A novel model of tumour formation in NF1

Ana Sara Varela Mendes Ribeiro

Thesis submitted for the degree of Doctor of Philosophy

Medical Research Council Laboratory for Molecular Cell Biology

University College London

Declaration

I, Ana Sara Varela Mendes Ribeiro confirm that the work presented in this thesis is my own. Where information has been derived from other sources, I confirm that this has been indicated in the thesis.

Signed…….Date……

Abstract

Neurofibromatosis type 1 (NF1) is a common genetic disorder that predisposes to the development of heterogeneous tumours of Schwann cell origin, termed neurofibromas. Neurofibromas are thought to arise from a combination of genetic events – loss of the Ras-GAP neurofibromin in the Schwann cell lineage – and microenvironmental cues. Schwann cells are specialised cells that ensheath and myelinate the axons in the peripheral nervous system (PNS). In the adult they are present in a quiescent state, however following damage to the PNS they have a remarkable ability to regenerate. Distal to the site of injury, Schwann cells dedifferentiate to a progenitor-like state, in which they contribute to nerve repair by recruiting a robust inflammatory response and helping axons return to their targets. Work from our laboratory has shown that activation of the Ras/Raf/ERK pathway plays a central role in driving the switch in Schwann cell state from a fully differentiated to a proliferating, "progenitor-like" cell. Crucially, neurofibromas resemble injured nerves in that they are composed of a mixture of inflammatory cells and Schwann cells that are found dedifferentiated and dissociated from axons, suggesting that deregulation of Ras/ERK may trigger tumourigenic events.

In this thesis I present work on how the Ras/Raf/ERK pathway may be regulated in Schwann cells. I show that the phosphatase MKP3 may be involved in controlling the levels of ERK activity in Schwann cells during differentiation and following nerve injury. I also describe a new model for neurofibroma formation. Using transgenic mice I show that *Nf1* loss in adult, myelinating Schwann cells has no effect on peripheral nerves and does not induce tumourigenesis. However, when coupled with an injury, the mice developed tumours at a high frequency. Furthermore, I show that in the absence of *Nf1*, ERK signalling is deregulated upon injury, implicating this pathway in the tumour formation. This may have therapeutic relevance, which is currently being tested in our animal model. In addition, we observed that tumours only arise at the wound site, despite Schwann cells dedifferentiating along the length of the nerve. This strongly implies that the microenvironment is a crucial player in the outcome of *Nf1* loss and reveals this new animal model as a promising system to further dissect molecular events involved in tumourigenesis.

Acknowledgements

I would like to thank Alison Lloyd for her enthusiasm, guidance and support during the course of my studies. I also thank the members of the Lloyd lab for being such a great team. I am particularly grateful to Sinead Roberts for reading and commenting on final drafts of this manuscript and to Melissa Collins for always finding time to listen to my doubts.

A very special thanks to Ilaria Napoli for being a teacher, a colleague and most of all, the best of the friends. I was truly fortunate to have her around.

Finally, I would not have made it without the support of my family. To my mother, in particular, thank you for being my rock and always putting things into perspective.

This work was supported by the Portuguese Foundation for Science and Technology (FCT) and the GABBA program (SFRH/ BD/ 33254/ 2007, with funds from the POPH-QREN).

Table of contents

Declaration ……..……..……..……..…….. 2
Abstract ……..……. 3
Acknowledgements ……..……...…..……. 4
Table of contents ……..……..…..……. 5
Figures and tables ……..…….. 10
Abbreviations used in this thesis ……..……....……..….. 13

Chapter 1: Introduction …….. 15
1.1 General introduction ……....15
1.2 Glial cells of the Peripheral Nervous System ……..…… 16
1.3 The Schwann cell lineage ……..……..……..……..……. 18
1.3.1. The origin of Schwann cells ……..18
1.3.2 NCS to SCP transition…….. 19
1.3.3 SCP to immature SC progression ……...……..… 23
1.3.4 Preparation for differentiation – radial sorting and proliferation …...…. 24
1.3.5 Threshold levels of NRG1 Type III dictate Schwann cell fate ……..... 25
1.3.6 Differentiation into non-myelinating SC …….. 27
1.3.7 Differentiation into myelinating SCs ……..……... 27
1.3.8 Signals mediating early events of myelination: SC-axon interaction 28
1.3.9 Signals and pathways mediating myelination ……..... 30
1.3.10 Transcriptional control of SC differentiation …… 31
1.4 Myelin structure and function ……. 34
1.4.1 Myelin composition …….. 37
1.5 Schwann cell basal lamina …… 40
1.6 The anatomy of peripheral nerves ……..……. 40
1.7 Wallerian degeneration and PNS repair ……..……..... 43
1.7.1 Axonal degeneration …….. 43
1.7.2 Schwann cell response: dedifferentiation and demyelination …… 45
1.7.3 Schwann cell plasticity is regulated by the Ras/RAF/ERK pathway……..46
1.7.4 The role of Schwann cells in WD: myelin and axonal clearance and recruitment of the inflammatory response …….. 47

1.7.5 The inflammatory response …… 48
1.7.6 Schwann cell proliferation ……....49
1.7.7 Axonal regrowth ……...…….. 51
1.7.8 Final steps of nerve repair: Schwann cell redifferentiation, axonal remyelination and resolution of the inflammatory response …….. 52
1.8 Neurofibromatosis type I …… 54
1.8.1 Incidence and symptoms …….. 54
1.8.2 Neurofibromas ……..... 55
1.8.3 The *NF1* gene …….. 57
1.8.4 Neurofibromin …… 58
1.9 Mouse models of NF1 ……..... 63
1.9.1 Initial models ……63
1.9.2 Properties of *Nf1* deficient cells …….. 64
1.9.3 *Nf1* chimeric mice ……65
1.9.4 Conditional *Nf1* knockout mice: the Krox-20 model …… 66
1.9.5 Evidence for a role of the microenvironment in neurofibroma formation..66
1.9.6 The neurofibroma cell of origin …….. 67
1.9.7 Mouse model of dermal neurofibromas …….. 71
1.9.8 Mouse models of malignant peripheral nerve sheath …….. 74
1.10 Insights into neurofibroma formation ……... 75
1.11 Thesis aims …… 77
Chapter 2: Materials and methods……..……79
2.1 Materials……...…..…… 79
2.1.1 Primers for genotyping ……..…… 79
2.1.2 siRNA oligos ……..…… 79
2.1.3 primers for qPCR ……..… 80
2.1.4 shRNA oligos ……...…..… 80
2.1.5 Antibodies……..…..…… 81
2.2. Animals ……..…...… 82
2.2.1 Mouse strains ……..….. 82
2.3 Cell culture ……...… 83
2.3.1 Primary Schwann cells ……...……..... 83

2.3.2 Rat Dorsal Route Ganglion (DRG) explants ……..…….. 83
2.3.3 Phoenix cell culture ……...… 83
2.4 Cell culture assays ……..... 84
2.4.1 Schwann cell differentiation assays ……84
2.4.2 Myelinating Schwann cell-DRGs co-cultures …… 84
2.4.3 Transfection of siRNA into Schwann cells ……... 84
2.4.4 Generation of shRNA expressing SC by Phoenix infection ….……..... 85
2.4.5 shRNA oligos design and vector cloning ……..…… 86
2.5 DNA/RNA manipulation ……..…… 87
2.5.1 DNA extraction from animal tissue …….. 87
2.5.2 Genotyping ……..... 87
2.5.3 RNA extraction from cultured cells …… 88
2.5.4 cDNA synthesis …… 88
2.5.5 qPCR ……..… 89
2.6 Protein analysis …… 89
2.6.1 Protein extraction from tissues …… 89
2.6.2 Protein extraction from cultured cells ……..…… 89
2.6.3 Western blotting ……...…. 90
2.7 Microscopy ……...…. 90
2.7.1 Tissue processing ……..…. 90
2.7.2 Histology and Tumour Grading ……..... 91
2.7.3 Hematoxylin/Eosin staining ……...…. 91
2.7.4 Alcian blue …… 91
2.7.5 X-gal staining …… 92
2.7.6 Immunohistochemistry ……....…… 92
2.7.7 Immunofluorescence ……...… 92
2.7.8 Semi-thin and ultrathin preparation ……..… 93
2.8 Administration of substances ……...… 93
2.8.1 Tamoxifen administration …… 93
2.8.2 Edu incorporation assay ……...…… 93
2.8.3 PD 0325901 administration ……..…… 94
2.9 Sciatic nerve transection …… 94
2.10 Statistical analysis ……...…… 95
Chapter 3: Results I …….. 96

3.1 Chapter introduction ……..…….. 96
3.2 Generation of a mouse model in which *Nf1* loss is induced specifically in myelinating Schwann cells in adult mice ……....… 97
3.3 Myelinating Schwann cells are not affected by *Nf1* ablation in adult mice ……... 105
3.4 Quiescent adult myelinating Schwann cells are refractory to tumourigenesis … 105
3.5 The ERK pathway is not activated by *Nf1* loss in adult mSchwann cells ……..…..109
3.6 Chapter summary and conclusions ……...… 112

Chapter 4: Results II …… 113
4.1 Chapter introduction ……....…… 113
4.2 Injury induces peripheral nerve tumour formation at high frequency ……. 113
4.3 Morphological characterization of sciatic nerves, at the site of injury …… 114
4.4 Tumours in NF1 mutants can be classified as Neurofibromas ……....… 117
4.5 Ultrastructural analysis confirms the multicellular nature of neurofibromas ….. 121
4.6 *Nf1*$^{-/-}$ Schwann cells are a major cellular component of the tumours that develop at the site of injury ……..… 124
4.7 Increased proliferation in *Nf1*-deficient tumours, 8 months following injury …. 129
4.8 Characterization of the tumour stroma - inflammatory cells and fibroblasts …. 129
4.9 Distal to the injury site, *Nf1*-deficient nerves regenerate normally …… 140
4.10 Distal to the tumour, *Nf1*$^{-/-}$ SCs redifferentiate and remyelinate axons ……144
4.11 Chapter summary and conclusions …… 147

Chapter 5: Results III …… 149
5.1 Chapter introduction ……....… 149
5.2 The ERK pathway is deregulated in *Nf1*-deficient mice following injury ……. 149
5.3 Increased proliferation in *Nf1*$^{-/-}$ Schwann cells …….. 151
5.4 Analysis of the extracellular matrix components ……..... 153
5.5 Enrichment of macrophages at the wound-site ……....… 163
5.6 Testing the therapeutic potential of MEK inhibitors ……..... 165
5.7 Chapter summary and conclusions ……... 168

Chapter 6: Results IV ……... 169
6.1 Chapter introduction ……..... 169
6.2 cAMP-differentiated Schwann cells show a dampened ERK signalling ……. 170
6.3 Pro-differentiating conditions quench ERK activation in *Nf1*-deficient SCs …..... 172
6.4 MKP3 is strongly induced by cAMP exposure …… ..172

6.5 MKP3 loss impairs Schwann cell cAMP-induced differentiation *in vitro*, but not in SC-DRG co-cultures 177
6.6 MKP3 is expressed *in vivo* at the onset of myelination and re-expressed following injury in the PNS 180
6.7 Chapter summary and conclusions 180

Chapter 7: Discussion 184
7.1 Adult, quiescent myelinating Schwann cells are not susceptible to *Nf1* loss 184
7.2 Adult *Nf1*$^{-/-}$ myelinating SCs form tumours, following injury 187
7.3 Following injury, tumours form independently of the *Nf1* background 190
7.4 The nerve is tumour-suppressive 192
7.5 The microenvironment at the injury site is tumour-promoting 193
7.6 Possible upstream signals of Ras signalling 194
7.7 Penetrance 195
7.8 Ras/Raf/ERK regulation in differentiating Schwann cells 195
7.9 Conclusions and therapeutic relevance 196
7.10 Further work 197

References 199

Figures and tables

Figure 1-1: Schematic representation of a peripheral nerve and associated glial cells ……..17
Figure 1-2: The Schwann cell lineage …… 20
Figure 1-3: NRG1 isoforms expressed in the peripheral nervous system and potential isoform-specific roles …….. 22
Figure 1-4: Major signalling pathways and transcriptional networks involved in Schwann cell differentiation …… 34
Figure 1-5: Diagrams of the structural regions of myelinated fibres ……..... 36
Figure 1-6: Myelinated axons and areas of compact and non-compact myelin ……..... 38
Figure 1-7: Schematic representation of peripheral nerves …….. 41
Figure 1-8: Wallerian Degeneration in the PNS ……....44
Figure 1-9: Structure of a normal peripheral nerve and a neurofibroma …… 56
Figure 1-10: Examples of dermal and plexiform neurofibromas …….. 56
Figure 1-11: Ras activation and downstream signals …… 60
Figure 1-12: Schematic representation of the functional domains of NF1 ……... 61
Figure 1-13: Pathways deregulated by *NF1* loss ……62
Figure 1-14: Susceptible stages for neurofibroma formation ……... 73
Figure 1-15: Model of neurofibroma initiation and progression …….. 77
Figure 1-16: Main questions addressed in this thesis ……... 78
Figure 2-1: Schematic representation of the partial transection performed in the right sciatic nerve …….. 94
Figure 3-1: Characterisation of transgenic mice expressing an inducible Cre recombinase in the peripheral nervous system …….. 98
Figure 3-2: Cre drives recombination in myelinating Schwann cells when expressed under the *P0* promoter ……...100
Figure 3-3: *P0-CreER* mice do not exhibit recombinase activity in p75+ nmSCs ……101
Figure 3-4: Generation of a mouse model to study *Nf1* disruption in myelinating Schwann cells, in adult peripheral nerves ……... 103
Figure 3-5: Animals used in this study …… 104
Figure 3-6: *Nf1* loss in Schwann cells does not induce Schwann cell dedifferentiation and proliferation …… 106
Figure 3-7: *Nf1* loss in adult, differentiated SCs does not affect nerve structure ……. 107
Figure 3-8: Remak bundles are maintained in the absence of *Nf1* ……..108
Figure 3-9: *Nf1* loss in adult mSchwann cells does not induce the recruitment of an inflammatory response ……..... 110
Figure 3-10: *Nf1* loss in adult mSCs does not induce activation of ERK signalling ……..... 111
Figure 4-1: *Nf1* mutant mice form tumours at the site of injury ……..... 115

Figure 4-2: Injured nerves from *Nf1* deficient mice are greatly enlarged at the site of injury and display increased cellular density …….. 116
Figure 4-3: Histological analysis of control and mutant sciatic nerves ……... 118
Figure 4-4: Tumours in *P0-Nf1*$^{fl/fl}$ and *P0-Nf1*$^{fl/-}$ mice display variable immunoreactividade for the Schwann cell marker S100β ……... 120
Figure 4-5: Morphological analysis of sciatic nerves at the injury site, 8 months following transection ……..... 122
Figure 4-6: EM analysis of the tumours developed in NF1 mutant mice, 8 months following peripheral nerve injury ……. 123
Figure 4-7: GFP+ positive cells are a major cellular component of the tumours developed in NF1 mutants ……. 125
Figure 4-8: In the tumour region, the majority of *Nf1*$^{-/-}$ Schwann cells do not express the S100β marker ……... 126
Figure 4-9: Most, but not all, *Nf1*$^{-/-}$ Schwann cells express p75 …….. 127
Figure 4-10: Striking resemblances between "perineurial-like" cells and p75+ Schwann cells or GFP+ SC-derived cells in a neurofibroma ……... 128
Figure 4-11: Few GFP+ cells are found at the wound site, in control animals, 6 months following injury …… 130
Figure 4-12: Increased proliferation in NF1 mutant nerves ……... 131
Figure 4-13: p75+ Schwann cells and macrophages proliferate in tumours formed in *Nf1*-deficient peripheral nerves after injury …… 132
Figure 4-14: Increased infiltration of mast cells in *P0-Nf1*$^{fl/fl}$ and *P0-Nf1*$^{fl/-}$ sciatic nerves … 134
Figure 4-15: Macrophages are present at elevated numbers in NF1 mutant nerves at the tumour region ……... 135
Figure 4-16: Inflammatory cells are recruited into the tumours in NF1 mutants …….. 137
Figure 4-17: A strong inflammatory response is observed in the neurofibromas …… 138
Figure 4-18: Variable expression of SMA in tumours from NF1 mutant mice …….. 139
Figure 4-19: Distal to the wound site, nerves regenerate normally in *P0-Nf1*$^{fl/fl}$ and *P0-Nf1*$^{fl/-}$ mice …….. 141
Figure 4-20: Analysis of the region distal to the injury site ……. 142
Figure 4-21: A few tumours spread along the distal stump of the nerve …….. 143
Figure 4-22: Distal to the tumour region, *Nf1*$^{-/-}$ Schwann cells are found redifferentiated and remyelinating ……. 145
Figure 4-23: GFP-positive expressing cells persist in the regenerated control nerves, 6 months following injury ……..... 146
Figure 5-1: ERK signalling is deregulated in sciatic nerves of *Nf1*-deficient mice, following injury …… 150
Figure 5-2: Increased proliferation in *Nf1*$^{-/-}$ Schwann cells 7 days following injury ……..... 152

Figure 5-3: Analysis of the extracellular matrix components, 7 days following injury- Laminin1 154
Figure 5-4: Analysis of the ECM, 7 days following injury- collagen1 157
Figure 5-5: Analysis of the ECM, 7 days following injury- collagen 1V 160
Figure 5-6: Analysis of the ECM, 7 days following injury- fibronectin 162
Figure 5-7: Enrichment of immune cells at the injury site, compared to the distal region of the nerve, 7 days following injury 164
Figure 5-8: PD treatment efficiently reduces activation of the ERK pathway 166
Figure 6-1: NRG1 stimulation elicits dampened ERK activation in Schwann cells induced to differentiate in the presence of db-cAMP 171
Figure 6-2: NF1 kd cells exhibit a marked quenching of ERK activation upon NRG1 stimulation 173
Figure 6-3: Dampening of ERK signalling occurs downstream of MEK 175
Figure 6-4: The ERK-specific phosphatase MKP3 is strongly induced by cAMP signalling...176
Figure 6-5: MKP3 knockdown does not prevent cAMP-mediated ERK dampening, but affects the kinetics of ERK activation following NRG stimulation 178
Figure 6-6: MKP3 kd impairs db-cAMP induced Schwann cell differentiation 179
Figure 6-7: MKP3 kd does not impair SC differentiation in SC-DRG co-cultures 181
Figure 6-8: MKP3 is expressed at P0 and re-expressed following injury to the PNS 182
Figure 7-1: Model of neurofibroma formation 199

Tables

Table 1-1: Clinical features of Neurofibromatosis type I 55
Table 2-1 Primers used for mice genotyping 79
Table 2-2 siRNA oligos 79
Table 2-3 Primers used in qPCRs 80
Table 2-4 shRNA oligos 80
Table 2-5 Primary antibodies 81
Table 2-6 Secondary antibodies 82
Table 2-7 Genotyping PCR reactions 87
Table 2-8: Solutions for protein extraction and Western blotting 89

Abbreviations used in this thesis

ANOVA	Analysis of variance
BCP	Boundary cap cell
bp	Base pair
cAMP	Cyclic adenosine monophosphate
cDNA	Complementary deoxyribonucleic acid
CNS	Central Nervous System
db-cAMP	Dibutyryl-cAMP
DMEM	Dulbecco's Modified Eagle Medium
DUSP	Dual specific phosphatase
ECM	Extracellular matrix
ERK	Extracellular related kinase
GAP	GTPase activating protein
GDP	Guanosine diphosphate
GEM	Genetically engineered mouse
GFP	Green fluorescent protein
GGF	Glial growth factor
GRD	GAP related domain
GTP	Guanosine triphosphate
HDAC	Histone deacetylase
ISC	Immature Schwann cell
kb	Kilobases
LOH	Loss of heterozygosity
mRNA	Messenger RNA
mSC	Myelinating Schwann cell
NCC	Neural crest cell
NCSC	Neural crest stem cell
Nf1	Neurofibromatosis type I gene
NF1	Neurofibromin/ Neurofibromatosis type I
NFAT	Nuclear factor of activated T cells
NMJ	Neuro-muscular junction
NRG1	Neuregulin-1
NFκB	Nuclear factor kappa-light-chain-enhancer of activated B cells

MAP	Mitogen activated protein
MHC	Major histocompatibility complex
MKP	Mitogen-activated protein kinase phosphatase
nmSC	Non-myelinating Schwann cell
PBS	Phosphate-buffered saline
PCR	Polymerase chain reaction
PI3K	Phosphatidylinositol-3-Kinase
PKA	Protein kinase A
PLL	Poly-L-lysine
PNS	Peripheral nervous system
RNA	Ribonucleic acid
ROS	Reactive oxygen species
RT	Reverse transcription
SC	Schwann cell
SCP	Schwann cell precursor
SEM	Standard error of the mean
siRNA	Short interfering RNA
shRNA	Short-hairpin RNA
UTR	Untranslated region protein-related domain

Chapter 1: Introduction

1.1 General Introduction

The identification of the original cell that gives rise to tumours has crucial implications for understanding the biology of cancer. In particular, the rigorous investigation of the early cellular events of tumourigenesis is dependent on the knowledge of the specific initiating-cell that acquires the initial genetic mutations (Alcantara Llaguno et al., 2009). Furthermore, the identification of the cell of origin of specific tumours may allow the development of unique treatment targets and strategies. In principle, any cell with a proliferative capacity may be a target for oncogenic transformation. Stem cells have become the most popular candidate given their inherent capacity to self-renew and longevity that would allow the sequential accumulation of the genetic or epigenetic modifications required for tumourigenesis. In mouse models of intestinal and prostate cancer, for example, it seems clear that the cancers originate in a bona fide stem cell that is capable of self-renewal and multilineage differentiation (Visvader, 2011). Nevertheless, it has also become clear that at least in some specific tumours, more differentiated cell populations, such as progenitors or even fully differentiated cells, may be the culprits. That certainly seems to be the case in neurofibromas, benign tumours of the peripheral nerve sheath that arise mainly in the context of the tumour predisposition syndrome, NF1 (Dirks, 2008). Neurofibromas, despite their mixed cell composition have been shown to originate from Schwann cells (SCs) that have lost neurofibromin, a negative regulator of Ras signalling. Importantly, differentiated SCs themselves, rather than a stem cell population, are the source for new cells in the adult, making it plausible that mature, fully differentiated cells may be prone to become transformed to neoplastic cells. Indeed, neurofibromas provide a powerful model to gain new insight into tumour biology: first because the initial genetic lesion driving the tumour is well defined and secondly because the developmental steps of the SC lineage are well characterized. Furthermore, given the complex interaction between neoplastic SCs and the non-neoplastic elements of the tumour, neurofibromas are also excellent models to study the role of tumour microenvironment and how its modulation may alter the susceptibility of specific cells to become tumour-initiating cells. Before presenting work aimed at testing the issues raised above, I shall introduce the biology of Schwann cells, reviewing the most relevant literature on SC development and differentiation. I will also characterize the events that follow injury to the peripheral nervous system (PNS), with a special focus on how Schwann cells and their inherent

plasticity play a central role in the regeneration of peripheral nerves. Finally, I will introduce Neurofibromatosis type I, the genetics behind the disease, and conclude by discussing the major findings, regarding the biology of neurofibroma formation.

1.2 Glial cells of the Peripheral Nervous System

Glial cells mediate key functions in the nervous system. In the PNS, the glial components can be divided into three major categories: the Schwann cells (SCs) surrounding the peripheral nerves, the satellite cells - associated with neuronal cells bodies in peripheral ganglia - and the enteric glia (Corfas et al., 2004; Jessen, 2004). Schwann cells form the majority of the glial population and based on their morphology, biochemical signature and type of neuron (or area of their axons) with which they associate can be divided into three classes: myelinating Schwann cells (mSCs), non-myelinating SCs (nmSCs) and perisynaptic SCs (also known as teloglia or terminal SCs) (Figure 1-1). The latter reside at neuro-muscular junctions (NMJ) where they cover, without completely wrapping around, the presynaptic terminal of motor axons and have active roles in the formation, function, maintenance and repair of the NMJ (Feng and Ko, 2008). Interestingly, they share markers expressed by both myelinating and non-myelinating SCs, including the small calcium binding protein S100, the glial fibrillary associated protein (GFAP) and the myelin protein P0, but the signals determining their differentiation remain poorly understood. Despite the crucial functions that these cells play at the NMJ, a detailed discussion of their biology is outside the scope of this thesis. The myelinating and non-myelinating Schwann cells are the most abundant glia in the PNS; mSCs associate with and myelinate single large calibre axons of all motor and some sensory neurons, whilst nmSCs ensheath multiple smaller axons emanating from many sensory and all post-ganglionic sympathetic neurons (Figure 1-1). Schwann cells play indispensable roles in supporting peripheral axons: during development they provide trophic support to the growing axons; in the adult, their main function is to ensheath and myelinate axons, protecting against axonal damage and enabling rapid conduction of nerve impulses (Taveggia et al., 2010). In addition they contribute to immune surveillance and ionic homeostasis in peripheral nerves (Brill et al., 2011). The role of Schwann cells may not be restricted to their interaction with peripheral axons- non-myelinating SCs present in the bone marrow have recently been implicated in the regulation of hematopoietic stem cell hibernation (Yamazaki et al., 2011). Moreover, SCs are behind the astonishing regenerative capabilities of the PNS in response to wounding.

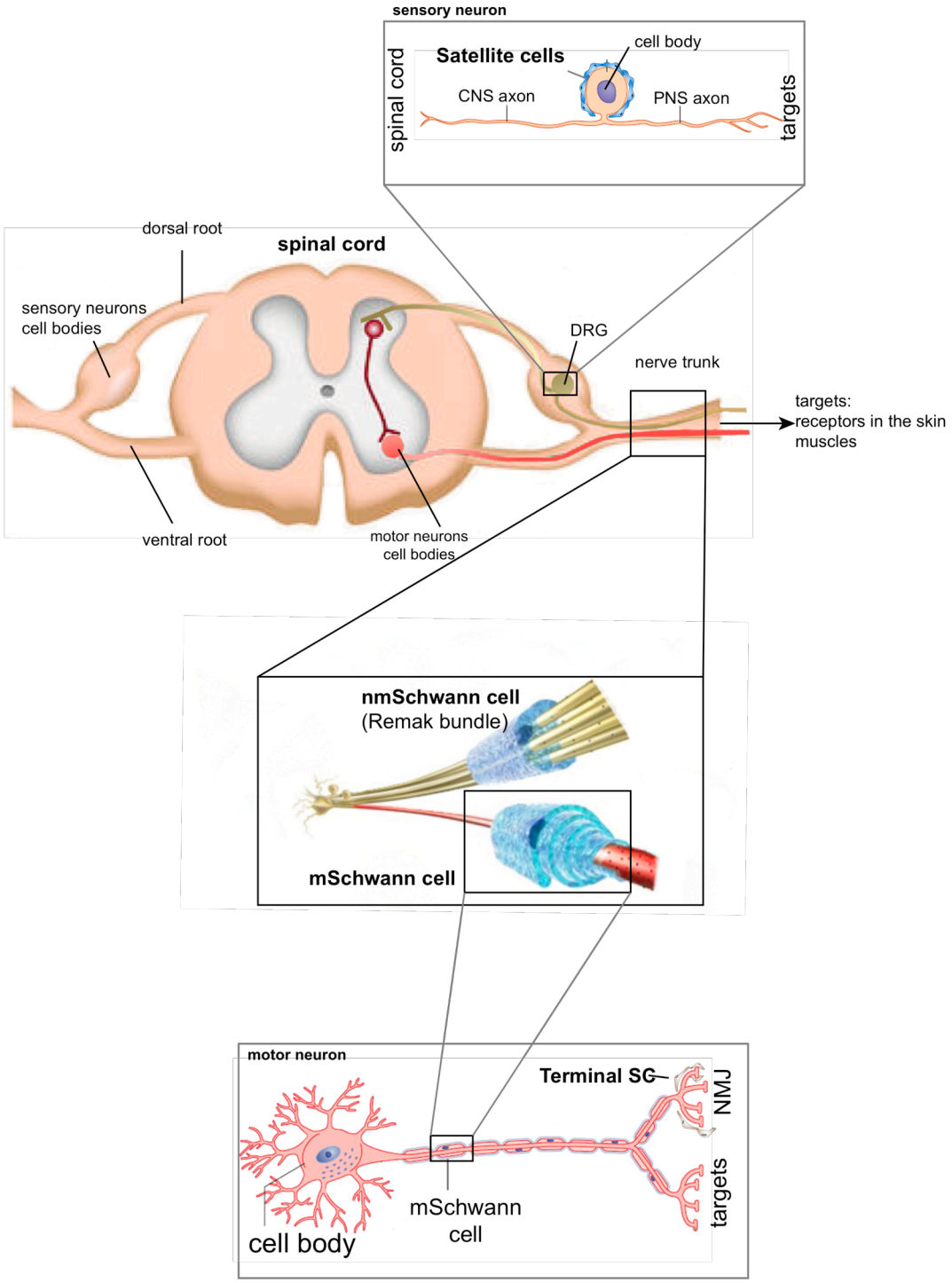

Figure 1-1: Schematic representation of a peripheral nerve and associated glial cells. A spinal nerve, emanating from the spinal cord is depicted. The cell bodies of sensory neurons reside in the PNS at the dorsal root ganglion (DRG), whereas motor neurons cell bodies reside in the CNS. Sensory axons, coming from the dorsal roots, meet motor neurons, coming from the ventral roots, to produce mixed spinal nerves. The image also shows the location of satellite cells, terminal SCs and myelinating and non-myelinating SCs.

Critical for their role in nerve repair is Schwann cells plasticity: following nerve injury, quiescent, fully differentiated cells revert to a "progenitor-like" phenotype that in many ways resembles the early stages of SC development. This striking feature is essential to provide a favourable environment for axonal regrowth.

Before discussing how Schwann cell plasticity underlies nerve regeneration and how it may be involved in the formation of peripheral nerve tumours, I will first discuss the process of SC development.

1.3 The Schwann cell lineage

1.3.1 The origin of Schwann cells

The course of Schwann cell development has been intensively studied (Figure 1-2). The majority of myelinating and non-myelinating SCs from spinal nerves derive from neural crest stem cells (NCSCs), a subset of neural crest cells (NCCs) characterized by the ability to self-renew and to undergo multilineage differentiation into myofibroblasts, glia and neurons (Morrison et al., 1999; Stemple and Anderson, 1992). Neural crest cells, that also give rise to other major cell types including satellite cells, boundary cap cells, melanocytes, craniofacial bones and cartilage and endocrine cells (Dupin et al., 2003; Maro et al., 2004), delaminate from the neural tube around embryonic day 8.5 (E8.5) in the mouse, and undergo extensive proliferation and migration along distinct pathways. To delaminate from the neural plate NCCs go through an epithelial-to-mesenchymal transition that appears to involve interplay between Noggin and bone morphogenetic protein-4 (BMP4) (Sela-Donenfeld and Kalcheim, 1999). The subpopulation of NCSCs can be identidified at this stage by the expression of several markers including the low affinity neurotrophin receptor p75, the neural adhesion protein L1, the intermediate filament nestin and the brain lipid-binding protein (BLBP). Importantly, NCSCs differentiate terminally by late gestation and cannot be detected postnatally in the PNS. An exception occurs in the gut, where NCSCs persist throughout adult life (Kruger et al., 2002).

Schwann cells in dorsal and ventral roots and satellite cells within the ganglion also originate, in part, via early cell pools other than NCSCs such as boundary cap cells (BCCs) (Maro et al., 2004). Boundary cap cells are neural crest derived multipotent cells, which can be identified in the embryo around day 10 (E10) by the expression of the transcription factor Krox-20 (as detailed below this gene will also be expressed in pro-myelinating SCs, but later in development). It is thought that BCCs differentiate

shortly after birth, however due to the lack of specific markers it remains possible that some BCCs persist in the adult, where they may constitute a reservoir of multipotent neural cells in the PNS. The processes by which BCCs give rise to different cell populations remain largely unknown, therefore I will focus my attention on the development of SCs in the spinal nerve trunks innervating the limbs, that originate from migrating neural crest stem cells that differentiate into Schwann cell precursors (SCPs).

Upon migration into peripheral nerves, NCSCs associate with outgrowing naked axons and commit to the SC lineage through a stepwise process, characterized by a strong dependence on axonal signals and involving three main transitions: the engagement of neural crest cells into the SC lineage, which leads to the formation of Schwann cell precursors (SCPs), the maturation of these precursors into immature Schwann cells (ISCs) and lastly, occurring around birth, the cell-cycle exit and differentiation into either the myelinating or the non-myelinating phenotypes (Figure 1-2). Importantly, this last step in SC development is reversible, as injury signals induce mature SCs to revert to a dedifferentiated state (discussed in section 1.7).

1.3.2 NCSC to SCP transition

Schwann cell precursors are the glial cells found in the limb nerves of the mouse embryo at E12/13 and represent the earliest well-defined stage of PNS glial development. Schwann cell precursors are highly migratory and proliferative cells, which are first found associated with outgrowing axons before starting to extend sheet-like processes that communally envelope axons in large bundles. SCPs, while sharing with NCSCs the expression of markers such as p75, L1 and the intermediate filament nestin (Jessen et al., 1994), can be distinguished by the expression of lineage specific markers such as Desert hedgehog (DHH), the growth associated protein-43 (GAP43), F-spondin and low levels of myelin protein zero (P0) and proteolipid protein (PLP) (Curtis et al., 1992; Dong et al., 1999; Jessen et al., 1994; Jessen and Mirsky, 1999). At this stage, SCPs depend strictly on axonal signals for survival and proliferation and, reciprocally, play a pivotal role in promoting axonal survival (Jessen and Mirsky, 2005). It is still unclear what drives NCSCs to commit to the glial lineage. Glial specification is blocked in mice lacking Sox-10, however Sox-10 expression is detected in all migrating neural crest cells indicating that Sox-10 expression alone is not sufficient to promote gliogenesis (Britsch et al., 2001). Sox-10 may exert at least

part of its functions by controlling the expression of ErbB3 receptors in NCSCs (Britsch et al., 2001).

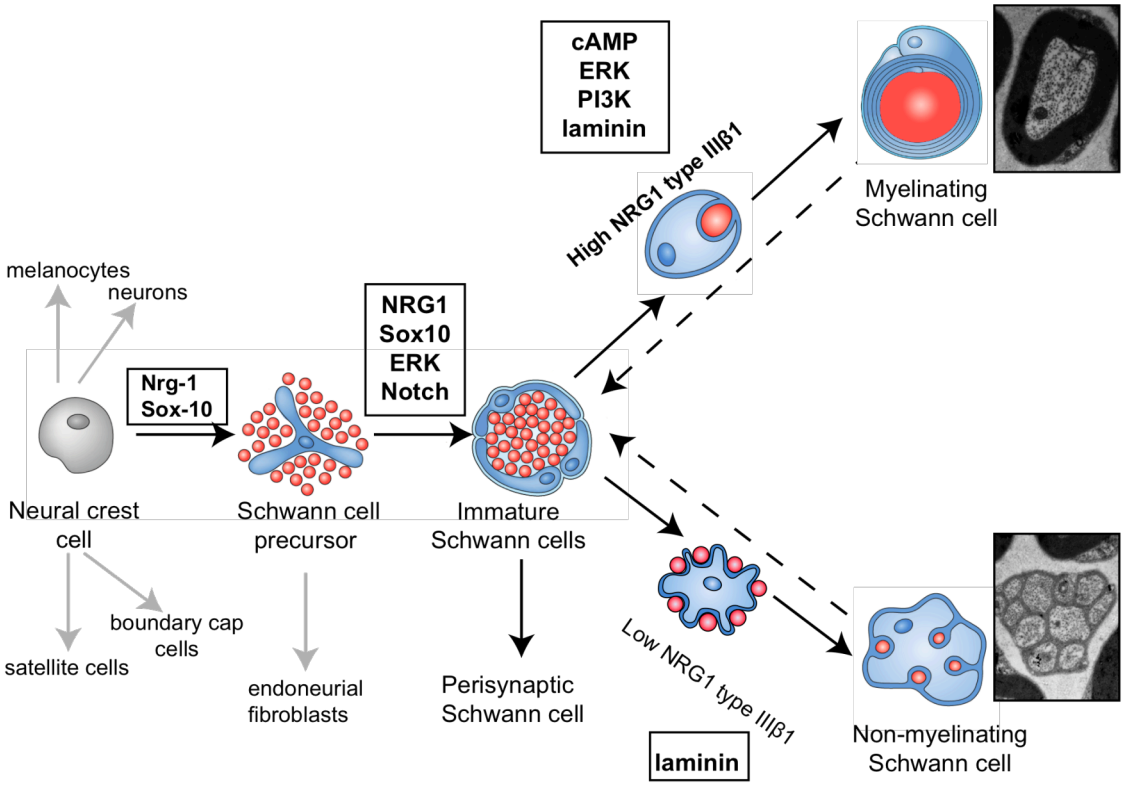

Figure 1-2: The Schwann cell lineage. Diagrammatic representation of the major transitions and signalling pathways involved in Schwann cell differentiation. The formation of fully differentiated myelinating and non-myelinating SCs begins around birth and is reversible (dashed lines) (adapted from Jessen and Mirsky, 2005). On the right, EM micrographs of a myelinating (top) and a non-myelinating SC ensheathing a group of axons (Remak bundle) (bottom), are shown.

Neuregulin-1 (NRG1)/ErbB signalling may also be involved in SC specification, since *in vitro,* the axonal derived factor NRG1 is able to block neuronal specification (Shah et al., 1994), which might lead indirectly to increased gliogenesis. Nevertheless, in the same cultures SCs develop readily with or without NRG1, indicating that NRG1 signalling is not required for glial specification. Instead, at this stage of development NRG1 signalling is critical for the proper migration of the neural crest cells (Britsch et al., 1998). Given the critical role that NRG1 and their receptors play in SC behaviour, a brief description of the main isoforms present in the PNS will follow.

The *NRG1* gene encodes more than 15 transmembrane and secreted protein isoforms, generated by alternative promoter usage and mRNA splicing. In the axonal membrane of peripheral axons, three major types of neuregulin-1 proteins can be found (I, II and III), all sharing an epidermal growth factor (EGF)-like domain and differing in their N-terminal sequences (Figure 1-3). Neuregulin-1 isoforms Type I (also known as heregulin or Neu) and II (also known as glial growth factor [GGF]) have N-terminal immunoglobulin-like domains that following proteolytic cleavage can be shed and released as soluble proteins from the neuronal surface. Two main isoforms of NRG1 Type III have been described in the PNS, β1a and β3 (Ho et al., 1995; Meyer et al., 1997), both defined by the presence of a cystein-rich domain (CRD). In the case of NRG1 Type III β1a, the CRD domain functions as a second transmembrane domain in that the mature form remains tethered to the axonal membrane after cleavage. The second type of NRG1 Type III present in the PNS, the β3 isoform (also known as sensory and motor neuron-derived factor- SMDF) lacks the transmembrane-domain C-terminal of the EGF-like domain and remains less studied. Consequently, NRG1 Type III can only function in a juxtracrine fashion, signalling only to cells that it is directly in contact with (Brinkmann et al., 2008). Neuregulin-1 isoforms mediate their effects in Schwann cells by binding the ErbB3 receptor (they can also bind to ErbB4, but this is only minimally expressed in SCs). Upon ligand binding, ErbB3, which lacks an active kinase, heterodimerizes with ErbB2 (that is unable to bind NRG1 but has an active kinase) leading to receptor co-phosphorylation, recruitment of adaptor proteins and activation of downstream pathways (specified below).

Neuregulin-induced signals are not only involved at this early stage of SC development, but have emerged as key regulators of axon-SC interactions at each stage of the Schwann cell lineage (Adlkofer and Lai, 2000). These include the survival and proliferation of SCPs: transgenic animals lacking NRG1 Type III isoforms or the ErbB2/3 receptors show a near complete absence of SCPs in developing nerve trunks, without affecting the formation of satellite glia within the dorsal root ganglia (DRG) (Dong et al., 1995; Erickson et al., 1997; Garratt et al., 2000a; Garratt et al., 2000b; Lee et al., 1995; Riethmacher et al., 1997; Wolpowitz et al., 2000). Importantly, these mice exhibited abnormal neuronal death, underscoring the importance of SC-neuron interactions in the support of neuronal survival (Wolpowitz et al., 2000). In contrast, deletion of the Type I and II neuregulin-1 isoforms did not affect the generation or survival of Schwann cells, indicating that different neuregulin isoforms perform distinct

functions in Schwann cells (Meyer et al., 1997). Figure 1-3 describes some of the specific biological functions that have been attributed to each of the NRG1 isoforms.

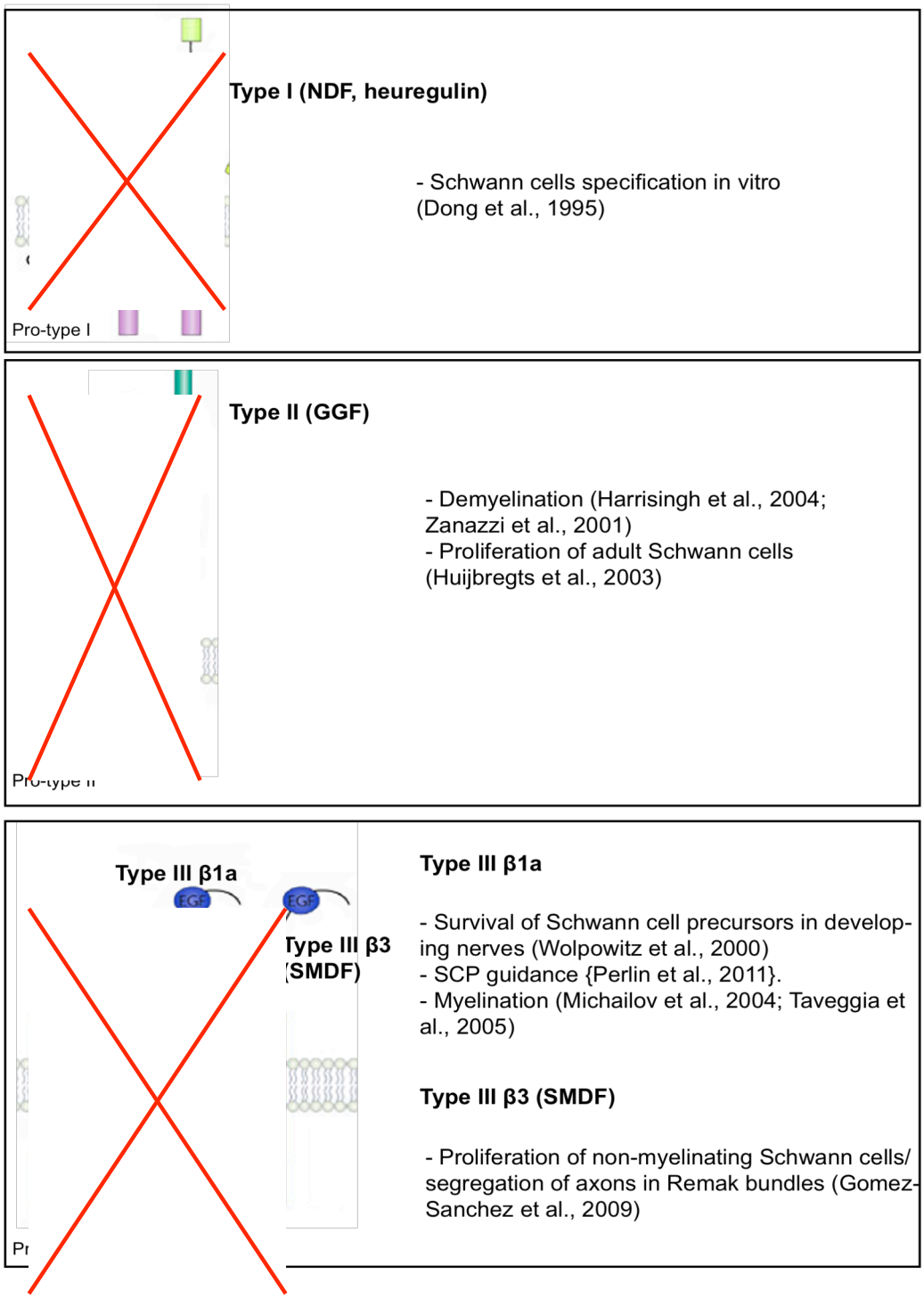

Figure 1-3: **Neuregulin-1 isoforms expressed in the PNS and potential isoform-specific roles**. Schematic representation of the three major isoforms of NRG1 expressed in peripheral axons, before and after proteolytic cleavage (adapted from Mei and Xiong, 2008). A brief description of the biological impact of each isoform is also shown. (Figures removed due to copyright restrictions).

It seems likely that, at this stage, the effects of the NRG1/ErbB signalling in Schwann cell proliferation/survival, are mediated, at least in part, through the ERK pathway, as a similar phenotype has been recently described in mice with selective inactivation of ERK1 and ERK2 kinases, suggesting that the ERK pathway is necessary to transduce NRG1/ErbB signals during the development of the Schwann cell lineage (Newbern et al., 2011). Moreover, NRG1 Type III may also act as an endogenous guidance cue controlling Schwann cell migration. Studies in zebrafish have shown that ectopic pan-neuronal expression of human NRG1 Type III in the spinal cord is sufficient to induce Schwann cells to trespass within the central nervous system (CNS), indicating that this signal promotes Schwann cell motility and attraction to ectopic locations (Perlin et al., 2011).

Interestingly, there is an emerging concept that SCPs can act as multipotent progenitors in the developing nervous system (Doetsch, 2003). This concept was fuelled by a fate-mapping study that demonstrated that the small number of fibroblasts present in the postnatal nerve originate from cells that are neural crest derived and express desert hedgehog (DHH) and are, therefore, presumably SCPs. In addition, SCPs have also been identified as a cellular origin of skin melanocytes (Adameyko et al., 2009). This idea is consistent with previous observations that P0 positive cells from early nerves or DRG in the rat have the potential to generate both neurons and fibroblasts (Hagedorn et al., 1999; Morrison et al., 1999).

Importantly, all SCPs differentiate during embryogenesis and are not found in adult peripheral nerves.

1.3.3 SCP to immature SC progression

As development proceeds, SCPs start to form basal lamina, proliferate and ensheath fasciculating axons and become immature Schwann cells (ISCs). The molecular mechanisms controlling this transition remain largely unknown. Again, neuregulin-1 might be involved because *in vitro*, the NRG1 Type I isoform has been shown to accelerate the conversion of SCPs to the immature phenotype (Dong et al., 1995). Nevertheless, Schwann cell development in transgenic mice lacking all Type I and Type II NRG1 isoforms occurs normally, indicating that probably *in vivo*, Type I and Type II isoforms are not involved in regulating the progression of SCP to immature Schwann cells (Meyer et al., 1997).

Recent studies have implicated Notch signalling at this developmental stage; inactivation of the major transcriptional mediator of canonical Notch (RBJP) delayed the transition from SCPs to the immature Schwann cell fate and, conversely, constitutive activation of the pathway resulted in premature Schwann cell generation (Woodhoo et al., 2009).

This transition occurs between E13-15 in mice and involves coordinated changes in molecular expression, regulation of survival and response to mitogenic signals. Contrary to SCPs that rely entirely on axonal-derived survival signals (in particular NRG1), immature SCs are able to maintain their own survival by setting in motion autocrine survival circuits. Importantly, these same autocrine signals likely maintain the survival of SCs after axonal degeneration, which is crucial for nerve regeneration. Major components of the autocrine loop have been identified and include insulin growth factor-2 (IGF-2), platelet-derived growth factor-β (PDGFβ), neurotrophin-3 (NT3), leukemia inhibitor factor (LIF) and lysophosphatidic acid (LPA). Also laminin, one of the major components of SC basal lamina, acts in concert with these components to promote longer-term survival (Lobsiger et al., 2000; Meier et al., 1999). The transition of SCP to ISC coincides with major changes in the architecture of the developing peripheral nerves: they become vascularised and a distinct layer of the developing epineurium appears at the nerve surface. A more detailed description of the structure of the peripheral nerve will be given in section 1.6.

1.3.4 Preparation for differentiation – radial sorting and proliferation

Immature Schwann cells, which can be identified by the expression a number of differentiation markers such S100, GFAP, and the sulfated O4 (Corfas et al., 2004; Jessen and Mirsky, 2005), are initially found arrayed around the edges of large axon bundles. At this point the fate of immature SCs begins to diverge to form myelinating or non-myelinating Schwann cells. The decision to commit to one of the two possible differentiated forms is not SC autonomous, but instead depends on the diameter of the axons SCs randomly associate with. Through a process termed radial sorting, Schwann cells extend radial extensions (lamellipodia) into the axons bundles and sort them into smaller fascicles. Then, immature Schwann cells contacting large-diameter axons pluck out one axon to ensheath establishing a 1:1 relationship, wrap their membrane around the axon (see Figure 1-5) and start expressing stage-specific factors, including Oct-6 - such cells have reached the pro-myelinating state. A large number of small unmyelinated axons are also radially sorted and achieve a 1:1 relationship with

non-myelinating SCs, indicating that this process, although required for myelination is not part of a myelin-specific program. The remaining small-calibre axons, destined to become non-myelinating, become surrounded and segregated by the cytoplasm of SCs in groups termed Remak bundles (Figure 1-1). To ensure that all the axons are ensheathed at the completion of radial sorting, SCs must adjust their numbers by controlling survival and proliferation and by coordinating the extension and stabilization of their processes (Raphael et al., 2011; Webster et al., 1973). The latter is known to involve interactions between β1-integrin in the SC membrane and laminin-γ1 present in their basal lamina, as transgenic mice lacking either laminin or integrin fail to extend cytoplasmic processes and therefore exhibit impaired radial sorting and myelination (Chen and Strickland, 2003; Feltri et al., 2002). Activation of this pathway mediates its effects, at least partially, through downstream activation of the Rho family GTPase Rac1 (Benninger et al., 2007; Nodari et al., 2007).

The importance of the burst in SC number at this stage was demonstrated by studies in a mouse model with conditional deletion of the focal adhesion kinase (FAK) in Schwann cells. FAK mutant Schwann cells are able to associate normally with axon bundles and extend lamellipodia but exhibit impaired proliferation, which in turn results in inefficient axonal sorting (Grove et al., 2007). Importantly, FAK is known to be activated by the presence of laminin and has also been shown to interact with ErbB receptors upon NRG binding (Fernandez-Valle et al., 1998; Vartanian et al., 2000), suggesting that it may represent a point of crosstalk between the ECM and axonal signals. In fact, axonal neuregulin-1 signalling through ErbB is again key to this process, as shown by studies in zebrafish where pharmacological or genetic disruption of ErbB signalling generates defects in radial sorting and myelination due to impaired lamellipodia extension and reduced SC proliferation (Lyons et al., 2005; Raphael et al., 2011).

1.3.5 Threshold levels of NRG1 type III dictate Schwann cell fate

Following birth, when the process of axonal sorting is mostly completed, Schwann cells, in response to environmental signals that may include ATP released from electrically active axons (Stevens and Fields, 2000; Stevens et al., 2004), cease to proliferate and become ready to complete their final engagement into one of the two mature differentiated cells. The Schwann cells associated with large diameter axons will engage into the complex program of myelination. An instruction to myelinate comes from the NRG1 Type III β1a expressed on the axonal membrane (Taveggia et al.,

2005). This was elegantly elucidated by *in vitro* studies using superior cervical ganglion neurons, which normally have small-calibre axons associated with non-myelinating Schwann cells. When NRG1 Type IIIβ1a was ectopically expressed in these neurons, SCs were instructed to change their fate and myelinate. Expression also rescued myelination in sensory neurons from NRG1 Type III-deficient mice that otherwise failed to myelinate (Taveggia et al., 2005). Furthermore, the levels of axonal NRG1 type III signalling through ErbB determines the myelin thickness. Mice heterozygous for NRG1 Type III exhibit severe hypomyelination in the PNS, while neuronal overexpression of NRGI Type III has the converse effect and leads to hypermyelination (Michailov et al., 2004; Taveggia et al., 2005). Importantly, the ensheathment and segregation of smaller calibre axons by the cytoplasm of non-myelinating SCs in Remak bundles is also controlled by Type III isoforms (Taveggia et al., 2005). Together, these studies provided compelling evidence that a threshold of NRG1 Type III signalling determines the binary choice between myelination and ensheathment: smaller axons that express low levels of membrane NRG1 Type III instruct SCs to become non-myelinating whereas larger axons express higher levels of this ligand and thereby induce SCs to myelinate (Michailov et al., 2004; Nave and Salzer, 2006; Taveggia et al., 2005). Proteolytic cleavage of NRG1 Type III regulates the levels of active neuregulin at the axon surface and hence plays a crucial role in the control of myelination. Two major metalloproteases that cleave NRG1 at different cleavage sites, the secretase β-amyloid converting enzyme-1 (BACE-1) and the tumour-necrosis factor-α-converting enzyme (TACE) have been shown to play opposing roles. $BACE^{-/-}$ mice show a phenotype similar to that seen in mice with mutations in NRG1 Type III or SC-specific ErbB2 knockouts, implicating BACE-1 in NRG1 processing and activation (Figure 1-3) (Hu et al., 2006; Willem et al., 2006). In contrast, processing by neuronal TACE (also known as ADAM19) appears to exert a negative effect in myelination, as reducing its activity rescues hypomyelination in NRG1 Type III haploinsufficient mice (La Marca et al., 2011).

In accordance to the pivotal role that NRG1 plays in SC differentiation, transgenic mice with targeted deletion of the ErbB2 gene at the pro-myelinating stage or expressing a dominant-negative form of the ErbB receptors in SCs display striking myelination defects (Chen et al., 2003; Garratt et al., 2000b). The levels of ErbB receptors at the Schwann cell membrane are also critical, as demonstrated by a study using erbin knock out mice. Erbin is an adaptor protein that stabilizes ErbB receptors;

its ablation leads to a reduction of ErbB2 levels in SCs, which resulted in aberrant axonal segregation and marked hypomyelination (Tao et al., 2009).

1.3.6 Differentiation into non-myelinating SCs

Not much is known about the molecular cues that drive SCs to become non-myelinating. Few molecular changes are likely to be involved in this transition given the similarities between immature and non-myelinating SCs. Both share identical molecular phenotypes, at least in morphology and expression of antigenic markers, exhibiting cell surface molecules that are not found on myelinating SCs such as the cell adhesion molecules L1, neural cell adhesion molecule (NCAM) and the neurotrophin receptor p75 (Jessen and Mirsky, 2002). Nevertheless, non-myelinating Schwann cells can be distinguished by the expression of the markers GalC, sGalC and integrins $\alpha_1\beta_1$ and $\alpha_7\beta_1$ (Jessen et al., 1985; Previtali et al., 2003a; Previtali et al., 2003b; Stewart et al., 1997). These cell surface molecules, however, are also expressed by mature myelinating Schwann cells, indicating that further study is needed to identify molecular changes restricted to this transition. Differentiation markers such as P0 are also downregulated during this transition and become undetectable in intact adult nmSC, probably as a result of inhibitory axonal signalling (Lee et al., 1997).

As mentioned, evidence exists that NRG1 may also be required for the differentiation into non-myelinating Schwann cells. Remak bundles in NRG1 Type III deficient mice contained abnormal number of axons and were incompletely segregated by the cytoplasm of non-myelinating SCs (Taveggia et al., 2005). Moreover, genetic inactivation of this NRG isoform using Nav1.8-Cre mice also resulted in aberrant Remak bundles (Fricker et al., 2009). Additionally, deposition of basal lamina also appears to be required for the proper formation of non-myelinating SCs, as mice with targeted ablation of laminin at the immature stage failed to form non-myelinating cells (Yu et al., 2009). However, it is difficult to conclude if such effects are direct consequences of defective differentiation of nmSCs or if it is a consequence of abnormal radial sorting.

1.3.7 Differentiation into myelinating SCs

The transition to myelinating Schwann cells involves far more complex morphological and genetic changes. Most of the antigens associated with immature SCs, such as the neurotrophin receptor p75, are downregulated and there is strong upregulation of a

number of genes associated with the control of myelination and formation of the myelin sheath such as Oct-6, Krox-20, myelin protein zero (P0), myelin-associated glycoprotein (MAG), peripheral myelin protein 22 (PMP22), myelin basic protein (MBP) and periaxin (Jessen and Mirsky, 2002).

In this part of my thesis, I shall begin by reviewing the initial events of myelination, during which SCs engage in multiple interactions with axons and basal lamina and establish a highly polarized organization. Next, I will discuss the major signalling pathways that appear to be involved in the process and will finish with a brief summary of the transcriptional networks implicated in the control of SC differentiation state.

1.3.8 Signals mediating early events of myelination: Schwann cell-axon interaction

Myelination involves an intimate interaction between axons and Schwann cells that results in dynamic morphological changes and the subsequent unidirectional wrapping of multiple layers of membrane concentrically around axons (Figure 1-5). Ensheathment and wrapping are initiated at the site of the SC-axon interface and require specific molecular mediators for recognition, adhesion and induction of the process. These mediators include the adhesion molecule N-cadherin, which is found enriched at the pre-myelinating SC-axon interface. Depletion of N-cadherin (N-cad) from SCs in co-cultures systems results in defective process extension and alignment with axons, despite normal deposition of basal lamina (Wanner and Wood, 2002). However, transgenic mice with targeted ablation of N-cadherin in SCs only exhibit a minor delay in myelination and myelin sheaths formed without any detectable defects, suggesting that N-cad, although likely playing a role in establishing the timely initiation of myelination is a nonessential component for the formation and maturation of the myelin sheath (Lewallen et al., 2011). Other adhesion molecules, the nectin-like proteins (Necl), have been implicated as critical mediators of SC-axonal adhesion and myelination. Nectin-like protein 4 is expressed by SCs and binds to Necl1 present along the axons and disruption of this specific interaction inhibits the initiation of myelination (Maurel et al., 2007; Spiegel et al., 2007).

Following the initial contact with axons, Schwann cells require the establishment of a radial organization in order to initiate the subsequent events of myelination. The establishment of this polarized organization is achieved at least in part due to the asymmetrical distribution of the Partitioning defective-3 (Par-3) protein at the sites of contact between SCs and axons. Using Par-3 transgenic mice Chan and co-workers

showed that this asymmetrical distribution is critical for myelination to proceed, as disruption of Par-3 localization lead to a block in myelination, despite the initial SC-axon adhesion and alignment not being affected (Chan et al., 2006).

The neurotrophins, a family of growth factors that include nerve growth factor (NGF), brain-derived neurotrophic factor (BDNF), neurotrophin 3 (NT-3) and NT 4/5, represent, together with NRG1 Type III, major signals controlling myelination. Neurotrophins mediate their effect through two different classes of receptors, the low affinity receptor p75 that binds all known neurotrophins and the more selective Trk family of tyrosine kinase receptors. Neurotrophins play distinct effects on SC myelination. Notably, depletion of BDNF or functional inactivation of p75 inhibits myelin sheath formation (Chan et al., 2001; Cosgaya et al., 2002). Once activated by BDNF, p75 interacts with Par-3, which results in the relocalization of the receptor to the sites of SC-axon contact where it mediates its promyelinating effects (Chan et al., 2006). What lies downstream of this interaction and exactly how it mediates myelination remains elusive. In contrast, NT-3, via Trk receptors, acts as an inhibitory regulator of myelination (Chan et al., 2001).

1.3.9 Signals and pathways mediating myelination

Given what has been discussed up to this point, it is clear that the coordination of diverse signals is required for the proper initiation of myelination. Once SCs have established the right organization around the axon, multiple pathways are activated and culminate in the promotion of a transcriptional network that ultimately drives the formation of the myelin sheath. In Schwann cells, most signals that promote myelination act through the transcription factors, Oct-6, Krox-20 and Sox-10. As emphasized earlier, NRG1 Type III plays a dramatic effect in the control of many aspects of neural development, in particular, in SC myelination. The binding of NRG1 to ErbB receptors in SCs results in the activation of a variety of downstream intracellular signalling pathways such as phosphatidylinositol 3 kinase (PI3K)/Akt, Ras/ERK and Calcineurin-NFAT (Newbern and Birchmeier, 2010). Evidence exist that all of these signalling pathways are required for myelination. Disruption of the PI3K pathway results in inhibition of axonal-mediated SC proliferation and myelination (Maurel and Salzer, 2000; Ogata et al., 2004). Conversely, overexpression of PI3K or activated AKT promotes myelin protein expression (Ogata et al., 2004). Interestingly, the extent of PI3K activation is directly graded by the amount of NRG1 present at the axonal surface. This was elegantly demonstrated using *in vitro* cultures of SCs treated

with membrane fractions isolated from different neurons. Treatment of SCs with axonal membranes from NRG1 wild-type (wt) neurons produced robust AKT phosphorylation, whilst no activation was observed when membranes from NRG1$^{-/-}$ neurons were used instead. An intermediary grade of AKT activation was achieved when membranes from NRG1 heterozygous neurons were used (Taveggia et al., 2005). Together, these studies suggest that the amount of myelin produced is a direct measure of the extent of PI3K/AKT activation.

Until recently, the ERK pathway was thought to exert opposing functions on myelination, since strong and sustained activation of ERK inhibits myelin gene expression and myelination *in vitro* (Harrisingh et al., 2004; Ogata et al., 2004; Syed et al., 2010) and *in vivo* (Napoli et al, 2012). However, a more complex involvement of the ERK pathway in Schwann cell development has emerged by recent findings. Selective deletion of ERK kinases in the Schwann cell lineage at approximately E13 using a *Dhh*-Cre recombinase resulted in a marked downregulation of Krox-20 and severe hypomyelination, suggesting that signalling through ERK is required for Krox-20 induction and consequently, myelination (Newbern et al., 2011). Supporting this notion, conditional ablation of the nonreceptor tyrosine phosphatase Shp2 (that acts to promote sustained signalling through the ERK pathway) at the onset of myelination using the Krox-20 promoter also resulted in marked hypomyelination (Grossmann et al., 2009).

Another mechanism by which NRG1 signalling is likely to positively regulate myelination is by increasing the Ca^{2+} levels in SCs through induction of the phospholipase C-γ. This activates the phosphatase calcineurin, which dephosphorylates and subsequently activates the nuclear factor of activated T cells-3 (NFATc3) and c4 resulting in their translocation into the nucleus. Conditional deletion of calcineurin β1 in SCs results in defects in radial sorting and severely disrupted peripheral myelination (Kao et al., 2009).

It has long been known that cAMP elevation *in vitro* induces SCs to express myelin markers, suggesting that cAMP is part of the signalling system that promotes myelination. cAMP exerts at least part of its pro-differentiative effects through activation of protein kinase A (PKA) that in turn phosphorylates and activates nuclear factor kappa-B (NF-κB), required for myelination (see below) (Howe and McCarthy, 2000; Nickols et al., 2003; Yoon et al., 2008). Two recent papers from the Talbot laboratory have finally demonstrated that cAMP signalling is also required for myelination *in vivo* and provided important insights of how this might be happening.

Using zebrafish and rodent models, the authors found that activation of the G-protein coupled receptor Gpr126 by an as yet unknown axonal ligand results in increased levels of cAMP, which is critical for myelination. Accordingly, deletion of the receptor induced arrest at the promyelinating state, which could be rescued by treatment with the adenylate cyclase activator, forskolin (Monk et al., 2009; Monk et al., 2011). This mechanism was independent of NRG1, given that the levels of NRG and SC receptors ErbB2/3 remained normal. Nevertheless, both pathways are likely to crosstalk and in fact, cAMP appears to switch NRG1 from a proliferative signal to a differentiation one (Arthur-Farraj et al., 2011).

Additional evidence for the interaction between both pathways come from studies showing that NRG1 Type III and cAMP-dependent activation of PKA act cooperatively to increase the activity of NF-κB (Limpert and Carter, 2010). In Figure 1-4, a summary of the main signalling pathways involved in SC myelination is represented.

1.3.10 Transcriptional control of SC differentiation

Myelination signals and their downstream signalling pathways converge on a number of transcription factors that initiate a genetic program to drive the transition of immature promyelinating proliferative cells to myelinating ones. The myelination process involves a coordinated balance between two opposing transcriptional programmes: negative regulators that act as myelination breaks, and positive regulators that lie downstream of myelination signals such as NRG and cAMP. Coordination between both programs ensures the timely onset and termination of myelination during development. Negative regulators may include the c-Jun-amino (N)-terminal kinase (JNK) and Notch: both pathways are active in immature SC, where they seem to be required for NRG1-signalling, and are then inactivated by Krox-20 dependent signalling when SCs start myelinating (Jessen and Mirsky, 2008; Woodhoo et al., 2009). If this is prevented and the JNK or the Notch pathway remain active, myelination is blocked (Jessen and Mirsky, 2005; Woodhoo et al., 2009). Other candidate transcription factors that might be involved in the negative regulation of myelination include Sox-2 and Id2 and Id4 (Le et al., 2005; Svaren and Meijer, 2008).

The positive regulation of myelination, however, has been much more extensively studied. The backbone of the positive circuit driving the transition from promyelination to myelination comprises the transcription factors Oct-6 (also known as SCIP), Brn-2, Sox-10 and the zinc-finger transcription factor Krox-20 (Svaren and Meijer 2008). In addition, other transcription factors, such as YY1 (Yin yang-1), NFκB

(nuclear factor of κ-light polypeptide gene enhancer in B cells) and NFAT also appear to be crucial for myelination.

The POU homeo-domain transcription factors Oct-6/SCIP and its close relative Brn-2 are first seen expressed in Schwann cells following initial axonal contact and its expression peaks when the 1:1 relationship with axons has been established (Arroyo et al., 1998; Blanchard et al., 1996; Lemke et al., 1991; Scherer et al., 1994). Deletion of Oct-6 and Brn-2 in mice results in a delayed onset of myelination, with pro-myelinating Schwann cells persisting into adulthood (Bermingham et al., 1996; Jaegle et al., 2003), indicating that both factors are important for regulating the timing of transition to the myelinated state. Importantly, the subsequent downregulation of Oct-6 and Brn-2 (both proteins becoming undetectable by two postnatal weeks) is critical for the later events of myelination (Scherer et al., 1994). Indeed, the forced expression of Oct-6 beyond the early myelinating stages, results in hypomelination and axonal loss (Ryu et al., 2007). Oct-6 has been shown to repress myelin genes such as P0 and MBP, which may indicate that Oct-6 downregulation if required for the de-repression of myelin associated gene expression in differentiating Schwann cells (Monuki et al., 1993; Monuki et al., 1990).

In contrast to the dynamic and transient pattern of expression of Oct-6/Brn-2, the specification factor Sox-10 is expressed throughout the Schwann cell lineage (Britsch et al., 2001; Schreiner et al., 2007). As mentioned before, peripheral glia are absent in Sox-10 deficient mice (Britsch et al., 2001), indicating that this factor is absolutely required for specification. Furthermore, selective loss of Sox-10 in immature SCs prevents Oct-6 and Krox-20 expression and consequently lineage progression (Finzsch et al., 2010). Ablation of Sox-10 in adult Schwann cells is sufficient to induce demyelination and axonal degeneration, revealing that its expression in the adult is also required for maintenance of a myelinating phenotype (Bremer et al., 2011). Sox-10 interacts synergistically with Oct-6 to activate Krox-20 in myelinating SCs. In addition to activating Oct-6 and Krox-20 expression, combinatorial interactions between Krox-20 and Sox-10 have been implicated in the regulation of a number of Krox-20 target genes (Ghislain and Charnay, 2006; Jones et al., 2007; Schreiner et al., 2007).

As mentioned, a major transcriptional target of Oct-6/Sox-10 regulation is the immediate early gene Krox-20/Egr2 (Chavrier et al., 1990; Ghislain and Charnay, 2006; Ghislain et al., 2002). Basal levels of Krox-20 are first detected during embryonic development in the boundary cap and then later upon transition of SCPs to the immature Schwann cell state (Golding and Cohen, 1997; Murphy et al., 1996;

Niederlander and Lumsden, 1996; Schneider-Maunoury et al., 1993; Wilkinson et al., 1989). Following birth, Krox-20 expression is downregulated in non-myelinating cells, whilst being robustly upregulated in pro-myelinating Schwann cells (Blanchard et al., 1996; Zorick et al., 1996a).

The transcription factor Krox-20 controls major myelin genes such as *P0*, *MBP*, *PMP22*, *Connexin32* (Cx32) and *MAG* and is therefore referred to as the master regulator of PNS myelination. Consistent with this designation, deletion of Krox-20 results in a differentiation arrest with SCs stalling at the pro-myelinating state and a failure of myelin formation. Moreover, despite being able to establish a 1:1 relationship with axons, pro-myelinating Schwann cells continue to proliferate in the absence of Krox-20 (Topilko et al., 1994) indicating that Krox-20 expression is required to promote the onset of myelination coupled to cell cycle withdrawal. Furthermore, continuous expression of Krox-20 throughout adulthood is required for the maintenance of myelination, as its ablation in adult Schwann cells results in progressive demyelination in the PNS characterized by Schwann cell dedifferentiation and degeneration of myelin sheaths (Decker et al., 2006).

Other transcription factors have been shown to be involved in the positive regulation of myelination. In particular, NFATc4 (as said, activated downstream of NRG/Calcineurin) complexes with and enhances Sox10 activity at the P0 and Krox-20 promoters (Ghislain and Charnay, 2006; Nagarajan et al., 2001; Schreiner et al., 2007; Topilko et al., 1994). In addition, NF-κB binding appears to stimulate both Oct-6 and Sox-10 activity (Jacob et al., 2011; Yoon et al., 2008). A simplified view of the transcriptional machinery involved in SC differentiation is depicted in Figure 1-4.

A flurry of recent studies has directed attention to the involvement of epigenetics in the regulation of the transcriptional machinery that control SC differentiation. Histone deacetylases (HDACs) in particular have been implicated in SC myelination, as HDAC1/2 double null Schwann cells arrest at the immature or the pro-myelinating stages. HDACs were shown to interact with and activate Sox-10 and the master regulator Krox-20. An independent study showed that both HDACs also interact with and deacetylate NF-κB, inducing binding of this complex to the Sox10 promoter and thereby increasing its activity (Chen et al., 2011; Jacob et al., 2011).

Finally, another level of transcriptional control has recently been unravelled. Conditional ablation of Dicer, the ribonuclease responsible for the generation of mature micro-RNAs, induced marked downregulation of positive regulators of the myelination program, including Krox-20 and upregulation of myelination inhibitors such

as Sox-2 and Notch. Consequently, SCs arrested at the promyelinating stage and failed to form myelin. Schwann cell gene expression is therefore critically regulated by

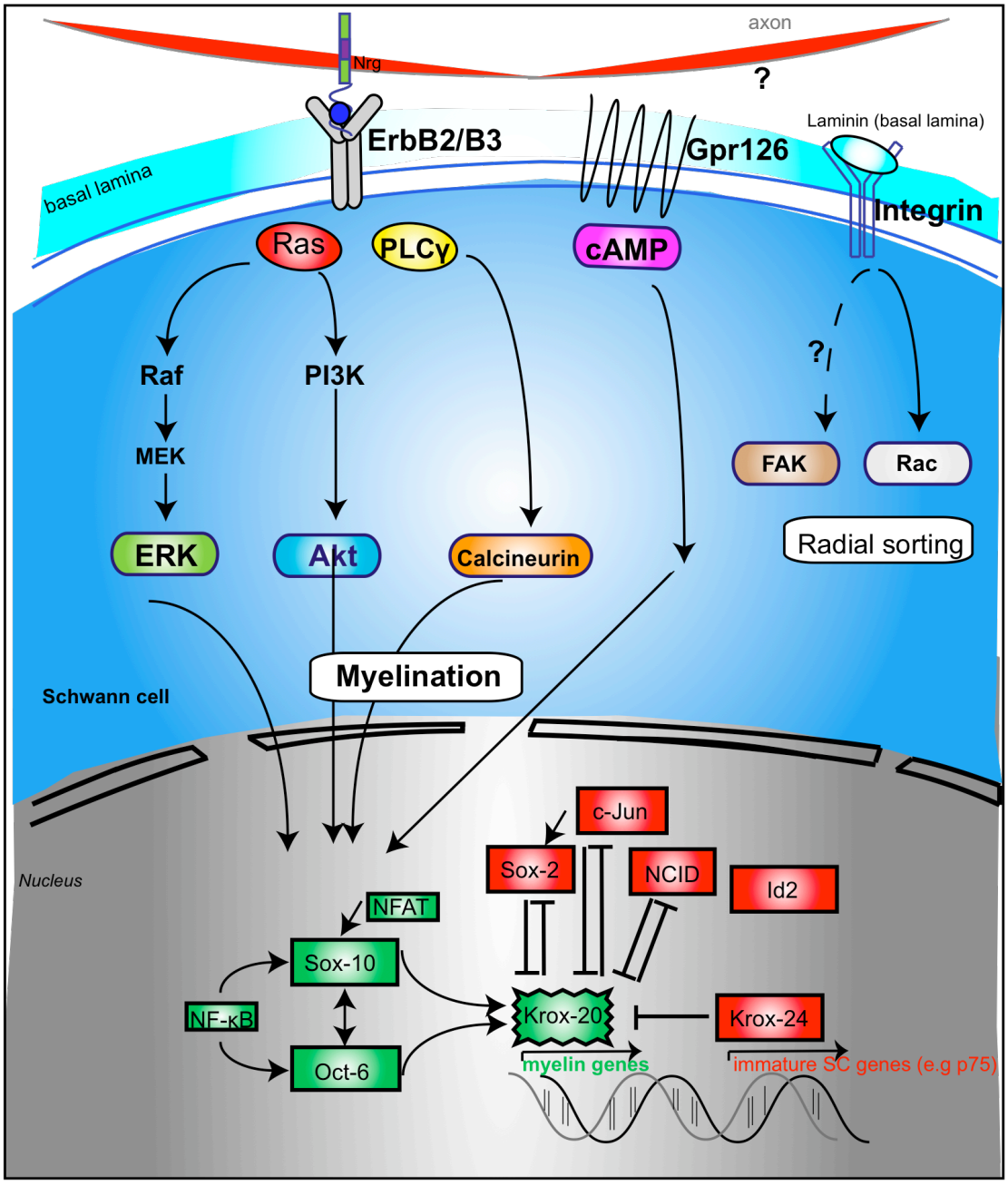

mature miRNAs (Pereira et al., 2010).

Figure 1-4: Major signalling pathways and transcriptional networks involved in SC differentiation. A) Signalling through ErbB, gpr126 and integrin receptors have been shown to activate various signalling pathways key to SC differentiation. **B**) Positive regulators are in green and negative regulators shown in red.

1.4 Myelin structure and function

Given the extraordinary relevance and complexity that the myelinated fibre represents I shall, in this part of the introduction, focus on the composition and organization of myelin mentioning, when appropriate, peripheral neuropathies associated with defective myelin production.

Myelination results in a dramatic increase in the velocity of impulse propagation and is critical for axon health and stability. The myelin sheath is a lipid-rich, specialised membrane that wraps around axons (typically larger than 1 μm in diameter) in a multilamellar spiralling manner (Figure 1-5A). The myelinating SC and its associated axons are organized into distinct molecular, structural and functional domains. These domains include the internodal region, juxtaparanode, paranodal junctions and Nodes of Ranvier (Nave, 2010; Poliak and Peles, 2003) (Figure 1-5B and C). The importance of myelin organization and integrity is emphasized in various demyelinating diseases where the disruption of these domains results in conduction block and axonal degeneration (Scherer and Wrabetz, 2008). Key to the function of myelinated fibres are the Nodes of Ranvier. They consist of discontinuous, small (1 micron wide) intermittent interruptions of exposed axons to which the voltage-gated sodium (Na^+) channels localize. It is this focal concentration of Na^+ channels, together with the increased resistance and reduced capacitance of the myelinate regions of the axons that allows for the rapid saltatory conduction of myelinated axons. The molecular composition of the node has been extensive characterized. Briefly, Nodes of Ranvier are highly enriched in neural adhesion molecules such as NrCAM and neurofascin, which bind glial matrix components like gliomedin (Eshed et al., 2005).

In the PNS, the nodes are filled with SC microvilli that emanate from the outer ends of the cell (Figure 1-5D). The microvilli, which express a specific matrix enriched in ezrin, radixin and moesin, play an important role in node formation and function. Flanking the nodes, Schwann cell membranes form loops that are connected to the axolemma by specialized axo-glial junctions (Figure 1-6A). These paranodal junctions, composed of a complex of axonal contactin and contactin-associated protein (Capsr) and glial neurofascin, promote tight attachment between axons and glia and are thought to provide a barrier to the lateral diffusion of proteins in order to maintain the composition of the nodes (Charles et al., 2002; Eshed et al., 2005; Poliak and Peles, 2003; Rios et al., 2000; Rios et al., 2003). The axon is further organized into the juxtaparanodes that are enriched in potassium channels, but which function remains

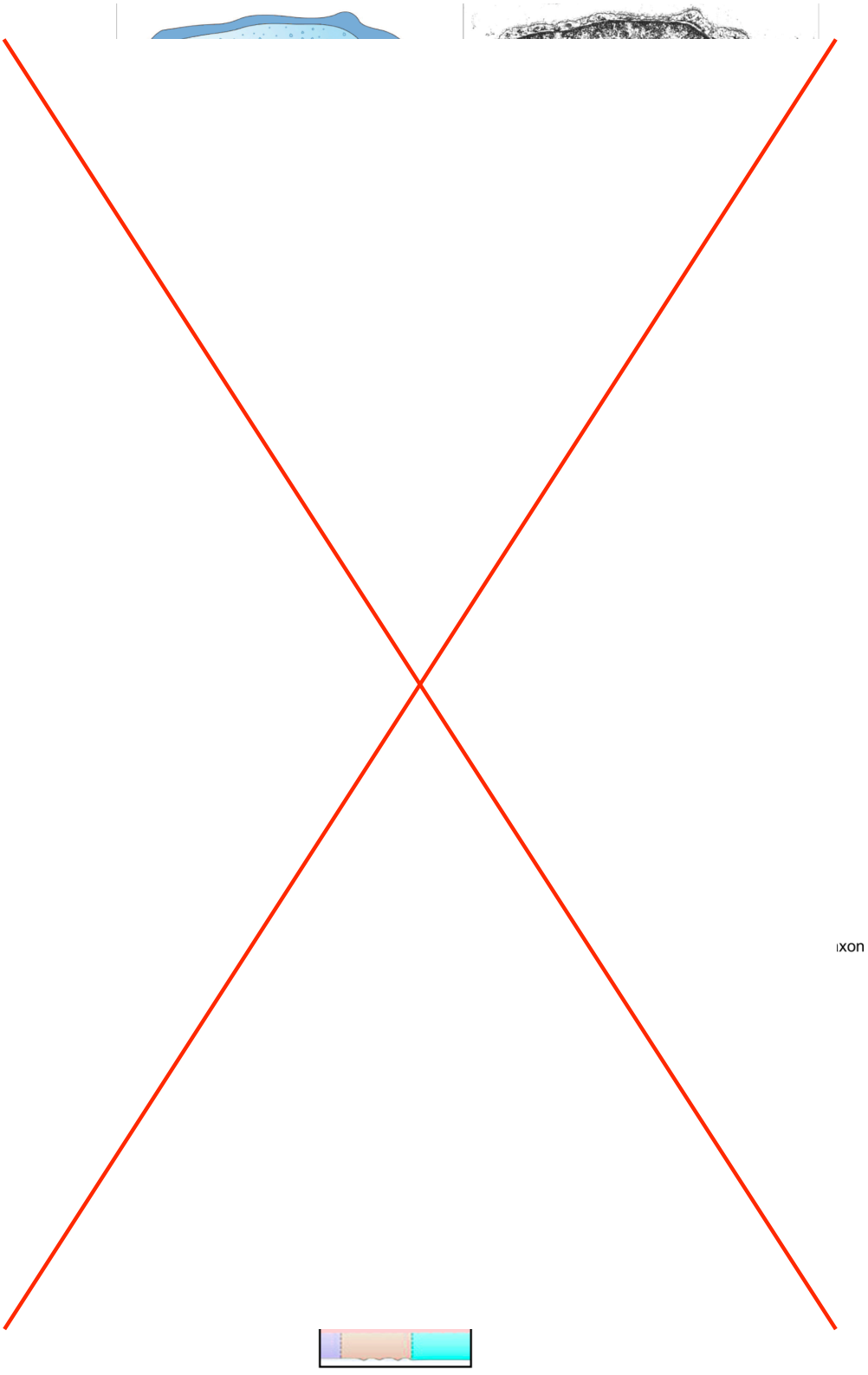

Figure 1-5: Diagrams of the structural regions of myelinated fibres. A) Schwann cells form myelin by enwrapping their membrane several times around the axon (Adapted from Lodish, 5th edition); **B**) Myelin covers the axons leaving regions of naked axons, the nodes of Ranvier; **C**) Schematic longitudinal view of a myelinated fibre showing the different domains; **D**) Detail showing the SC microvilli and basal lamina (Adapted from Poliak and Peles, 2005). (Figures removed due to copyright restrictions).

unknown (Salzer et al., 2008). The remaining domain in the myelinated fibre comprises the internode that can reach up to 1mm in length in the adult PNS (Abe et al., 2004) Along the internode the inner SC membrane (adaxonal), uniformly separated from the axon by a periaxonal space of 15nm, interacts with the axon through a set of adhesion molecules that include the nectin-like (Necl) cell adhesion molecules, a family of Ig-like CAM (also known as cell adhesion molecules Cadm) and the synaptic cell adhesion molecules (SynCAMs). A simplified view of a myelinated fibre is shown in Figures 1-5 and 1-6.

1.4.1 Myelin composition

The myelin membrane is organized into two structurally and biochemically distinct areas: compact, which is found at the internodes and results from the apposition of adjacent layers of SC membrane and exclusion of the cytoplasm, and regions of non-non-compact myelin. Compact myelin in the PNS is largely composed of lipids, mainly cholesterol and sphingolipids, including galactocerebroside (GalC) and sulfatide (Snipes and Suter, 1995). The main myelin proteins are protein zero (P0), peripheral myelin protein 22 kDa (PMP22), myelin basic protein (MBP) and proteolipid protein (PLP) (Figure 1-6B).

As mentioned before, P0 is first expressed at low levels in SCPs, becoming strongly upregulated at the onset of myelination in mSCs (Baron et al., 1994). In the myelin sheath, P0 accounts for more than half of the PNS myelin protein and plays a key role in mediating the stabilization and compaction of consecutive layers of myelin (Kirschner and Ganser, 1980). P0 is a 28kDa glycoprotein containing an extracellular Ig-like domain, a hydrophobic transmembrane region, and a small, basic intracellular domain (Lemke et al., 1988). The extracellular domain mediates homotypic interactions across the extracellular space, in that way keeping together opposing myelin membranes (Filbin et al., 1990; Shapiro et al., 1996) (Figure 1-6B). The intracellular domain forms heterotypic interaction with lipids and promotes the close apposition of intracellular membranes. In humans, mutations in the P0 gene are associated with demyelinating diseases such as Charcot-Marie Tooth 1B (CMT1B), Dejerine-Sottas syndrome (DSS) and congenital hypomyelination (CH) (Hayasaka et al., 1993a; Hayasaka et al., 1993b; Warner et al., 1996). The phenotypes of these diseases resemble those that develop in transgenic mice expressing targeted mutations in P0. In *P0*-null mice Schwann cells form a multilamellar spiral of membrane around axons, but the myelin does not compact (Giese et al., 1992).

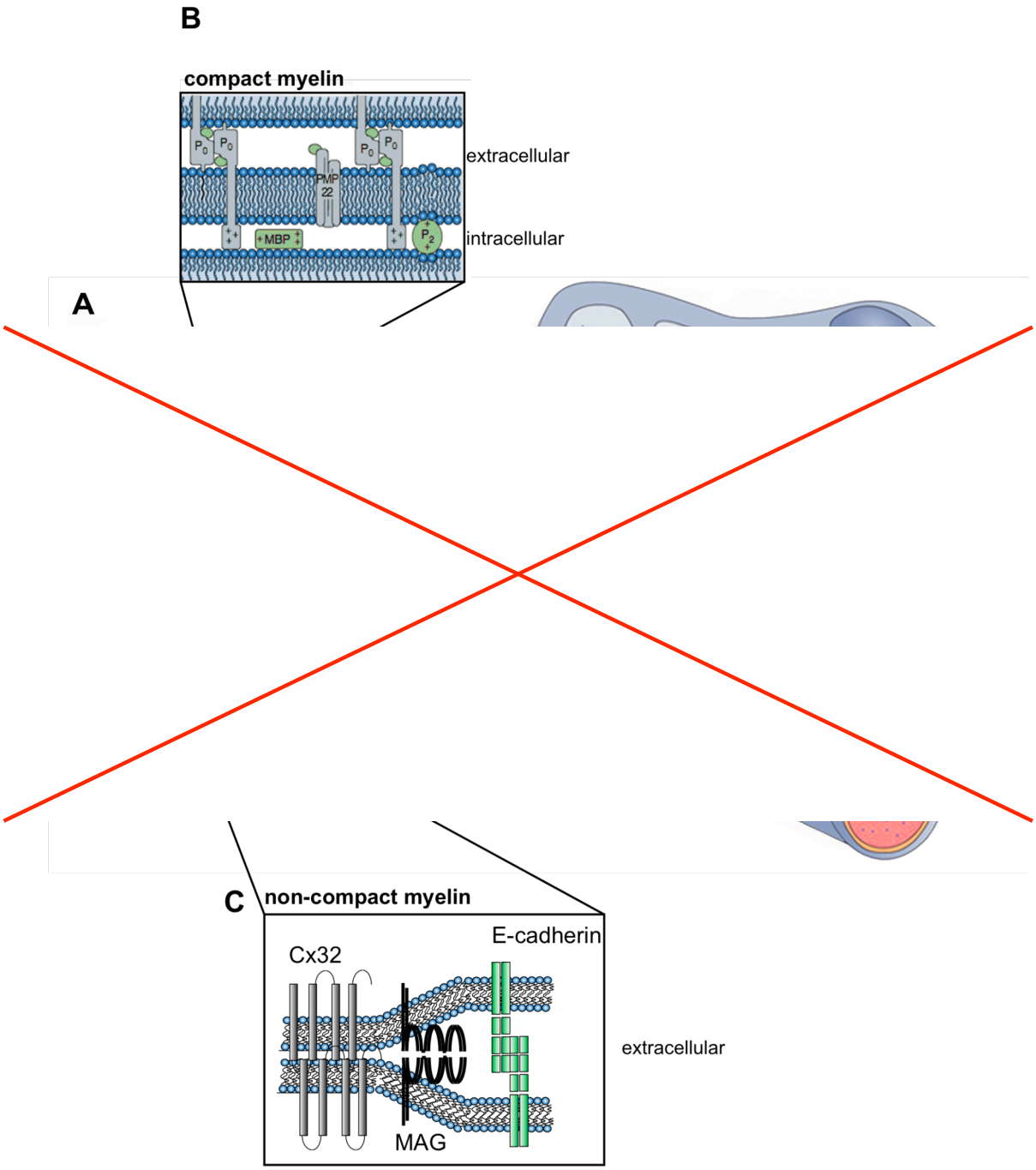

Figure 1-6: Myelinated axons and areas of compact and non-compact myelin. **A**) Schematic representation of a myelinated axon; Compact myelin is shown in pale blue; Non-compacted myelin is shown in dark blue. The Schmidt-Lanterman incisures (SLIs) correspond to areas of non-compacted myelin that spiral around the axon (adapted from Nave, 2010); **B**) major components of compact myelin; **C**) major components of non-compact myelin. (Figures removed to copyright restrictions).

P0 heterozygous mice also develop a late-onset demyelinating neuropathy, indicating that even a modest reduction in the amount of P0 causes instability of compact myelin (Martini et al., 1995; Shy et al., 1997; Zielasek et al., 1996). Thus, a single allele of P0 is sufficient for the normal compaction of the myelin, but both are required for its long-term maintenance. Other protein elements of the myelin sheath have also been implicated in human disease. PMP22, for example, is a hydrophobic membrane protein (Figure 1-6B) whose levels appear to be crucial for the maintenance of the myelin sheath (although its function remains unknown). Accordingly, three copies of the PMP22 gene lead to CMT1A disease, probably owing to a modest increase of PMP22 protein in the compact myelin (Hanemann and Muller, 1998; Vallat et al., 1996).

The role of lipids in myelin composition has been much harder to study. Nevertheless, targeted disruption of the UDP-galactose-ceramide galactosyltransferase gene (*cgt*) provided an unprecedented opportunity to perturb the lipid components of myelin (Bosio et al., 1998; Dupree et al., 1998). CGT is necessary for the synthesis of galactocerebroside and sulfatide, therefore, these glycolipids are completely absent in $cgt^{-/-}$ mice. $Cgt^{-/-}$ mice develop neurological signs with the onset of myelination, and most die between 18 and 30 days. Surprisingly, despite the normal ultrastructure appearance of most PNS myelin sheaths, axonal conduction velocity is dramatically slowed, which may be related to abnormal paranodes (Bosio et al., 1998; Dupree et al., 1998). Collectively, these observations highlight the importance of the stoichiometric organization of the myelin sheath, as perturbations in any one component can alter the entire structure.

In myelinating SCs, regions of non-compact myelin are found at the paranodal loops, the Schmidt-Lanterman incisures (SLI), nodal microvilli and the inner and outer edges of the myelin sheath (Figure 1-5 and 1-6). Non-compact myelin contains a significant amount of cytoplasm and its components include periaxin, myelin-associated glycoprotein MAG, E-cadherin and the integrins $\alpha6\beta1$ and $\alpha6\beta4$ which interact with the basal lamina and connexin 32 (Figure 1-6C). The specialized Schmidt-Lanterman incisures are inclusions of cytoplasm present in each layer of myelin connecting the Schwann cell nucleus to the consecutive layers of myelin membranes (Figure 1-6A) (Salzer, 2003; Scherer, 1999).

1.5 Schwann cell basal lamina

SCs typically form a basal lamina around their abaxonal cytoplasmic membrane that separates the cell from the mesenchymal endoneurial space of the peripheral nerve. In

longitudinal sections, SC basal lamina forms a continuous tube that even bridges the nodal gaps. The SC basal lamina is a complex and organized network of secreted proteins rich in extracellular matrix (ECM) components such as laminin heterodimers (composed of α2/merosin, β1, and γ1 laminin chains), collagens I and IV, fibronectin, entactin/nidogen and proteoglycans (perlecan, N-syndecan and bamacan) (Bunge, 1993; Chernousov and Carey, 2000; Court et al., 2006). The ECM proteins provide the substrate on which SCs reside. In this way, they play not only a supportive role, providing strength and structure to Schwann cells, but may also regulate key aspects of SCs behaviour through sequestration and local release of growth factors. Indeed, as discussed before, interactions between laminin in the basal lamina and integrin receptors at SC membranes trigger many different intracellular signals required to control SC proliferation and differentiation (reviewed in (Yu et al., 2007)). In addition, some ECM components of the basal lamina may play an important role in the process of nerve regeneration by providing a guidance structure that promotes axonal regrowth (Stoll and Muller, 1999; Zhang et al., 1995). In the next sections of this thesis, I shall briefly describe the anatomy of the peripheral nerves, and then proceed to discuss, in more detail, the events that follow injury to the PNS and how SCs and their associated basal lamina are critical mediators of nerve regeneration.

1.6 The anatomy of peripheral nerves

To understand the biology of Schwann cells in the context of nerve regeneration and tumourigenesis it is relevant to first consider some basic concepts of the anatomy of peripheral nerves. From the central nervous system (CNS) emerge multiple branches of two different categories of peripheral nerves- cranial and spinal, whose terminals reach all body districts. Although nerve trunks located in distinct parts of the organism may differ with respect to the fibre-type composition and number of fascicles, the morphology of these nerves trunks is remarkably similar (with the olfactory and optic nerves being exceptions) (Sunderland, 1990; Sunderland and Bradley, 1949). In this thesis, most of the experiments were performed on one of the largest spinal nerves present in both human and rodent organisms, the sciatic nerve. The sciatic nerve, as all the spinal nerves, contains mixed axons, i.e., sensory and motor, and is therefore composed of a mixture of myelinated and unmyelinated nerve fibres (Williams, 1999). A schematic representation of a peripheral nerve is shown is Figure 1-7.

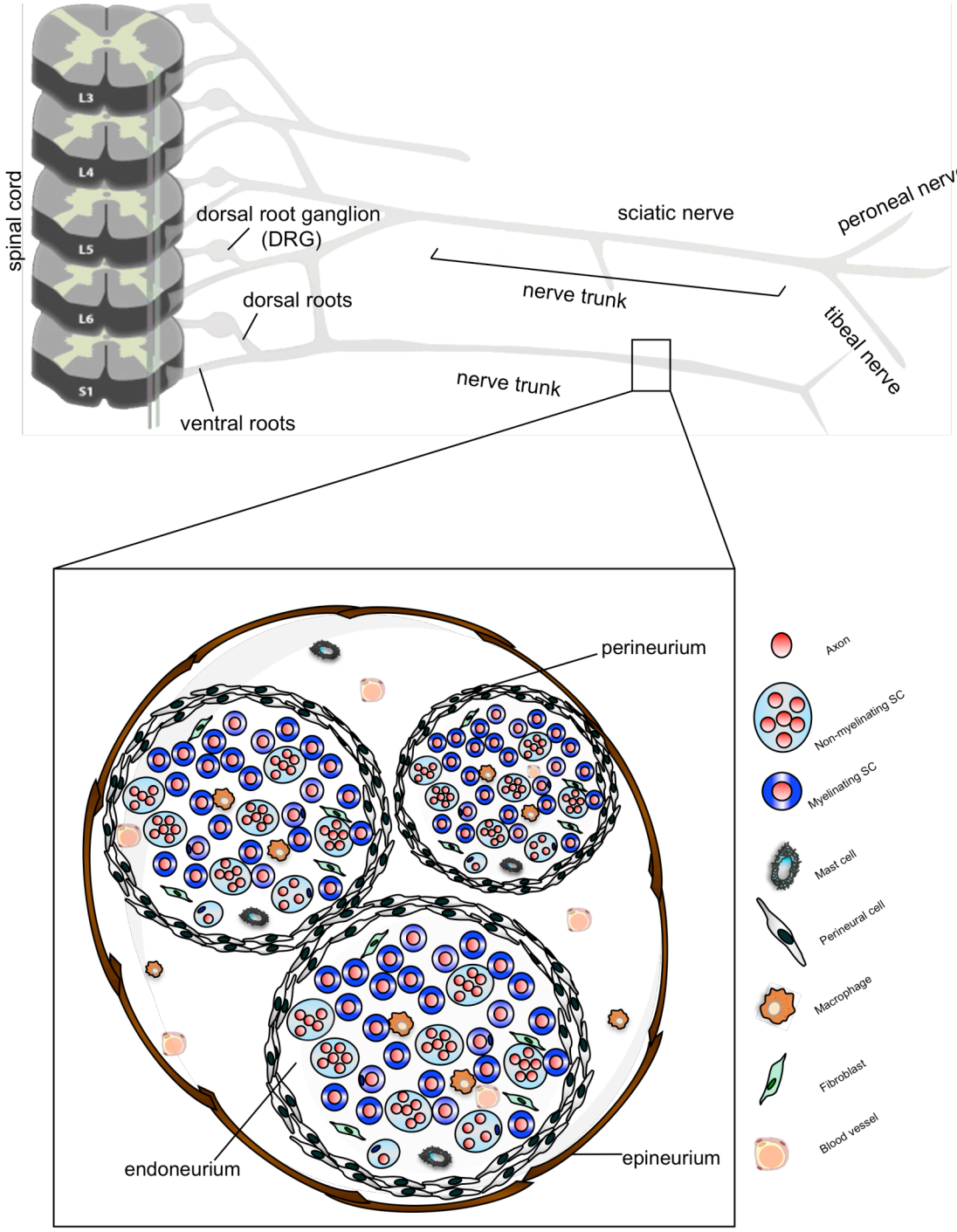

Figure 1-7: Schematic representation of peripheral nerves. The sciatic nerve and other spinal nerves are represented. Schwann cells in the nerve trunks (nerves that innervate the limbs) are derived from SCPs; Schwann cells in the nerve roots (ventral and dorsal) and satellite cells in the DRG, originate from distinct progenitors, the boundary cap cells. A cross-section of a nerve trunk composed by 3 fascicles is also shown, together with the major contributing cell types.

Classically, two types of layers can be distinguished in the nerve trunks: the epineurium, which is an outer layer that encloses the entire nerve whether this is uni- or multifascicular and the more internal, multilayered perineurium that surrounds individual fascicles (Figure 1-7). The epineurium is composed of a supporting and protective connective tissue, which includes a collagen tissue sheath and a plexus of blood vessels that pass across the perineurium to communicate with the network of arterioles and venules within the endoneurium. In addition, it may also contain fibroblasts, some resident macrophages and mast cells and variable amounts of adipose tissue (Geuna et al., 2009).

Within the epineurium, fascicles of nerve fibres are individually ensheathed by the perineurium, a dense and mechanically strong, yet flexible cellular sheath that consists of alternating layers of collagen and uninterrupted, concentric rings of flattened, specialized, fibroblast-like cells that are connected by tight junctions (Akert et al., 1976; Key and Retzius 1876). Such cells, termed perineurial cells, contain a patchy basal lamina and numerous pinocytic vesicles and often, bundles of microfilaments.

The perineurial sheath serves as a metabolically active barrier, protecting axons from ionic flux, toxins and infection (Kristensson and Olsson, 1971; Olsson, 1990). Despite the essential function that the perineurial cells play in the peripheral nerve function, their origin is not fully clarified. Previous studies have suggested that during development the perineurium appears to form by a series of steps in which nearby mesenchymal or fibroblasts cells first assemble as a loosely organized tube around the nerve and then mature to create a multilayered barrier (Du Plessis et al., 1996; Thomas and Jones, 1967). In support of this idea, fibroblasts cultured in the presence of neurons and Schwann cells form "perineurial-like" structures (Bunge et al., 1989). However other characteristics, such as association of perineurial cells with basal lamina, are quite different from fibroblasts. Studies in zebrafish have suggested that in these animals, the perineurium develops from glial cells that originate in the CNS (Kucenas et al., 2008). Whether there is similar origin in mammals remains to be demonstrated. Regardless of their origin, it is known that the final maturation step requires the signalling molecule desert hedgehog (DHH), which is expressed by Schwann cells. In the absence of DHH, the perineurium is disorganized and is permeable to macromolecules and inflammatory cells (Parmantier et al., 1999).

The compartment within the perineurium, the endoneurium, represents a loose, soft, connective tissue that embeds and protects the fascicles during movement and external trauma (Lundborg 2005). It contains the SC-axon units (often referred as the

nerve fibres) embedded in a collagenous matrix that also supports a capillary network, a population of resident macrophages and a variable, but generally reduced, number of fibroblasts (Thomas, 1993). Schwann cells represent the majority of the cell population within the endoneurium, followed by endothelial cells and resident macrophages (2-9%), while fibroblasts represent less than 4% of the total (Causey and Barton, 1959; Mueller et al., 2003).

1.7 Wallerian degeneration and PNS repair

In contrast to the CNS, peripheral nerves have a remarkable ability to regenerate following an injury. Underlying the success of this process is the plasticity of Schwann cells that respond to the injury by reverting from a seemingly stable, specialised cell state to a proliferating precursor-like cell (Parrinello et al., 2010; Scherer and Salzer, 2001; Zochodne, 2008).

Traumatic injury to the PNS produces abrupt tissue damage at the lesion site where the physical impact occurred. Additionally, the nerve stump distal to the wound site and a small reactive zone at the end of the proximal stump, despite not having encountered the physical trauma directly, also undergo a series of well-characterized molecular and cellular events collectively known as Wallerian Degeneration (WD). During Wallerian degeneration, axons downstream of the injury site, degenerate leaving behind SCs that dedifferentiate and divide inside the basal lamina tubes that surrounded the original nerve fibres, organizing themselves into columns termed Bands of Bungner (Figure 1-8). Meanwhile, SCs together with resident and infiltrating macrophages clear the axonal and myelin debris, thereby generating a conducive environment for newly formed axons, that can then associate with the SC columns and re-grow distally until reaching their targets. Following axonal regeneration, Schwann cells then re-differentiate to give rise to a fully repaired and functional nerve (Fernandez-Valle et al., 1995; Shamash et al., 2002; Stoll et al., 1989; Zhang et al., 2000). The same process is triggered in both crushed and transected nerves, although the success of repair may vary depending on the type of injury. Most strikingly, the maintenance of an intact basal lamina that occurs during a crush, but not in a transection, is thought to improve the success of regeneration by preserving the integrity of the original axonal paths and allowing accurate reinnervation (Nguyen et al., 2002). More severe injuries, such as nerve transections, involve more complex tissue remodelling. Upon cut, the nerve stumps on either side of the cut retract, generating a gap, which must be bridged by new tissue; moreover, the regrowing

axons from the proximal stump must travel through this newly formed tissue - the nerve bridge - to reach the distal stump and their targets (McDonald et al., 2006) (Figure 1-8).

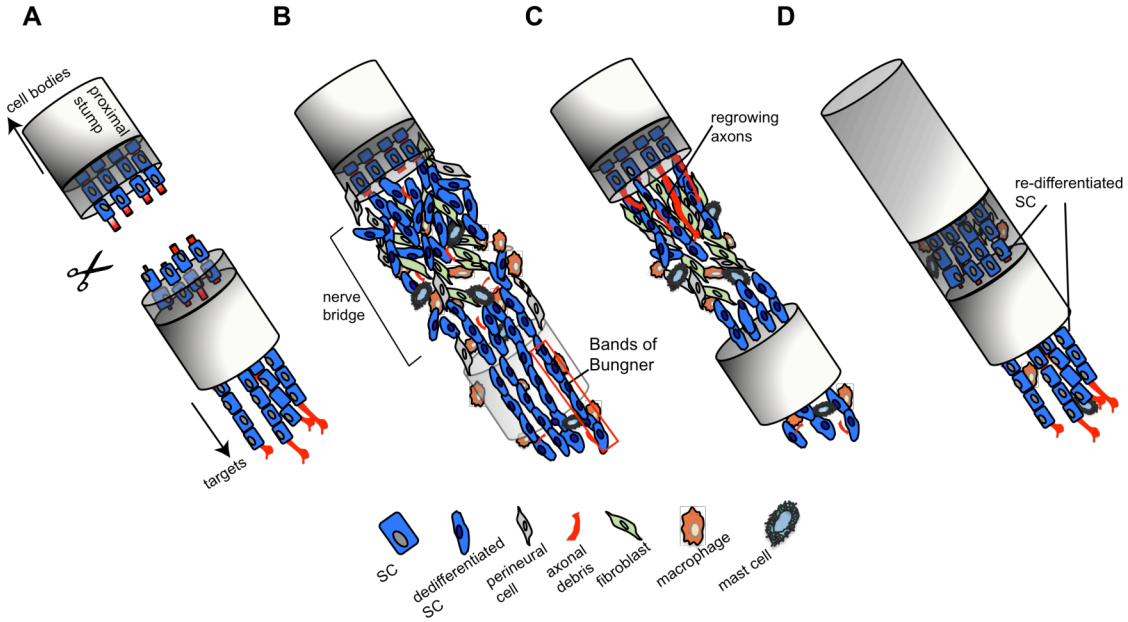

Figure 1-8: Wallerian Degeneration in the PNS. Schematic representation of the events that follow an injury: **A**) nerve transection leaves a gap separating both stumps of the nerve; **B**) axonal degeneration, SC dedifferentiation and infiltration of inflammatory cells; **C**) regenerating nerve with axons sprouting from the proximal stump and growing towards target tissue along the SC cords (in the nerve bridge) and the bands of Bungner (in the distal stump); **D**) a repaired and functional nerve.

1.7.1 Axonal degeneration

Within 24-48 hours of physical injury, the axolemma and cytoskeleton of the axons downstream of the lesion begin to degenerate. Evidence that axonal degeneration results from an active process rather than from mere axonal starvation secondary to the lack of cell body derived signals came from the discovery of the naturally occurring Wallerian Degeneration Slow (*Wld*^{s}) mutant mice whose axons survive for as long as a month after transection (Brown et al., 1994; Lunn et al., 1989; Tsao et al., 1994). It is now thought that axonal degeneration is a caspase-independent process, mediated by the rapid activation of calcium-dependent axonal proteases, such as calpain (Glass et al., 2002). Moreover, the ubiquitin-proteasome system (UPS) is also involved, since blockage of proteasome activity has been shown to delay axon degeneration from injury both *in vivo* (Ehlers, 2004; Hoopfer et al., 2006; MacInnis and Campenot, 2005; Zhai et al., 2003) and *in vitro* (Gerdts et al., 2011). The genetic mutation underlying the

Wld^{s} mice was found to result in the formation of an abnormal fusion protein consisting of the N-terminal 70 amino acids (N70) of the multi-ubiquitination factor Ube4b (the 70 amino acid portion, however, was found not to influence ubiquitination) and the full-length NAD^{+} synthesizing enzyme nicotinamide mononucleotide adenylyl transferase 1 (Nmnat1), separated by a short linker sequence (Mack et al., 2001). A recent study has shown that expression of both Nmnat-1 and the first 16 base pairs of N70 is required to protect axons from degeneration (Conforti et al., 2009). Exactly how they act to protect axonal integrity, however, remains to be elucidated. One plausible explanation suggests that as Nmnat1 shares with Nmnat2 (a known axonal survival signal), the same enzymatic domain for NAD+ synthesis (Jia et al., 2007; Yan et al., 2010), the WldS protein may exert its protective effect by augmenting or substituting for Nmnat2 to maintain sufficient levels of Nmnat enzyme activity in the distal axons after injury (Gilley and Coleman, 2010; Wang et al., 2012).

1.7.2 Schwann cell response: dedifferentiation and demyelination

As a prompt response to degenerating axons, SCs in the distal stump rapidly convert from a mitotically quiescent differentiated phenotype, to a dedifferentiated, proliferative, progenitor-like state. This transition involves the coordinated downregulation of myelin-associated genes, such as P0, MBP and periaxin and the upregulation of genes associated with the embryonic development such as the neurotrophin receptor p75, cell adhesion molecules, and many basement membrane components, including, NCAM, GFAP and L1 (Hall et al., 1997; Taniuchi et al., 1986; Trapp et al., 1988). In *Wld*^{s} mutants, the dedifferentiation of SCs is also delayed until the onset of axonal degeneration, implicating the requirement of axonal derived instructions in the process (Lunn et al., 1989). The exact injury signals remain unknown, although there is some evidence that NRG1 may act as one of these early signals between damaged axons and SCs, promoting myelin breakdown. Within minutes of axonal transection, ErbB2 phosphorylation is observed at the paranodes of myelinating SCs. Moreover, rats treated with the pharmacological inhibitor PKI-166, which blocks the ErbB2 receptor, exhibit retarded demyelination following nerve injury, despite undergoing axonal degeneration (Guertin et al., 2005). However, the role of NRG1 has not yet been conclusively demonstrated, as the inhibitor used also acts on the epidermal growth factor receptor (EGFR) (which is expressed by SCs upon injury (Guertin et al., 2005)), and so a number of ligands (including NRG1) may be implicated. In support of the involvement of the NRG/ErbB pathway in driving SC

dedifferentiation, addition of high levels of NRG1 Type II to SC-axonal co-cultures results in SC demyelination and proliferation (Guertin et al., 2005; Harrisingh et al., 2004; Zanazzi et al., 2001). Moreover, transgenic mice that overexpress NRG1 Type II in myelinating SCs (onset of expression at postnatal day 5) develop hyperplasia and demyelination (Huijbregts et al., 2003). Further investigation is needed however to obtain experimental evidence supporting a role for NRG1 Type II in Wallerian Degeneration. Importantly, at least *in vitro*, the effect of NRG1 Type II is blocked by treatment with MEK inhibitor (but not by a PI3K inhibitor), implicating this branch of Ras signalling as the intracellular pathway transducing the dedifferentiation signal (Harrisingh et al., 2004).

1.7.3 Schwann cell plasticity is regulated by the Ras/RAF/ERK pathway

Work from our laboratory has provided a major contribution towards the establishment of Ras/Raf/ERK as the central pathway driving quiescent, differentiated SCs to revert to a proliferative, "progenitor-like" state. Using myelinated SC-axonal co-cultures we have shown that sustained activation of Raf/ERK signalling is sufficient to trigger SC dedifferentiation. To address whether activation of this pathway also regulates SC plasticity *in vivo* we have recently generated a transgenic mouse model expressing a Tamoxifen (Tmx)-inducible Raf-kinase/estrogen receptor fusion protein (RafTR) specifically in myelinating Schwann cells (Napoli et al., 2012). We found that strong and sustained activation of Raf/ERK signalling in the adult PNS is, indeed, sufficient to induce SCs to revert to a "progenitor-like" state, even in the presence of intact axons. Moreover, we found that SCs persist in the dedifferentiated state for as long as Raf/ERK remains activated. Importantly, this state is reversible as dedifferentiated SCs readily redifferentiated and remyelinated axons as soon as the RafTR kinase was inactivated by Tmx withdrawal.

Consistent with Raf/ERK being the pathway controlling the Schwann cell plasticity following nerve injury, we and others have shown that as rapidly as within 20 min post-lesion there is a strong and robust activation of ERK signalling both at the lesion site and throughout the entire distal stump of the injured nerve. What is more, ERK is activated specifically in Schwann cells and the signal is sustained for several days (Harrisingh et al., 2004; Sheu et al., 2000). Strikingly, injured mice treated with the MEK inhibitor PD0325901 exhibit a dramatic inhibition in the switch in Schwann cell differentiation state (Napoli et al., 2012).

As mentioned, the upstream dedifferentiation signal(s) that acts to induce the strong and sustained activation of Ras/ERK signalling has yet to be identified. *In vitro*, NRG1 stimulation results in a strong, but transient, activation of the Ras/Raf/ERK pathway in SCs (Echave et al., 2009). Thus, it seems clear that even if NRG1 acts as an early damage signal, other signals must account for the sustained ERK activation that follows injury.

Upon nerve damage, the blood-nerve-barrier (BNB) breaks-down and leaks components from the vasculature, hence altering the ECM composition. One of these components is fibrinogen that following leakage is converted into fibrin, which can be deposited in the matrix (Akassoglou et al., 2000). In a study by Akassoglou and co-workers, fibrin was found to induce strong phosphorylation of ERK in cultured Schwann cells, which correlated with upregulation of the dedifferentiated SC marker p75 (Akassoglou et al., 2002). Furthermore, the authors demonstrated that the timing of remyelination/regeneration correlates with fibrin clearance, suggesting that its presence may prolong the period of ERK activation and therefore be inhibitory for SC redifferentiation (Akassoglou et al., 2002). Exactly how Raf/ERK acts on the transcriptional machinery to drive dedifferentiation remains under investigation. Studies from our lab, however, have shown that ERK activation appears to act by coordinating the blockage of Krox-20 dependent activity via repression of myelin gene promoters and by inducing the activity of negative regulators of myelination, such as c-jun and Sox-2 (Rosenberg et al., in preparation).

It is thus striking that Ras/Raf/ERK induces opposing biological outcomes promoting differentiation during development and dedifferentiation following injury. The explanation for such context-specific effects may reside in differential levels of activity and implies that strict regulatory mechanisms must be in action both in embryogenesis and later following an injury to ensure the adequate outcome. Interestingly, the same seems to hold true for neuregulin signalling since, in a recent study, a soluble form of NRG1 type III was shown to, depending on the concentration present, play a dual effect, either promoting or inhibiting myelination (Syed et al., 2010).

1.7.4 The role of Schwann cells in WD: myelin and axonal clearance and recruitment of the inflammatory response

The process of SC dedifferentiation becomes most evident 2 days after injury, when myelin sheaths start to disintegrate as a result of Krox-20 and myelin genes downregulation. SCs become separated from degenerating myelin and phagocytose

myelin debris (myelin ovoids) in a process that is dependent of binding of the galactose-specific lectin MAC-2 (expressed by SCs) and sGalcC and GalC in myelin debris (Reichert et al., 1994). Besides contributing to myelin clearance, dedifferentiated SCs play an important role in the orchestration of an inflammatory response (Napoli et al., 2012). Importantly, recent work from our laboratory has shown that activation of the Raf/ERK pathway in SCs in sufficient to recapitulate these effects. Strikingly, we have shown that dedifferentiated Schwann cells, by means of as yet unknown Raf-activated signals, induce the BNB breakdown independently of trauma. Furthermore, they actively secrete cytokines such as MCP-1 (monocyte chemoattractant protein-1) and c-Kit ligand, implicated in attracting inflammatory cells (Napoli et al., 2012). Together, these findings have highlighted Schwann cells and Ras/Raf/ERK signalling as central mediators of nerve regeneration.

1.7.5 The inflammatory response

Wallerian degeneration is strictly dependent on the activation of an inflammatory response. Shortly following an injury, the endoneurial levels of early inflammatory cytokines such as MCP-1, tumour necrosis factor alpha (TNF-α) and interleukin 1α (IL-1α) mostly secreted, as mentioned, by ERK-activated-SCs start to increase both at the lesion site and distal stump of the damaged nerve. Within days, this network is amplified by cytokines, chemokines and other bioactive molecules released by recruited inflammatory cells and activated endothelial cells (Be'eri et al., 1998; Shamash et al., 2002; Stoll et al., 2002). Different types of inflammatory cells are seen at the injury site:

Neutrophils

The phagocytic neutrophils (polymorphonuclear granulocytes) are the first inflammatory leucocytes to invade the injured tissue, to phagocytose debris and recruit other leucocytes during WD (Nathan, 2006). However, their response is very limited in time and extent, peaking at 24 hours within an injury and only a few cells infiltrating the more distal areas of the distal stump (Perkins and Tracey, 2000). They quickly undergo apoptosis after a brief period of phagocytosis, and are normally absent one week post-injury (Hall, 2005; Kennedy and DeLeo, 2009; Perry et al., 1987).

Macrophages

Macrophages are important effector cells in immune-mediated debris clearance. Resident macrophages, which express major MHC molecules and complement receptor 3, have a prompt response to injury. They are later joined by chemokine c-c

motif receptor 2 (CCR2) positive, bone-marrow derived macrophages (Bruck, 1997; Bruck and Friede, 1991; Mueller et al., 2003). The recruitment of macrophages to the distal nerve begins 3-4 days following trauma by diapedesis across a temporarily leaky BNB and peaks at about 7 days. Monocytes, which differentiate into macrophages in the tissue, are attracted by locally produced cytokines and chemokines including MCP1, macrophage inflammatory protein1 (MIP-1) TNFα and LIF, expressed by dedifferentiating SCs and resident macrophages (Ousman and David, 2001; Toews et al., 1998). Macrophages invade the tubes of SCs by passing through the basal lamina and degrade and phagocytose the myelin debris (Hall, 2005). At least two mechanisms are involved in myelin recognition and uptake. Macrophages express complement component receptor 3 (CR3) and the corresponding complement component 3 (C3) is expressed at the surface of degenerating myelin, indicating that myelin is opsonized by the complement during WD (Bruck and Friede, 1990). In addition, the galactose specific lectin MAC-2 is also induced in phagocytosing macrophages, at least partially by fibroblast-secreted granulocyte macrophage colony stimulating factor (GM-CSF) and contributes to myelin clearance (Stoll and Muller, 1999). Removal of degenerated myelin is critical for successful repair since some of the myelin components such as MAG, are highly inhibitory to axonal regeneration (McKerracher et al., 1994; Mukhopadhyay et al., 1994; Schafer et al., 1996). Myelin clearance begins 3-4 days after the injury and is completed approximately 2 weeks following injury. Besides their role in myelin clearance, macrophages also produce cytokines that activate SCs, including IL-1 (La Fleur et al., 1996), and trophic factors, like NGF that promote axonal regeneration (Hikawa and Takenaka, 1996; Perry et al., 1987). Although many macrophages remain free in the endoneurium for several weeks, the majority eventually disappears either by apoptosis or migration to lymph nodes and spleen (Kuhlmann et al., 2001).

Mast cells

There is a sustained increase in the number of mast cells within the epineurium and endoneurium distal to a traumatic injury. Mast cell-derived vasoactive agents, together with metalloproteinases secreted by endothelial cells and TNFα and ILβ secreted by macrophages increase the permeability of the BNB (Hall. 2005). However, little is known about their contribution to WD and nerve repair.

T-cells

T-cells are the last immune cell to arrive at the lesion site, peaking at 14-28 days following injury (Moalem et al., 2004). T-cells produce pro- or anti-inflammatory

cytokines that support cellular and humoral immunity. Type 1 helper (Th1) T cells secrete pro-inflammatory cytokines (e.g. TNFα, INFγ) that activate nearby macrophages, neutrophils and NK cells. Anti-inflammatory cytokines (IL4, IL10) produced by Th2 T cells inhibit macrophage functions and pro-inflammatory cascades.

1.7.6 Schwann cell proliferation

As Schwann cell dedifferentiation proceeds, SCs re-enter the cell-cycle. Accordingly, 3 to 4 days following nerve injury, SCs are found proliferating at the lesion site and throughout the entire distal stump (Liu et al., 1995). Given the absolute requirement for NRG1 for SC proliferation during development it is not surprising that NRG1 was one of the first candidates to be considered to play a similar role in adult SCs following injury. Fuelling this idea, elevated expression of NRG1 Type II and ErbB2/3 is observed in a time frame consistent with SC proliferation (Carroll et al., 1997; Guertin et al., 2005). It was hence quite unexpected when analysis of a transgenic mice with targeted disruption of ErbB2 revealed that signalling through ErbB2 is not only dispensable for the maintenance of myelinated SCs, but is also not required for the SC proliferation following an injury (Atanasoski et al., 2006). In spite of ErbB2 disruption, ERK and cyclinD1 (that, as will be detailed below, are required for SC proliferation) were still activated (although slightly reduced). It therefore seems clear that other mitogenic signals, which likely include growth factors and cytokines secreted by inflammatory cells, must be involved (Chen et al., 2007; Fawcett and Keynes, 1990; Hirata et al., 1999). Additional evidence that different mechanisms govern SC proliferation in development and in injury came from analysis of the cyclinD1 knockout mice. Schwann cell development and proliferation is unimpaired in cyclinD1$^{-/-}$ mice, indicating that cyclinD1 is mostly dispensable downstream of the mitogenic actions of NRG1. In sharp contrast, SC proliferation following injury was completely absent in cyclinD1 mutants, indicating that the proliferative response of adult SCs to damage is strictly dependent on this cyclin. Interestingly, Schwann cell dedifferentiation and demyelination were not affected in cyclinD1 mutant mice demonstrating that these events can be uncoupled (Kim et al., 2000). Despite this apparent independence between proliferation and dedifferentiation the same pathway drives the two processes since ERK, besides driving dedifferentiation as detailed before, is also required for cyclinD1-dependent proliferation of adult SCs (Napoli et al., 2012). Accordingly, MEK treatment completely abolished SC proliferation following injury (Napoli et al., 2012).

Surprisingly, nerve regeneration in cyclinD1 knockout mice was normal, in spite of the

blockage in Schwann cell proliferation, suggesting that SC proliferation is not required for successful nerve repair. Importantly, these studies were performed in crushed nerves (Kim et al., 2000; Yang et al., 2008). It is possible that in this type of injury, the maintenance of an intact basal lamina might be sufficient to provide guidance to the regrowing axons. In more severe injuries, such as nerve transection, both stumps are separated and retract creating a bridge between them. In these cases, proliferating SCs form cellular cords that appear to serve as tracks for axonal regrowth across the gap formed between both stumps (Parrinello et al., 2010). In support of the critical importance of this event, studies have shown that if local mitosis is blocked at the bridge, using mitomycin-C, Schwann cells do not migrate from the proximal stump and, consequently, axonal regrowth is impaired (Chen et al., 2005; Pellegrino and Spencer, 1985). Work from our laboratory has provided further insight regarding the molecular and cellular events underlying this process. We have shown that following transection, at the region of the nerve bridge (see Figure 1-8), fibroblasts interact with Schwann cells inducing a switch in SC behaviour from repulsion to attraction. This switch, which we have shown to be mediated by the activation of EphB2 receptors on SCs by ephrinB on fibroblasts, induces SCs to migrate as cords from the proximal stump, through the nerve bridge. Importantly, disruption of such interactions and failure to properly form SC cords results in axonal mismigration (Parrinello et al., 2010). Together, these results suggest that contrary to crush injuries in which SC proliferation appears to be dispensable, likely due to the prominent role played by the basal lamina, in nerve transections SC proliferation and subsequent migration as cellular cords appears to be required for proper axonal regrowth and nerve repair.

1.7.7 Axonal regrowth

The success of nerve regeneration depends on the reinnervation of the correct axonal targets (Nguyen et al., 2002). As already stated, Schwann cells promote PNS repair by providing trophic support and physical guidance to regrowing axons by forming Bands of Bungner, which are rail-track-like structures upon which axons can efficiently regenerate (Chen et al., 2007; Nguyen et al., 2002). In crush injuries most of axons find their original targets, a process that is more difficult in transected nerves. Dedifferentiated SCs also produce and present a plethora of neurotrophic factors that include NGF, BDNF and NT-3 among others (Funakoshi et al., 1993; Heumann et al., 1987). Additionally, SCs express a series of adhesion molecules including N-cadherin, L1 and NCAM that, at least *in vitro*, enhance the outgrowth of neurites (Bixby et al.,

1988; Bixby and Zhang, 1990; Martini and Schachner, 1988; Tacke and Martini, 1990; Thornton et al., 2005). Axonal regrowth is also mediated by interaction with ECM molecules. Following nerve injury, SCs increase the expression of proteins that are integrated in their basal lamina, such as laminins and fibronectin. Interaction between these proteins and axonal components facilitates axonal regrowth by providing structural and trophic support (Agius and Cochard, 1998; Lefcort et al., 1992; Toyota et al., 1990; Vogelezang et al., 2001). Most of the axon sprouts arising from parent axons in the proximal stump find and follow Schwann cell columns, whilst a more reduced number of axons might also grow at random into the connective tissue of the nerve (Geuna et al., 2009). Since an excess number of axons invade the distal SCs columns, the initial number of axons present in the distal nerve may considerably exceed the original number (Aguayo et al., 1973; Sanders and Young, 1946). Other branches that fail to reach the targets are pruned away and disappear. After a few months of nerve regeneration there is a reorganization of the nerve trunk into a large number of miniature compartments or "minifascicles", each surrounded by a new perineurium (Geuna et al., 2009). This process, known as compartimentalization (Morris et al., 1972a, b), also occurs in the end part of the proximal stump and in the gap between the two stumps. The process of compartimentalization is likely to be a response to the disturbance of the endoneurial environment resulting from a damaged perineurium and likely expresses the need for a quick reconstitution of the normal endoneurial space by restoring the perineurial barrier (Lundborg, 2004).

1.7.8 Final steps of nerve repair: Schwann cell redifferentiation, axonal remyelination and resolution of the inflammatory response

Unlike proliferation, Schwann cell redifferentiation and remyelination seems to largely recapitulate events during development, in both timing and sequence of gene-expression pattern (Chen et al., 2007; Hall, 2005; Walikonis and Poduslo, 1998; Zang et al., 2000). Redifferentiation is triggered when SCs re-establish contact with regenerated axons. This induces a transient expression of Oct-6, followed by Krox-20 upregulation and induction of myelin genes (Scherer et al., 1994; Zorick et al., 1996a). Similar signals and signalling pathways seem to be involved in the induction of remyelination in both development and regeneration. Of note, NRG1/ErbB2/3 signalling is likely a key signal for remyelination, as both $NRG1^{-/-}$ and BACE1-null (that lack mature NRG1 Type III) are severely hypomyelinated following nerve injury (Fricker et al., 2011; Hu et al., 2008). Similar to their functions during development,

neurotrophic factors also appear to be involved in the modulation of remyelination during repair (Terenghi, 1999; Cosgaya 2002). Following injury, NT3 is downregulated whereas BDNF and p75 are upregulated. Consistent with a role in promoting redifferentiation, p75 null mice have an abnormal response to injury showing a reduced number of myelinated axons and thinner myelin sheaths (Song et al., 2006).

Extracellular matrix components are also important players in promoting regeneration. Accordingly, injured nerves undergo a strong upregulation of laminin, collagens, fibronectin and specific integrins (Lefcort et al., 1992) to resemble the specific set of ECM component expressed during embryogenesis (Chernousov and Carey, 2000). As detailed earlier, laminins and their β1-integrins are required for proper SC differentiation during development. Similarly, γ1-laminin mutants show impaired axonal regrowth following injury, suggesting that also during redifferentiation laminin/integrin signalling may be involved in SC-mediated axonal sorting and in the regulation of SC proliferation and survival (Chen and Strickland, 2003). Again, scarce information could be found regarding the mechanisms driving redifferentiation into non-myelinating Schwann cells. Nevertheless, it is likely that is follows the same molecular and cellular events that mediate their differentiation during development.

In terms of the fate of the inflammatory cells in the regenerating nerve, not much has been reported. Likewise, the kinetics and signals underlying the resolution of the inflammatory response remain poorly understood. Interestingly, analysis of the RafTR transgenic mice in our laboratory has shown that the inflammatory response elicited by Raf/ERK activation in SCs could be resolved upon signalling inactivation, suggesting the elegant possibility that SCs differentiation status can somehow coordinate both the initiation and the later termination of the inflammatory process (Napoli et al., 2012). This may have relevant implications as deregulation of the inflammatory response is frequently observed in diseases such as neuropathies.

It should be easy, by this point, to recognize the major role Ras/Raf/ERK signalling plays in controlling and coordinating key events in Schwann cell biology. In particular, Ras/Raf/ERK is a central regulator of SC plasticity, regulating both differentiation and mediating SC dedifferentiation and proliferation following injury. It is therefore not surprising that deregulation of the pathway is likely to be involved in several inherited and infectious peripheral neuropathies (Fisher et al., 2008; Nadra et al., 2008; Tapinos et al., 2008) and in various pathological conditions associated with Neurofibromatosis type I.

1.8 Neurofibromatosis type 1

1.8.1 Incidence and symptoms

Neurofibromatosis type 1 (NF1) is one of the most common tumour-predisposition syndromes, affecting 1 in 3500 individuals worldwide (Brannan et al., 1994). NF1 is inherited as an autosomal dominant disease with the most common phenotypic manifestations resulting from abnormalities of neural crest-derived tissues (Riccardi, 1981). Patients with NF1 develop a wide spectrum of clinical presentations, including bony dysplasias, pigmentary lesions of the skin (café-au-lait macules and axillary freckling) and iris (Lisch nodules) and learning disabilities. In addition, NF1 patients have increased risk for specific kinds of benign and malignant tumours, including optic gliomas, astrocytomas, glioblastomas, pheochromocytomas (adrenal medullary cancers), juvenile myelomonocytic leukemias and embryonal rhabdomyosarcomas (Bader, 1986). However, as the name of the disease implies, the development of neurofibromas is the hallmark lesion of NF1. Neurofibromas are benign tumours of the peripheral nerve sheath that may develop in different parts of the body (neck, head, trunk, limbs) and extend into surrounding structures including skin, bone, muscle and internal organs (Williams et al., 2009). Neurofibromas can cause significant morbidity - severe disfigurement, pain, functional impairment - and even mortality, due to its continuous growth and frequent surgical inaccessibility. A summary of the clinical manifestations of the disease and the criteria used for its diagnosis is displayed in Table 1-1.

Individuals with NF1 are born with one mutated (non-functional) and one wild-type *NF1* allele. The *NF1* heterozygous condition, although sufficient to cause some of the clinical symptoms such as learning disabilities and pigmentary defects, is, by itself insufficient for tumourigenesis. Neurofibroma formation, in particular, follows Knudson's "two-hit" model for inactivation of tumour suppressor genes, in that tumours only develop upon inactivation of the remaining wild-type *NF1* allele and consequently complete loss of neurofibromin expression, the protein product of *NF1* (Upadhyaya et al., 1994; Zhu et al., 2002).

Table 1-1: Clinical features of Neurofibromatosis type 1

Established diagnostic criteria for NF1- patients are diagnosed with NF1 if they meet two or more of the following criteria:
• Multiple dermal neurofibromas or one plexiform neurofibroma • Multiple café-au-lait macules • Multiple skinfold freckles • Iris hamartomas (Lisch nodules) • Optic pathway glioma • Bony dysplasias • First-degree relative with NF1
Other associated features of NF1
• Specific learning disabilities • Short stature • Cardiovascular abnormalities • Malignant peripheral nerve sheath tumours • Other malignancies; leukaemia, pheochromocytoma, etc.

1.8.2 Neurofibromas: *Composition, Genetic and Cellular origins*

Neurofibromas are highly heterogeneous, benign tumours that arise within the peripheral nerves. Histologically, neurofibromas resemble a disordered version of the normal nerve. In fact, reminiscent of an injured nerve, neurofibromas are composed of axonal processes, increased numbers of "perineurial-like" and endothelial cells, fibroblasts, mast cells and Schwann cell-like elements (that may represent 40%-80% of all cellular components), all of which are embedded in an abundant collagenous matrix (Figure 1-9). Clinically, human neurofibromas may be classified as dermal or plexiform (Figure 1-10). Dermal neurofibromas are superficial tumours that arise in small nerves and are generally well circumscribed. In contrast, plexiform neurofibromas, which arise almost exclusively in the context of NF1, arise within large nerves or nerve plexus causing diffuse enlargement of the affected nerve. Dermal neurofibromas typically arise in patients entering puberty or pregnant women, and increase in number and size with age. These are almost invariably benign tumours, rarely progressing into malignancy. In contrast, plexiform tumours can be either congenital or appear later in life and are prone to undergo malignant progression to Malignant Peripheral Nerve Sheath Tumours (MPNSTs), a clinically aggressive and almost invariably lethal cancer, that affects approximately 8-13% of individuals with the condition (Evans et al., 2002; Rubin and Gutmann, 2005).

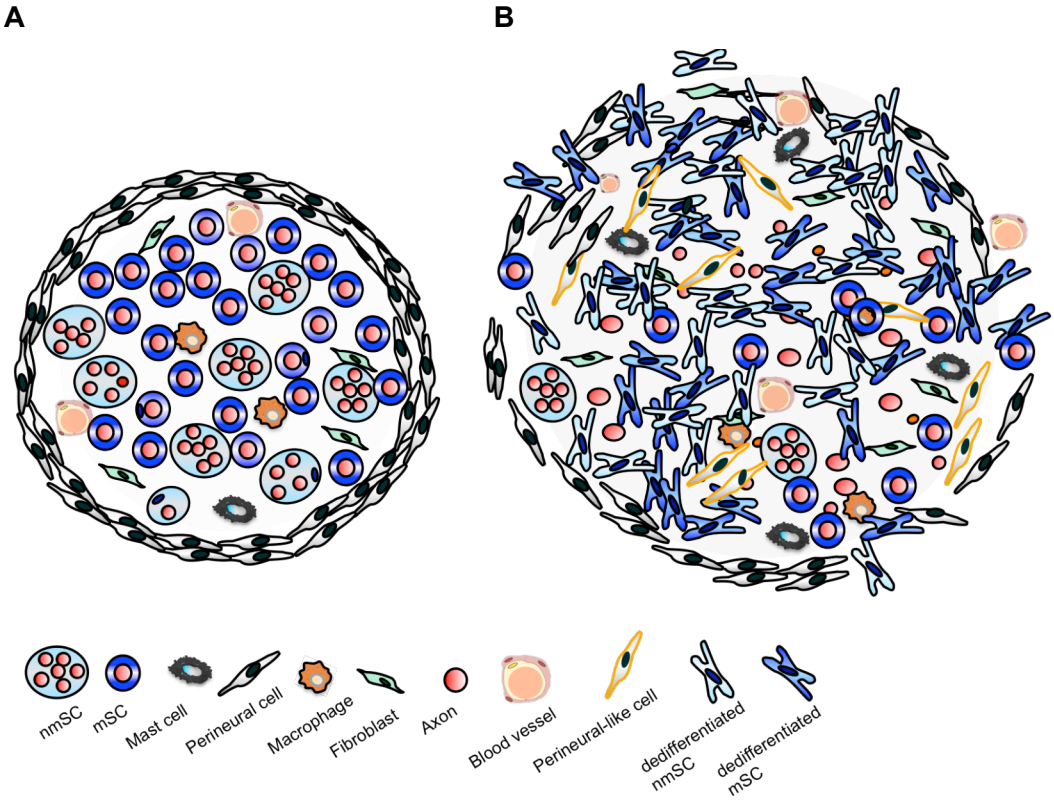

Figure 1-9: Structure of a normal peripheral nerve and a neurofibroma.

A) Schematic representation of a normal nerve fascicle (see Figure 1-7 for details); **B**) Neurofibromas are heterogeneous tumours composed of hyperproliferative Schwann cells that are found abnormally dedifferentiated and devoid of axonal contact. Other cell components include perineurial-like cells, macrophages, mast cells and fibroblasts. The perineurium is often disrupted.

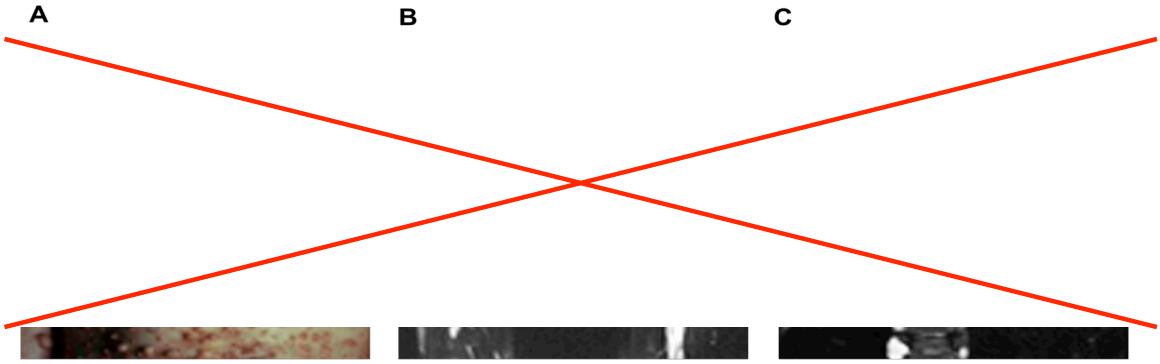

Figure 1-10: Examples of dermal and plexiform neurofibromas. A) Dermal neurofibromas growing on the chest and abdomen. **B**) Magnetic resonance image of plexiform neurofibromas growing in the sciatic nerves of an NF1 patient. **C**) Magnetic resonance image of plexiform neurofibromas in the nerve roots, causing compression of the spinal column. Photographs from the Children's Tumor Foundation; www.ctf.org. (figures removed due to copyright restrictions).

Despite the heterogeneity of neurofibromas in terms of location, age of onset and cellular composition, it is now well established that Schwann cells are the neoplastic element in these lesions and their transformation is known to result from loss of the remaining *Nf1* allele. Accordingly, in neurofibromas isolated from human patients, somatic inactivation of the second *Nf1* allele is found specifically in Schwann cells and not in other $Nf1^{+/-}$ cellular components (Serra et al., 2000). Importantly, in neurofibromas Schwann cells are found abnormally dedifferentiated, dissociated from axons and hyperproliferating.

1.8.3 The *NF1* gene

The *NF1* gene was identified in 1990 by positional cloning (Viskochil et al., 1990; Wallace et al., 1990). The human *NF1* gene localizes at chromosome 17q11.2 (in chromosome 11 in mice), spans 350 kilobases (Kb) of genomic DNA containing 61 exons, of which four (9a, 10a-2, 23a and 48a) are alternatively spliced in *NF1* transcripts (Barker et al., 1987; Cawthon et al., 1990b; Marchuk et al., 1991; Viskochil et al., 1990; Wallace et al., 1990). These alternatively spliced exons remain poorly studied but are thought to reflect tissue-specific or differentiation-regulated RNA splicing events. *NF1* is highly conserved with regards to its organization and structure in both coding and non-coding regions (Bernards et al., 1993; Buchberg et al., 1990). It's promoter region contains a number of perfectly conserved potential transcription regulatory elements including multiple AP2 binding sites, an SP1 site, a cAMP response element and a serum response element (Hajra et al., 1994). There are 3 small genes embedded within exon 27 of *NF1* gene, encoded in the opposite strand: EVI2A, EV12B and OMGP (Cawthon et al., 1991; Cawthon et al., 1990a). However, there is no clear evidence that any of these genes is involved in NF1 pathogenesis. *NF1* has one of the highest rates of *de novo* mutations, with already more than 1200 germline and 160 somatic mutations identified (Thomas et al., 2010). Mutations include whole gene deletions (in about 5% of the patients), nonsense, missense, frameshift and mutations affecting mRNA splicing (Messiaen et al., 2000; Wimmer et al., 2007; Wimmer et al., 2006). Although NF1 is completely penetrant, its expressivity is highly variable even between individuals with identical mutations, and a well-defined correlation between genotype-phenotype is not observed (Carroll, 2011).

1.8.4 Neurofibromin

The product of the *NF1* gene, neurofibromin, is a large 220-250 kDa cytoplasmic protein highly expressed in neurons, oligodendrocytes, astrocytes, leukocytes and Schwann cells (Daston et al., 1992; DeClue et al., 1991; Gutmann et al., 1991). As shown in Figure 1-12, several putative domains have been identified (Aravind et al., 1999; D'Angelo et al., 2006; Gregory et al., 1993; Izawa et al., 1996; Vandenbroucke et al., 2004). However, the most well characterized functional domain of neurofibromin corresponds to a GTPase activating protein (GAP)-related domain (GRD) that shares strong sequence homology with the GAP family members, such as IRA1 and IRA2 in yeast (Tanaka et al., 1990) and GAP1 in *Drosophila* (Gaul et al., 1992). Accordingly, neurofibromin is now recognized as a member of the mammalian family of RasGAPs that includes *RASA1* (p120GAP), *RASA2* (Gap1^{m}), *RASA3* (GAP1^{IP4BP}), *RASA4* (CAPRI), among others (Carroll, 2011). The GAP proteins function as negative regulators of Ras-mediated signalling by accelerating the conversion of the active Ras-GTP-bound form to the inactive Ras-GDP-bound form (Ballester et al., 1990; Xu et al., 1990). Ras are small G proteins encoded by a family of genes that includes *H-RAS*, *N-RAS* and *K-RAS* (K-RAS encodes two isoforms, K-Ras4A and K-Ras4B) that regulate cellular responses by transducing extracellular signals to the nucleus via a series of downstream effectors (Figure 1-11). Ras signalling can be activated by a variety of extracellular stimuli including growth factors, hormones, cytokines and neurotransmitters via interaction with receptor tyrosine kinases (RTK), G-protein coupled receptors, cytokine receptors and ECM receptors. Activation through RTK is perhaps the best characterized and is initiated upon binding of a growth factor, which causes RTK autophosphorylation. This creates intracellular docking sites for adaptor proteins and signal-relay proteins that recruit and activate guanine nucleotide exchange factors (GEFs), such as members of the Sos family. GEFs bind Ras and stimulate nucleotide dissociation. Nucleotide displacement allows the passive binding to GTP, given that the intracellular levels of GTP are much higher than those of GDP. Activated Ras-GTP can then interact and activate multiple downstream effector pathways, including Raf/MEK/ERK, phosphatidylinositol 3'-kinase (PI3K) and Ral guanine-dissociation stimulator (RalGDS), which ultimately communicate with the cell nucleus to regulate cell proliferation, survival, migration and differentiation (Schubbert et al., 2007). Keeping with the critical role that Ras plays in major cellular processes, it is not surprising that constitutively active mutations in Ras are frequently associated with human cancers as a result of permanent simulation of the Raf-ERK and/or PI3K

pathways that lead to uncontrolled cell proliferation and escape of apoptosis (Weiss et al., 1999).

The Raf/MEK/ERK cascade is the best characterized Ras effector pathway (Repasky et al., 2004). Activation of the pathway involves a coordinated multistep process that is initiated upon Ras induced activation of Raf. Activated Raf initiates a cascade whereby Raf phosphorylates and activates MEK1/2, which in turn phosphorylates ERK1/2. Activated ERK can phosphorylate cytosolic substrates and/or be translocated into the nucleus where it regulates transcription by phosphorylating a number of targets including transcription factors such as JUN and ELK1 (an ETS family member that forms part of the serum response that regulates the expression of FOS) (Wasylyk et al., 1998). Activation of these transcription factors can lead to the expression of proteins involved in the control of cell-cycle progression, such as cyclinD1 (reviewed in (Schubbert et al., 2007)). Ras/Raf/ERK can mediate opposing effects in the same cell type depending on the intensity and duration of the signal. For example, in the PC12 cell line NGF addition results in prolonged and sustained ERK activity leading to cell cycle exit and differentiation into a neuronal phenotype, while transient activation is associated with proliferation (Marshall, 1995). In Schwann cells Ras/ERK signalling also mediates multiple and complex effects: whilst signalling through this branch is required for proper differentiation during development, its sustained activation in adult SC drives dedifferentiation and proliferation, both *in vitro* and *in vivo* (Newbern et al., 2011; Harrisingh, et al., 2004; Napoli et al., 2012).

Ras-GTP also binds and activates PI3K. PI3K phosphorylates phosphatidylinositol-4,5-bisphosphate (PIP2) to generate phosphatidylinositol-3,4,5- triphosphate, which in turn activates downstream effectors such as 3-phosphoinositide-dependent protein kinase I (PDK1) and AKT (Bader et al., 2005). AKT is a kinase that promotes survival in many cell types by inactivating several pro-apoptotic proteins including BAD (Vivanco and Sawyers, 2002). AKT can also phosphorylate and inactivate the tuberous sclerosis complex 2 (TSC2), which leads to activation of TOR signalling. Importantly, constitutive activation of TOR is found in both *Nf1*$^{-/-}$ Schwann cells and in human neurofibromas (Johannessen et al., 2005) and treatment with rapamycin (a TOR inhibitor) has been shown to suppress the growth of malignant tumours in a mouse model of MPNSTs (Johannessen et al., 2008). However, given that ERK has also been found to be capable of phosphorylating TSC2 and consequently, inducing TOR activation (Ma et al., 2005), it remains to be clarified if the aberrant TOR signalling observed in the absence of *Nf1* is a consequence of increased signalling through PI3K,

ERK or both.

Inactivation of Ras proteins and termination of the downstream signalling is dependent upon GTP hydrolysis by the intrinsic Ras-GTPase activity. However, the intrinsic Ras-GTP hydrolysis is very inefficient, cleaving GTP at very low rates; GAP proteins, such as NF1, facilitate Ras inactivation by binding to Ras and augmenting its GTPase activity by several orders of magnitude.

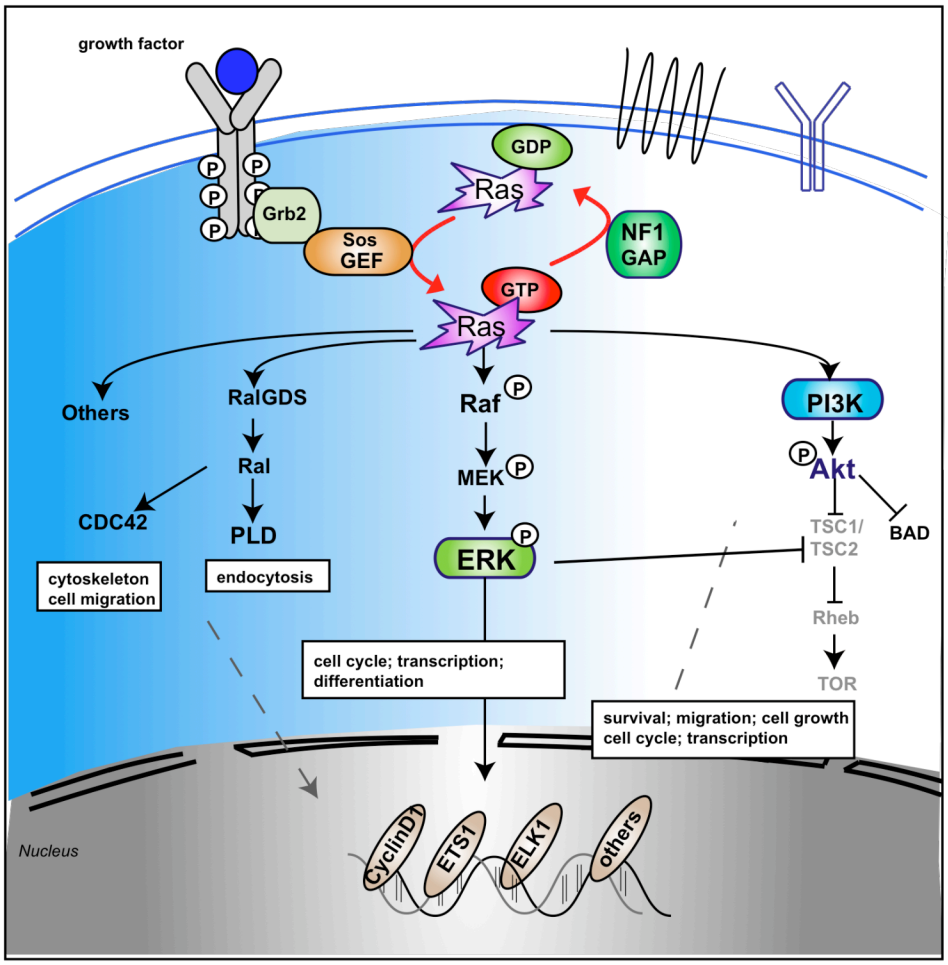

Figure 1-11: Ras activation and downstream signals. Ras activation in response to growth factors is mediated by RTK activation of adaptor proteins (e.g. Grb2), which interact with Ras-GEFs (e.g. Sos). GEFs promote the displacement of GDP, leading to binding of GTP and activation of Ras. Activated Ras interacts with a number of effector pathways to transduce signals into the cytoplasm and nucleus. Some examples of pathways downstream of the best characterized Ras effectors.

NF1, via its GRD domain, inhibits Ras and suppresses Ras-mediated mitogenic signalling and is therefore considered a tumour suppressor. In addition to the GRD domain, several other domains have been identified and include a tubulin-binding domain

(TBD), a cystein/serine rich domain (CSRD), a Sec14 homology domain (Sec14), a pleckstrin homology domain (PH) and a nuclear localization sequence (NLS). The TBD and CSRD modulate the GAP activity of neurofibromin; binding to tubulin inhibits, whereas phosphorylation of CSRD, enhances GAP activity (Bollag et al., 1993; Mangoura et al., 2006). Regarding the remaining domains, their function is still unclear. Neurofibromin also contains a FAK interacting domain, which may be involved in regulating cell adherence (Kweh et al., 2009) (Figure 1-12).

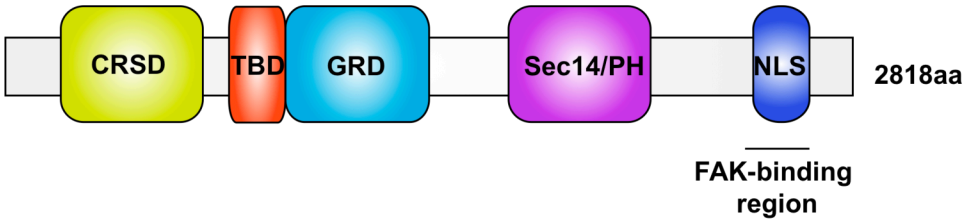

Figure 1-12: Schematic representation of the functional domains identified in neurofibromin. Several domains have been identified in neurofibromin and include a cysteine/serine rich domain (CSRD), a tubulin-binding domain (TBD), a GAP related domain (GRD), a Sec14 homology domain (Sec14), a pleckstrin homology domain (PH) and a nuclear localization sequence (NLS). The GRD domain is by far the best studied and appears to mediate most of neurofibromin's functions.

Neurofibromin also appears to be involved in the regulation of cAMP/PKA pathways. Initial work in *Drosophila* suggested that this effect was independent of Ras activity as the phenotypes presented by the *Nf1*$^{-/-}$ flies, including a growth deficiency, could be rescued by increasing signalling through the cAMP-dependent PKA pathway, but not by manipulating Ras strength (Guo et al., 1997; Guo et al., 2000; The et al., 1997). However, later work by Walker and colleagues has detected aberrant levels of activated ERK in Ras2 (paralog of mammalian R-Ras)-expressing larval neurons, suggesting that aberrant signalling through Ras was the primary cause of the *dNf1*$^{-/-}$ mutants systemic growth deficiency. Accordingly, the size defects could be rescued by expression of a functional NF1-GAP or a *Drosophila* p120RasGAP ortholog in larval neurons (Walker et al., 2006). In agreement with this, a recent report has demonstrated that genetic or pharmacological inhibition of the RTK Anaplastic Lymphoma Kinase (Alk) (which was found to be located upstream of NF1-regulated Ras/ERK signalling) is sufficient to restore normal levels of ERK signalling in neurons of

dNf1$^{-/-}$ mutants and, consequently, to rescue the small size phenotype of *Nf1*$^{-/-}$ flies (Gouzi et al., 2011). Together, these studies argued against separable Ras and cAMP-related functions and, instead, suggested that cAMP/PKA activation occurs downstream of Ras signalling. Moreover, the mechanisms through which neurofibromin can regulate cAMP dependent signalling seem to be cell-specific, given that its loss decreases cAMP levels in astrocytes while increasing them in Schwann cells (Dasgupta et al., 2003; Kim et al., 2001). Finally, there is some evidence that neurofibromin loss influences calcium signalling (Dang and DeVries, 2005), although the domains of the protein involved in this effect are still unknown. Figure 1-13 summarizes the signalling pathways that have been reported to be affected by neurofibromin loss.

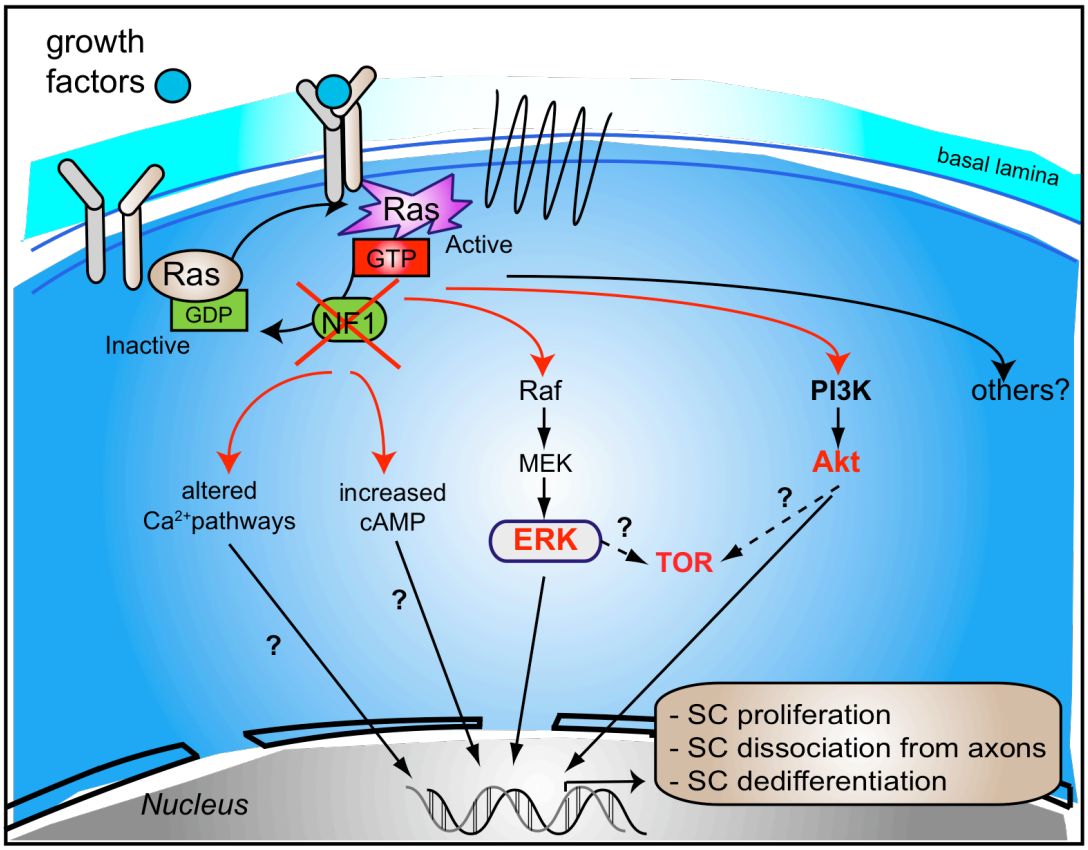

Figure 1-13: Pathways deregulated by *NF1* loss. Schematic representation of the intracellular pathways that seem to be affected by neurofibromin loss and how these may alter SC behaviour, ultimately leading to neurofibroma formation.

In terms of the molecular mechanisms regulating neurofibromin expression, only limited information is available. *In vitro* studies have shown neurofibromin is subject to rapid and transient proteasomal degradation following growth factor treatment

(Cichowski et al., 2003). This prompt degradation of neurofibromin upon activation of either G-coupled receptors or receptor tyrosine kinases, appears to be involved in the initial activation of the Ras signalling pathway, whereas its rapid-re-expression is required for proper attenuation of the pathway. Furthermore, *Nf1* deficient cells are more sensitive to low concentrations of growth factors, showing Ras activation at levels that $Nf1^{wt}$ cells did not respond. Thus, it seems that neurofibromin is required for maintaining an appropriate sensitivity to growth factors and for limiting and narrowing the period of Ras activation (Cichowski et al., 2003). It is precisely this biological function of NF1 that is believed to underlie most clinical presentations of *NF1* mutations. Importantly, elevated levels of active Ras are detected in $NF1^{-/-}$ Schwann cells isolated from neurofibromas (Cichowski and Jacks, 2001; Sherman et al., 2000) and MPNSTs and have been shown to be critical for the maintenance of a transformed phenotype (Basu et al., 1992; DeClue et al., 1992; Kim et al., 1997; Kim et al., 1995). Thus, increased Ras activity appears to be important for both the formation and maintenance of Schwann cell tumors.

Although most evidence points to Ras hyperactivation in Schwann cells being the key event triggering tumourigenesis in NF1, many questions remain to be answered. These include which precise signals are involved in promoting Ras activation during neurofibroma formation and which downstream pathways are important in this process. Nevertheless, great progress in the understanding of NF1 and neurofibroma formation in particular, has been accomplished mostly due to the generation of various genetically engineered mouse (GEM) models of NF1. In the next part of this introduction I shall review the major existing NF1 models and the key findings that can be taken from them also referring, when appropriate, to observations made from the analysis of human neurofibromas.

1.9 Mouse models of NF1

1.9.1 Initial models

Over the past several years different approaches have been taken to develop models for the tumours seem in individuals affected with NF1. The first attempts to directly test the role of NF1 *in vivo* were described independently by the Copeland and Weinberg labs in 1994. Both laboratories generated an *Nf1* knockout mouse model harbouring a targeted mutation in the exon 31 of the *Nf1* gene (Brannan et al., 1994; Jacks et al., 1994). The heterozygous mice ($Nf1^{+/-}$) were viable and fertile, but disappointingly failed to develop classical features of human NF1 such as neurofibromas

or pigmentation defects (Brannan et al., 1994). However, *Nf1*$^{+/-}$ mice did develop other NF1 related symptoms such as learning disabilities. Importantly, these defects were later demonstrated to be due to increased ERK activation in inhibitory neurons leading to greater GABA release and long-term potentiation (LTP) (Costa et al., 2002; Cui et al., 2008; Silva et al., 1997). Critically, genetic or pharmacological inhibition of ERK reversed the learning deficits indicating that brain dysfunction in NF1 may be a direct consequence of Ras hyperactivation (Costa et al., 2002).

Furthermore, *Nf1*$^{+/-}$ mice were prone to tumour development, notably myeloid leukaemias and pheochromocytomas, both of which occur with increased frequency in NF1 patients (Jacks et al., 1994). Loss of the wild-type allele was commonly found in the tumours. Interestingly, the pathogenesis of pheochromocytomas was strain specific, as the elevated incidence of these tumours in an *Nf1*$^{+/-}$ mouse in a mixed sv/129xC57BL/6 background disappeared when the mutant allele was bred onto a s/129 background (Tischler et al., 1995).

Otherwise, the heterozygous mice were indistinguishable from wild-type until 12-15 months of age, when their survival declined sharply due to the development of lymphomas, leukemias, lung adenocarcinomas, hepatomas, fibrosarcomas and adrenal tumours (Jacks et al., 1994). As these malignancies are also observed in older wild-type mice (24 months), this suggested that germline loss of one *Nf1* allele accelerated the development of tumours for which the mice are already predisposed (Brossier and Carroll, 2011).

The absence of neurofibromas in the *Nf1* heterozygous mouse model led to the hypothesis that inactivation of the remaining functional *Nf1* allele in other cell types, in particular Schwann cells, was required for neurofibroma development. However, this possibility could not be tested in mice homozygous for the *Nf1* null mutation (*Nf1*$^{-/-}$) as these mice die at day E12.5-E13.5 as the result of cardiac failure (Brannan et al., 1994; Jacks et al., 1994). Nevertheless, *Nf1*$^{-/-}$ mice provided a powerful tool to study the effects of neurofibromin loss on Schwann cell function *in vitro*.

1.9.2 Properties of *Nf1* deficient cells

In accordance with neurofibromin's role as a Ras-GAP, and similar to human neurofibroma-derived Schwann cells, *Nf1* null Schwann cells isolated from *Nf1*$^{-/-}$ mice, showed increased Ras activity and refractile morphologies characteristic of Ras expressing cells (Kim et al., 1997; Kim et al., 1995). In addition, *Nf1* deficient cells exhibit functional abnormalities including angiogenic and invasive properties (Muir,

1995; Sheela et al., 1990). However, in contrast to the initial expectation that Ras hyperactivation would lead to enhanced mitogenesis, *Nf1*$^{-/-}$ Schwann cells instead demonstrated reduced proliferation in response to the mitogenic signal NRG1 or axonal contact (Kim et al., 1995). It soon became clear that *Nf1* loss leads to oncogene-induced senescence (OIS). Similarly, introduction of activated Ras mutants into Schwann cells, in the absence of additional insults, induced DNA synthesis inhibition and growth arrest, that can only be bypassed through genetic disruption of the Rb or p53 pathways (Courtois-Cox et al., 2006; Lloyd et al., 1997; Mathon et al., 2001; Ridley et al., 1988; Serrano et al., 1997). This, together with the observation that human neurofibromas express markers of senescence, may explain the benign nature and the growth pattern of these tumours (Courtois-Cox et al., 2006). In humans it has been observed that the growth of neurofibromas seems to be self-limited with the enlargement periodically stopping and then restarting. In light of these findings one may imagine a scenario in which oncogene-induced senescence limits the growth of neurofibromas, with periods of growth occurring when tumour cells escape from this process via as yet unknown mechanisms (Carroll and Ratner, 2008). Curiously, *Nf1* deficient cells can be induced to hyperproliferate through cAMP-mediated PKA activation (Kim et al., 1997), demonstrating how *Nf1*$^{-/-}$ SC behaviour can be strikingly modulated by environmental factors. Importantly, hyperplasia of *Nf1*$^{-/-}$ mouse Schwann cells can be reversed by treatment with inhibitors of Ras farnesylation (a modification required for Ras maturation and appropriate localization) (Kim et al., 1997).

Furthermore, as will be discussed below, progression to malignancy seems to be dependent on loss of p53 and/or Rb signalling which underscores the importance of OIS in restricting neurofibroma growth.

1.9.3 *Nf1* chimeric mice

In an effort to circumvent the embryonic lethality of *Nf1* knockout mice *Nf1*$^{-/-}$; *Nf1*$^{+/-}$ chimeras were generated by injecting *Nf1*$^{-/-}$ embryonic stem cells into *Nf1*$^{+/-}$ C57BL/6 blastocysts. Chimeric mice partially composed of *Nf1*$^{-/-}$ cells survived postnatally and developed neurofibromas in spinal nerve roots and peripheral nerves nerve trunks (see Figure 1-7, for clarity), reminiscent of human plexiform neurofibromas (Cichowski et al., 1999). Importantly the tumours derived exclusively from *Nf1*$^{-/-}$ cells, indicating that complete loss of *Nf1* in one or more cell types is rate-limiting and an obligate step in neurofibroma formation and explaining the absence of neurofibromas in the heterozygous *Nf1*$^{+/-}$ mice. However, the reasons underlying the fact that inactivation of

the second *Nf1* allele appears to be a frequent event in humans (NF1 patients are heterozygous) and rare in $Nf1^{+/-}$ mice are still unclear, but may involve interspecies differences in lifespan, target cell number, proliferative properties or interspecies differences in the mutability of the *NF1* locus (Cichowski et al., 1999).

1.9.4 Conditional *Nf1* knockout mice: the Krox-20 model

The generation of $Nf1^{-/-}$ chimeras was a major step in our understanding of neurofibroma formation. However, given that the chimeras contained multiple cell types that were *Nf1* null, these experiments were not sufficient to definitively establish that loss of neurofibromin in cells of the Schwann cell lineage was sufficient to trigger neurofibroma formation. To test if this was the case, the Parada lab generated transgenic mice in which floxed *Nf1* alleles were conditionally ablated in Schwann cells by Cre recombinase under the control of the Krox-20 promoter (a more detailed characterization of this technique will be given in chapter 3) (Zhu et al., 2002). Surprisingly, *Krox-20Cre;*$Nf1^{fl/fl}$ mice did not develop any frank tumours, although they exhibited microscopic Schwann cell hyperplasia within peripheral nerves. However, when *Nf1* ablation occurred in an $Nf1^{+/-}$ background (*Krox-20Cre;*$Nf1^{fl/-}$) neurofibromas developed in peripheral nerve roots with 100% penetrance by one year of age (Zhu et al., 2002). These observations, together with the fact that neurofibromas in NF1 patients are similarly composed of $Nf1^{-/-}$ Schwann cells intermingled with a variety of $Nf1^{+/-}$ cells, led to the hypothesis that an *Nf1* haploinsufficient tumour microenvironment is required to cooperate with neurofibromin loss in Schwann cells to drive neurofibroma formation.

1.9.5 Evidence for a role of the microenvironment in neurofibroma formation

The suggestion that *Nf1* heterozygous, non-neoplastic cells were required to potentiate neurofibroma formation raised the question of which cell types were essential for this effect and what were the signalling pathways involved in this interaction. As mentioned earlier, neurofibromas are composed not only of neoplastic Schwann cells, but of a heterogeneous mixture of other cell types - fibroblasts, endothelial cells, mast cells and perineurial-like cells - all of which could be contributing to this process. To date, however, the most compelling evidence has come from work focusing on mast cells. Initial *in vitro* experiments have shown that $Nf1^{-/-}$ Schwann cells secrete elevated levels of Kit ligand (KitL), a growth factor that activates the c-Kit

receptor tyrosine kinase (Yang et al., 2003). In turn, *Nf1*$^{+/-}$ mast cells show increased c-Kit receptor expression and enhanced proliferation, migration and survival in response to KitL (Chen et al., 2010; Ingram et al., 2000). Additionally, KitL induces mast cell secretion of concentrations of the pro-fibrotic transforming growth factor-beta (TGF-β), a process that is enhanced in *Nf1* haploinsufficient mast cells. In response to TGF-β both murine *Nf1*$^{+/-}$ fibroblasts and fibroblasts from human neurofibromas proliferate and synthesize excessive collagen, a hallmark of neurofibromas (Yang et al., 2006).

Recently, Yang and colleagues, in a study using bone marrow transplantation in knockout mice, unveiled a crucial role for *Nf1*$^{+/-}$ mast cells in neurofibroma formation in the Krox-20 model. The authors have shown that when *Krox-20Cre:Nf1*$^{fl/fl}$ mice (that, as mentioned earlier do not form tumours) were lethally irradiated and transplanted with *Nf1*$^{+/-}$ bone marrow they developed multiple neurofibromas that were infiltrated by donor mast cells. Furthermore, on the basis that c-Kit receptor activation controls the release of mast cells from the bone-marrow (Ingram et al., 2000), the authors generated mice harbouring hypoactive *Nf1*$^{+/-}$ mast cells by intercrossing *Nf1*$^{+/-}$ mice with animals harbouring point mutations in c-Kit receptors (*Nf1*$^{+/-}$*;cKit*$^{W41/W41}$). When bone marrow from these mice was used to replace the lethally irradiated *Krox-20Cre:Nf1*$^{fl/fl}$ no tumours formed, indicating that c-Kit signalling in bone marrow-derived cells is critical for neurofibroma development (Yang et al., 2008). Importantly, when *Krox-20Cre:Nf1*$^{fl/-}$ mice (that normally form tumours) were transplanted with wild-type bone marrow, mast cell recruitment to peripheral nerves was not observed and mice no longer developed neurofibromas, pinpointing recruited mast cells as the critical haploinsufficient player cooperating with *Nf1*$^{-/-}$ Schwann cells in this particular mouse model (Yang et al., 2008). What remains unclear is exactly what pro-tumourigenic effects mast cells perform at the location of the developing tumour and if these effects are directed at the *Nf1*$^{-/-}$ SCs themselves or at any other component of the tumour.

Furthermore, although it is clear that mast cell recruitment is essential for tumour development in the Krox-20 model, it appears that in other neurofibroma models other cell components might promote neurofibroma development. In fact, the requirement of an *Nf1* haploinsufficient tumour microenvironment has been subsequently challenged by studies of distinct mouse models of NF1 (discussed below).

1.9.6 The neurofibroma cell of origin

With the work on the mouse models describe above together with the analysis of *Nf1*$^{-/-}$ Schwann cell properties *in vitro*, it became evident that the neoplastic cell that

gives rise to neurofibromas is derived from the Schwann cell lineage. However, precisely which cell type within this lineage undergoes the genetic mutations that initiate the tumourigenic process remained unknown. The observation that plexiform neurofibromas are often detected at birth, and therefore thought to be congenital had raised the possibility that neural crest stem cells or early SC progenitors undergoing *NF1* loss of heterozygosity (LOH) might be the neurofibroma-initiating cell. Supporting this idea, astrocytomas that developed in an NF1-related mouse model (*NestinCreER;Nf1$^{fl/fl}$;p53$^{fl/fl}$*) were shown to originate from neural stem cells (Alcantara Llaguno et al., 2009). In contrast, arguments favouring an adult, differentiated SC origin also existed. These included the unusual ability of fully differentiated cells to revert to a dedifferentiated phenotype with proliferative capabilities, the lack of a known stem cell population that can give rise to SCs in the adult organism and the observation that the majority of cells within neurofibromas retain a SC phenotype (Parrinello and Lloyd, 2009). In 2008 three independent groups have addressed whether neurofibromas arise from embryonic stem cells or a differentiated population, by generating conditional mouse models in which *Nf1* ablation in Schwann cells was induced at different stages of development (Joseph et al., 2008; Wu et al., 2008; Zheng et al., 2008).

Neural crest cells are not rendered tumourigenic by Nf1 loss

As noted earlier, NCSCs terminally differentiate by late gestation and cannot be detected post-natally in peripheral nerves (Kruger et al., 2002). Nonetheless, *Nf1* loss during earlier embryogenesis could render NCSCs tumourigenic, leading to a sustained expansion of these cells and their postnatal persistence such that they can give rise to tumours in the adult. To test this hypothesis Joseph and colleagues analysed the frequency of Schwann cell progenitors with stem cell properties in the embryonic and postnatal PNS in mice in which *Nf1* was inactivated in neural crest cells using *WntCre;Nf1$^{fl/-}$* mice (Wnt is expressed by E9.5 migrating neural crest cells - (Gitler et al., 2003)). Importantly, they found that, although *Nf1* loss induced a transient increase in the number of NCSCs in most regions of the fetal PNS at E13, their numbers decreased progressively in later stages of embryogenesis and could no longer be detected post-natally. These findings suggested that *Nf1*-deficient NCSCs differentiate during late gestation in a similar manner as wild-type NCSCs. *WntCre;Nf1$^{fl/-}$* mice died at birth so it remains to be tested if SCs derived from *Nf1$^{-/-}$* NCSCs can give rise to tumours. Nevertheless, E13 NCSC/SCPs isolated from *Nf1$^{-/-}$* mice could not form tumours when engrafted in the sciatic nerves of *Nf1$^{+/-}$* mice (Joseph et al., 2008),

indicating that NCSCs are not rendered tumourigenic by *Nf1* deficiency and thus suggesting that more differentiated cells are the targets for tumourigenesis.

Nf1 loss in Schwann cell precursors gives rise to neurofibromas later, in adulthood

In parallel studies *Nf1* deletion in Schwann cell precursors at E12.5 using a *P0aCre driver* (P0 expression begins at E12.5 and is restricted to SCPs) was shown to result in the development of neurofibromas in adult nerve trunks by 15-20 months (Joseph et al., 2008; Zheng et al., 2008). This was in contrast with the previous *Krox20-Nf1*$^{fl/-}$ model that developed tumours in the nerve roots and never in the nerve trunks (see Figure 1-7 to note the differences between nerve trunks and nerve roots). Possible reasons for this discrepancy include the different origins of SCs in both regions of the peripheral nerves. As noted earlier, whilst Schwann cells in the nerve roots originate from boundary cap cells that express Krox-20 at E10.5, SCs in the nerve trunks originate from SCPs that express P0 at E12.5 and Krox-20 at E15.5 (immature SCs). Therefore the distinct locations of the tumours in both models led to the suggestion that *Nf1* loss in boundary cap cells at E10.5 induces neurofibromas in nerve roots, whereas *Nf1* loss in SCPs at E12.5 drives neurofibroma formation in the nerve trunks. The observation that *Nf1* loss at the stage of immature SCs (E15.5) did not lead to tumour formation, raised the possibility that the timing of *Nf1* inactivation was the key determinant of neurofibroma formation, with *Nf1* loss being restricted to a window of opportunity (NCSC-SCP) and that more differentiated cells were not susceptible to undergo tumourigenesis by *Nf1* loss.

The attempt to isolate *Nf1*$^{-/-}$ stem cells from adult *P0aCre;Nf1*$^{fl/-}$ animals that developed neurofibromas failed once again, suggesting that the tumours were not the result of the presence of *Nf1*-deficient NCSCs. Instead, analysis of the neurofibromas in this mouse model revealed that the majority of proliferating cells within neurofibromas lacked markers characteristic of primitive SC progenitors (e.g. BLBP) and, rather, expressed markers of adult non-myelinating/dedifferentiated Schwann cells such as p75 and GFAP. Together, these findings argued against a classical stem cell origin of neurofibromas and rather suggested that neurofibromas were being driven by proliferation of mature SCs (Joseph et al., 2008).

Interestingly, analysis of post-natal nerves from *P0aCre;Nf1*$^{fl/-}$ animals revealed that embryonic loss of *Nf1*, despite giving rise to tumours in the adult animals, did not automatically alter the mitogenic or differentiative abilities of SCs (Joseph et al., 2008; Zheng et al., 2008). Instead, Schwann cells in *P0aCre;Nf1*$^{fl/-}$ mice developed normally

and were present in the correct numbers in neonatal nerves (Zheng et al., 2008). This was particularly surprising given that elevated levels of Ras/ERK, which would be expected to result from *Nf1* loss, have been consistently shown to induce Schwann cell dedifferentiation and proliferation (Harrisingh et al, 2004; Napoli et al., 2012). This led us to propose that during SC differentiation other mechanisms are in place, that regulate Ras/ERK signalling to ensure that the right levels of ERK are achieved (this will be further discussed in chapter 6).

Thus, based on these studies it seemed that *Nf1* deficiency did not directly affect the stem/precursor cells that had undergone *Nf1* loss, but instead it somehow conferred the downstream/differentiated progeny with aberrant properties that ultimately led to uncontrolled proliferation and tumour formation. Possible explanations of how embryonic *Nf1* loss may drive tumourigenesis in the adult will be discussed below.

In agreement with this window of opportunity for tumour development an independent study by Wu and co-workers showed that when *Nf1* is ablated at the same developmental stage (E12.5) using a *Dhh* driven Cre recombinase (expressed by E12-5 in both SCP and boundary cap cells), it also resulted in rapid and extensive neurofibroma formation, causing high morbidity and mortality by 13 months of age (Wu et al., 2008). However, tumours developed at the nerve roots, but not in the nerve trunks, suggestive of a boundary cap cell of origin rather then an SCP origin. Nevertheless, although no full blown tumours developed at nerve trunks, they did show hyperplasia and axonal dissociation that, as will be discussed below, were the first neoplastic events detected in the *P0aCre;Nf1*$^{fl/-}$ model (Wu et al., 2008; Zheng et al., 2008). It is thus plausible that had the mice not developed tumours in the nerve roots and hence survived longer (the tumours developed much more rapidly and extensively in this mouse model compared to *P0aCre;Nf1*$^{fl/-}$ animals) neurofibromas would have also eventually developed in the limb nerves.

Importantly, in contrast to the Krox-20 model in which the development of tumours only occurred in the context of an heterozygous (*Nf1*$^{+/-}$) background (there is no available information on the phenotype of the *P0aCre;Nf1*$^{fl/fl}$ animals), in the *DhhCre;Nf1*$^{fl/fl}$ mice, neurofibroma development occurred independently of an *Nf1* haploinsufficient microenvironment. This may be particularly relevant in the pathogenesis of the sporadic neurofibromas that arise in patients without NF1. Analysis of the neurofibromas that developed in this mouse model revealed additional differences in comparison with the *P0aCre;Nf1*$^{fl/fl}$ models. In particular, the molecular profile of the tumour cells was distinct - exhibiting immunoreactivity for BLBL, a

marker of progenitor cells that was not detected in the tumours of the previous models, supporting the idea that the plexiform neurofibromas that developed in both mice have different origins (SCPs versus BCCs).

In summary, these models suggested that although the apparent requirement for embryonic loss of *Nf1* (NCSC/SCP), *Nf1*$^{-/-}$ embryonic Schwann cells differentiate normally into mature SCs that later in life become the neurofibroma initiating cells. Importantly, *Nf1* loss at the immature SC stage did not give rise to tumours, suggesting that these more differentiated cells are no longer susceptible to become tumourigenic by *Nf1* depletion. In addition, it also suggested that different neurofibromas, despite their similar composition, may derive from distinct cells within the SC lineage of origin. This is in agreement with the extreme variability seen in human patients with NF1 and raises the tempting speculation that the timing of *Nf1* loss may affect the severity of the clinical manifestations with *Nf1* inactivation in earlier SC precursors leading to the most severe phenotypes (Parrinello and Lloyd, 2009).

1.9.7 Mouse model of dermal neurofibromas

The idea that distinct cells within the SC lineage could give rise to neurofibromas was further supported by a study focused on the development of dermal tumours (Le et al., 2009). In fact, despite the histological similarities shared between dermal and plexiform neurofibromas, the distinct location and clinical behaviour of these different neurofibromas had already raised the question of whether the cell of origin of dermal tumours is distinct from the population that gives rise to plexiform neurofibromas. Contributing to this supposition, the P0 and Krox-20 models failed to develop dermal neurofibromas, although efficiently developing plexiform tumours.

With this idea in mind, Le and colleagues proposed that dermal neurofibromas may arise from a neural crest-derived adult progenitor cell known as skin-related neural precursor cells (SKP) (Fernandes et al., 2008). SKPs can be isolated from the dermis of adult mice and humans and *in vitro*, can be induced to self-renew and differentiate into glial, neuronal and melanocytic lineages (Fernandes et al., 2008). To test the idea that SKPs can be the source of neoplastic SCs within dermal neurofibromas, the authors isolated SKPs from the skin of *CMVCreER;Nf1*$^{fl/-}$ mice (in this mouse model, *Nf1* is ubiquitously recombined upon Tamoxifen administration) and then, *in vitro*, induced their recombination. Subsequently, *Nf1* recombined SKPs were transplanted back into the same heterozygous host. The authors observed that these cells formed tumours when transplanted in the dermis of pregnant recipients or when implanted in the

proximity of the sciatic nerve (Le et al., 2009). The reasons underlying the fact that tumours only formed in these two contexts were not further investigated, but likely involve the critical importance of the microenvironment during neurofibroma formation. In addition, Le and colleagues applied Tamoxifen topically onto the skin of *CMVCreER;Nf1*$^{fl/-}$ animals to induce Cre recombination *in vivo* and observed that this led to local dermal neurofibroma formation. However, this protocol induces *Nf1* recombination in all the cell types in the skin (including SCs in the peripheral nerves). Therefore, until an SKP-specific promoter is generated to allow targeted disruption of *Nf1* in these cells, it can only be concluded that the cell of origin of dermal neurofibromas resides in the skin. Nevertheless, dermal neurofibromas also arose in the *DhhCre;Nf1*$^{fl/fl}$ model and *Dhh* is also expressed by SKPs (Fernandes et al., 2004; Wong et al., 2006), supporting the idea that dermal and plexiform neurofibromas may derive from different progenitors. However, attempts to define differences in the transcriptomes of dermal and plexiform neurofibromas have thus far been unsuccessful (Carroll, 2011; Miller et al., 2009), suggesting that even if the cell of origin is distinct in both tumours, they share similar subsequent molecular and cellular events that culminate in tumourigenesis. A summary of all the mouse models described, the promoters used to drive *Nf1* loss and the major phenotypes generated, is depicted in Figure 1-14.

Relevance to human disease

While the models described may be a relatively faithful representation of some of the neurofibromas that develop in NF1 patients (particularly those that develop in early life), it likely does not cover all the mechanisms of tumourigenesis experienced by humans. The hypothesis that neurofibromas might develop from mutations occurring in even more differentiated SCs is backed up by the finding that multiple tumours within the same patients exhibit different somatic mutations (Thomas et al., 2010). Hence, at least in some NF1 patients, it seems that different tumours have resulted from independent loss of heterozygosity (LOH) events. If the loss of the second *Nf1* allele had occurred in early SC progenitors one might expect that the same somatic mutations was found in different tumours, which does not seem to be the case.

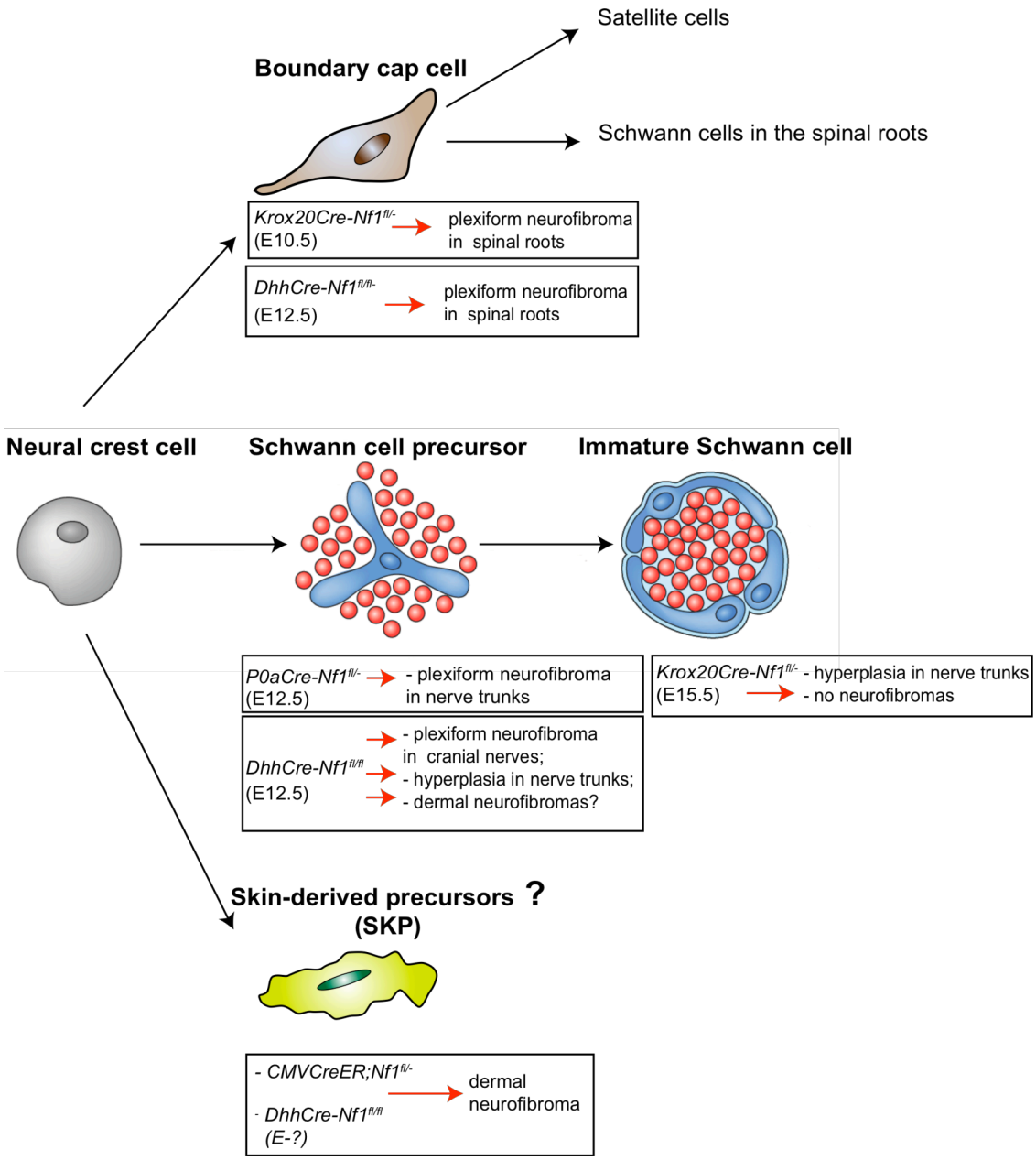

Figure 1-14: Susceptible stages for neurofibroma formation. Schematic representation of multiple GEM models generated to ablate *Nf1* at different stages of SC development; the promoters used to direct recombination, the target cells and the main phenotypes achieved are represented.

1.9.8 Mouse models of malignant peripheral nerve sheath tumours

Before discussing possible mechanisms that may be involved in triggering the development of neurofibromas in the mouse models described, I will briefly review available models of MPNSTs. In contrast with the human condition in which the frequency of plexiform neurofibromas progressing to MPNSTs is relatively high, in mouse models malignant tumours only rarely develop from pre-existing plexiform neurofibromas. This probably reflects the fact that mice that develop large plexiform neurofibromas have to be sacrificed, thus precluding the study of the natural progression of these tumours. Furthermore, the significantly shorter lifespan of a mouse may reduce the window of opportunity for acquisition of additional mutations in *Nf1*$^{-/-}$ SCs required to drive MPNST formation. In order to overcome this limitation, mice harbouring mutations in different tumour suppressor genes in addition to *Nf1* deficiency were created. As stated earlier, Ras hyperactivation in SCs leads to growth arrest that can be overcome by inhibition of the p53 function. With this observation in mind the Jacks and Parada laboratories bred mice heterozygous for *Nf1* to mice heterozygous for p53 (Cichowski et al., 1999; Vogel et al., 1999). As these genes are both located on mouse chromosome 11, trans and cis *Nf1*$^{+/-}$*;p53*$^{+/-}$ animals were generated, with the latter, as might be predicted, exhibiting a more severe phenotype and developing MPNSTs in approximately 30% of the cases. Importantly, LOH at both *Nf1* and *p53* loci was identified in all the MPNSTs developed in these mouse models, suggesting that the complete loss of both genes cooperates in the formation of these lesions. MPNSTs also formed when *Nf1*$^{+/-}$ mutants were crossed with *p16Ink4a*$^{-/-}$*; p19Arf*$^{-/-}$ animals. However, when *Nf1*$^{+/-}$ mice were crossed with either *p16* null or *p19* null alone no tumours formed, indicating that deregulation of both products encoded by *CDKN2A* (the locus containing both *p16INK4a* and *p19ARF* genes) and thus deregulation of p53 and Rb pathways, is required to promote MPNSTs in the context of *Nf1* heterozygosity (Joseph et al., 2008; King et al., 2002). Importantly, mutations in p53 and in the CDKN2A genes are commonly found in human MPNSTs (Birindelli et al., 2001; Kourea et al., 1999; Menon et al., 1990; Nielsen et al., 1999).

Malignant peripheral nerve sheath tumours and neurofibromas are histologically distinct with the first displaying reduced expression of genes involved in SC specification and differentiation, such as Sox10 and S100, whilst presenting elevated expression of markers characteristic of migrating neural crest such as Twist1 and Sox9. This likely reflects loss or suppression of SC differentiation signals and is probably an important step in the progression of neurofibromas into MPNSTs (Joseph

et al., 2008; Levy et al., 2004; Miller et al., 2009; Miller et al., 2006).

1.10 Insights into neurofibroma formation

Early events of tumourigenesis

As mentioned, embryonic loss of *Nf1* during embryogenesis leads to tumour formation in the adult mice, despite not causing a detectable immediate effect in early *Nf1*$^{-/-}$ Schwann cell behaviour. Instead, at birth, Schwann cells are found in the right numbers and without any major differentiation defects. So how can they form tumours later in life? A possible explanation came from a closer examination of the *P0Cre:Nf1*$^{fl/-}$ mutant nerves in the early post-natal period. As noticed by Zheng and colleagues, *Nf1* deficiency, although not inducing hyperproliferation or tumourigenesis in early life, did result in a subtle defect in the segregation of axons associated with non-myelinating Schwann cells, in that Remak bundles displayed an increased number of unsorted axons. Over time subsequent degeneration of abnormal Remak bundles occurred, leading to the dissociation of nmSC that, once devoid of axonal contact, re-entered the cell cycle and hyperproliferated. It is thus plausible that embryonic loss of *Nf1* is necessary to prime non-myelinating SCs for later tumourigenesis by disrupting the normal interactions between axons and SCs. At later stages, probably in response to the degeneration of naked axons and dedifferentiated nmSCs, there is the recruitment of an inflammatory response with extensive mast cell infiltration and dedifferentiation of mSCs, reminiscent of what happens during injury. However, unlike injury that is generally a self-limited process, inflammation and SC dedifferentiation in *Nf1*$^{-/-}$ nerves appears to be perpetuated, and in that way contributes to neurofibroma formation (Parrinello and Lloyd, 2009).

Ras/Ras/ERK signalling and neurofibroma formation

How does neurofibromin loss induce the cellular events that culminate in neurofibroma formation? Some insight of how this may be happening came from work in our laboratory. Using a DRG-SC co-culture system we have shown that the ERK activation resulting from *Nf1* loss is sufficient to impair SC-axon interactions, via a mechanism dependent on the ERK-mediated downregulation of the Schwann cell surface molecule Semaphorin4F (Sema4F) (Parrinello et al., 2008). Importantly, we have also shown that, in contrast to *Nf1* wild-type cells that become quiescent upon establishing a more stable interaction with the axons, Sema4F knocked-down cells readily proliferated in response to external mitogens, even after establishing long-term

contact with axons (Parrinello et al., 2008). This, together with the fact that Ras/Raf/ERK activation in Schwann cells drives differentiated cells to revert to a more "progenitor-like", proliferative state, led us to delineate a model of neurofibroma formation. In this model we proposed that the increased Ras/Raf/ERK signalling that results from *Nf1* loss leads to Sema4F downregulation; this may be initially involved in the defective nmSC-axon interaction and the later dissociation from axons. Dissociated cells, freed from the growth-suppressive signals coming from the axons, are able to respond to external growth factor signals (that may be produced by inflammatory cells or other components of the nerve microenvironment). Dissociated *Nf1*$^{-/-}$ Schwann cells respond to external signals with an abnormal and sustained Ras/ERK activation (due to the lack of neurofibromin), which as shown by Napoli et al., is sufficient to induce SC dedifferentiation. Dedifferentiated SCs secrete pro-inflammatory factors that recruit inflammatory cells (Napoli et al., 2012). These, in turn, actively secrete factors that stimulate Ras/ERK in Schwann cells, which may contribute to the perpetuation of cycles of SC dedifferentiation/proliferation and recruitment of an inflammatory response, which ultimately leads to neurofibroma formation (Parrinello and Lloyd, 2009). Figure 1-15 shows a schematic representation of the proposed model of neurofibroma formation.

This model hinges on the assumption that adult SCs are strictly dependent on neurofibromin to properly regulate Ras/Raf/ERK signalling. This implies that different signals inducing Ras activation in *Nf1*$^{-/-}$ SCs may represent possible triggers to tumourigenesis by inducing abnormal SC dedifferentiation and proliferation.
To test this model we decided to 1) generate a new mouse model in which *Nf1* loss could be induced in fully differentiated myelinating SCs, testing the susceptibility of fully differentiated cells to foster tumour formation; 2) activate Ras/ERK in adult *Nf1*$^{-/-}$ Schwann cells, by means of nerve injury, to test if strong signalling through the pathway can modulate the fate of an *Nf1*$^{-/-}$ Schwann cell (Figure 1-16).

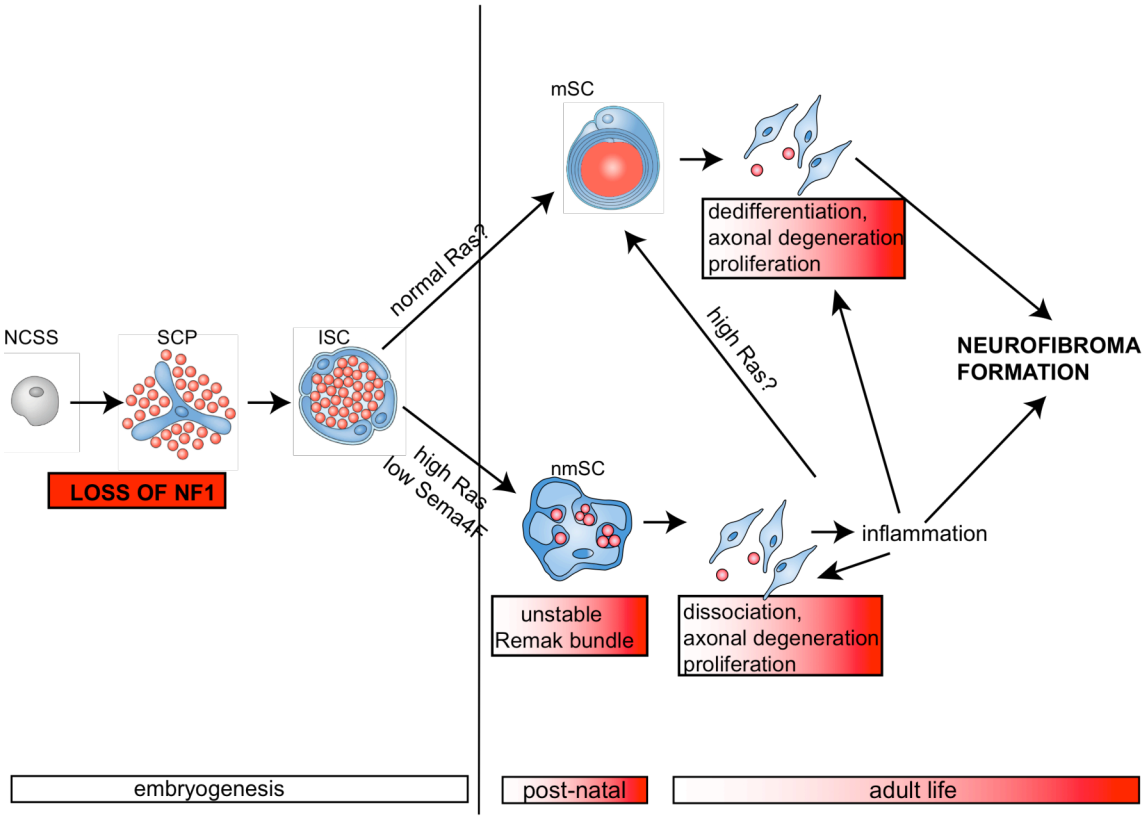

Figure 1-15: Model of neurofibroma initiation and progression. Slightly elevated levels of Ras resulting from *Nf1* loss in SCPs, leads to unstable Remak bundles. Later in life, low levels of Sema4F secondary to elevated Ras/ERK may lead to Remak bundle disruption and subsequent axonal degeneration. This leads to the recruitment of an inflammatory response that in turn induces elevated ERK in myelinating SCs that then dedifferentiate and proliferate also contributing to neurofibroma development (adapted from Parrinello and Lloyd 2009).

1.11 Thesis aims

Schwann cells are highly plastic cells that retain the ability to self-renew throughout adult life. Underlying this remarkable ability there is a Ras/Raf/ERK driven process through which fully mature differentiated SCs revert to a dedifferentiated "progenitor-like" state that is able to undergo proliferation. This is of great importance following nerve injury when dedifferentiated SCs proliferate creating a suitable environment for axonal regrowth. Deregulation of this process seems, however, to be involved in pathological conditions, as abnormally dedifferentiated SCs are found in

neurofibromas, a very common tumour arising in patients with NF1. Importantly, neurofibroma formation appears to be somehow driven by Ras hyperactivation as tumours only form upon complete loss of neurofibromin, a negative regulator of Ras signalling. Important insights into the biology of neurofibromas have already been taken from diverse mouse model of NF1. However, many questions remain to be solved. In this thesis, I aimed to solve some of the unanswered questions, by addressing the effects of *Nf1* loss in fully mature SCs and the impact of nerve injury and the associated Ras/ERK activation in *Nf1*-deficient nerves. This thesis describes work with relevant implications not only for the understanding of neurofibroma development and the signalling pathways involved, but also for possible therapeutic strategies.

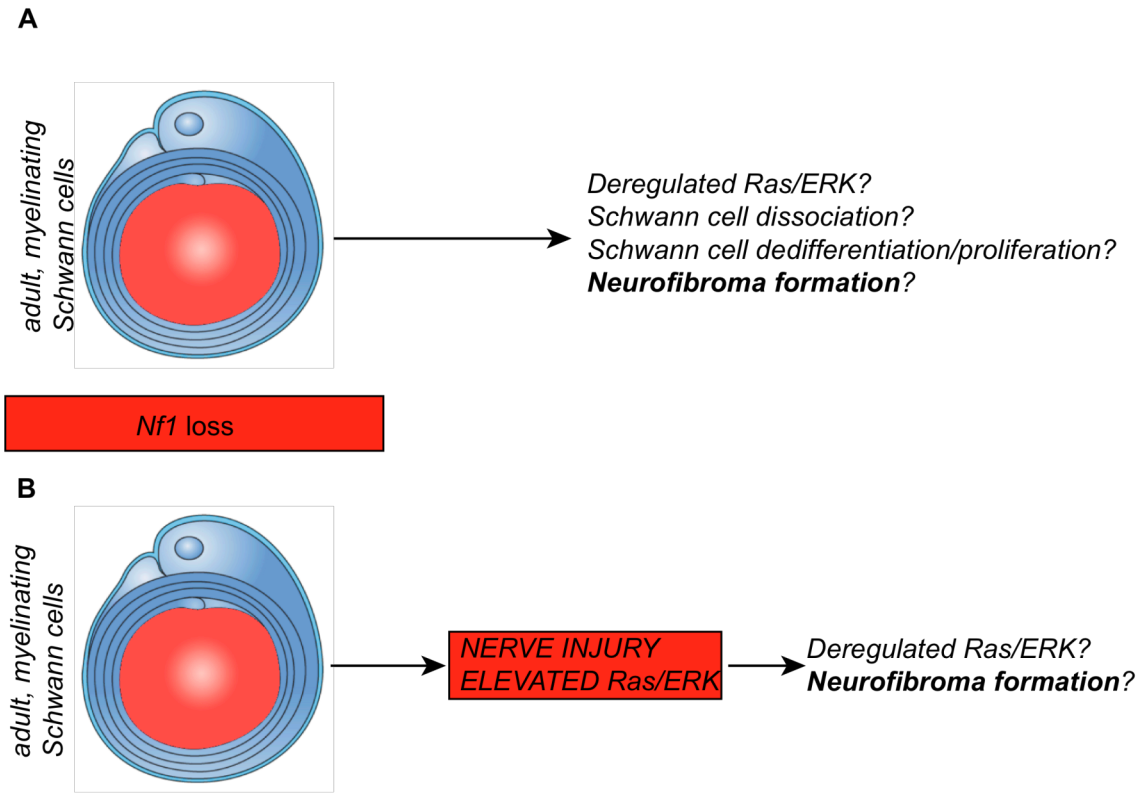

Figure 1-16: Main questions addressed in this thesis. A) Testing the effect of *Nf1* loss in a fully differentiated, myelinating Schwann cell. **B**) Testing the effect of injury in the context of *Nf1*$^{-/-}$ Schwann cells.

Chapter 2: Materials and methods

2.1 Materials

Reagents were obtained from Sigma, unless otherwise stated. Al kits were used according to manufactures instructions.

2.1.1 Primers for genotyping

Gene name	Sequence (5'-3')
Nf flox	(P1) CTT CAG ACT GAT TGT TGT ACC TGA (P3) ACC TCT CTA GCC TCA GGA ATGA (P4) TGA TTC CCA CTT TCT GGT TCT AAG
Nf1 +/-	(NF31a) GTA TTG AAT TGA AGC ACC TTT GTT TGG (NeoTkp) GC GTG TTC GAA TTC GCC AAT G (NF131b) CTG CCC AAG GCT CCC CCA G
Nf1Δ	(P1) CTT CAG ACT GAT TGT TGT ACC TGA (P2) CAT CTG CTG CTC TTA GAG GAA CA
P0-CreER	(Pcx) CTG CAC AGA CAT GAG ACC ATA GG (Cre)TCG GAT CCG CCG CAT AAC C
YFP(R26) wt	(P_{R26-F}) AAA GTC GCT CTG AGT TGT TAT (P_{R26-R}) GGA GCG GGA GAA ATG GAT ATG
YFP(R26) mutant	(P_{R26-F}) AAAGTC GCT CTG AGT TGT TAT ($P_{R26-Rmut}$) GCG AAG AGT TTG TCC TCA ACC

Table 2-1 Primers used for mice genotyping

2.1.2 siRNA oligos

Gene	Target sequence	Cat No.
NF1 (3)	5'-CAAGCTAGAAGTGGCCTTGTA -3'	SI01919505
NF1 (5)	5'-TGGCCTAAGATTGACGCTGTA -3'	SI01919512
Dusp6 (1)	5'- CACGGATATTATGATCACTAA-3'	SI00278271
Dusp6 (5)	5'-CTCCCTGCAATCTACGTGAAA-3'	SI03089835
Scram	5'-AATTCTCCGAACGTGTCACGT-3'	S1022563

Table 2-2 siRNA oligos

2.1.3 Primers for qPCR

Gene name	Forward/Reverse	Sequence
B2M	Forward	TGACCGTGATCTTTCTGGTG
	Reverse	ATTTGAGGTGGGTGGAACTG
K20	Forward	TGACCGTGATCTTTCTGGTG
	Reverse	ATTTGAGGTGGGTGGAACTG
P0	Forward	CTGGTCCAGTGAATGGGTCT
	Reverse	CATGTGAAAGTGCCGTTGTC
MBP	Forward	CACAAGAACTACCCACTACG
	Reverse	GGGTGTACGAGGTGTCACAA

Table 2-3 Primers used in qPCRs

2.1.3 shRNA oligos

Construct	Target sequence Top strand/Bottom strand
shScr	TGCGTTGCTAGTACCAACT
shMKP3-2	GTGCCAAGGACTCTACTAA
5'-gatccGTGCCAAGGACTCTACTAATTCAAGAGATTAGTAGAGTCCTTGGCACTTTTTTACGCGTg-----3' 5'-aattcACGCGTAAAAAAGTGCCAAGGACTCTACTAATCTCTTGAATTAGTAGAGTCCTTGGCACg-----3'	
shMKP3-5	AGGGGAGTTCAAGTACAAG
5'-gatccAGGGGAGTTCAAGTACAAGTTCAAGAGACTTGTACTTGAACTCCCCTTTTTTTACGCGTg-----3' 5'-aattcACGCGTAAAAAAAGGGGAGTTCAAGTACAAGTCTCTTGAACTTGTACTTGAACTCCCCTg-----3'	
shMKP3-9	CCTCCAACCAGAATGTCTA
5'-gatccGCCTCCAACCAGAATGTCTATTCAAGAGATAGACATTCTGGTTGGAGGTTTTTTACGCGTg-----3' 5'-aattcACGCGTAAAAAACCTCCAACCAGAATGTCTATCTCTTGAATAGACATTCTGGTTGGAGGCg-----3'	

Table 2-4 shRNA oligos

2.1.4 Antibodies

Primary antibody	**Species**	**Dilution**	**Source**
Immunofluorescence/ Immunohistochemistry			
P0 (myelin protein zero)	Mouse	1:1000	Astex Clone 18
p75NGFR	Rabbit	1:500	Millipore 07-476
GFP	Chicken	1:400	Abcam ab13970
	Rabbit	1:2000	Abcam ab290-50
Neurofilament	Chicken	1:1000	Abcam ab4680
	Rabbit	1:2000	Millipore ab1987
P-ERK1/2	Rabbit	1:100	Cell signalling 9191S
S100β	Rabbit	1:1000	DAKO Z0311
Smooth alpha actin (SMA)	Mouse	1:100	Sigma A5228
Iba-1	Rabbit	1:10000	WAKO 019-19741
CD-117 (c-Kit)	Rat	1:300	BDpharmigen 553356
CD3	Biotin	1:300	BDpharmigen Cl.125-2C11
NIMP-R14	Rat	1:300	Abcam ab2557
Collagen I	Rabbit	1:1000	Abcam ab292
Collagen IV	Rabbit	1:1000	Abcam ab19808
Laminin1	Rabbit	1:2000	Abcam ab11575
Western blotting			
NF1	Rabbit	1:100	Santa Cruz sc-67
P-ERK1/2	Mouse	1:1000	Sigma M8159
ERK1/2	Rabbit	1:10000	Sigma M5670
MKP3	Rabbit	1:500	Cell signalling 3058
beta-tubulin	Mouse	1:2000	Sigma T4026
Vinculin	Mouse	1:1000	Sigma V9131
DNA dyes			
DAPI		1:100	
Hoechst		1:2000	

Table 2-5 Primary antibodies

Secondary antibody	**Species**	**Dilution**	**Source**
Immunofluorescence/ Immunohistochemistry			
Alexa-Fluor 594	Mouse	1:500	Invitrogen -Molecular Probes A11032
	Rabbit	1:500	Invitrogen -Molecular Probes A11012
Alexa-Fluor 488	Chicken	1:500	Invitrogen -Molecular Probes A11039
	Mouse	1:500	Invitrogen -Molecular Probes A1029
	Rabbit	1:500	Invitrogen -Molecular Probes A11034
	Rat	1:500	Invitrogen -Molecular Probes A11006
IgY Texas Red	Chicken	1:500	Abcam 7116
Streptavidin-FITC	Biotin	1:500	Invitrogen -Molecular Probes S32354
Western blotting			
Anti-HRP	Mouse	1:5000	GEhealthcare NA9340
	Rabbit	1:5000	GEhealthcare NA9310

Table 2-6 Secondary antibodies

2.2 Animals

All animal work was performed in accordance with the United Kingdom Home Office legislation. Mice were housed in a temperature and humidity controlled vivarium on a 12-hour light-dark cycle with free access to food and water.

2.2.1 Mouse strains

Nf1$^{flox/flox}$ (Zhu et al., 2001) and *Nf1*$^{flox/-}$ (Jacks et al., 1994) on a mixed 129/Bl/6 background were crossed with *P0CreER* C57Bl/6 mice to generate *P0-Nf1*$^{fl/fl}$ and *P0-Nf1*$^{fl/-}$ mice (Leone et al., 2003). *P0-Nf1*$^{fl/fl}$ and *P0-Nf1*$^{fl/-}$ mice were bred to lacZRosa (Soriano, 1999) and to YFPRosa (Srinivas et al., 2001).

2.3 Cell culture

2.3.1 Primary Schwann cells

Primary Schwann cells were isolated from postnatal 7 (P7) Sprague Dawley rat sciatic and brachial nerves as previously described (Cheng et al., 1995) and maintained on poly-L-lysine (2,4μg/ml) [Sigma P-6282] coated plastic dishes [Nunc]. Cells were routinely cultured in DMEM [Lonza 12-707, 1g/l glucose] supplemented with 3% charcoal stripped foetal calf serum [Biosera], 4mM L-glutamine [Gibco 25030], 0,1mg/ml kanamycin [Sigma K1377], 2μg/ml gentamycin [Gibco 15710], 1μg/mL forskolin [Calbiochem 344270] and GGF produced in our laboratory. Cell cultures were maintained at 37°C in 10% CO_2 and 95% humidity. Medium was changed every two days and cells were passaged every three days. Schwann cells were routinely plated at a density of 4,8 x10^5 cells per 10cm dish.

2.3.2 Rat Dorsal Route Ganglion (DRG) explants

DRG were extracted from P0 or P1 Sprague Dawley rats and stored in ice cold L-15 [Gibco 11415-064] media. DRG were then plated into the centre of PLL and laminin-coated [25μg/ml, Sigma] glass-coverslips (13mm) in 200μl of defined basal media supplemented with 50ng/ml of NGF [Alomone labs N-245]. The defined basal media consisted of DMEM F-12 with glucose [Gibco 21041-025] complemented with SATO (100μg/mL BSA [Gibco], 60 ng/ml progesterone, 16μg/ml putrescine, 50 ng/ml thyroxine, 50 ng/ml triidothyrine and 40ng/ml selenium), 10μg/ml insulin [Lonza] and 100μg/ml transferrin [Calbiochem]. Following overnight incubation at 37°C and 5% CO_2, DRG were treated with 10^{-5}M β-D-arabinosylcytosine (AraC), a DNA synthesis inhibitor, to eliminate endogenous Schwann cells and fibroblasts. After 48 hours of AraC treatment, cultures were medium changed into defined conditions for a further 72 hours before use.

2.3.3 Phoenix cell culture

The retroviral packaging line, Phoenix [Nolan lab, Stanford University] was used to introduce genetic material into Schwann cells, as described below. Phoenix cells were maintained on uncoated plastic dishes, in DMEM+Glutamax™ [Gibco 31966, 4.5mg/ml D-glucose] supplemented with 10% foetal bovine serum (FBS) [Sigma], 0,1mg/ml kanamycin [Sigma K1377] and 2μg/ml gentamycin [Gibco 15710]. Before seeding, cells

were passaged through an 18G needle, to ensure an even distribution on the plate. Cells were incubated at 37°C in 10% CO_2 and 95% humidity.

2.4 Cell culture assays

2.4.1 Schwann cell differentiation assays

Primary Schwann cells were cultured to confluence, washed three times with serum free defined medium and transferred to defined medium alone or containing 1mM dbcAMP [Sigma] to induce differentiation, for the duration of the experiment. Defined medium consisted of DMEM with glucose, supplemented with SATO (described above), 10μg/ml insulin [Lonza] and 100μg/ml transferrin [Calbiochem]. In some of the experiments, shorty before harvesting (see Chapter 6 for details) cultures were stimulated with 20ng/ml of human recombinant neuregulin (EGF domain) [R&D Systems].

2.4.2 Myelinating Schwann cell-DRG co-cultures

Sub-confluent Schwann cells were trypsinised and re-suspended in Schwann cell medium (3 % serum) to inhibit trypsin activity. The cells were then centrifuged at 1100 rpm to pellet and re-suspended in DRG defined basal medium containing NGF (detailed above) and 1% of serum. The number of cells was determined using a coulter counter [Beckman Coulter]. 60 000 cells/per coverslip (in a final volume of 400μl) were plated onto the dissociated DRG. Co-cultures were medium changed every 48 hours into fresh DRG medium plus 1% serum, for a total period of 7 days. After 7 days, when Schwann cells reached confluence, co-cultures were medium changed into myelination promoting medium (defined DRG medium plus 50μg/ml ascorbic acid, 1% serum and 1:300 matrigel [R&D 356231]). Cultures were left to myelinate for up to 3 weeks and fed every 2-3 days with fresh myelination medium.

2.4.3 Transfection of siRNA into Schwann cells

Schwann cells were plated on 60mm dishes at a density of 220, 000 in SC medium (3% serum). The following day, cells were medium changed with 2,3 ml of fresh SC medium and transfected with siRNA duplexes. SiRNA stocks were diluted from 20μM (stock solution) to a concentration of 0,2μM (2μL of stock solution plus 198μL of plain DMEM). SiRNA/lipid complexes were then prepared by the sequentially adding 88μL DMEM + 12μL sRNA working solution (0,2μM) + 6μL Hiperfect solution [Qiagen].

Complexes were allowed to form by incubating the mixture for 10 minutes at room temperature. SiRNA/lipid complexes were then added directly to the 60mm dishes and incubated overnight (final concentration of approx. 1nM of siRNA). Medium was changed 18 hours later, to remove transfection complexes. A second round of transfections was performed 48 hours following the first, to achieve an extended period of knockdown.

2.4.4 Generation of shRNA expressing SCs by Phoenix infection

Five million Phoenix cells were seeded on a 10cm plate for each transfection and left ON at 37°C. Five μg of plasmid DNA (pSIREN-RetroQ vector + shRNA- see 2.4.5) was mixed with 500μl of serum free medium, followed by 17.5μl of PLUS™ [Invitrogen 18324-012] and left at room temperature for 15 minutes. A separate tube was prepared for each of the constructs. In fresh tubes, 25μL of Lipofectamine reagent [Invitrogen 11514-015] was mixed with 500μl of serum free medium and the DNA/ PLUS™ mix from the previous step. The transfection mixture was left for further 15 minutes at room temperature to allow DNA/lipid complexes to form. Medium on Phoenix cells was replaced by 4ml of serum-free medium per plate, washing once with serum-free medium. The DNA/lipid complexes were then carefully added dropwise to the Phoenix plate, gently mixed and incubated at 37°C, 10% CO_2. Four hours later, the transfection medium was removed and replaced with normal Phoenix medium. Medium was again replaced after 24 hours with 6ml of fresh medium and the cells were left ON to produce the virus. Five ml of viral supernatant was then collected from each plate, polybrene [Sigma H9268] was added at a final concentration of 8μg/ml and the solution was filtered to remove cellular debris before adding to the sub-confluent SC plates. Phoenix cells were topped up with an extra 5ml of fresh medium to continue virus production. Schwann cells (which had been plated at a density of $6x10^5$ cells per 10 cm dish the previous day) were incubated for 3 hours with the viral supernatant, then left to recover ON in normal 3% medium. Twenty-four hours later, a second 3-hour infection was carried as just described. Infected cells were left to recover for 2 days in normal medium and then cultured for 6 days in medium containing puromycin (1μg/ml), to remove non-vector expressing cells. Selective medium was replaced every 2-3 days.

2.4.5 shRNA oligos design and vector cloning

ShRNA oligos targeting MKP3 were design using the Clontech RNAi designer (http://bioinfo.clontech.com/rnaidesigner/sirnaSequenceDesign.do). Briefly, the online program designs shRNA duplexes suitable for cloning into retroviral expression vectors by identifying a 19bp sequence targeting the gene of interest, which is then incorporated into longer 66bp oligos that contain BamHI and EcoRI overhangs for insertion into the pSIREN vector, plus a MluI restriction site for insert identification. The target sequences and the shRNA duplexes generated are shown in Table 2-4.

ShRNA duplexes were purchased from Sigma and cloned into the retroviral expression vector RNAi-Ready pSRIEN-RetroQ Vector [Clontech 631526]. Preparation of the shRNA expression vectors were carried out according to manufacturer's instructions:

1) shRNA duplexes were annealed by mixing 100μM of each shRNA oligo (reverse and forward) in a 1:1 ratio and heating to 95°C for 30 seconds, followed by gradual cooling over 6 minutes;

2) Annealed shRNAs were diluted to 0,5μM concentration (1:100 dilution) in TE buffer and then ligated to the linearized vector by incubating the following mixture at room temperature for 3 hours:

- 2μL pSIREN-RetroZ Vector (25ng/μL)
- 1μL shRNA oligos (0,5μM)
- 1,5μL T4 DNA ligase buffer (10x)
- 0,5μL BSA (10 mg/mL)
- 9,5μL nuclease-free water
- 0,5μL T4 DNA ligase enzyme (400 U/mL)

A ligation reaction was set up as above for each of the MKP3 target oligonucleotides, control shRNA, plus a vector-only control.

3) Each ligation reaction was transformed into competent HB101 bacteria by adding 2μL ligation mixture to 50μL of bacterial cell suspension, incubating on ice for 5 minutes and then heat shocking at 42°C for 30 seconds in a water bath before replacing on ice.

4) Transformed bacteria were grown in 250μL of SOC medium, shaking for 1 hour at 37°C. 30μL of each transformation was then spread onto agar plates containing the selection antibiotic ampicilin and incubated at 37°C ON.

5) 3 to 4 well separated colonies were picked from each plate and grown up in small starter cultures of LB medium+ampicilin for 8 hours.

6) Plasmids were then isolated and purified from the bacteria using the Mini-Prep kit [Qiagen] and digested to check the presence of the shRNA insert (see below).
7) Once the presence of the insert was confirmed by restriction digest, 0,5 mL of the starter culture was inoculated into 250mL LB medium+ampicilin and grown up at 37°C ON with vigorous shacking. Plasmids were purified from these bacterial cultures by Maxi-Prep [Qiagen] and kept as a stock dissolved in TE and frozen at -20°C.

Restriction enzyme digests

Restriction digest to check for the presence of an Mlu1-containing insert were carried out on plasmids from 3-4 colonies. All buffers and restriction enzymes were obtained from Promega. Restriction digests were performed at 37°C for 1 hour in 20μl reactions containing the following:

μl	**Reagent**	**Final**
	DNA	0.5-1.0 μg
0.5	Enzyme (10u/μl)	5u
2.0	10x reaction buffer	
0.2	BSA (10mg/ml)	0.1 mg/ml
	Water	to 20μl

The MKP3 shRNAs plasmids stocks from the Maxi-prep, having been checked at the mini-prep stage for Mlu1 sites by restriction digest, were further verified by sequencing.

2.5 DNA/RNA manipulation

2.5.1 DNA extraction from animal tissue

Genomic DNA was extracted from ear notches. Animal tissue was lysed ON at 55°C in 400μL of Lysis Buffer (100mM Tris-HCl pH8.5, 5mM EDTA, 0.2% SDS and 200mM NaCl) and 4μL of Proteinase K [Roche] (1:100). Following lysis, 50 μL were rapidly frozen in dry ice and the SDS pelleted by 15 minutes of centrifugation at 13000 rpm at 4°C. Supernatant was used for PCR reactions.

2.5.2 PCR/ Genotyping

Mice were genotyped by PCR. Reactions were set up using 1μL genomic DNA in a final volume of 25 μl. Reactions were set up as described in Table 2-7 using Promega Taq polymerase. Primers used for PCR reactions are detailed in Table 2-1.

	Nf1 flox	*Nf1* +/-	*P0*	*YFP*
Buffer 5X	5	5	5	5
$MgCl_2$ (50mM)	4.2	2.5	1.5	2
Primers (10μm)	1	1	2.5	1
dNTPs (10mM)	0.5	0.5	0.5	0.5
Taq pol (U)	0.2	0.2	0.2	0.2
H_2O	13.1	14.8	14.3	15.3

Table 2-7 Genotyping PCR reactions

and the program:

- 94°C for 3 min;
- 94°C for 30 sec
- 55°C for 1 min } X 35
- 72°C for 2 min
- 72°C for 10 min
- 4°C

2.5.3 RNA extraction from cultured cells

Total RNA was isolated using Trizol Reagent (Ambion), according to manufacturer's instructions, and precipitated in isopropanol. Following precipitation, salts and contaminants were washed away with 70% ethanol and RNA was eluted in RNAse free H_20.

2.5.4 cDNA synthesis

The SuperScript™ II Reverse First-Strand Synthesis System (Invitrogen) was used with random hexamers to reverse transcribe 500ng-1 μg of RNA to produce cDNA for quantitative RT-PCR reactions. Reactions containing RNA, 1μl random hexamers and 1μl of 10mM dNTPs were made up to 12 μl with DEPC treated water, incubated at 65°C for 5 minutes and placed on ice for > 1 minute. A reaction mix was then prepared containing 2μl 10xPCR buffer, 4μl of 25mM $MgCl_2$, 2μl of 0.1M DTT for n x reactions and 9μl of this reaction mix was added to each sample and incubated at 25°C for 5 minutes. 1μl of RT (200U/μl) was then added to each tube and incubated for 10 minutes at room temperature and then at 42°C for 50 minutes. The reactions were terminated at 70°C for 15 minutes and then chilled on ice. Finally, 1 μl RNase H

(2U/μl) was added to each tube and incubated at 37°C for 20 minutes to degrade the RNA strands.

2.5.5 qPCR

Quantitative PCR was performed using the DyNAmo SYBR Green qPCR Kit (Finnzymes, NEB) and the Opticon 2 DNA engine (MJ Research). PCR reactions (25μl) contained 10μl of PCR Sybr Green mix and 0,5μL of each sense and anti-sense 10mM primers. All reactions were performed in duplicate. Intron-spanning gene-specific primer pairs were designed using the OligoPerfect™ Designer [Invitrogen]. Cycle parameters were as follows: 10 min at 95°C for Taq activation, followed by 35 cycles of 15 sec at 95° C for denaturation, 20 sec at 58°C for annealing, 20 sec at 72° C and 1 min at 77°C for annealing/extension. Relative expression values for each gene of interest were normalized to *B2M* and calculated as follows: $2^{-\Delta\Delta Ct}$ where $\Delta\Delta Ct = \Delta Ct_{(gene\ interest)} - \Delta Ct_{(normalizer)}$

2.6 Protein analysis

2.6.1 Protein extraction from tissues

Sciatic nerves were frozen in liquid nitrogen immediately after dissection. Frozen nerve samples were homogenised in liquid nitrogen, using and Eppendorf tube micro-pestle. Samples were lysed in directly in Laemli buffer, boiled and passaged through an insulin syringe.

2.6.2 Protein extraction from cultured cells

Cells were washed 1x in PBS and scraped off the dish in 1ml PBS with a rubber bung. Cell pellets were collected by spinning at 4°C in a cooled microfuge at 13,000 rpm and pellets were snap frozen in liquid nitrogen. Harvested cell pellets were lysed in RIPA buffer (Table 2-8) and samples vortexed and incubated on ice for 15 minutes, vortexing every 5 minutes. Lysates were centrifuged at 13,000 rpm for 15 minutes at 4°C to remove cell debris and supernatants were transferred to fresh 1.5ml tubes on ice. Protein concentrations were measured against standard BSA solutions using the BCA microplate assay [Pierce] and RIPA added to normalise protein concentrations in all samples. 4x sample buffer was then added and samples boiled for 5 minutes at 95°C to denature proteins.

Solutions	Components and additional information
RIPA lysis buffer	1% Triton X-100, 0.5% sodium deoxycholate, 50mM Tris pH7.5, 100mM NaCL, 1mM EGTA pH8, 20mM NaF, 100μg/ml PMSF, 15μg/ml aprotonin, 1mM Na_3VO_4.
4x Sample buffer	200mM Tris pH 6.8, 8% SDS (BioRad), 40% glycerol, 400mM DTT, 0.25% bromophenol blue.
10x Running buffer	2.5M glycine (BDH), 250mM Tris, 1% SDS.
10x Transfer buffer	200mM Tris, 1.5M glycine, 20% methanol (BDH)
Blocking solution	5% milk, 0.05% Tween-20 (BioRad) in PBSA
Stripping buffer	200mM glycine, pH2.5, 0.4% SDS.
1x PBSA Tween wash	0.05% Tween-20 in PBSA
20x TBS Tween	200mM Tris pH8, 3M NaCl, 1% Tween-20
PBSA	137mM NaCL, 2.7mM KCL, 1.47mM KH_2PO_4, 8.1mM NA_2HPO_4
20X TBS	200mM Tris pH8, 3M NaCl

Table 2-8: Solutions for protein extraction and Western blotting

2.6.3 SDS-PAGE and Western blotting

Protein samples were loaded onto polyacrylamide gels and resolved by SDS gel electrophoresis (SDS-PAGE). 10% gels were used, except for NF1 in which 5% gels were used. Proteins were transferred to PVDF membrane [Millipore] using transfer apparatus (see Table 2-6). Membranes were blocked for 1 hour at room temperature or overnight at 4°C. Blots for re-probing were washed in stripping buffer for 20 minutes and blocked in milk. Blocked membranes were incubated overnight in primary antibody in block solution in rolling 50ml Falcon tubes. Membranes were then washed in TBST and incubated for one hour with horseradish peroxidase-conjugated secondary antibody diluted in milk block. Membranes were then washed 4x in TBST and once in TBS before chemiluminescent detection using ECL Plus™ reagent [GE Healthcare].

2.7 Microscopy

2.7.1 Tissue processing

For histological analysis, both paraffin section and frozen sections were used. For paraffin sections, mice were sacrificed and sciatic nerves were dissected, post-fixed in 10% formalin for 24 hours at 4°C and processed for paraffin embedding (see below). Sciatic nerves were cut longitudinally or transversally at 8 μm using a microstat [Leica].

For frozen sections, sciatic nerves were dissected and fixed for 2 hours in 4% paraformaldehyde (PFA) [TAAB] at room temperature. Fixed nerves were cryoprotected in 30% sucrose in PBS overnight at 4°C, transferred to a 1:1 mixture of 30% sucrose with O.C.T compound [TissueTek, Sakura] and finally embedded in O.C.T and snap-frozen in liquid nitrogen. 8-12 μm thick longitudinal or transversal sections were cut using a cryostat [Leica].

2.7.2 Histology and Tumour Grading

For hematoxylin and eosin (H&E) histology analysis, sciatic nerves were harvested and fixed in 10% formalin ON at 4°C. Nerves were then rinsed in water and then dehydrated through a graded ethanol series: 70%, 80% and 95% ethanol washes (30 minutes each), followed by 3 washes in 100% ethanol (15, 30 and 45 minutes). Nerves were then washed twice in xylene for 15 minutes total and incubated in paraffin at 60°C for two hours. A second incubation in fresh paraffin [VWR] was performed for 1 hour before final inclusion in paraffin.

8μm thick sections were cut using a microstat, placed onto Superfrost (VWR) slides and deparaffinized. For deparaffinization, slides were first incubated at 62°C for 2-3 minutes and then placed in xylene for 2 minutes (2X). Next, sections were rehydrated through a graded ethanol series to water (2 washed in 100% ethanol for 2 minutes, one wash in 95% for 2 minutes, one wash in 70%, ethanol, final rinse in cold tap water).

2.7.3 Hematoxylin/Eosin staining

Rehydrated sections were overstained with hematoxylin [Sigma] for one 2 minutes. Excess stain was removed by washing in tap water for 5 minutes. Sections were then destained for a few seconds in acidic ethanol (95ml absolute ethanol and 5ml HCl 10M) and washed in ethanol 70% for 3 minutes. Eosin [Sigma] staining was performed for 10 seconds. Slides were then dehydrated through a series of ethanol and xylene: 3 washes in ethanol 95% (5 minutes each); 2 washes in ethanol 100% (2 minutes each) and 2 washes in xylene (2 minutes each) before mounting in DPX [VWR].

2.7.4 Alcian blue

Sections of paraffin-embedded sciatic nerves were rehydrated as described above, stained with Alcian blue pH 2,5 for 15 minutes and then rinsed in distilled water. Sections were then dehydrated trough a series of ethanol grades and mounted in DPX.

2.7.5 X-gal staining

Sciatic nerves from *P0:LacZ* mice were dissected, fixed in lacZ fixative (1% formaldehyde; 0,2% glutaraldehyde; 2mM $MgCl_2$; 6mM EGTA in PBS) for 1 hour, followed by cryoprotection in 20% sucrose/PBS ON at 4°C. Nerves were then embedded in OCT and frozen in liquid nitrogen. 8 μm section were cut and washed 3X 30 min in LacZ wash buffer (1ml 1M $MgCl_2$; 5ml 1% Sodium deoxycholate; 5 ml 2% Nonidet-P40; 489 ml PBS w/o $MgCl_2$ or $CaCl_2$). Following washes, sections were incubated in the dark at 37°C for 3-4 hours with LacZ stain (98ml lacZ wash buffer; 2ml 5mg/ml X-gal (dissolved in dimethyl-formamide); 0,21 g K-ferrOcyanide and 0,16g K-ferrIcyanide). Slides were washes in water, post-fixed in 4% PFA ON at 4°C and then dehydrated in a series of ethanol grades and xylene (see below) before mounting in DPX.

2.7.6 Immunohistochemistry

Immunohistochemistry was performed in paraffin sections. Nerve sections were deparaffinized, rehydrated, and subjected to antigen retrieval: slides were submersed in a 10mM citrate buffer solution (pH 6,0) and heated in a microwave until boiling. After 5 minutes at room temperature, slides were transferred to a fresh sodium citrate solution and boiled again. A second 20 minutes incubation at RT was performed before permeabilization. Section were permeabilized with 0.5% TritonX in PBS for 30 minutes and blocked in 10% Goat serum for 1 hour. Before incubation with primary antibodies, the endogenous peroxidase activity was quenched by incubating slides with 3% H_2O_2 for 10 minutes at RT. The primary antibodies (dilutions used in Table 2-5) (4°C ON) were visualized by treating the sections with HRP secondary antibodies (2 hours RT) (Table 2-6), followed by incubation with 3.3'-diaminobenzidine substrate per manufacturer's protocol [Vector Labs]. Sections were then, in most of the experiments, stained with H&E (see below), dehydrated and mounted in DPX medium.

2.7.7 Immunofluorescence

Immunofluorescence was performed in both frozen and paraffin sections. Nerves sections were processed as described above, permeabilized in 0.3% Triton in PBS for 30 min, blocked in 10% goat serum/PBS for ≥1 hour and incubated in primary antibodies in blocking buffer overnight at 4°C. Following staining with primary antibodies, sections were washed 3 times with PBS and detection was performed using the appropriate fluorescent secondary antibodies (Tabe 2-6), for 2 hours at RT. Nuclei

were counterstained with Hoechst or DAPI in PBS and mounted in FluormountG [Southern Biotechnology Associates].

For p-ERK immunofluorescence, sciatic nerves were dissected and directly snap frozen in OCT and liquid nitrogen. Cryosections (14μm thick) were post-fixed in PFA for 10 minutes. Following incubation with the primary and the HRP-conjugated secondary antibody, the signal was amplified using the tyramide signal amplification kit [Invitrogen].

Imaging was performed on a Zeiss Axioskop 2 [Zeiss], with OpenLab software [Perkin Elmer] (immunohistochemistry). Confocal microscopy was performed using a Leica TCS SPE Confocal Microscope, with accompanying Leica LAS AF software (immunofluorescence).

2.7.8 Semi-thin and ultra-thin preparation

Sciatic nerves were dissected and fixed ON at 4°C with 2% glutaraldehyde in 0.2M phosphate buffer. Nerves were then post-fixed in osmium tetroxide for 1.5 hours at 4°, followed by 45 minutes in 2% uranyl acetate at 4°C. Nerves were then dehydrated in an ethanol series before embeddeding in epoxy resin. Semi-thin sections were cut with a glass knife at 0.3 μm and stained with 1% toluidine blue in 2% borax at 75°C for 2 minutes, for visualization. Ultra-thin sections were cut with a diamond knife at 70 nm, collected onto formvar coated slot grids and visualized using transmission electron microscope (TEM).

2.8 Administration of substances

2.8.1 Tamoxifen administration

Tamoxifen [Sigma] was dissolved in sunflower oil (20mg/mL) and filtered through a 0.2μm filter. Controls and mutant mice, aged 4-5 weeks old, received intraperitoneal injections (i.p.) of 2mg of Tamoxifen (100μL) once a day for 5 consecutive days.

2.8.2 Edu incorporation assay

Cell proliferation was measured by 5-ethynyl-2'-deoxyuridine (EdU) incorporation [Invitrogen]. Mice were pulsed with 2mg of EdU three times; 48h, 24h and 4 hours before sacrifice. Sciatic nerves were dissected and processed for immunostaining with the appropriate primary and secondary antibodies. Following immunostaining, nerves were post-fixed in PFA for 10 min, washed in PBS and permeabilized in 0.3% Triton for

15 min. Edu staining was performed using the EdU kit [Invitrogen] according to the manufacturer's instructions.

2.8.3 PD 0325901 administration

200mg of the MEK inhibitor PD 0325901 [LC labs] were reconstituted in 400 μL of DMSO and then dissolved in 0.5% hydroxylpropyl methylcellulose plus 0.2% tween. NF1 mutants received i.p. injections of PD 0325901 at a dose of 8mg/Kg, once a day for 14 days, beginning 48 hours following surgery. In the control group, NF1 mutants received i.p. injections of vehicle only (DMSO in hydroxylpropyl methylcellulose solution).

2.9 Sciatic nerve transection

The right sciatic nerve of anaesthetized 6-7 weeks mice (Isofluorane), was exposed at the sciatic notch. The nerve was partially transected and the wound closed with clips. The entire nerve was recovered 7 days or 6-8 months after surgery. Nerves were immediately fixed in 4% PFA for immunohistochemistry or frozen in liquid nitrogen for protein analysis. Contralateral nerves were used as unlesioned control samples. A schematic is shown in Figure 2-1.

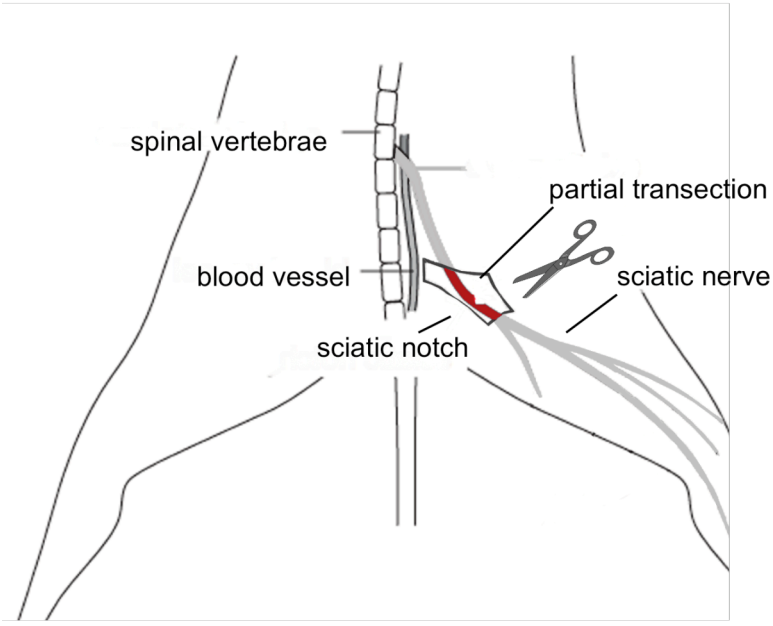

Figure 2-1. Schematic representation of the partial transection performed in the right sciatic nerve.

2.10 Statistical analysis

The data are represented as mean values plus/minus standard error of the mean (SEM). One-way ANOVA with post-hoc Bonferroni tests were used for statistical analysis in all experiments, except the one depicted in Figure 6-6 in which data were analysed using Repeated Measures ANOVA with post-hoc Newman-Keuls analysis (*$p \leq 0.05$; ** $p \leq 0.01$; *** $p \leq 0.001$). All statistical analyses were performed in Prism4 (GraphPad).

Chapter 3: Results I

3.1 Chapter introduction

A cell to be rendered tumourigenic has to acquire the ability to evade the mechanisms that control cell proliferation, growth and survival. It is widely accepted that genetic and/or epigenetic lesions are crucial in providing cells with these capabilities. However, the outcome of the initial genetic lesion is now known to be strongly dependent on the combinatorial action of a variety of cell-intrinsic and cell-extrinsic factors. Thus, activation of the same oncogenic pathway in different cellular contexts may have profoundly distinct tumourigenic potentials (Visvader, 2011). Similarly, a specific genetic lesion occurring at different developmental stages of a cellular target may have very different outcomes (Guerra et al., 2007). In addition to cell-intrinsic determinants, the interactions between the genetically altered cells and the surrounding microenvironment can be critical in determining if the early genetic changes will progress to the development of frank tumours.

It is well established that neurofibromas arise from Schwann cells that undergo LOH at the *NF1* locus. What has been less clear is the cell type within the Schwann cell lineage in which *NF1* LOH occurs. The development of conditional mouse models in the past few years has allowed this question to be addressed. Using different genetic murine models, three different groups have induced loss of *Nf1* at different developmental stages and demonstrated that neurofibromas can develop from differentiated, non-myelinating Schwann cells, but only when *Nf1* loss occurs during a limited time window (E12.5-E13.5) (Joseph et al., 2008; Wu et al., 2008; Zheng et al., 2008). However, it is still not clear how these studies translate to the human disease. Moreover, the heterogeneity of neurofibroma formation at the level of number, severity and location, may be indicative of the existence of different cells of origin.

To address this possibility, we sought to test if fully differentiated, myelinating Schwann cells have tumourigenic potential. Furthermore, we wanted to investigate the controversial issue of whether *Nf1* haploinsufficiency affects the outcome of *Nf1* loss in adult Schwann cells. It is relevant to mention that during the course of this study, two articles addressing somewhat similar questions to those addressed in this thesis were published (Le et al., 2011; Mayes et al., 2011). Their findings, and how they relate to this work, will be discussed later, in Chapter 7.

3.2 Generation of a mouse model in which *Nf1* loss is induced specifically in myelinating Schwann cells in adult mice

To test if *Nf1* loss in adult myelinating Schwann cells (mSCs) could elicit tumour formation, we needed a system in which *Nf1* disruption could be spatially and temporally controlled. To do this, we employed the well-documented Cre-lox technology. The Cre-lox mechanism requires two components, a) the enzyme Cre recombinase that catalyzes recombination between two *loxP* sites, and b) two *loxP* sites that consist of specific 34-base pair long DNA sequences. By mating mice expressing Cre under ubiquitous or specific promoters, with mice carrying genes in which *loxP* sites have been introduced via homologous recombination, genetic modifications can be achieved (Nagy, 2000).

In order to specifically target myelinating Schwann cells, we selected a conditional transgenic mouse line expressing the Cre recombinase (Cre-ERT2) under the myelinating Schwann cell specific promoter - *P0* (Leone et al., 2003) (Figure 3-1Bi). The *P0-CreERT2* mice express a Tamoxifen-inducible variant of Cre recombinase. In this inducible system Cre is fused to a mutated estrogen receptor ligand-binding domain (ER). The CreER fusion protein is not able to bind endogenous estrogen but does bind to the synthetic ligand 4-hydroxy-Tamoxifen (4-OHT), produced in the liver by Tamoxifen (Tmx) hydroxylation. The CreER fusion protein expressed by these mice is incapable of entering the nucleus due to binding to HSP90 and is therefore rendered inactive. In the presence of the ligand 4-OHT, HSP90 is released and CreER translocates into the nucleus where it exerts its enzymatic activity (Figure 3-1C).

We initially characterized the ability of P0Cre to ablate genes of interest in the PNS by crossing it into the Rosa26 Reporter LacZ (*R26R-LacZ*) (Figure 3-1A). This reporter strain contains a targeted insertion of the *LacZ* gene, preceded by a *loxP*-flanked transcriptional termination sequence (tpA), into the ubiquitously expressed Rosa26 locus (Soriano, 1999). Upon Tmx treatment, the termination sequence is removed, inducing the expression of the β-galactosidase (β-gal) protein (Figure 3-1B ii).

Five to six week-old mice were administrated 2mg of Tmx a day over a period of 5 consecutive days, since this protocol had proven to be the most efficient at inducing Cre activity by Leone and colleagues (Leone et al., 2003) (Figure 3-1D). *P0Cre*-mediated recombination, revealed by X-gal staining, was detected 15 days following the first Tmx injection (d15pTmx) in sciatic nerves of *P0:LacZ* mice (Figure 3-2A). The need to use substrates to visualize β-gal made it difficult to co-label the tissues with Schwann cell markers, affecting the accuracy in assessing the efficiency of Cre activity.

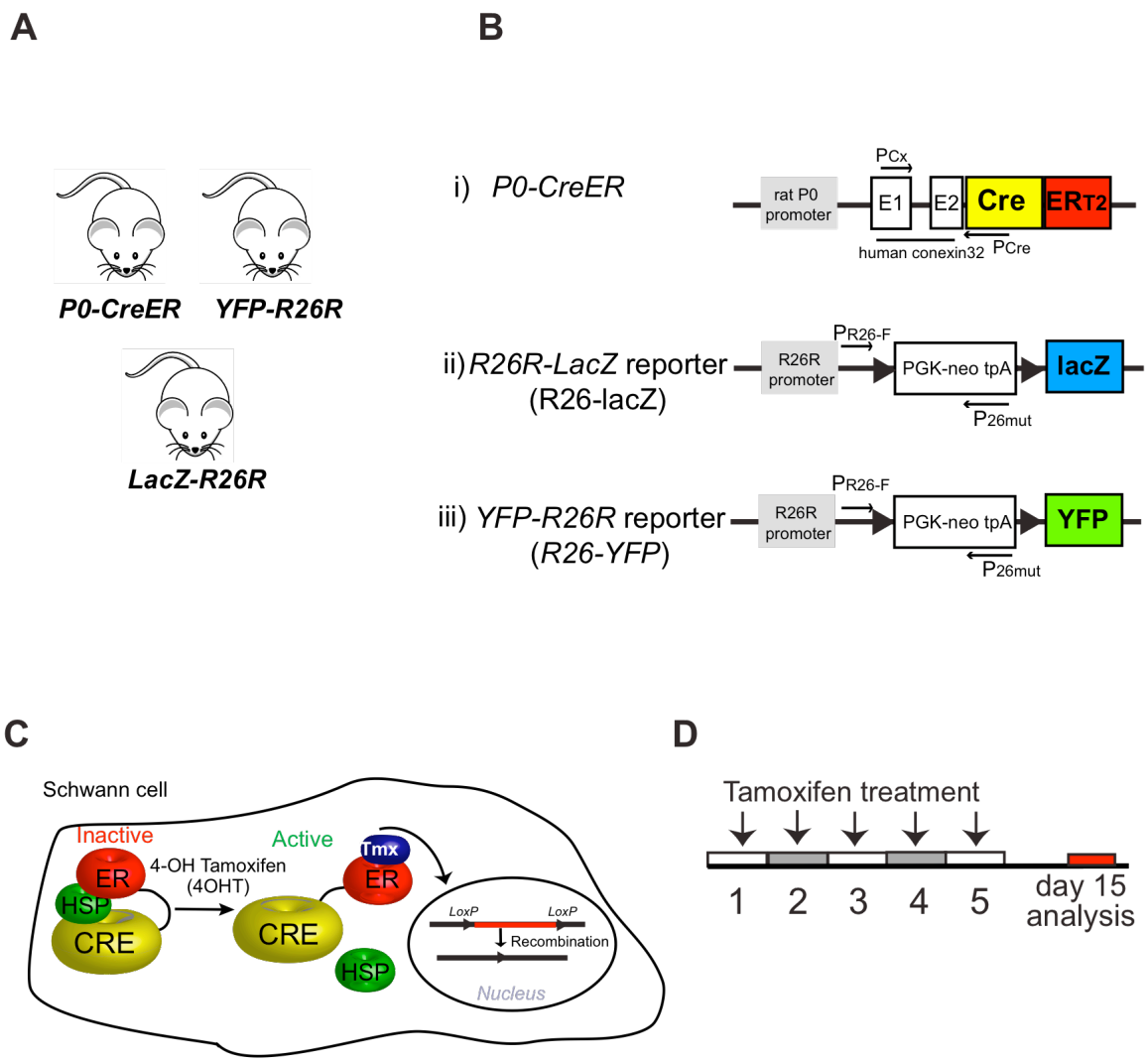

Figure 3-1: Characterisation of transgenic mice expressing an inducible Cre recombinase in the peripheral nervous system. **A**) *P0-CreER* mice were crossed with mouse reporter lines *R26R-LacZ* and *R26R-YFP*. **B**) Schematics of: (i) the *P0-CreER* construct; (ii) the modified Rosa26 locus in the *LacZ-R26R* and in the *YFP-R26R* mice (iii). Arrows indicate primers used for PCR analysis. Arrowheads represent loxP sites. **C**) Model of CreER regulation: in the presence of 4-OH Tamoxifen, the CreER fusion protein is released from HSP90 and translocates into the nucleus where it mediates recombination using the *loxP* sites. **D**) Protocol of Tamoxifen administration.

Furthermore, the efficiency of Cre recombination is known to vary depending on the target gene (for example, the distance between the two loxP sites) (Richardson et al., 2011). Therefore, we decided to make use of a second reporter mouse – *R26-YFP*, structurally similar to the *R26-LacZ*, except that it contains the yellow fluorescent protein gene in the place of *LacZ* (Srinivas et al., 2001) (Figure 3-1B iii). *P0-CreER* mice were crossed with *R26-YFP* and their progeny treated with Tmx. Fifteen days later, sciatic nerve cryosections were immunostained for GFP (that labels YFP) and the mSchwann cell marker, P0. As shown in Figure 3-2B and quantified in Figure 3-2C, the percentage of P0 positive cells that were also positive for Cre activity was variable between animals, ranging from a minimum of 15.3% to a maximum of approximately 50%. The reason for this variability is not known, but may result from batch variations of Tmx.

In the *P0-CreER* transgenic, Cre recombinase is driven by the well-characterized 1.1kb *P0* rat promoter fused to the 5'-untranslated region of the human connexin32 gene upstream of *CreER* (Messing et al., 1992; Messing et al., 1994) (Figure 3-1Bi). The activity of the *P0* promoter has previously been documented as being confined to myelinating Schwann cells, whilst being inactive in non-myelinating Schwann cells (Messing et al., 1992). Nevertheless, to confirm the specificity of the cells targeted by the *P0-CreER* driver, we co-stained sciatic nerves from Tmx treated animals with GFP and the marker of non-myelinating or dedifferentiated Schwann cells, p75. Four-hundred-eighty p75 positive cells from 6 different animals were counted, and we failed to find a single p75+GFP+ cell, confirming the specificity of the promoter to myelinating Schwann cells (Figure 3-3A). As mentioned in Chapter I, following injury to the PNS, Schwann cells revert to a dedifferentiated, progenitor-like state characterized by the expression of the p75 receptor, amongst other markers. Therefore, as a positive control, we analysed sciatic nerves from *P0:YFP* mice seven days following nerve transection and confirmed the co-localization of p75 and GFP (Figure 3-3A iv).

Once characterized, *P0-Cre*ER transgenics were mated with mice homozygous for the conditional *Nf1* allele ($Nf1^{fl/fl}$), in which *loxP* sites flank *Nf1* exons 31 and 32 (Zhu et al., 2001) (Figure 3-4A and 3-4B-i). Importantly, exon 31 is frequently found mutated in NF1 patients. These are well-characterized animals in which *Nf1*flox ($Nf1^{fl}$) has been shown to represent a functional conditional allele: $Nf1^{fl}$ behaves as a wild-type allele and once floxed, is a phenocopy of the null allele (Zhu et al., 2001). Finally, we also crossed *P0- CreER* to $Nf1^{fl/-}$ mice in which only one *Nf1* allele is functional (flox) and the second has been rendered null by integration of a knockout (KO) cassette at exon 31

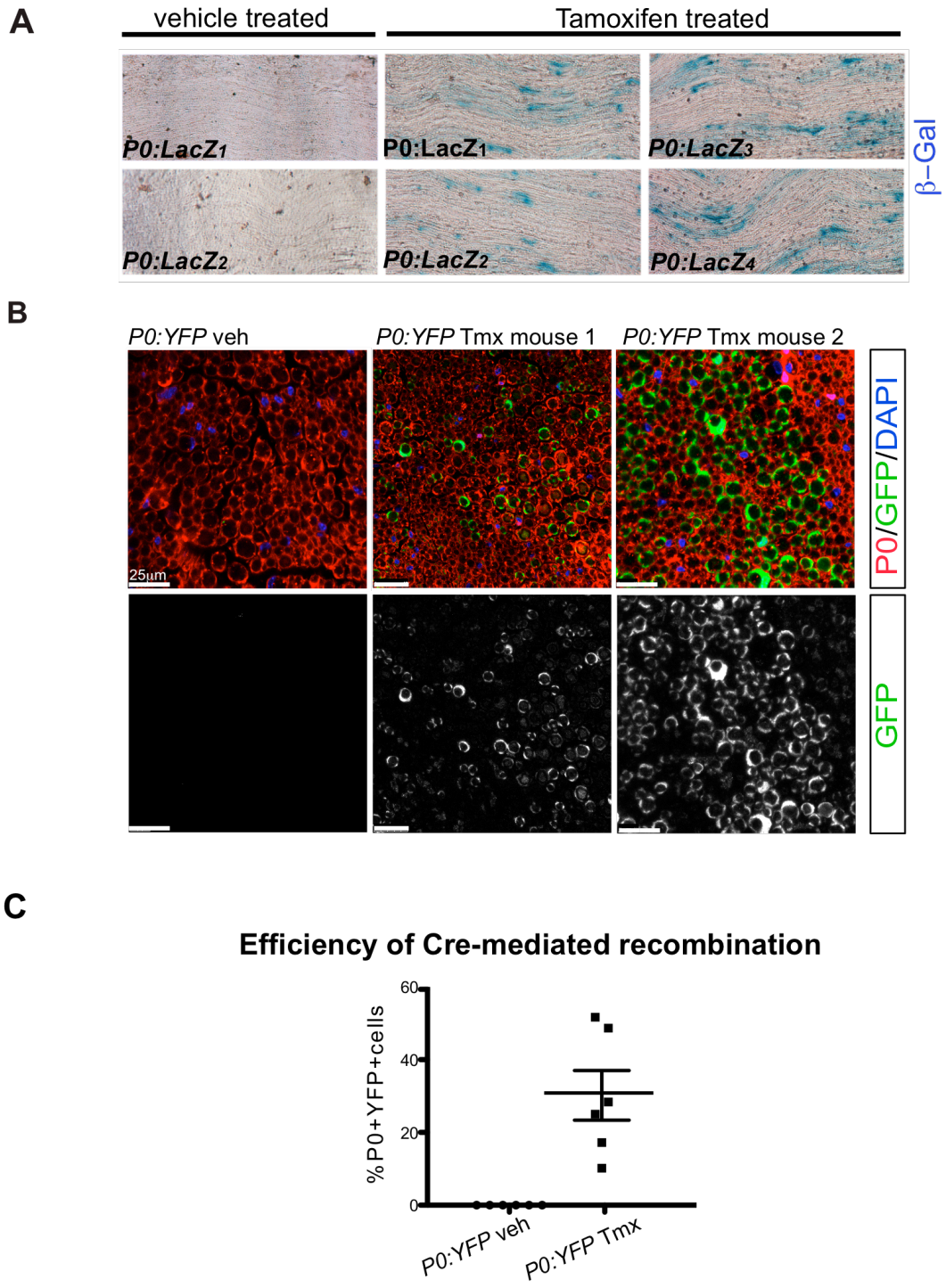

Figure 3-2: Cre drives recombination in myelinating Schwann cells when expressed under the *P0* promoter. **A**) X-gal staining demonstrates Cre activity in sciatic nerves of 4 different *P0:LacZ* mice, 15 days following Tamoxifen administration. Vehicle treated mice were used as controls. **B**) Efficiency of Cre activity shows variability between animals. Frozen sections of *P0:YFP* sciatic nerves were stained for the Schwann cell marker P0 (red) and GFP (green). Nuclei were counterstained with DAPI. Controls were performed in *P0:YFP* mice injected with vehicle. Two different mice, representative of the variability in Cre activity are shown. **C**) Quantification of the percentage of P0+GFP+ cells in 7 different animals. Graph shows mean ±SEM.

A

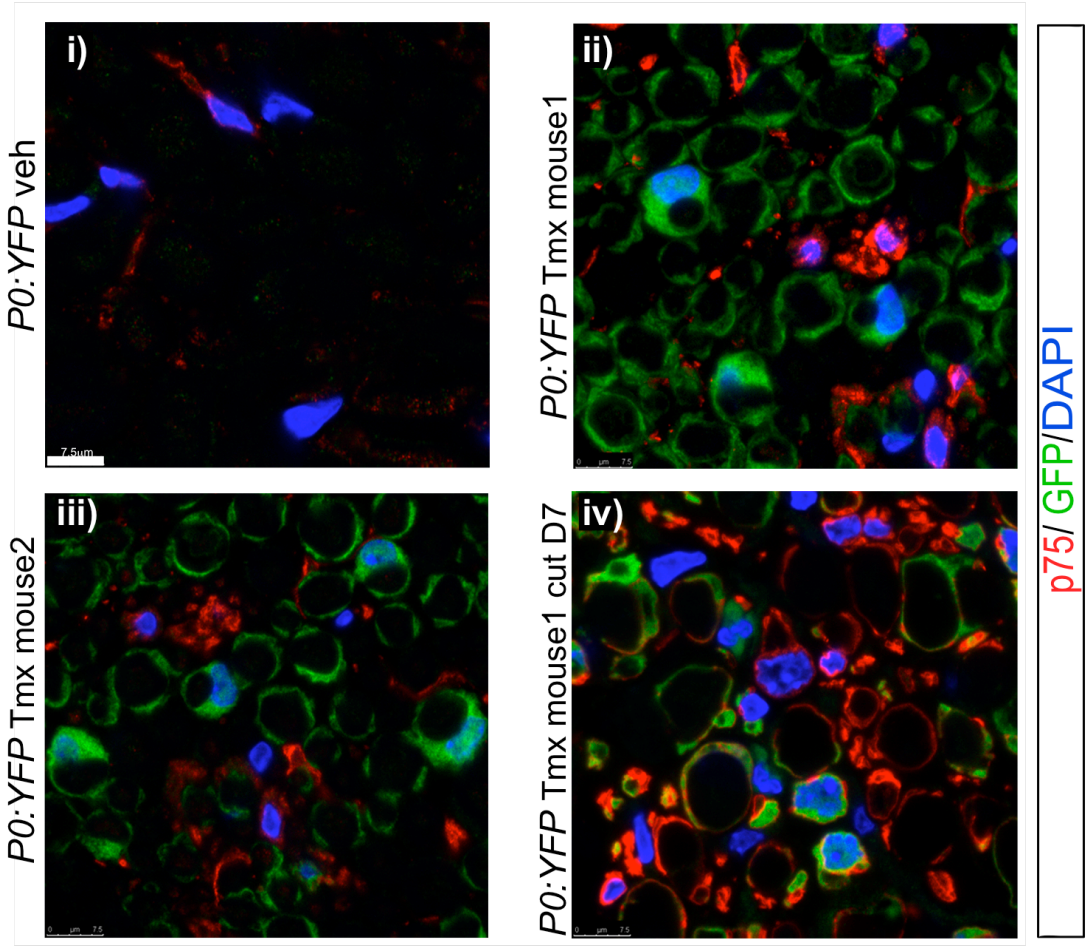

Figure 3-3: *P0-CreER* mice do not exhibit recombinase activity in non-myelinating p75+ Schwann cells. **A**) Sciatic nerve cryosections of Tmx-treated *P0:YFP* animals were stained for GFP (green) and for the non-myelinating/dedifferentiated Schwann cell marker p75 (red). No co-localization was found in intact nerves. Two mice are shown (**ii** and **iii**). Negative controls were performed in vehicle treated *P0:YFP* mice (**i**). **iv** shows injured nerves from Tmx treated mice in which dedifferentiating GFP positive cells are found to co-localize with p75, 7 days following nerve transection. 480 p75+ cells from 6 different animals were analysed and no p75+GFP+ cells were found in uninjured nerves.

(Brannan et al., 1994). This strategy yielded *P0-Nf1*$^{fl/fl}$ and *P0-Nf1*$^{fl/-}$ mice (referred as NF1 mutants). In both mutant mice, activation of Cre produces *Nf1*$^{-/-}$ Schwann cells, however, while in *P0-Nf1*$^{fl/fl}$ all other cells in the animal are *wild-type, P0-Nf1*$^{fl/-}$ mice have a heterozygous background and this more faithfully resembles the human pathogenesis (NF1 patients are haploinsufficient for *NF1*). By using both wild-type (*Nf1*$^{fl/fl}$) and heterozygous backgrounds (*Nf1*$^{fl-/}$), we sought to dissect possible effects of NF1 haploinsufficiency on tumour development.

Throughout this thesis most of the studies described were done in *P0-NF1*$^{fl/fl}$ and *P0-NF1*$^{fl/-}$ mice, using Cre negative littermates (*NF1*$^{fl/fl}$ and *Nf1*$^{fl/-}$) as controls. Additionally, in some experiments in which selective analysis of the *Nf1*$^{-/-}$ Schwann cells was pertinent, we have used animals resulting from crosses between *P0-NF1*$^{fl/fl}$ and *P0-NF1*$^{fl/-}$ and the YFP reporter (*P0:YFP-Nf1*$^{fl/fl}$ and *P0:YFP-Nf1*$^{fl/-}$ - also designated as NF1 mutants). In these cases, *P0:YFP-Nf1*$^{+/+}$ and *P0:YFP-Nf1*$^{+/-}$ were used as controls. Figure 3-5 summarizes all the genotypes used in this study.

Once the correct genotypes were achieved through multiples crosses (Figure 3-4-C i-iii), we tested the success of P0-CreER-mediated *Nf1* recombination. To do this, we treated *P0-Nf1*$^{fl/fl}$ and *P0-Nf1*$^{fl/-}$ mice with the Tmx protocol detailed above and, 15 days later, harvested the sciatic nerves for DNA and protein analysis. A 280 bp product corresponding to the deleted *Nf1* allele (*Nf1Δ* - represented schematically in 3-4B-iv) appeared exclusively in the PCR analysis of sciatic nerve DNA from Tmx treated mutants, but not in DNA from Cre negative controls (Figure 3-4C-iv), thus confirming the genomic deletion at the *Nf1* locus. Additionally, Western blot analysis using nerve lysates revealed that neurofibromin (NF1) levels were reduced in NF1 mutants upon Tmx treatment. However, it is relevant to consider that, as I have shown before, the efficacy of Cre activity seems to vary between animals (Figure 3-2B and C) and hence it is likely that the amount of neurofibromin present in mutant mice may also be variable. Interestingly, the levels of neurofibromin do not seem to be significantly affected by *Nf1* heterozygosity.

In conclusion, we have generated a mouse model in which *Nf1* can be ablated specifically in fully differentiated myelinating Schwann cells in adult sciatic nerves.

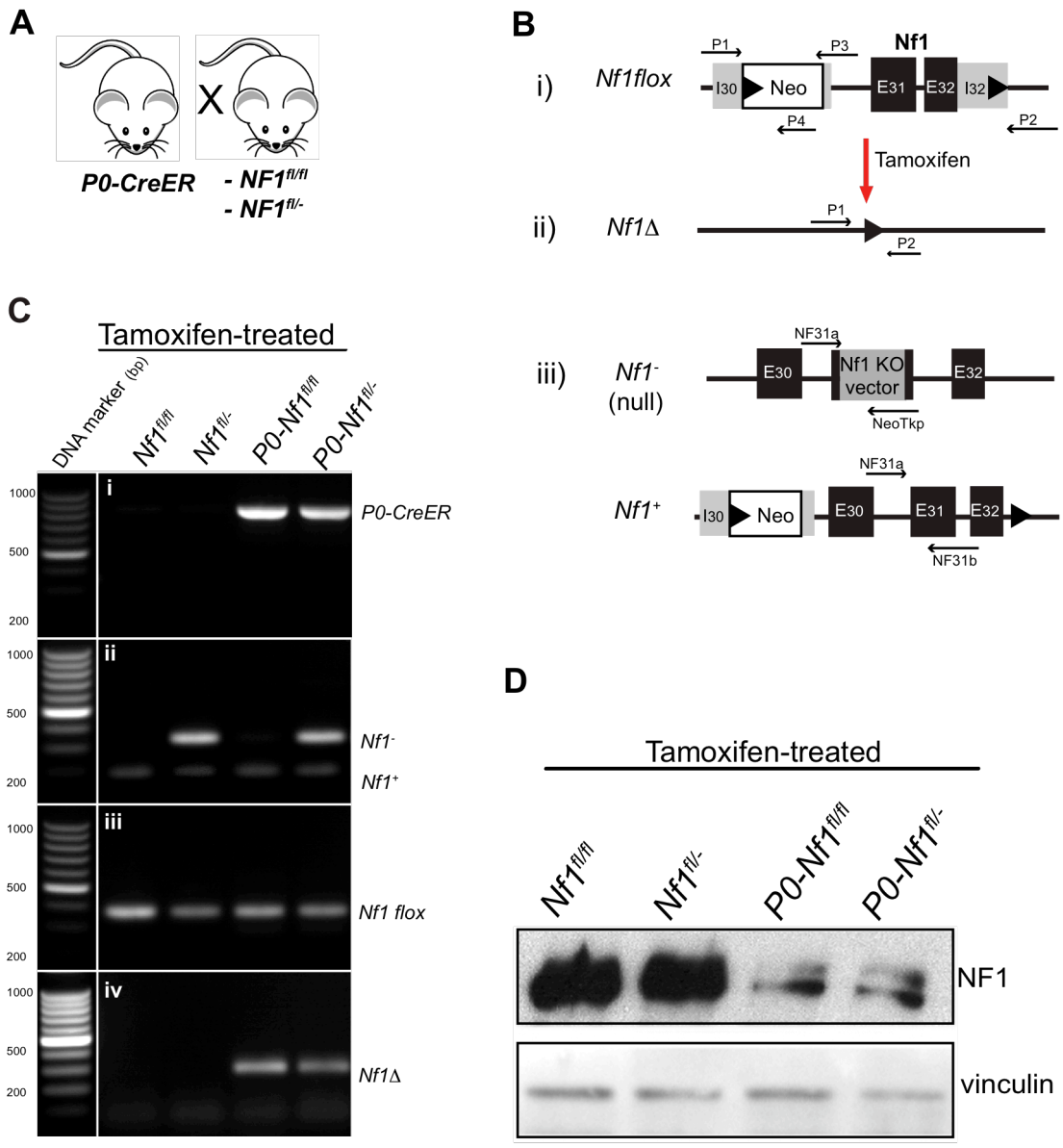

Figure 3-4: Generation of a mouse model to study *Nf1* disruption in myelinating Schwann cells, in adult peripheral nerves. **A**) *P0-CreER* mice were crossed with *Nf1*$^{fl/fl}$ and *Nf1*$^{fl/-}$ mice to generate *P0-Nf1*$^{fl/fl}$ and *P0-Nf1*$^{fl/-}$ mice. *P0-CreER* negative littermates were used as controls. **B**) Schematic representation of (**i**) the *Nf1* flox allele with two *loxP* sites (arrowheads) flanking exons 31 and 32; (**ii**) the recombined allele (*Nf1Δ*) resulted from Cre-mediated recombination and (**iii**) the *Nf1* null allele (*Nf1*$^{-}$) and the *Nf1*$^{+}$ allele in *Nf1*$^{fl/-}$ mice. Positions of the primers used are shown (arrows). **C**) PCRs detecting the presence of **i**) the *P0-CreER* construct, **ii**) the *Nf1* null and *wt* allele, **iii**) the *Nf1* floxed allele and **iv**) the recombined *Nf1Δ* allele in genomic DNA from adult sciatic nerves of Tmx treated mice. **D**) Western blot analysis of NF1 expression in mouse sciatic nerves, 15 days following Tamoxifen administration.

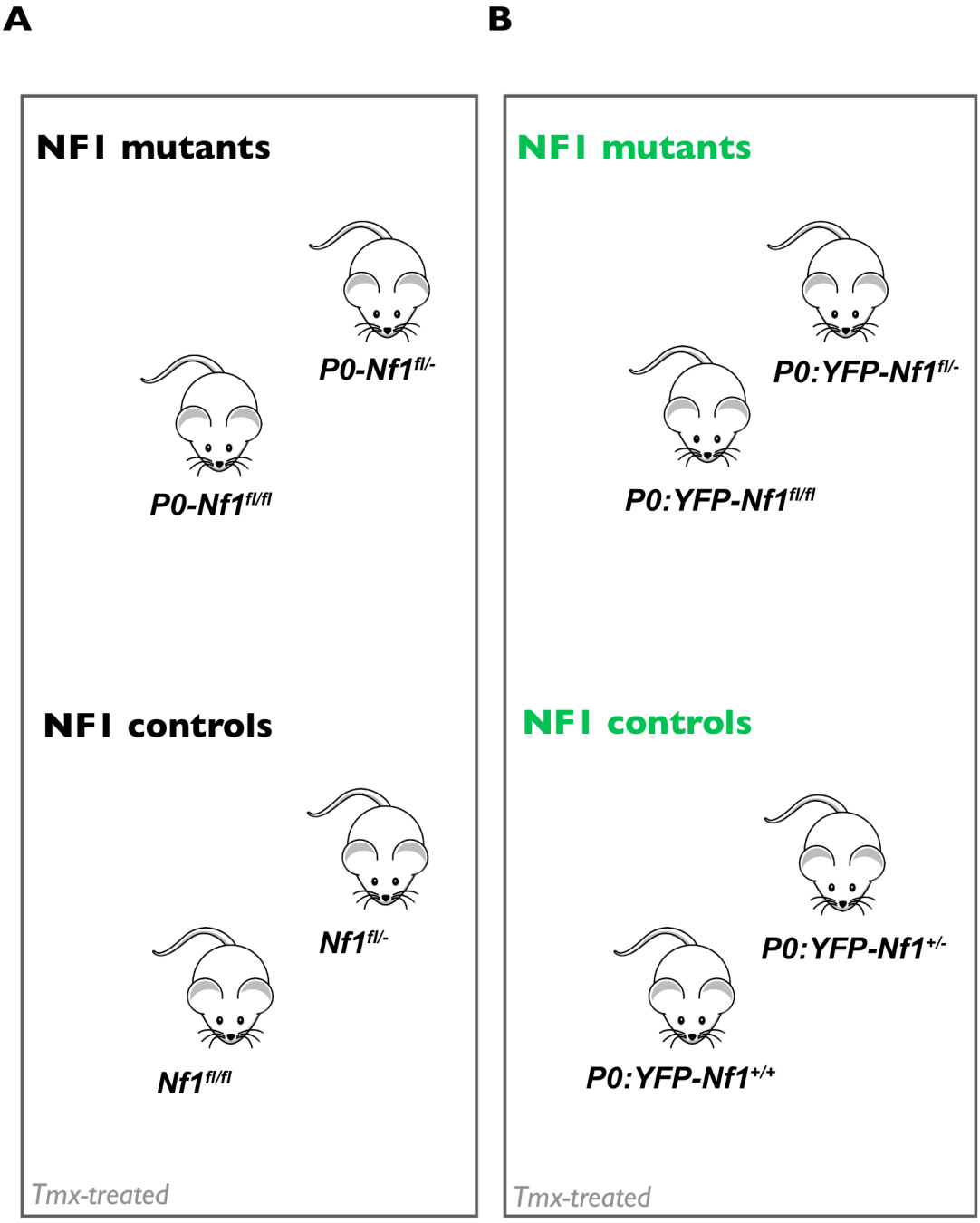

Figure 3-5: Animals used in this study. **A**) NF1 mutants *P0-Nf1*$^{fl/fl}$ and *P0-Nf1*$^{fl/-}$ were compared with Cre negative *Nf1*$^{fl/fl}$ and *Nf1*$^{fl/fl}$ littermates. **B**) In some experiments, *P0:YFP-Nf1*$^{fl/fl}$ and *P0:YFP-Nf1*$^{fl/-}$ mutants were used, instead. When this was the case, *P0:YFP-Nf1*$^{+/+}$ and *P0:YFP-Nf1*$^{+/-}$ were used as controls. All groups of mice were Tmx-treated, unless otherwise specified.

3.3 Myelinating Schwann cells are not affected by *Nf1* ablation in adult mice

We started by examining whether the selective loss of *Nf1* affects the Schwann cell differentiation state two weeks following Tmx administration, as we had previously verified that at this time-point neurofibromin levels were already reduced (Figure 3-6A). Observation of sciatic nerves from NF1 mutants showed no increase in the number of p75 positive cells, revealing that myelinating Schwann cells are not induced to dedifferentiate by *Nf1* loss (Figure 3-6B and C). Moreover, we analysed cell proliferation by pulsing the animals with EdU for 48 hours (one daily pulse, during days 13-15pTmx) and found no mitotically-active $Nf1^{-/-}$ Schwann cells, as shown by co-labelling with GFP and EdU (Figure 3-6D iii and iv). On the contrary, a few EdU-positive cells were found in the epineurium, probably reflecting the higher turnover of this structure (arrow in Figure 3-6D iv). These rare GFP-/EdU+ cells were equally found in NF1 mutants and controls, eliminating a possible non-cell autonomous effect of *Nf1* mutant Schwann cells.

3.4 Quiescent adult myelinating Schwann cells are refractory to tumourigenesis

In order to investigate the long-term effects of *Nf1* disruption in myelinating Schwann cells, we characterized sciatic nerves 8 months following *Nf1* ablation (Figure 3-7A). Gross dissection of NF1 mutants did not reveal any macroscopic alterations (n>10 of each genotype). Consistent with this, *Nf1*-deficient and control sciatic nerves looked similar under histological examination of H&E stained sections. In addition, we could not detect any differences in the structure or degree of myelination when analysing semi-thin sections of NF1 mutants and control mice (Figure 3-7B). Similarly, immunolabelling with the myelin marker P0 and the axonal marker neurofilament showed no alterations in the myelin sheaths or any signs of axonal degradation in NF1 mutants, when compared to controls (Figure 3-7C).

In previous mouse models of NF1, neurofibroma formation was preceded by Remak bundle disruption (Zheng et al., 2008). To determine if $Nf1^{-/-}$ mSchwann cell could play a non-autonomous effect in these structures, we performed EM analysis in sciatic nerve sections. As represented in Figure 3-8, we failed to detect any differences between control and mutant mice: Remak bundles remained intact in the presence of *Nf1* deficient mSCs.

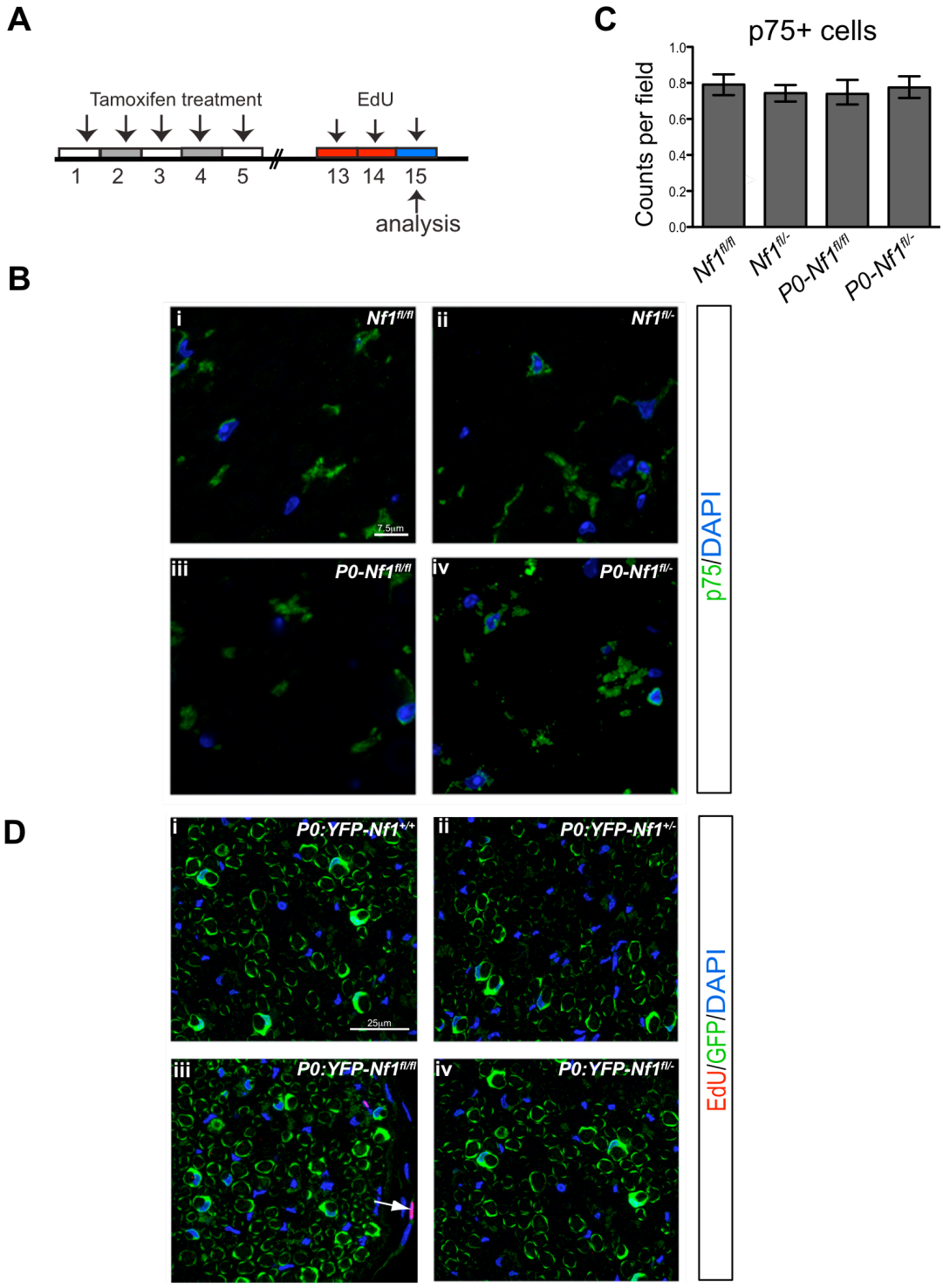

Figure 3-6: *Nf1* loss in Schwann cells does not induce Schwann cell dedifferentiation and proliferation. **A**) Tmx and EdU protocol. **B**) Cross-sections of sciatic nerves from control and NF1 mice were stained for the non-myelinating/dedifferentiated Schwann cell marker p75. **C**) Quantifications of p75+ cells (n=3 for each group, 8 fields were counted per section; 3 sections per animal, data represents mean values ±SEM) **D**) Controls *P0:YFP-Nf1*$^{+/+}$ and *P0:YFP-Nf1*$^{+/-}$ and mutants *P0:YFP-Nf1*$^{fl/fl}$ and *P0:YFP-Nf1*$^{fl/-}$ were pulsed with EdU (in red). No proliferation was observed in the Schwann cells (green). Arrow points to an epineurial EdU positive cell (3 animals of each genotype were analysed).

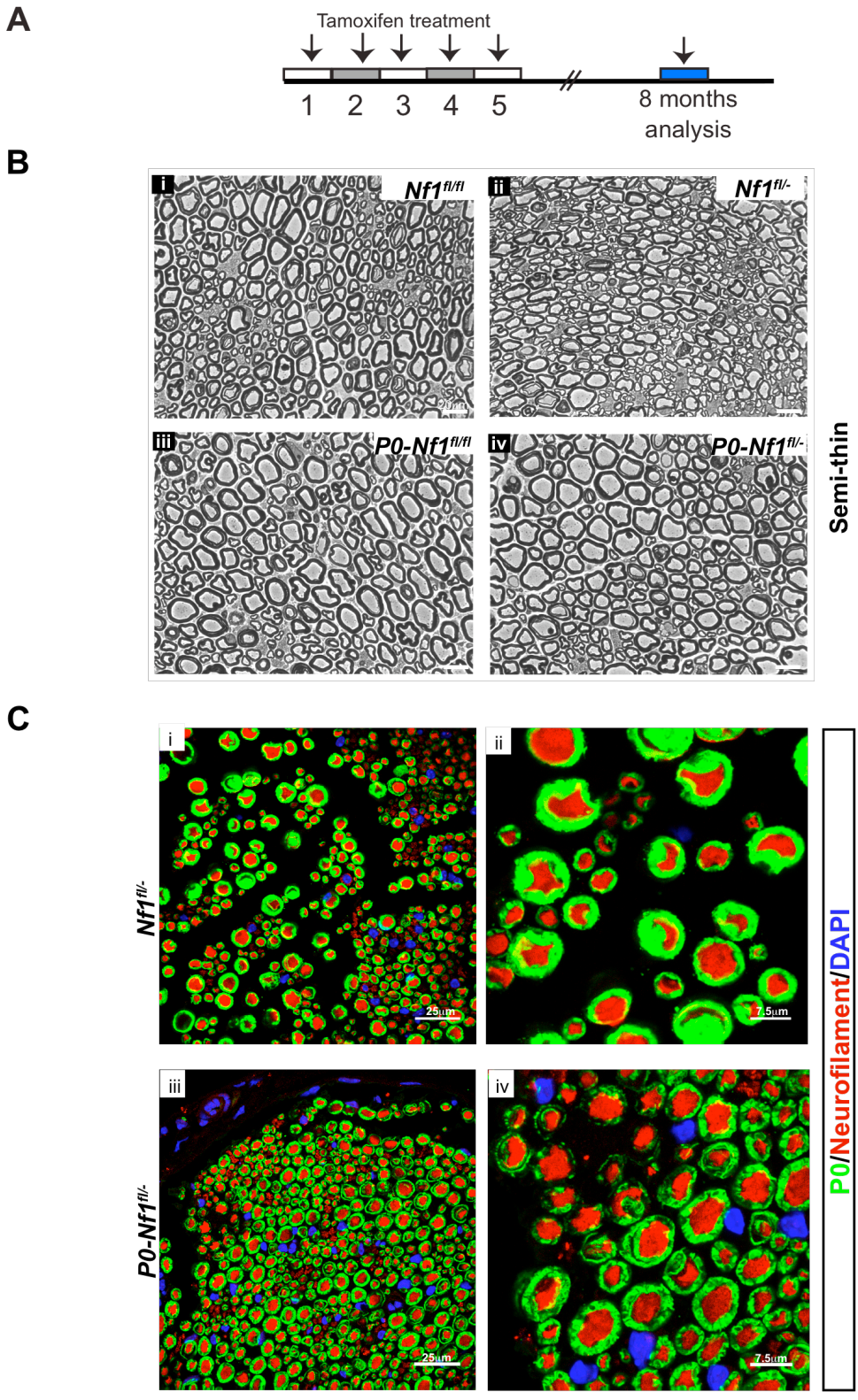

Figure 3-7: *Nf1* loss in adult, differentiated Schwann cells does not affect nerve structure. A) Sciatic nerves were processed 8 months following Tmx injections. **B**) Representative transverse semi-thin sections of control (**i** and **ii**) and mutant mice (**iii** and **iv**) stained with toluidine blue. **D**) Immunostaining of cross-sections for P0 - marker for myelinating Schwann cells (green) and neurofilament - marker for axons (red). Myelinated fibers are not altered despite loss of *Nf1* (n=3 for each genotype).

A

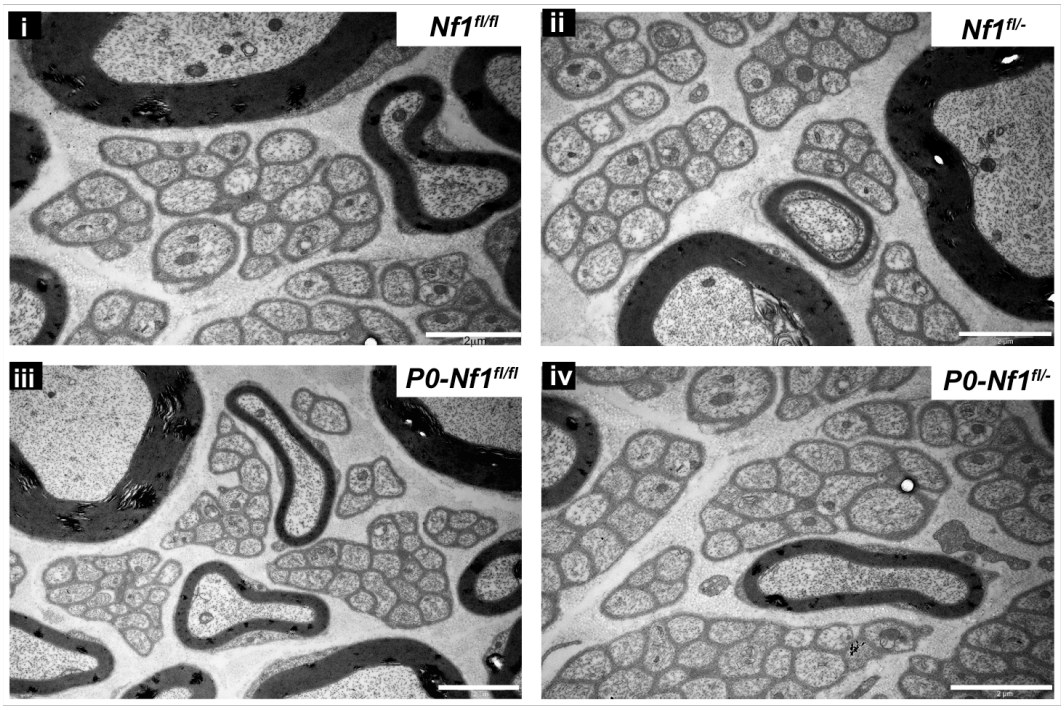

Figure 3-8: **Remak bundles are maintained in the absence of *Nf1***. Cross-sections were processed for EM analysis and revealed no disruption of Remak bundles, 8 months after Tmx treatment. Representative images of two controls (**i** and **ii**) and two mutants (**iii** and **iv**) are shown. 4 animals of each genotype were analysed.

Mast cells have been implicated as critical mediators of neurofibroma initiation (Yang et al., 2008). Given that the infiltration of these cells in peripheral nerves is frequently seen well in advance of tumour development (Zhu, 2002), we investigated if mast cells were present in sciatic nerves, 8 months following *Nf1* disruption (Figure 3-9A). As revealed by Alcian blue staining in paraffin sections, no mast cells were found in NF1 mutant nerves (Figure 3-9B). Likewise, no alterations in the number of macrophages, another cell type frequently found in these tumours, were detected (Figure 3-9C and D).

Taken together these observations indicate that mSchwann cells are not rendered tumourigenic by loss of *Nf1*. What is more, disruption of *Nf1* in myelinating Schwann cells does not impact the maintenance of adult peripheral nerves, in the context of an otherwise normal adult nerve,

3.5 The ERK pathway is not activated by *Nf1* loss in adult myelinating Schwann cells

As discussed in Chapter 1 of this thesis, *NF1* is a Ras-GAP that negatively regulates Ras and its downstream pathways, including Ras/Raf/MEK/ERK (Cichowski and Jacks, 2001). Work from our lab has shown that Raf/ERK activation is sufficient to drive Schwann cell dedifferentiation *in vitro* (Harrisingh et al., 2004) and *in vivo* (Napoli et al., 2011). Furthermore, we have also shown that *in vitro, Nf1* loss via Ras/ERK signalling, induces disruption of Schwann cell/axonal interactions rendering Schwann cells more susceptible to mitogenic signalling (Parrinello et al., 2008). Thus, it was tempting to speculate that loss of *Nf1 in vivo* would induce activation of Ras/Raf/ERK signalling and, consequently, dedifferentiation, axonal dissociation and proliferation of Schwann cells. Nevertheless, as just described, *Nf1* ablation in adult, myelinating Schwann cells does not cause any detectable effect. To understand why this was the case we examined the expression levels of activated ERK (p-ERK) by Western blot analysis of sciatic nerve lysates and by immunostainings of nerve cryosections (Figure 3-10). In both NF1 mutants, ERK activation was not detected, revealing that *Nf1* loss in fully differentiated mSchwann cells is not sufficient to produce a detectable alteration in the signalling through Ras/Raf/ERK, providing a plausible explanation for the absence of any noticeable phenotype.

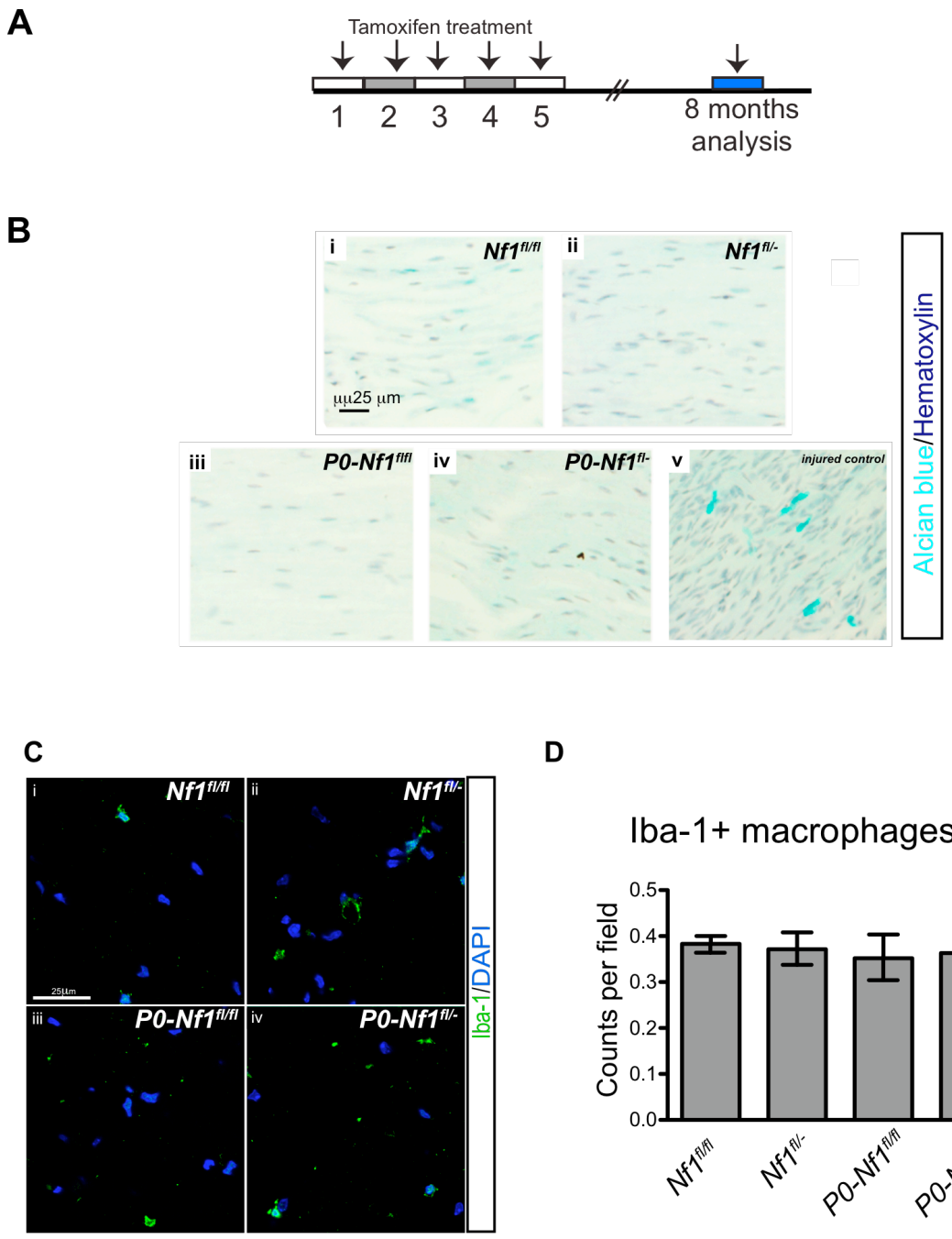

Figure 3-9: *Nf1* loss in adult mSchwann cells does not induce the recruitment of an inflammatory response. **A**) Sciatic nerves from control (**i** and **ii**) and mutant sciatic nerves (**iii** and **iv**) were harvested 8 months following Tamoxifen treatment, and processed for analysis. **B**) Paraffin sections were stained with Alcian Blue and the nuclei counterstained with hematoxylin. Three animals of each group were examined; mast cell recruitment was not observed in controls (**i-ii**) and in NF1 mutants (**iii-iv**); **v**) an injured positive control shows mast cell recruitment 5 days after nerve transection. **C** and **D**) Nerve cryosections were immunostained for the macrophage marker Iba-1 (green) and revealed no increase in the number of these cells, 8 months after *Nf1* loss (n=3 for each group, 8 fields were counted per section, 3 sections per animal, data are represented as mean values ±SEM).

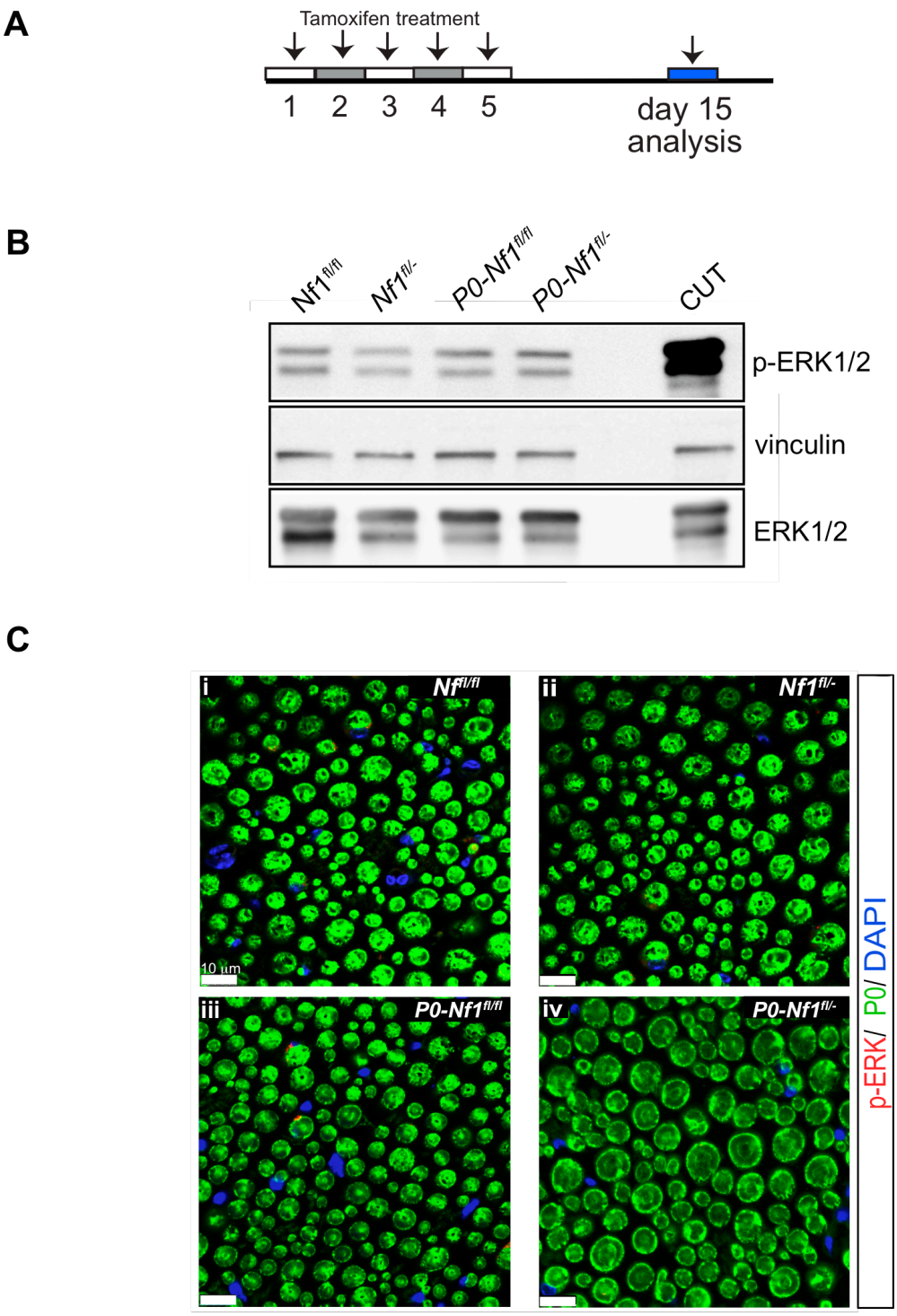

Figure 3-10: *Nf1* loss in adult myelinating Schwann cells does not induce activation of ERK signalling. A) 5-6 weeks-old mice were treated with Tamoxifen and sciatic nerves were harvested for analysis, 15 days following the first Tmx dose. **B**) Western blot analysis of sciatic nerve extracts shows no alteration of p-ERK levels upon *Nf1* loss (third and fourth lane). On the right, nerve extracts from control mice 24 hours post nerve transection are shown as a control for ERK activation. **C**) Representative images of cross-sections of sciatic nerves immunostained for p-ERK (red) and P0 (green) in the controls *Nf1*$^{fl/fl}$ and *Nf1*$^{fl/-}$ (**i** and **ii**) and in the *Nf1*-deficient mice *P0-Nf1*$^{fl/fl}$ and *P0-Nf1*$^{fl/-}$ (**iii** and **iv**) (n=3 for each group).

3.6 Chapter summary and conclusions

In this chapter I have described the generation of a mouse model to study the selective loss of *Nf1* in myelinating Schwann cells, in adult mice. Importantly, in this model, p75 positive, non-myelinating Schwann cells are negative for Cre activity, confirming the specificity of *Nf1* ablation in mSchwann cells. Characterization of the peripheral nerves shortly after *Nf1* disruption revealed that the loss of this tumour suppressor does not have an automatic impact on Schwann cell differentiation status and proliferation. Importantly, long-term analysis of NF1 mutants revealed that $Nf1^{-/-}$ Schwann cells do not give rise to tumours in either an $Nf1^{+/+}$ *or* $Nf1^{+/-}$ background. Moreover, the overall structure of the peripheral nerve is not affected and no inflammatory response is induced. Consistently with these findings, we observed that the ERK pathway is not detectably activated upon *Nf1* loss, suggesting two possibilities: 1) the differentiated, myelinated nerve microenvironment is able to suppress Ras activation or 2) in the adult homeostatic peripheral nerve, NF1 does not play a relevant role as a Ras regulator.

Altogether, we have shown that *Nf1* loss in quiescent, adult mSchwann cells, by itself, is not sufficient to drive tumourigenesis.

Chapter 4: Results II

4.1 Chapter introduction

In the previous chapter I have shown that loss of *Nf1* in myelinating Schwann cells in the context of a normal, adult nerve is not tumourigenic, at least as a result of a "single-hit" mechanism. Surprisingly, the levels of ERK signalling were not affected by *Nf1* loss, suggesting that in an intact nerve, NF1 is mostly dispensable for the maintenance of the basal levels of Ras/ERK signalling or that other regulatory mechanisms are induced upon *Nf1* loss and able to suppress the Ras pathway.

A link between injury and tumourigenesis was postulated over a century ago (Balkwill and Mantovani, 2001). Several lines of evidence, including clinical observations and studies in transgenic mice, have demonstrated that wounding and/or inflammation can strongly modulate the tumourigenic potential of genetically altered cells (Schuh et al., 1990; Wong and Reiter, 2011).

Injury to the PNS results in a sequence of well-defined molecular and cellular events known as Wallerian degeneration. Following nerve injury, axons downstream of the wound degenerate, Schwann cells dedifferentiate to a proliferative, progenitor-like state and a robust inflammatory response is elicited. Upon axonal regrowth, the inflammation is resolved and Schwann cells redifferentiate to restore the function of the nerve. Importantly, work in our lab has shown that the switch in Schwann cell differentiation state to a progenitor-like cell is dependent on strong signalling through the Ras/Raf/MEK/ERK pathway (Harrisingh et al., 2004; Napoli et al., 2011). We therefore decided to investigate if wounding to the sciatic nerve and its associated activation of Ras/Raf/ERK pathway would alter the tumourigenic properties of *Nf1*$^{-/-}$ mSchwann cells.

4.2 Injury induces peripheral nerve tumour formation at high frequency

To test if wounding of the sciatic nerve may cooperate with lack of *Nf1* to induce tumourigenesis, we performed partial-transections of the right sciatic nerve, 15 days following Tmx treatment (Figure 4-1A). Partial-transection was favoured over full-transection to facilitate the reconnection of the two stumps during regeneration and reduce variability among experiments (See Figure 2-1). Six-to-eight months following the injury - we would expect that by this time point, the cellular remodelling that takes place during the regeneration process should be mostly resolved - mice were

sacrificed and gross dissections were performed in control and mutant groups. Strikingly, we detected visible tumours at the injury site in approximately 35% of all NF1 mutant mice subjected to nerve transection (n=75 of *P0-Nf1*$^{fl/fl}$ and n=52 of *P0-Nf1*$^{fl/-}$). The frequency of tumour development was not significantly different between *Nf1*$^{+/+}$ and *Nf1*$^{+/-}$ backgrounds, ruling out a fundamental role for *Nf1* haploinsuficiency in tumour formation in this mouse model (Figure 4-1C).

In sharp contrast to the high frequency of tumour formation observed in NF1 mutants, we did not detect abnormal nerve enlargements in the injured nerves from control mice (n=78 of *Nf1*$^{fl/fl}$ and n=61 *Nf1*$^{fl/-}$). A single exception was an *Nf1*$^{fl/-}$ mouse, which had a macroscopically enlarged sciatic nerve at the wound site. Given the rarity of this event and the fact that it occurred in an animal with a heterozygous background, it is tempting to speculate that this tumour may have resulted from LOH at the *Nf1* locus.

In agreement with the results described in the previous chapter, the unwounded contra-lateral nerves of the NF1 mutants (in which mSchwann are *Nf1*$^{-/-}$) were consistently found unaltered. This was true even when sciatic nerves were analysed up to 15 months following *Nf1* disruption and further confirms that, by itself, *Nf1* loss in adult mSchwann cells fails to drive tumourigenesis.

4.3 Morphological characterization of sciatic nerves, at the site of injury

Hereafter, NF1 mutants refer to mice with visibly enlarged sciatic nerves only; macroscopically normal mutant nerves were not included in any of the following analyses.

The structure and composition of the tumours that developed in *Nf1*-deficient mice at the site of injury were characterized and compared with the equivalent region of control animals (roughly 2 mm above the sciatic notch), 8 months following injury. Figure 4-2A illustrates the remarkable enlargement of the peripheral nerves in *Nf1*-deficient mice, when compared with controls (approximately six fold, as quantified in 4-2B). Also, frozen cross-sections were prepared from sciatic nerves, stained with Hoechst nuclear staining (Figure 4-2C) and the number of nuclei per field counted using epifluorescence microscopy. As shown in Figure 4-2D, NF1 mutants exhibit significantly increased cellular density, in addition to increased size.

A

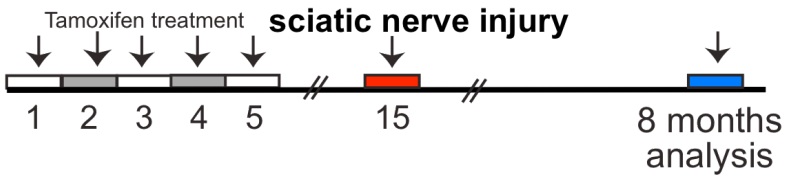

B

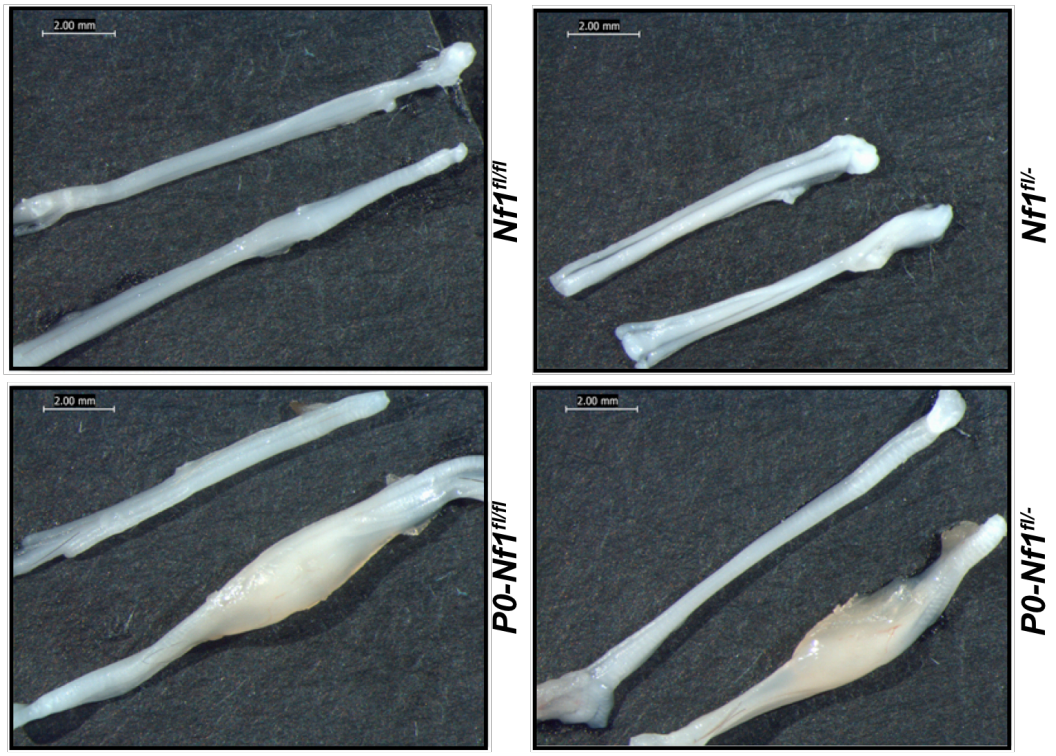

C

	number tumours	total of injured mice	% tumours/ total injured mice
***Nf1*$^{fl/fl}$**	0	78	0.0
***Nf1*$^{fl/-}$**	1	61	1.6
***P0-Nf1*$^{fl/fl}$**	25	75	33.3
***P0-Nf1*$^{fl/-}$**	18	52	34.6

Figure 4-1: NF1 mutant mice form tumours at the site of injury.

A) Schematic representation of the protocol used to assess the effect of injury. **B**) Gross micrographs show sciatic nerves (uninjured nerve on the left and injured on the right) of age-matched controls (**i** and **ii**) and NF1 mutants (**iii** and **iv**) Tmx-treated, 8 months following injury. **C**) Table shows the frequency of tumour development in all the 4 genotypes studied. Tumours form only (*) in mice lacking NF1 in Schwann cells and at a similar frequency in *Nf1*$^{+/+}$ and *Nf1*$^{+/-}$ background (*see main text).

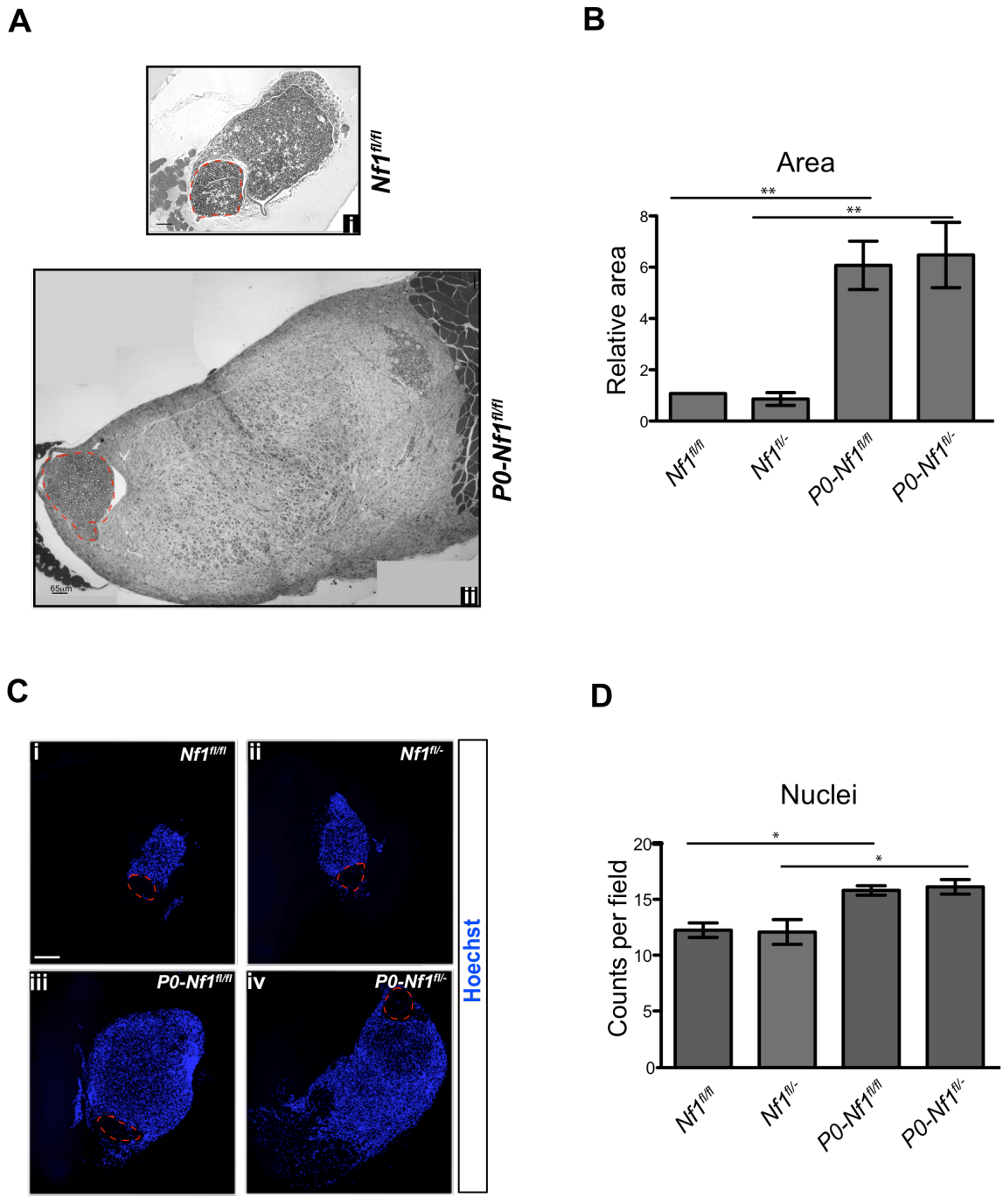

Figure 4-2: Injured nerves from *Nf1*-deficient mice are greatly enlarged at the site of injury and display increased cellular density. **A**) Transverse semi-thin sections stained with toluidine blue show enlargement of the sciatic nerve in NF1 mutant nerves (ii). **B**) Quantification of the relative area (n=3 of each genotype). Note that similar results were obtained for *Nf1*$^{+/+}$ and *Nf1*$^{+/-}$ backgrounds. **C**) Hoechst staining shows nuclei density, 8 months following partial nerve transection. **D**) Quantification of C (n=4 of each genotype). Red dashed lines delineate the unwounded region of the nerves. Data represents mean values ±SEM.

4.4 Tumours in NF1 mutants can be classified as Neurofibromas

We performed histological analysis on the tumours and used published criteria to define grades of mouse peripheral nerve tumours (Stemmer-Rachamimov et al., 2004). Paraffin sections from more than 10 tumours were evaluated by H&E and S100 staining by our collaborating pathologist. Tumours were classified as GEM Grade I neurofibromas, exhibiting the classical characteristics of human neurofibromas, including being composed by a heterogeneous cell population containing S100β positive and S100β negative cells, abundant ECM deposition and numerous spindle-shaped cells (Figure 4-3 and 4-4).

As illustrated in Figure 4-3B, three distinct areas could typically be recognized in the tumours: i) the uninjured region of the nerve; ii) an apparently regenerated region and iii) the neoplastic lesion itself. These 3 areas were easily recognizable in terms of morphological organization, cellular density and S100β expression. The unwounded area remained surprisingly unaffected, displaying regular fibre alignment and sparse nuclei, comparable to unwounded controls (Figure 4-3Ai and 4-3Bi). The second identifiable area appeared similar to the regenerated control (Figure 4-3Aii and 4-3Bi and ii); in both cases, despite an increased cellularity when compared to uninjured nerves (Figure 4-3Ai), the nerve fibres are aligned in a fairly regular way, resulting in a comparatively reorganized structure (note the aligned nuclei in 4-3Aii). Finally, the lesion surrounding the nerve displayed evident cellular disorganization, abundant blood vessels (black arrows in 4-3Aiii and 4-3B) and numerous inflammatory cells, recognized by H&E staining (red arrows in 4-3Biii).

The distribution of S100β immunoreactive cells - a parameter conventionally used for neurofibroma diagnosis - was also markedly divergent between the different areas of the tumour. As illustrated by the neurofibroma shown in Figure 4-4B, homogeneous S100β positive staining was observed exclusively associated with the unwounded, entrapped nerve (i). In the "regenerated area", S100 expression appeared similar to the repaired controls (compare 4-4Bii with 4-4Aii): immunoreactivity was sparsely found, mirroring the presence of intermingled S100 positive and S100 negative cells (ii). Finally in the lesion itself, only minimal S100 staining was observed (Figure 4-4).

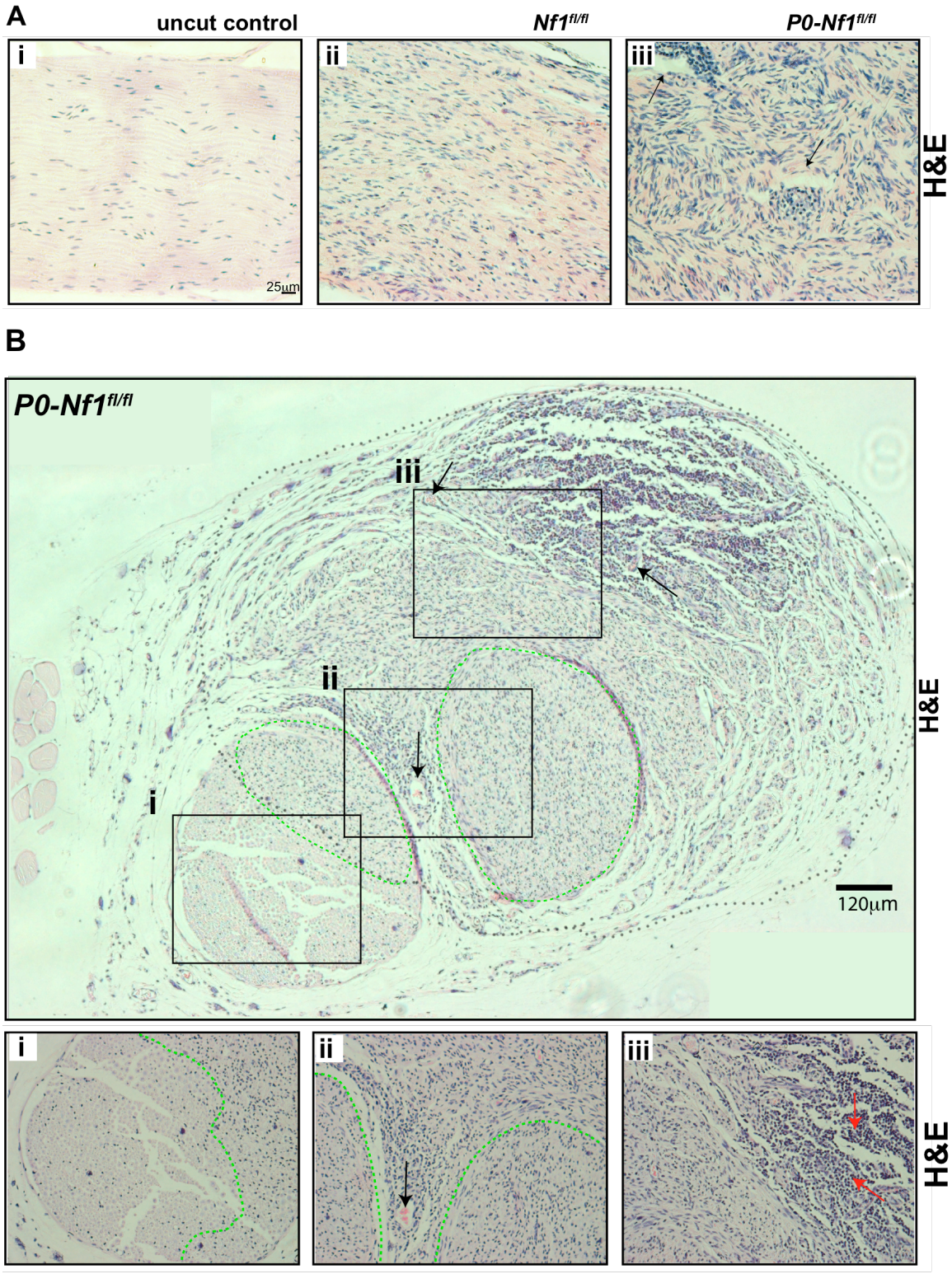

Figure 4-3: Histological analysis of control and mutant sciatic nerves. **A**) Control and mutant nerves were sectioned longitudinally and stained for hematoxylin and eosin (H&E). **i)** uncut control; **ii**) control nerve *Nf1*$^{fl/fl}$ appears regenerated 8 months following injury; note the fairly aligned nuclei in contrast with **iii**. **iii**) NF1 mutants developed neurofibromas at the site of injury. Note the disordered, convoluted bundles of cells exhibiting spindle-cell morphology with ovoid and spindle shaped nuclei, characteristic of these tumours.

→

B) Cross-section of a paraffin embedded sciatic nerve from a *P0-Nf1*$^{fl/fl}$ mouse displays morphologically distinct areas; grey dashed line outlines (**i**) uninjured and (**ii** and **iii**) injured regions; green dashed line demarcates the regenerated area from the tumour lesion. Black arrows point to blood vessels; red arrows to immune cells.

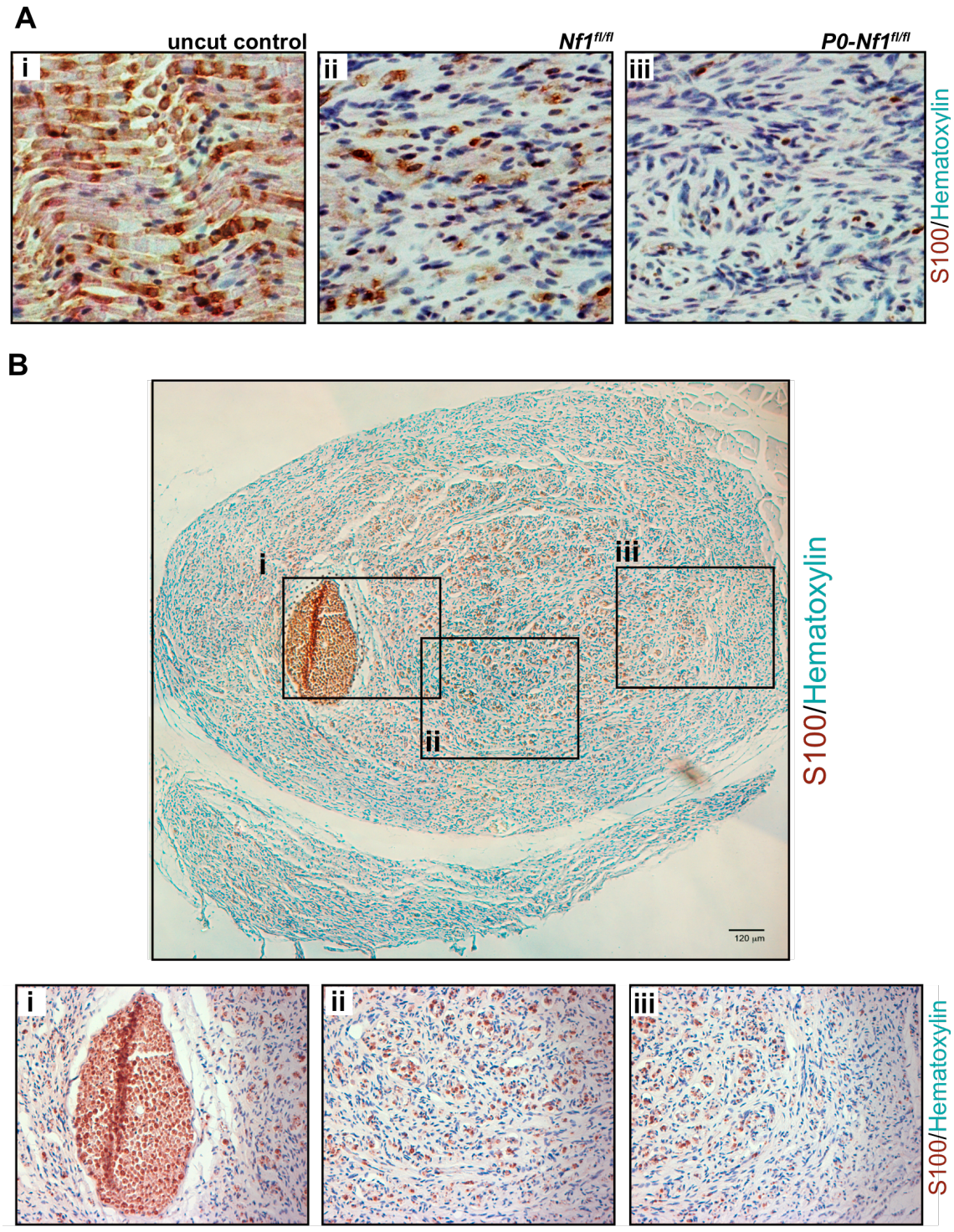

Figure 4-4: Tumours in *P0-Nf1*$^{fl/fl}$ and *P0-Nf1*$^{fl/-}$ mice display variable immunoreactividade for the Schwann cell marker S100β. A) Sciatic nerves from NF1 mutants were embedded in paraffin, sectioned longitudinally and stained for S100β. **i**) uncut control; **ii**) control nerve: *Nf1*$^{fl/fl}$ exhibits a relatively homogeneous staining for S100β in contrast to the scarce staining observed in some areas of neurofibromas (**iii**). **B**) Cross-section of a paraffin embedded neurofibroma; **i**, **ii** and **iii** represent distinct areas, where S100β is differentially expressed. Similar results were obtained with *P0-Nf1*$^{fl/-}$ transgenics (3 animals of each genotype were analysed).

4.5 Ultrastructural analysis confirms the multicellular nature of neurofibromas

Human neurofibromas contain a variety of cell types found in normal peripheral nerves, including Schwann cells, fibroblasts, neurons, perineurial cells and mast cells. To better define the cellular composition of the tumours that developed in our NF1 model we prepared semi-thin and ultra-thin sections from control and NF1 mutants, 8 months following injury (Figure 4-5A illustrates the regions that sections were prepared from). The overall ultrastructural appearance of neurofibromas and regenerated controls is illustrated in Figure 4-5B.

Repaired sciatic nerves from control mice, visualized by toluidine blue staining of cross-sections, were found tightly packed with myelinated axons, with little intervening interstitial space (Figure 4-5Bi). Under EM analysis, they were composed of well-organized minifascicles or compartments, which are known to form as part of the regeneration process (Figure 4-5Biii). The formation of these structures, consisting of groups of Schwann cell-axon units delimited by perineurial-like layers, has been speculated to represent an attempt by the nerve to preserve some level of protection within their immediate microenvironment (Morris et al., 1972).

Overall, despite the increased cellularity as compared to unwounded controls - that can be explained by an increased number of Schwann cells, resulting from the process of axonal sprouting, and by the presence of the fascicle-forming cells - control nerves appeared reorganized and well regenerated. Importantly, contrary to a study by Atit and colleagues in which *Nf1* haploinsufficient mice exhibited impaired skin wound repair (Atit et al., 1999), here the success of nerve repair was not affected by *Nf1* heterozygosity.

In contrast, the tumours that formed at the injury site in NF1 mutants were significantly enlarged by an expanded interstitial compartment and by increased cellularity between myelinated axons (Figure 4-5Bii). Electron micrographs of these tumours revealed the presence of mast cells - confirmed by numerous intracellular granules, "perineurial-like" cells - traditionally identified by numerous pinocytic vesicles and patchy or continuous basal lamina, and rare myelinated axons, most of which were found intact. Schwann cell cytoplasmic processes, as defined by continuous basal lamina, were frequently found devoid of axonal association, sometimes wrapping abundant collagen pockets (Figure 4-6C). Unsheathed or misegregated axons could also be identified (Figure 4-6C and D), which may suggest that, following injury and in the context of a $Nf1^{-/-}$ nerve, the redifferentiation process of non-myelinating Schwann

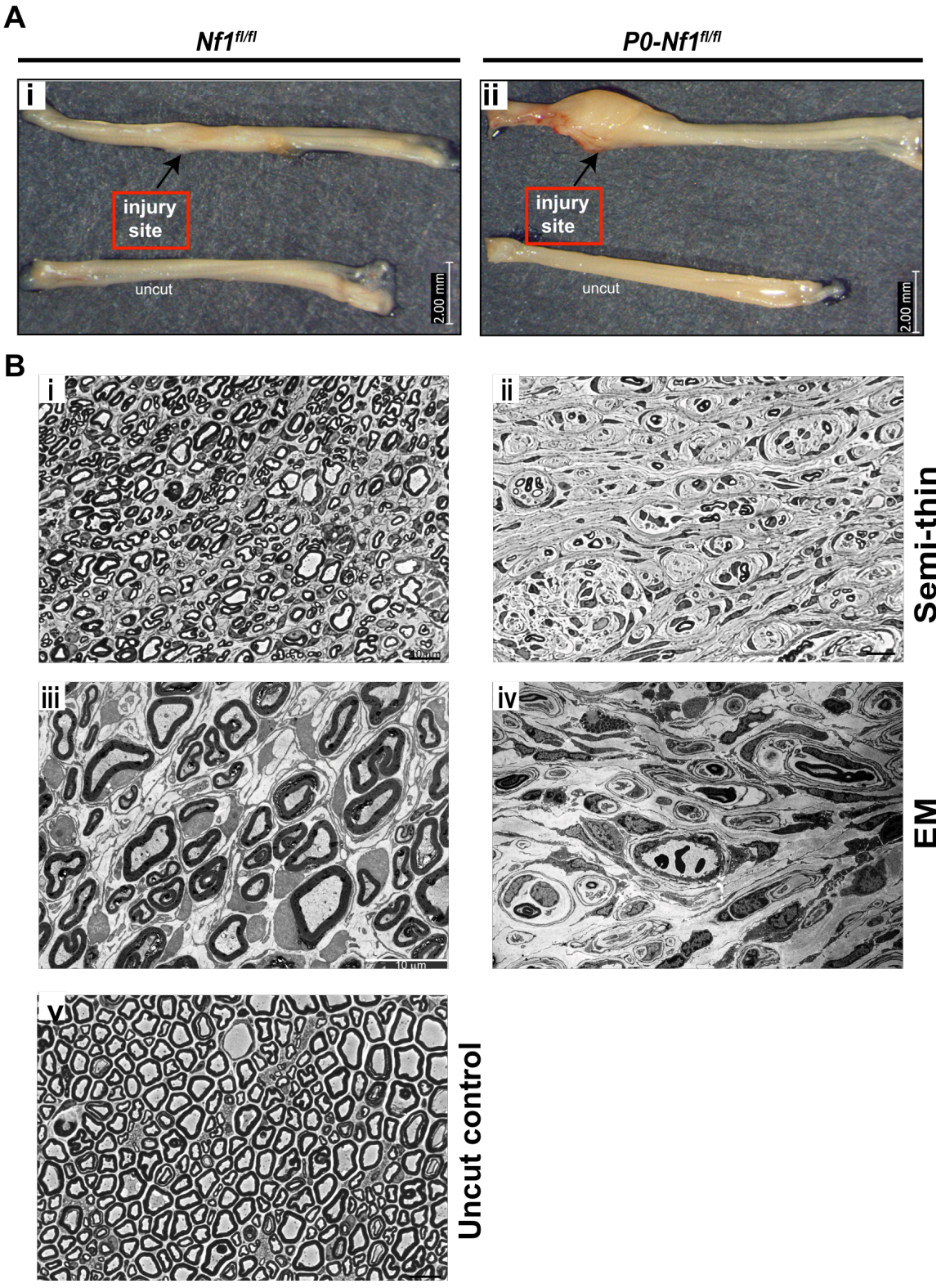

Figure 4-5: Morphological analysis of sciatic nerves at the injury site, 8 months following transection. A) Sections were prepared from the injured site in (**i**) control and (**ii**) *Nf1*-deficient nerves. **B**) Representative images of semi-thin (**i** and **ii**) and ultra-thin (**iii** and **iv**) sections from control and NF1 mutant peripheral nerves. In control animals, sciatic nerves appeared well-organised and regenerated. Mutant mice developed macroscopic tumours with disrupted morphology (4 animals of each genotype were processed for analysis).

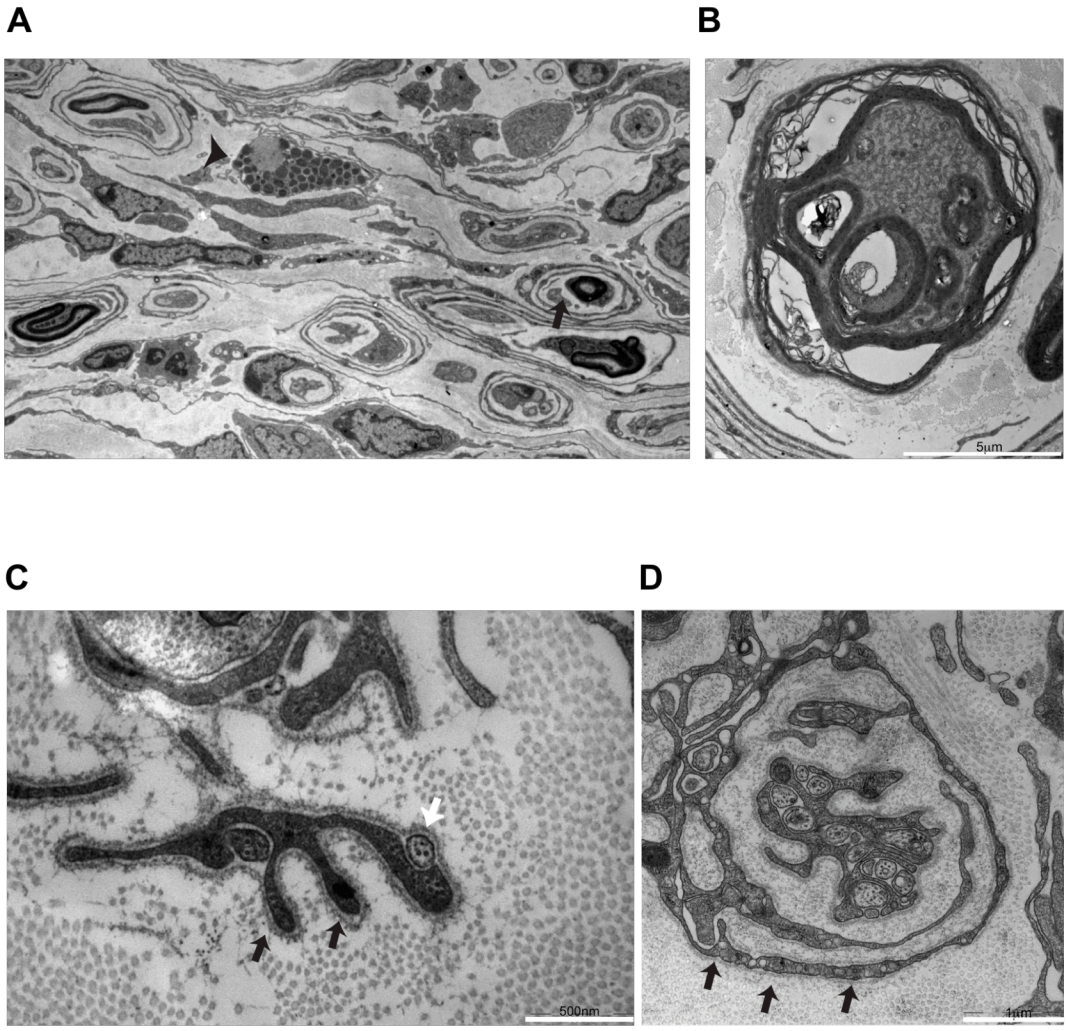

Figure 4-6: EM analysis of the tumours that developed in NF1 mutant mice, 8 months following peripheral nerve injury. A) Representative image of an EM micrograph of a *P0-Nf1*$^{fl/fl}$ sciatic nerve shows a mixture of intact mSchwann cells (arrow), "perineurial-like" cells and mast cells (arrowhead). **B**) A rare example of demyelination found in an NF1 mutant mouse. **C**) Black arrows point to prominent Schwann cell cytoplasmic processes identified by continuous basal lamina. White arrow point to a "naked" axon. Abundant collagen deposits are also observed. **D**) Arrows point to "perineurial-like" cells identified by patchy basal lamina and intracellular pinocytic vesicles. Note the presence of unsegregated axons (3 to 4 tumours of both *P0-Nf1*$^{fl/fl}$ and *P0-Nf1*$^{fl/-}$ were analysed by EM, 8 months following injury).

cells is impaired. Alternatively, it might reflect disruption of Remak bundles, an event frequently witnessed in neurofibromas.

The data demonstrates a close similarity in the pathology of the lesions developed in this novel model of tumourigenesis and previously described human neurofibromas (Dickersin, 1987).

4.6 *Nf1*$^{-/-}$ Schwann cells are a major cellular component of the tumours that develop at the site of injury

The contribution of *Nf1*$^{-/-}$ Schwann cells to the neurofibromas that developed in this murine model was assessed using *P0:YFP-Nf1*$^{fl/fl}$ and *P0:YFP-Nf1*$^{fl/-}$mice. Six months following *Nf1* loss and sciatic nerve partial-transection, mice were sacrificed and sciatic nerves processed for immunofluorescence. Strikingly, near uniform GFP expression was observed in the lesions that developed at the site of injury, demonstrating the extensive contribution of *Nf1*$^{-/-}$ Schwann cells. GFP positive cells were mostly found deprived of axonal association, enwrapping other cells or forming parallel layers (Figure 4-7). Isolated cells invading the adjacent muscle were also observed, suggesting that *Nf1*$^{-/-}$ Schwann cells have the potential to invade surrounding tissues (Figure 4-7iii and iv). Importantly, we observed that at the tumour region, the majority of GFP+ cells are negative for the mature Schwann cell marker S100β; only the myelinating cells appear to express this marker (Figure 4-8). This is consistent with the histological analysis represented in Figure 4-4, in which most of the S100β positive cells were found in the "regenerated" area and only sparsely detected in the lesion itself. How these observations relate with previous described model of NF1 and possible implications for the histopathological analysis of these tumours will be addressed later, in chapter 7.

Most of the GFP+ cells were also positive for the p75 marker, providing strong evidence that these are dedifferentiated, *Nf1*$^{-/-}$ Schwann cells (Figure 4-9A). Importantly, comparison of EM micrographs and immunofluorescence images, revealed a striking resemblance between many of these GFP/p75 expressing cells– which exhibit long cytoplasmatic processes enwrapping other cells – and the cells frequently found in neurofibromas and traditionally identified as "perineurial-like" (Figure 4-10). This suggests that, at least some of these cells, despite their distinct ultrastructural morphology, are in fact, mSchwann cells derived. Furthermore, we were able to identify some GFP positive/p75 negative cells in these tumours (Figure 4-9B). This raises the possibility that neurofibromas contain rare cell populations derived from P0-

A

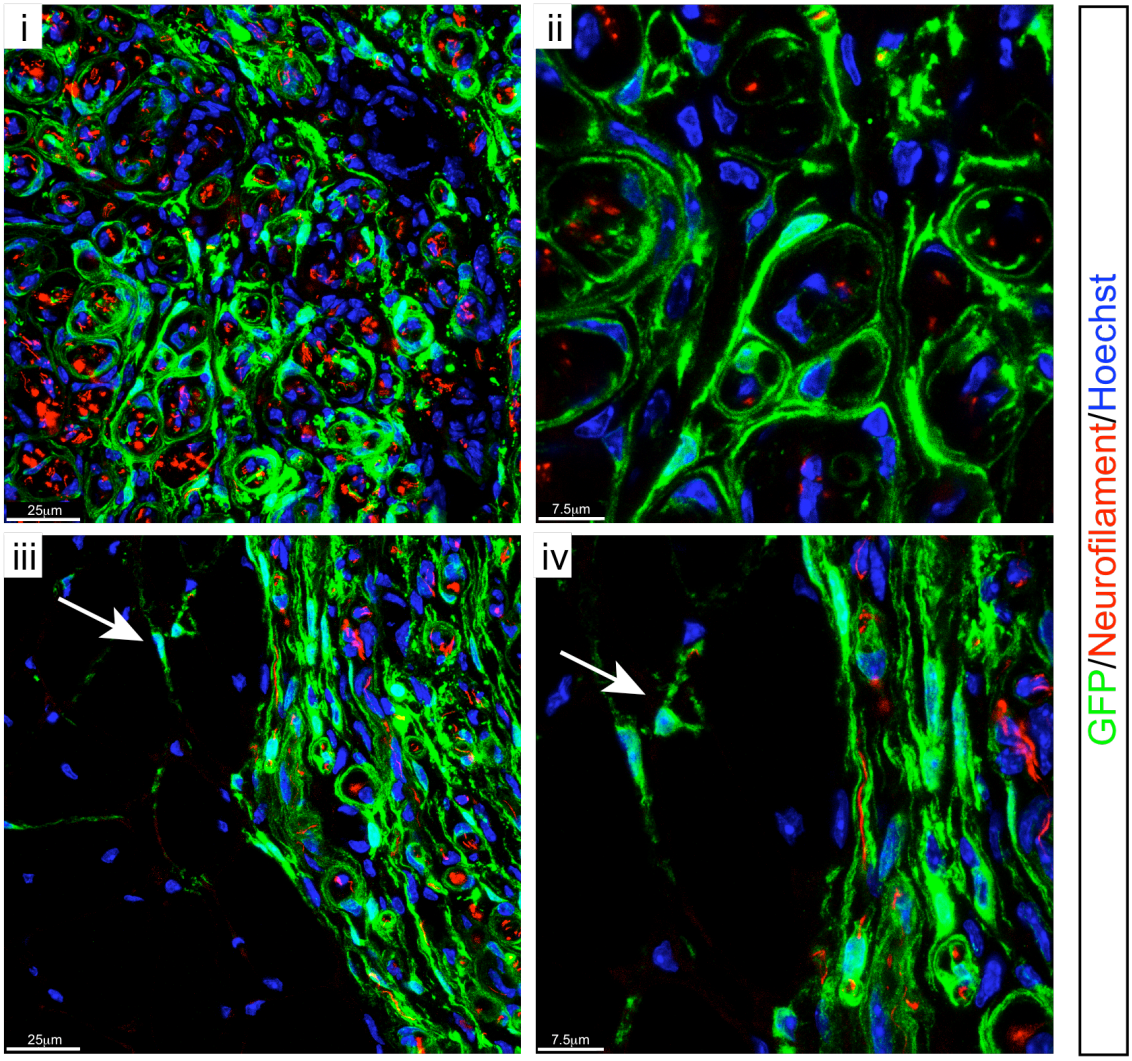

Figure 4-7: GFP+ positive cells are a major cellular component of the tumours that developed in NF1 mutants. Cross-sections of a tumour from a *P0:YFP-Nf1$^{fl/fl}$* mouse were co-stained for GFP (green) and the axonal marker, neurofilament (red). Note that GFP+ cells are devoid of axonal contact. Arrows in **iii** and **iv** point to *Nf1$^{-/-}$* Schwann cells (GFP+), invading the adjacent muscle tissue.

A

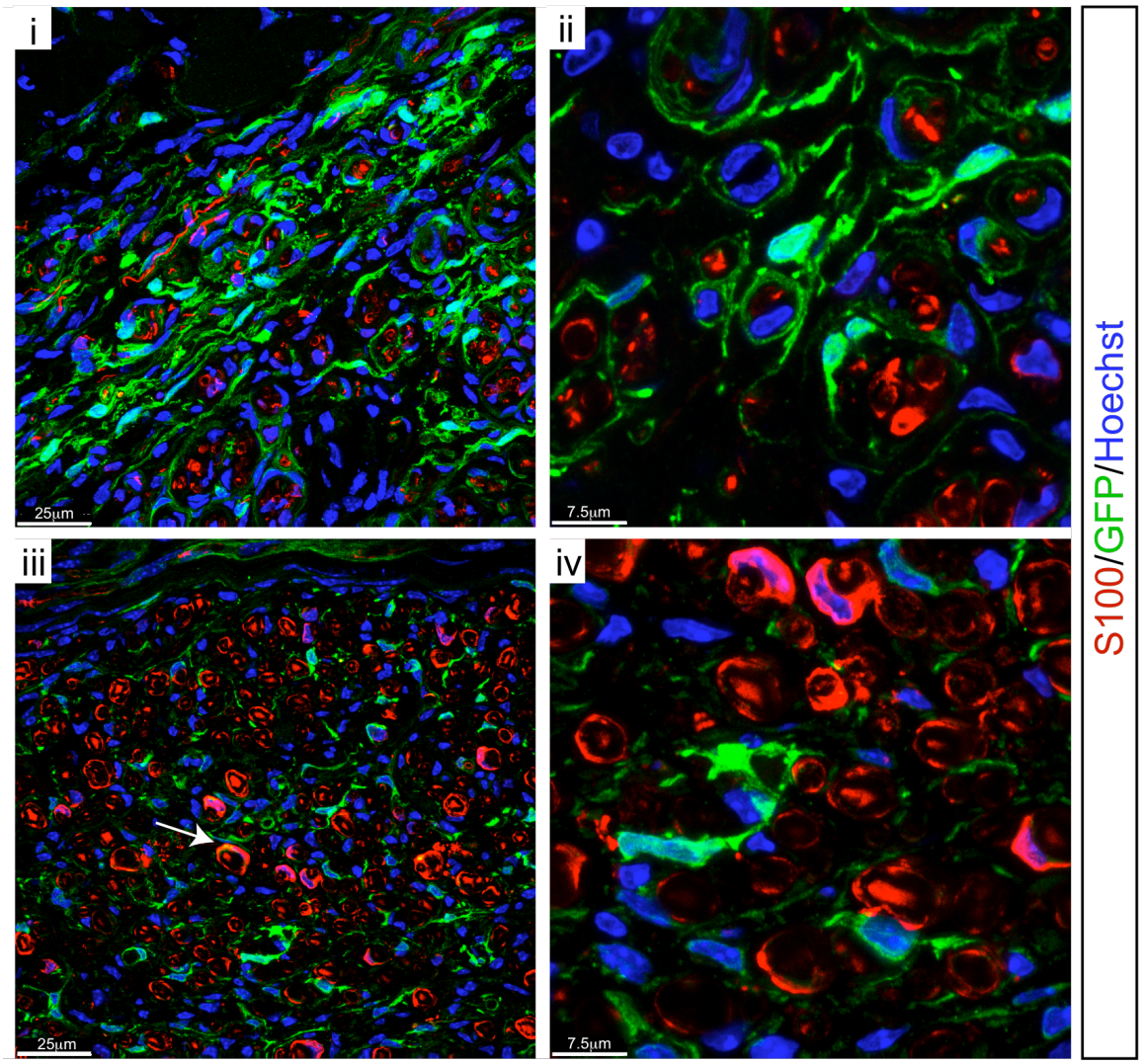

Figure 4-8: In the tumour region, the majority of *Nf1*$^{-/-}$ Schwann cells do not express the S100β marker. Neurofibroma cryosections from a *P0:YFP-Nf1*$^{fl/fl}$ mouse, were immunolabelled for GFP (green) and S100β (red); nuclei were counterstained with Hoechst (blue). **i** and **ii** show representative images of the neoplastic tissue (note the scarce S100β positivity); iii and iv images were taken from the "regenerated" area. The white arrow in **iii** points to a rare GFP+S100β+ cell.

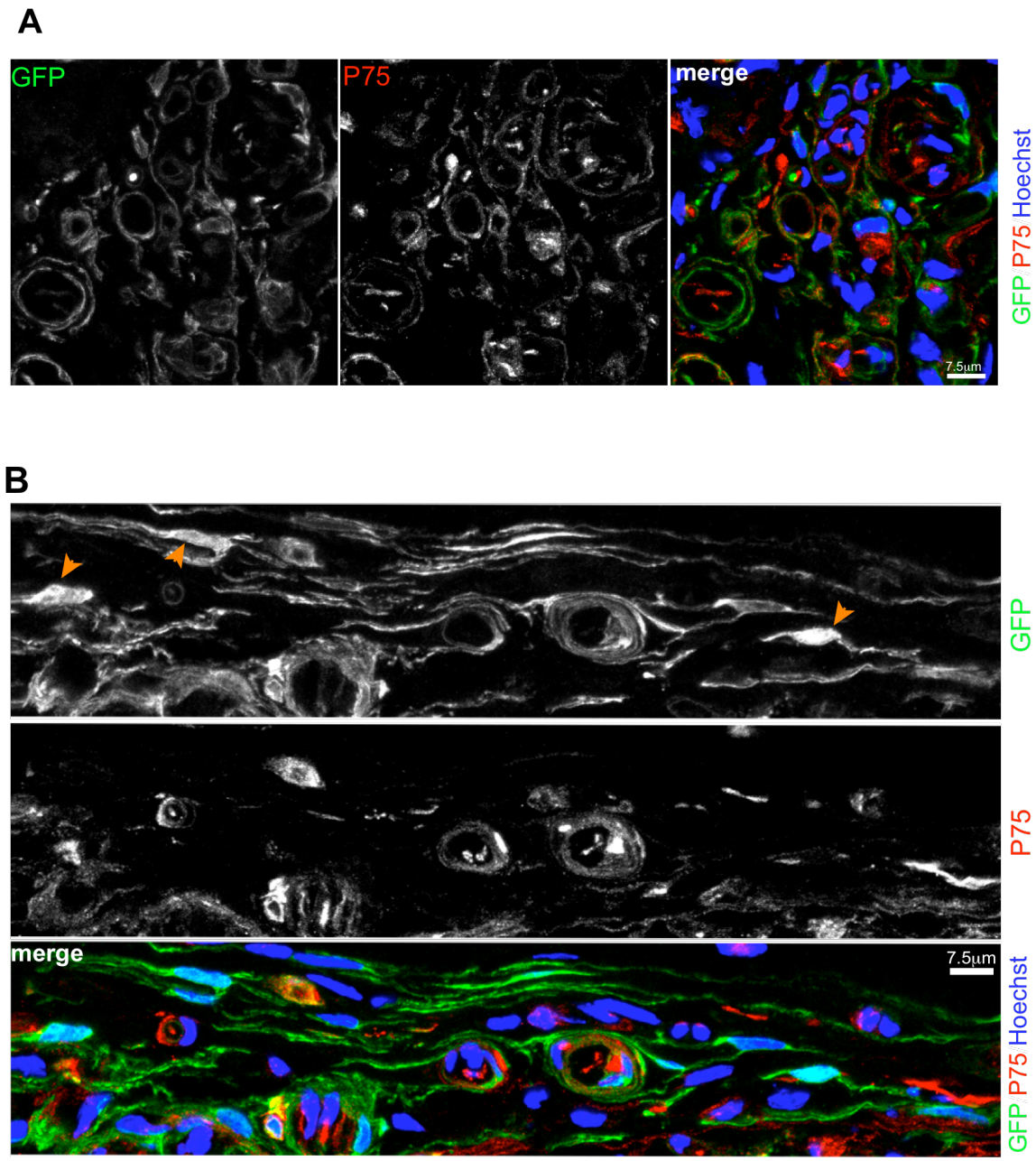

Figure 4-9: Most, but not all, *Nf1*$^{-/-}$ Schwann cells express p75.

A neurofibroma was dissected from a *P0:YFP-Nf1*$^{fl/fl}$ animal, 6 months after Tmx treatment and nerve injury. Cryosections of the tumour were immunostained for GFP (first panel in A and B) and p75 (second panel in A and B); nuclei were stained with Hoechst (blue). **A**) The majority of the GFP+ cells were also positive for the non-myelinating/dedifferentiated Schwann cell marker p75. **B**) Arrowheads identify some GFP positive cells that are negative for p75.

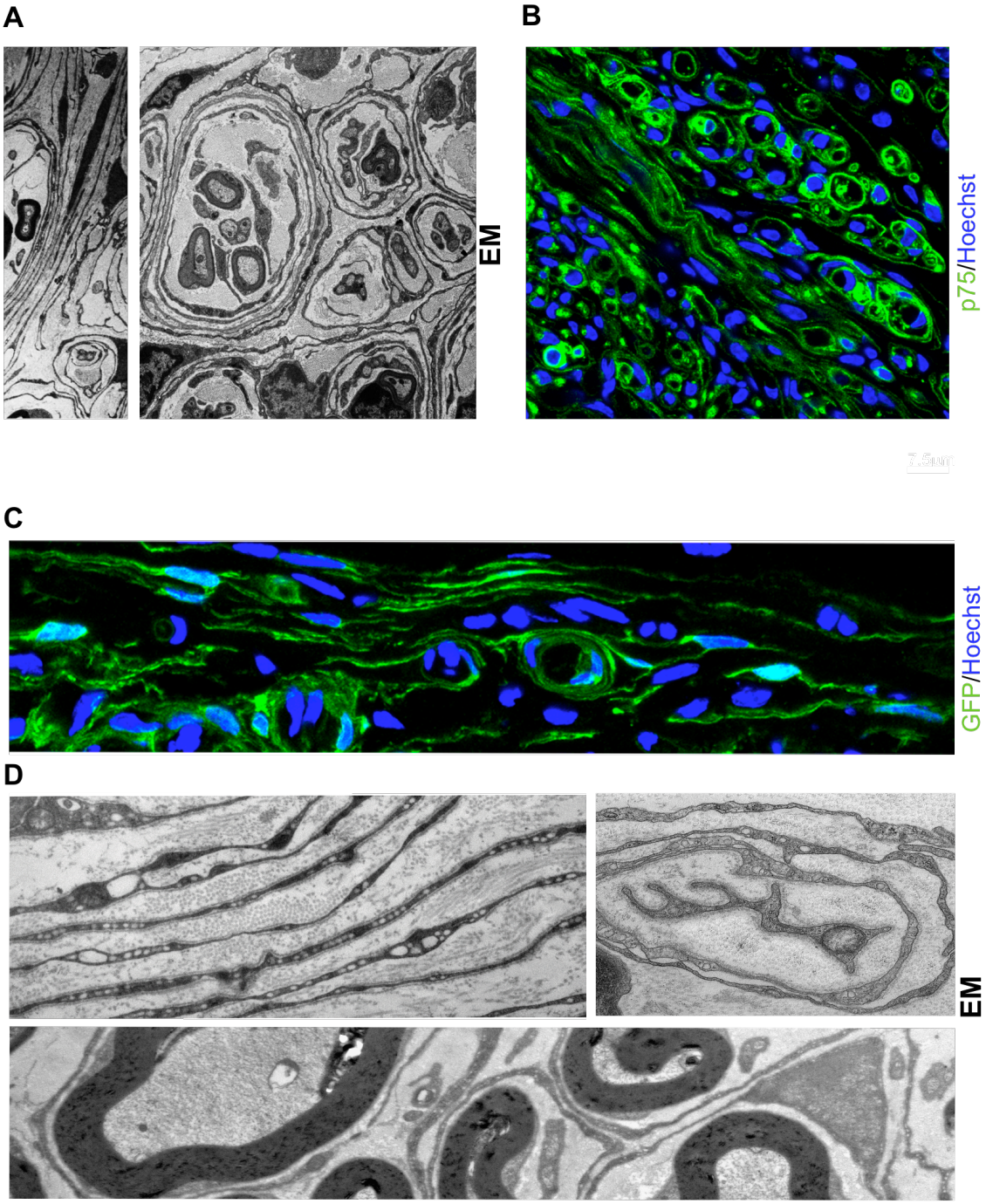

Figure 4-10: Striking resemblances between "perineurial-like" cells and p75+ Schwann cells or GFP+ SC-derived cells in a neurofibroma. **A** and **D**) EM micrographs showing representative images of "perineurial-like" cells enwrapping minifascicles or forming parallel layers of cytoplasmic processes. **B** and **C**) Immunofluorescence images showing p75 positive Schwann cells (green in B) and GFP positive (green in C) mSC-derived cells with remarkable morphological similarities to the "perineurial-like" cells represented in A and D.

expressing cells that have lost their original identity. It would be interesting to investigate this further.

In contrast to the homogenous distribution of GFP+ cells in neurofibromas, only a few positive cells were found at the injury site in controls (Figure 4-11). This might suggest that the Schwann cells at the injury site do not derive from P0-expressing cells, but instead are mostly derived from the non-myelinating population. A more extensive characterization of injured control nerves is needed to investigate if "perineurial-like" mSC-derived are also present in the context of a normal regeneration process. Together, these results provide strong evidence that neurofibroma is driven by expansion of *Nf1* deficient cells, derived from myelinating Schwann cells.

4.7 Increased proliferation in *Nf1*-deficient tumours, 8 months following injury

We monitored cell proliferation in neurofibromas and control nerves, 8 months after nerve transection. By administering EdU 2 days before analysis, we found that cells were more likely to be dividing in neurofibromas as compared to normal regenerated tissues from controls (Figure 4-12). To address which cells were proliferating within the neurofibromas, we stained tumour sections with antibodies for the dedifferentiated Schwann cell marker p75. We observed that only 4% of the proliferating cells are p75+. Although surprising, this is consistent with the low proliferative index that characterises established benign neurofibromas. Interestingly, when we co-stained tumours sections with the macrophage marker Iba-1, we found that nearly 50% of the proliferating cells were positive for this marker (Figure 4-13). This may suggest that, although proliferating slowly at this stage of tumourigenesis, $Nf1^{-/-}$ Schwann cells may have a non-autonomous effect on other cellular constituents of the tumour. By propagating the inflammatory response, $Nf1^{-/-}$ cells may contribute to the maintenance of a pro-tumourigenic microenvironment and, consequently, the tumour itself.

4.8 Characterization of the tumour stroma - inflammatory cells and fibroblasts

A role for inflammation in tumourigenesis is now widely accepted, and it has become evident that an inflammatory microenvironment is an essential component of the stroma in most tumours (Grivennikov et al., 2010). Histological analysis of H&E stained sections of the neurofibromas that developed at the injury-site had already indicated the presence of a strong associated inflammatory response.

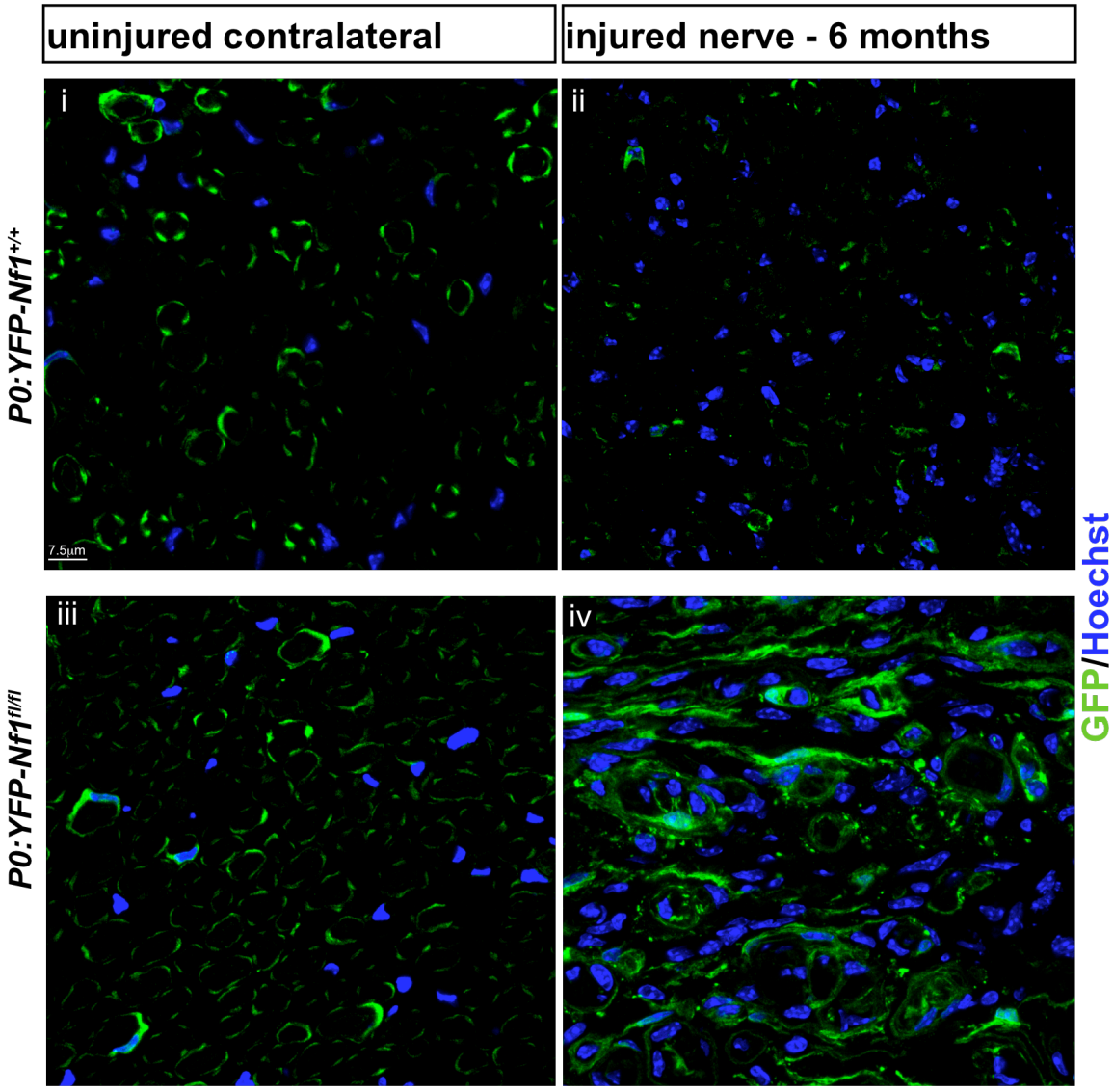

Figure 4-11: Few GFP+ cells are found at the wound site, in control animals, 6 months following injury. Cross-sections of sciatic nerves from control and *Nf1*-deficient mice were immunostained for GFP (green). Figure compares the injured nerve at the wound site (that corresponds to a neurofibroma in *Nf1*-deficient nerves) (**ii** and **iv**) with the respective unwounded contralateral nerve (**i** and **iii**). Note that in contrast to the neurofibroma where abundant GFP staining is observed, only a few positive cells are found in regenerated controls at the injury site.

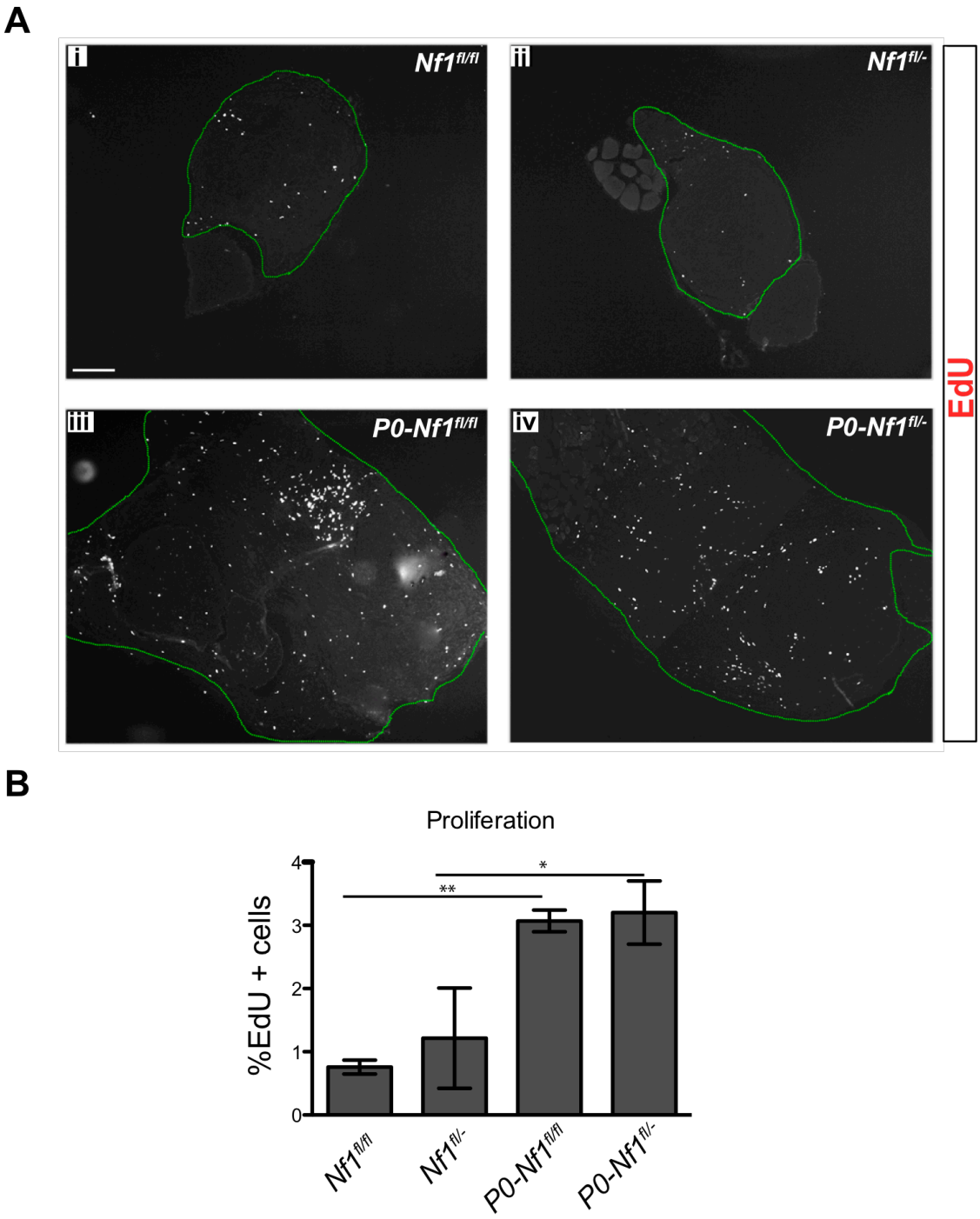

Figure 4-12: **Increased proliferation in NF1 mutant nerves**.

A) EdU staining showing that 8 months following transection, *Nf1*-deficient sciatic nerves exhibit increased cell proliferation at the site of injury when compared to the same region of control animals. Note that proliferation varies greatly between regions within the same nerves. The green dashed line delimits injured regions. **B**) Quantification of EdU positive cells in all 4 genotypes (n=3 or 4 of each group, data are mean values, error bars represent ±SEM).

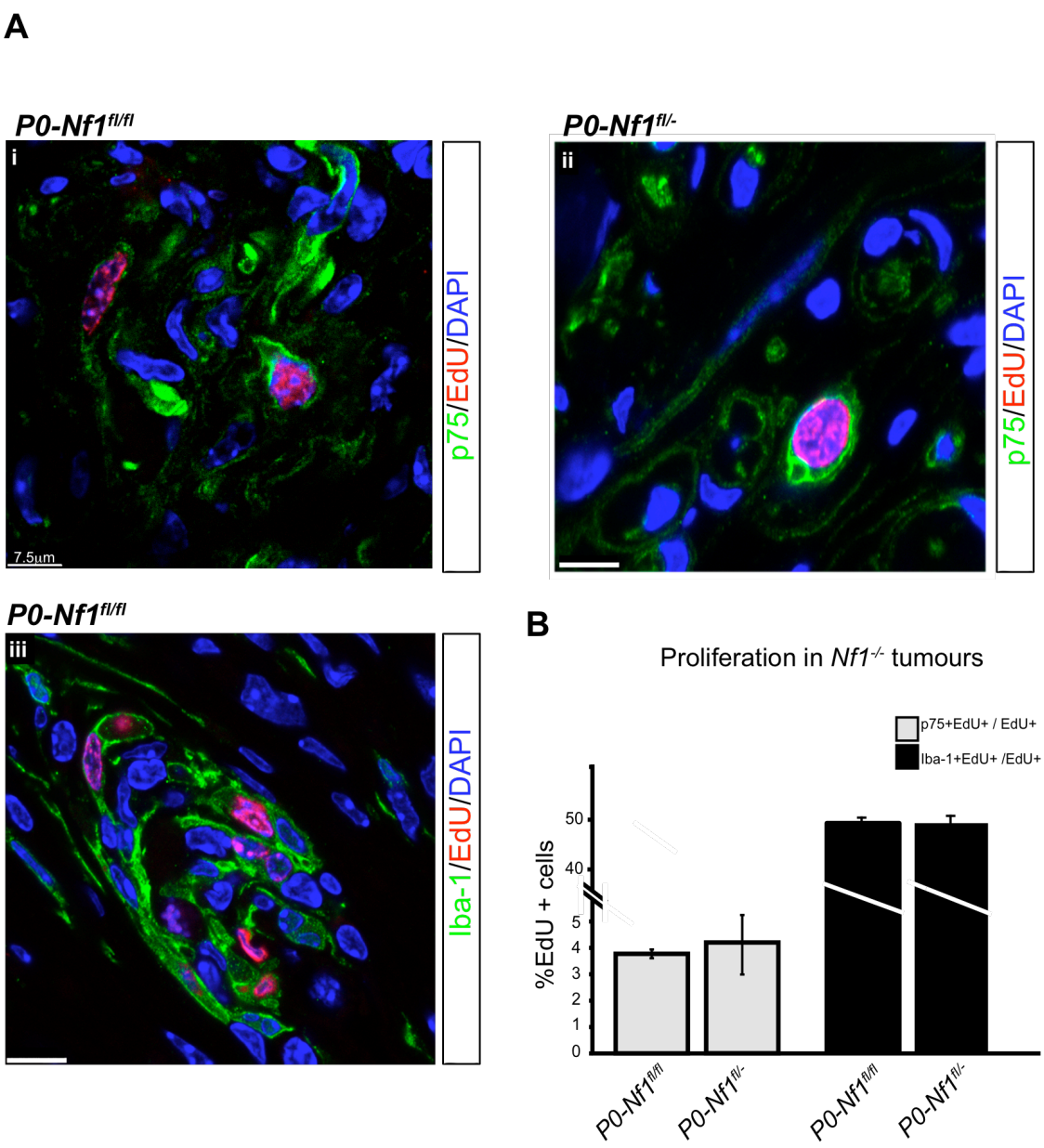

Figure 4-13: p75+ Schwann cells and macrophages proliferate in tumours formed in *Nf1*-deficient peripheral nerves after injury.

A) 8 months after nerve transection, mice were injected with EdU and sciatic nerves were harvested and processed for immunostaining. Cross-sections of tumour samples from NF1 mutants were stained for: EdU (red) and p75 (green) (**i** and **ii**); and EdU and Iba-1 (green) (**iii**); **B**) Quantification of p75+EdU+/EdU+ and Iba1+EdU+/EdU+ (data represent means and ±SEM of 3 animals per group).

To further characterize the inflammatory component of the tumours, we sectioned enlarged *Nf1*-deficient sciatic nerves and regenerated controls, 8 months following injury and performed a series of stainings for a variety of immune cells. Mast cells, a component of the innate immune response, were shown to be a critical player in a distinct mouse model of neurofibroma development and their presence is one of the hallmarks of these tumours. To investigate if this was the case in the neurofibromas developed in our NF1 model, we stained paraffin sections with Alcian blue and observed that tumours contained an increased number of mast cells when compared to regenerated control nerves (Figure 4-14A). Consistent with the Alcian blue staining, immunolabelling with the mast cell receptor, c-Kit, also showed an increased number of mast cells in the tumours (Figure 4-14B and C). Regenerated nerves, although having fewer mast cells than the neurofibromas, still exhibited higher numbers of mast cells comparatively to unwounded nerves, which suggests that mast cells persist in the nerve long after regeneration. Interestingly, all the animals with an $Nf1^{+/-}$ background displayed more mast cells than their $Nf1^{+/+}$ littermates. This observation, despite being found consistently in all the mice analysed, did not reach statistical significance likely due to the reduced number of animals used in the experiment (n=4). If proven true, this would be in accordance with reports from the Clapp group that showed that $Nf1^{+/-}$ mast cells are hypermotile in response to the KitL secreted by Schwann cells and that this effect is exacerbated in the presence of $Nf1^{-/-}$ Schwann cells (Yang et al., 2003). Still, because the frequency of tumour formation did not vary with the *Nf1* background, we can eliminate a determining role for $Nf1^{+/-}$ mast cells in our neurofibroma model. Tumour-associated macrophages are a major component of the infiltrate of most tumours (Balkwill and Mantovani, 2001). Macrophages derive from circulating monocytic precursors and are directed into tumours by chemoattractants. In accordance with the high proliferative rate described earlier in Figure 4-11, macrophages are present at elevated numbers in these tumours (Figure 4-15). Neutrophils are the first immune cell to arrive at site of injury, but are usually cleared within few days following wounding. We assessed the presence of these phagocytic cells in sciatic nerves of control and NF1 mutants, 8 months following injury. NIMP positive cells, although in a reduced number, were only found in the tumours and not in the regenerated nerves (Figure 4-16 A and C). Finally, we have analysed the presence of T cells, a sub-group of lymphocytes that play a central role in the adaptative immune response.

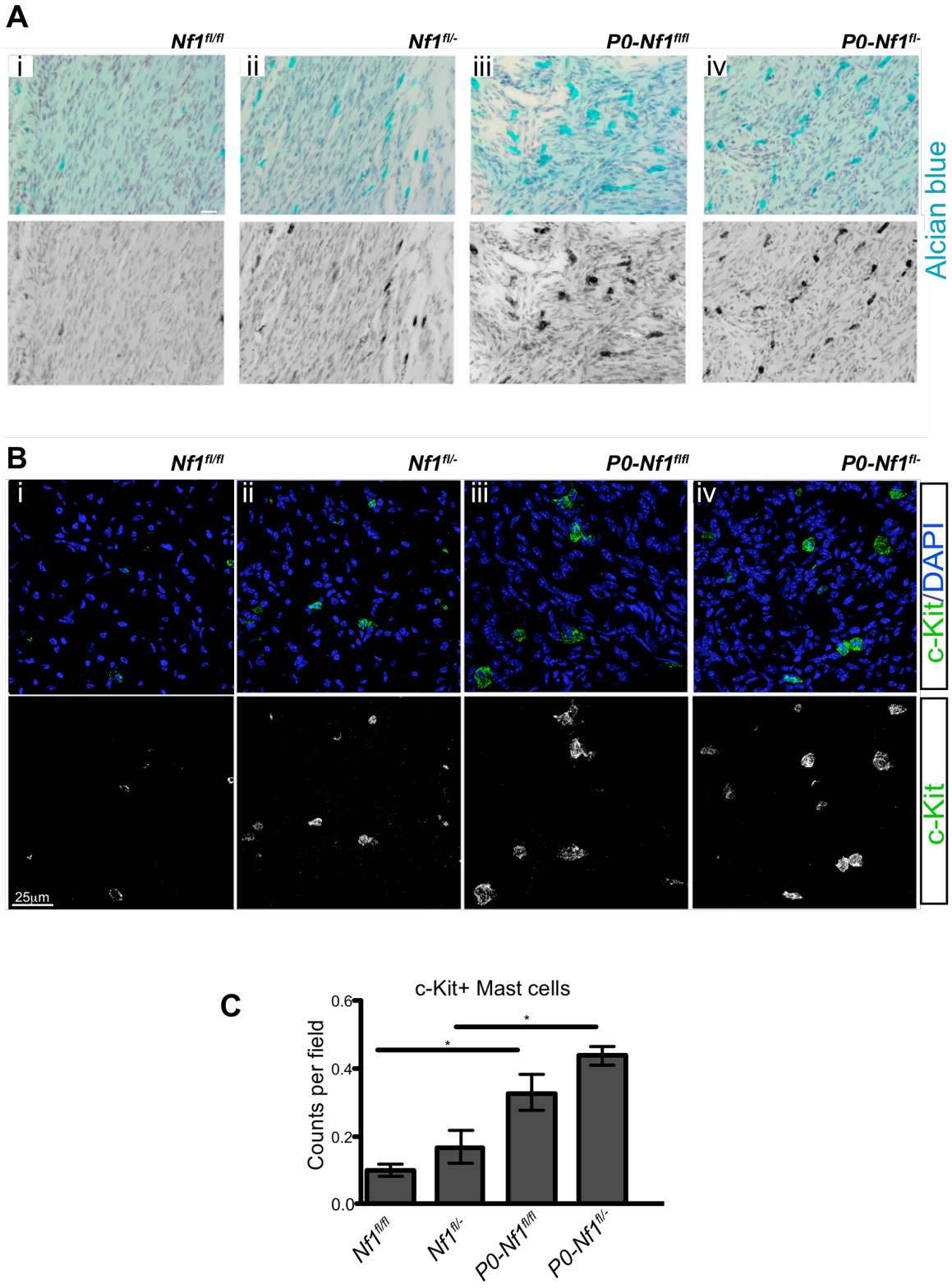

Figure 4-14: Increased infiltration of mast cells in *P0-Nf1^{flfl}* and *P0-Nf1$^{fl/-}$* sciatic nerves. **A**) Alcian blue and **B**) c-Kit immunolabelling show increased numbers of mast cells in the injured region of NF1 mutants when compared to controls, 8 months following nerve transection. **C**) Quantification of mast cells as determined by c-Kit staining of sciatic nerve cryosections (n=3 animals for each group; 8 fields per section and 3 sections per animal were counted, data are represented as mean values ±SEM).

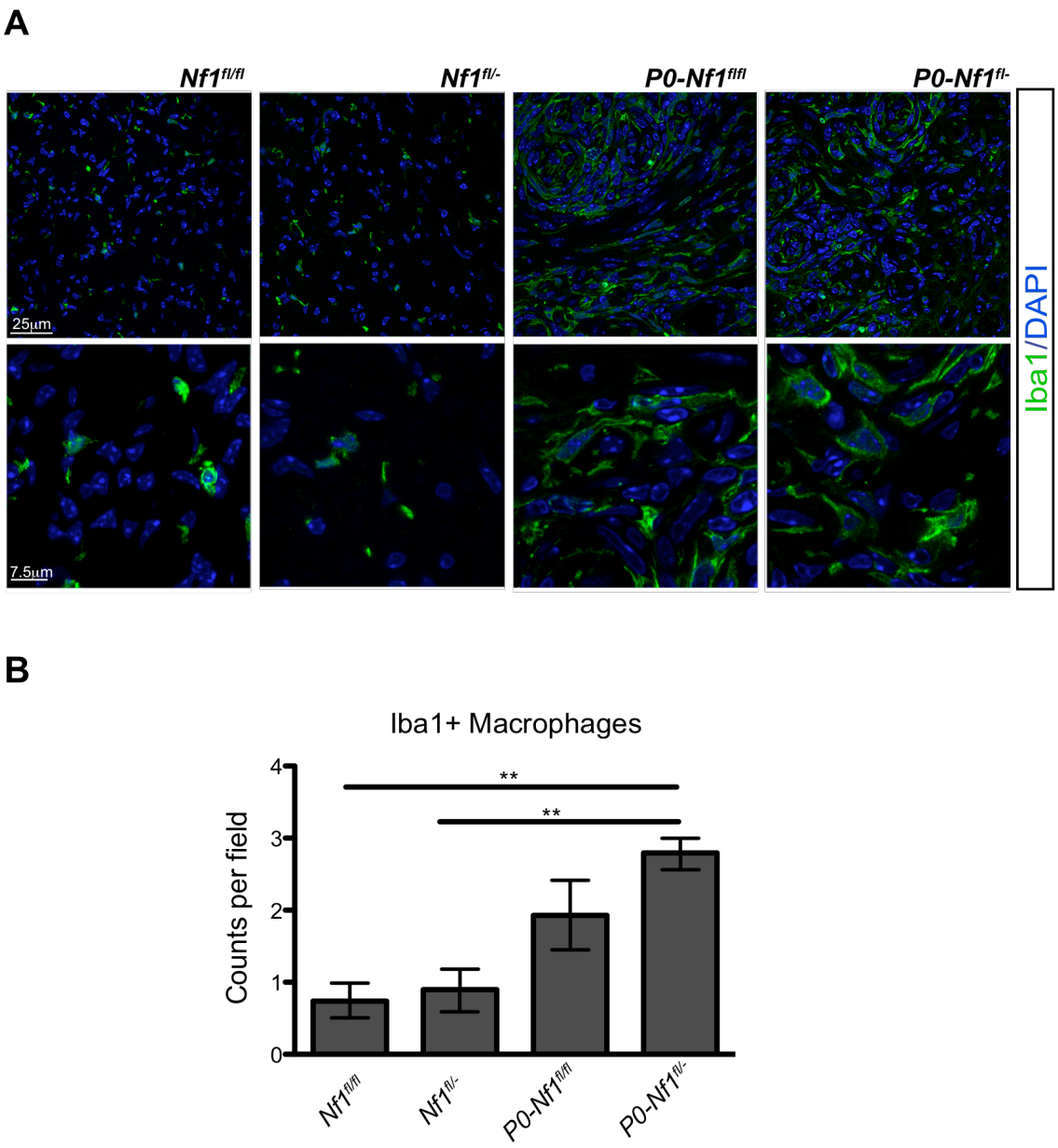

Figure 4-15: Macrophages are present at elevated numbers in NF1 mutant nerves at the tumour region. A) Representative images of sciatic nerve cross-sections stained for the macrophage marker Iba-1 and counterstained with DAPI. **B**) Quantification of Iba1+ cells (n=3 animals for each group, 10 fields were counted per section, 3 sections were analysed for each animal, data are represented as mean values ±SEM).

In tumour immunity, T cells are generally more recognized for their antitumour activity, however they may also exert tumour-promoting effects under certain circumstances (Grivennikov et al., 2010). CD3 staining revealed the occurrence of a few positive cells, exclusively in the tumours (Figure 4-16B and D). To summarize; we confirmed the presence of a strong inflammatory component in the neurofibromas that formed at the site of injury in *Nf1*-deficient sciatic nerves. These immune cells were differentially distributed throughout the tumours, with most found in clusters in the proximity of blood vessels within the tumours (Figure 4-17). In addition to inflammatory cells, it is becoming increasingly clear that fibroblasts are also prominent modifiers of tumourigenesis (Kalluri and Zeisberg, 2006). Fibroblasts are the principal cellular component of connective tissue and are best known for the prominent role that they play in wound repair. Activated fibroblasts at the lesion site, proliferate, generate large amounts of extracellular matrix and contribute to the contraction of the healing wound. Work from our laboratory has discovered an additional and important role for these cells in peripheral nerve injury; interactions between fibroblasts and Schwann cells, through ephrin-B/EphB2 signalling, result in cell sorting, which in turn enables the directional collective cell migration of Schwann cells out of the nerve stumps to guide regrowing axons across the wound (Parrinello et al., 2010). In normal circumstances, once the wound is repaired, fibroblasts decrease in number and revert to a resting phenotype. Instead, at the site of a tumour, they are frequently found perpetually activated and play an increasingly acknowledged role in fostering tumourigenesis. To investigate if activated fibroblasts were present in neurofibromas 8 months following injury, we performed immunohistochemistry for Smooth-muscle-actin (SMA). This marker, although frequently used to identify activated fibroblasts, also labels other cell types such as pericytes. Indeed, in all the nerves examined, SMA+ cells were found surrounding blood vessels (Figure 4-18iii). Nevertheless, outside the blood vessels, positive cells were detected exclusively in tumours and never in regenerated nerves, suggesting that activated fibroblasts are a component of the tumour stroma, in some of the neurofibromas. However, as illustrated in Figure 4-18, not all tumours were positive for this marker, implying that activated fibroblasts do not play a critical role in neurofibroma development in the model described here. This is evocative of the pathology of human neurofibromas, in which fibroblast contribution to tumour composition is highly variable (Thomas et al., 2011). The presence of these different cell types so long after injury is consistent with the presence of a chronically

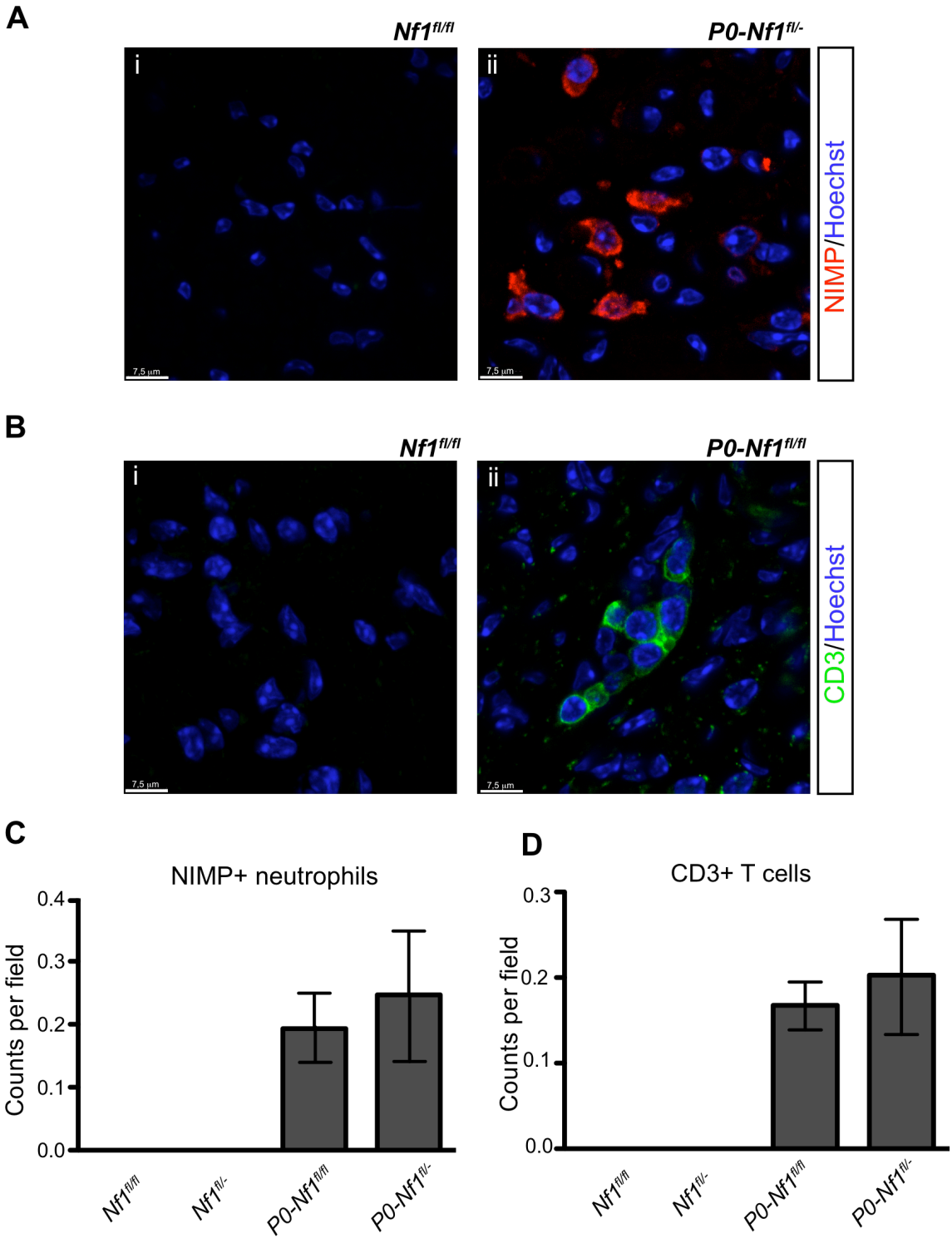

Figure 4-16: Inflammatory cells are recruited into the tumours developed by NF1 mutants. Eight months following injury, Tmx-treated mice were harvested and cryosections of sciatic nerves were immunostained for **A**) the neutrophil marker NIMP-R14 and for **B**) the T-cell marker CD3. Representative images of cross-sections are shown. **C**) Quantification of CD3+ and NIMP+ cells (n=3 animals for each group, 10 fields were counted per section, 3 sections were analysed for each animal, data are represented as mean values ±SEM).

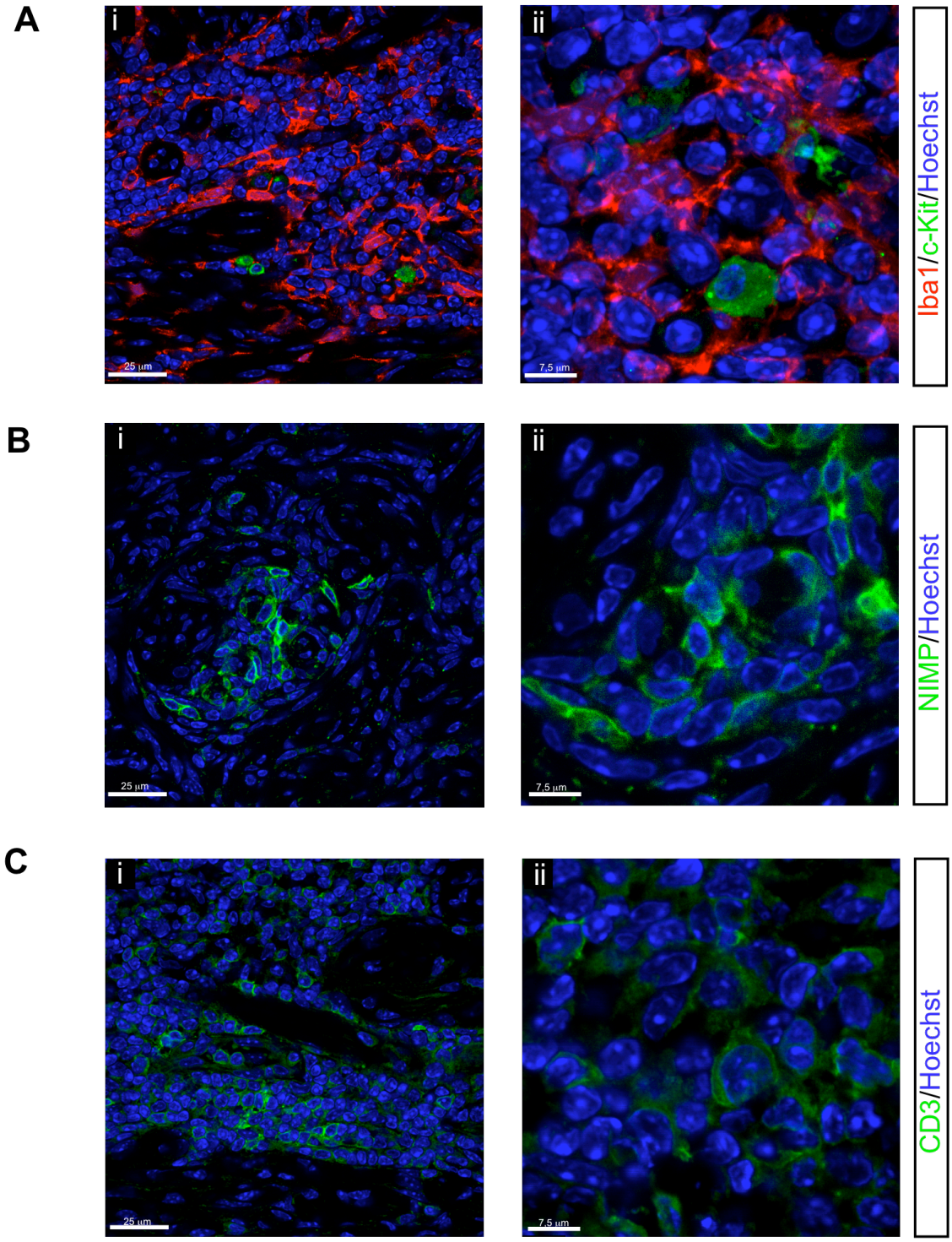

Figure 4-17: A strong inflammatory response is observed in the neurofibromas. Immunostainings of cryosections of peripheral nerve tumours, 8 months after injury show clusters of immune cells, heterogeneously distributed. Examples of regions strongly positive for **A**) the macrophage and mast cell markers (Iba1 and c-Kit, respectively); **B**) the neutrophil marker NIMP and **C**) the T-cell marker CD3. **ii** shows higher magnifications of **i.**

A

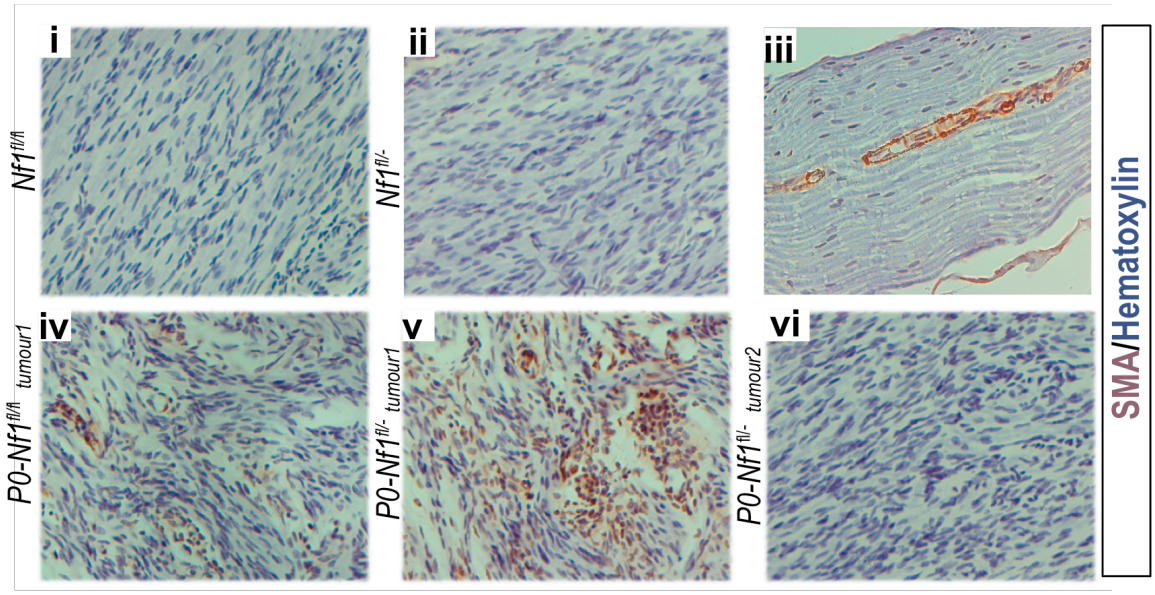

Figure 4-18: Variable expression of Smooth Muscle Actin in tumours from NF1 mutant mice. A) Sciatic nerves were embedded in paraffin and processed for SMA staining, 8 months following surgery. Control mice (**i** and **ii**) were consistently negative for the activated fibroblasts marker SMA. **iii** shows SMA+ pericytes in an uncut control. Tumours developed by *P0-Nf1*$^{fl/fl}$ and *P0-Nf1*$^{fl/-}$ mice (**iv-vi**) showed variable expression of SMA. Shown are three examples representative of this variability (3 animals of each genotype were analysed).

activated inflammatory response and is strongly reminiscent of Dvorak's description of tumours as "wounds that do not heal" (Dvorak, 1986).

4.9 Distal to the injury site, *Nf1*-deficient nerves regenerate normally

Up to this point, I have shown that adult *Nf1*$^{-/-}$ mSchwann are protected from tumourigenesis in the context of a normal nerve; yet, when in concert with a nerve injury, they give rise to neurofibromas. Thus, it seems that the dedifferentiated, progenitor-like state to which mSchwann cells revert upon injury is more susceptible to tumourigenesis. Nevertheless, the dedifferentiated state is not, *per se*, sufficient to render Schwann cells tumourigenic. As detailed before, upon wounding to a peripheral nerve, all Schwann cells distal to the site of injury dedifferentiate along the length of the nerve. However, interestingly, neurofibromas arose exclusively at the site of injury. We examined the structure of sciatic nerves downstream of the injury site in both controls and NF1 mutants (Figure 4-19A). Figure 4-19Bi shows representative images of semi-thin sections stained with toluidine blue and visualized by phase-microscopy. Control and *Nf1*-deficient nerves were indistinguishable; both appeared packed with myelinated axons and reduced interstitial space (similar to the site of injury in controls- see Figure 4-5i). This was further confirmed at the ultrastructural level using electron microscopy; the distal region of controls and mutants were well regenerated and, most importantly, comparable in all the 4 genotypes studied (Figure 4-19Bii).

In agreement with the structural analysis, the inflammatory response in controls and mutants was found to be mostly resolved and equivalent between groups. Accordingly, the cell density was not significantly different in regenerated controls and mutant distal nerves (Figure 4-20). Nevertheless, repaired nerves exhibited slightly higher numbers of mast cells and macrophages when compared to unwounded tissue, even when mice were analysed up to 12 months after nerve transection, suggesting that a basal inflammatory response persists long after wounding (compare Figure 4-20 and 3-9). Together, this data suggests that distal to the site of injury, *Nf1*$^{-/-}$ Schwann cells are protected from tumourigenesis. What is more, the nerve region downstream of the injury site seemed to regenerate similarly in control and NF1 mutants. Exceptionally, in a very small number of tumours (n=3 out of 25 in *P0-Nf1*$^{fl/fl}$ and 1 out 18 in *P0-Nf1*$^{fl/-}$), the distal region was also enlarged, in a manner indicative of the tumours spreading along the nerves (Figure 4-21). This is consistent with the human pathogenesis of

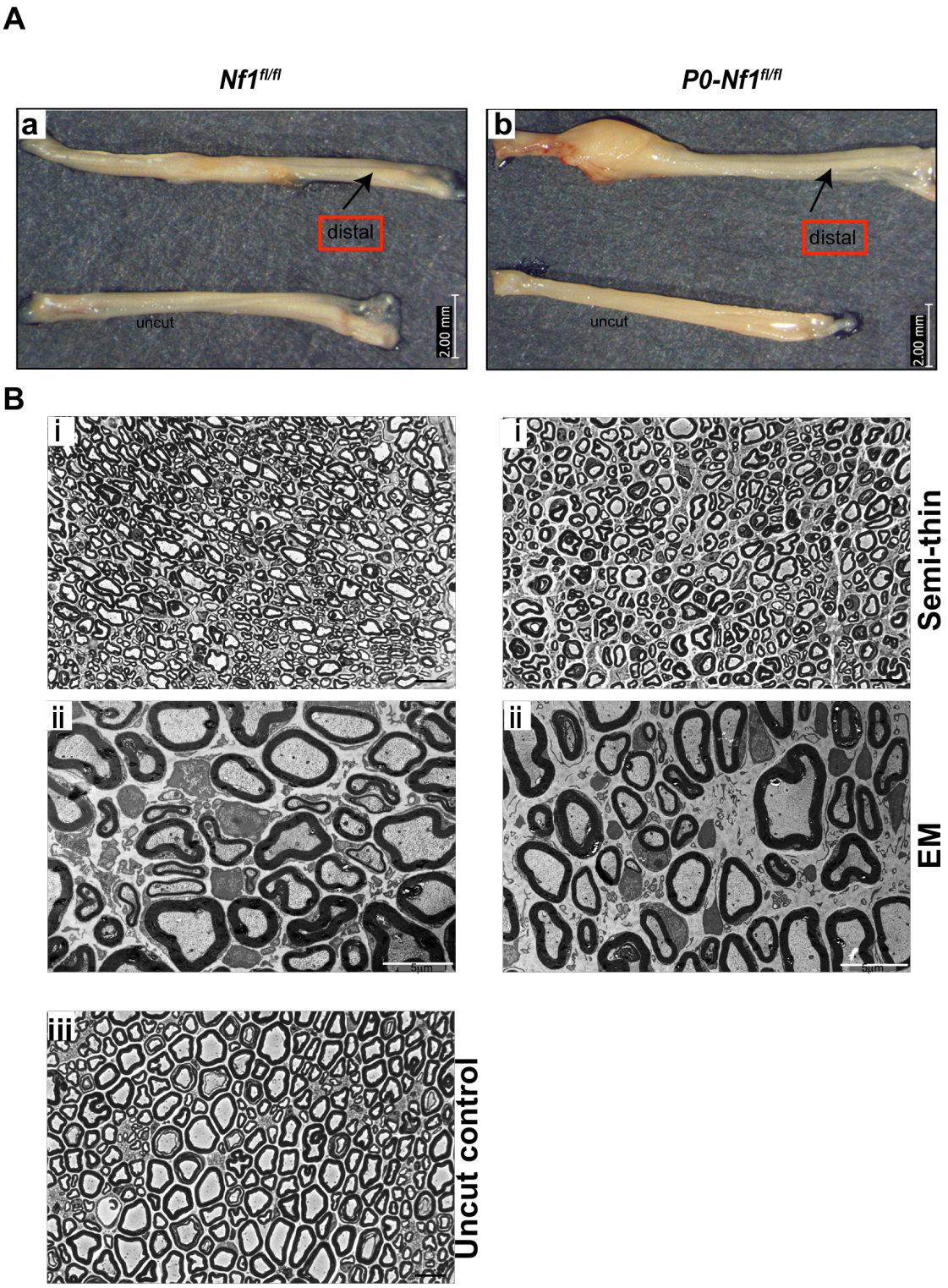

Figure 4-19: Distal to the wound site, nerves regenerate normally in *P0-Nf1*$^{fl/fl}$ and *P0-Nf1*$^{fl/-}$ mice. The distal region of injured sciatic nerves is indistinguishable between control (**A**) and mutant mice (**B**). **i** shows representative phase-microscopy images of semi-thin sections stained with toluidine blue; **ii** shows electron micrograph images. **iii** represents a semi-thin section from a control uncut nerve (4 animals of each genotype were processed for analysis, similar results were obtained for *Nf1*$^{+/+}$ and *Nf1*$^{+/-}$ backgrounds).

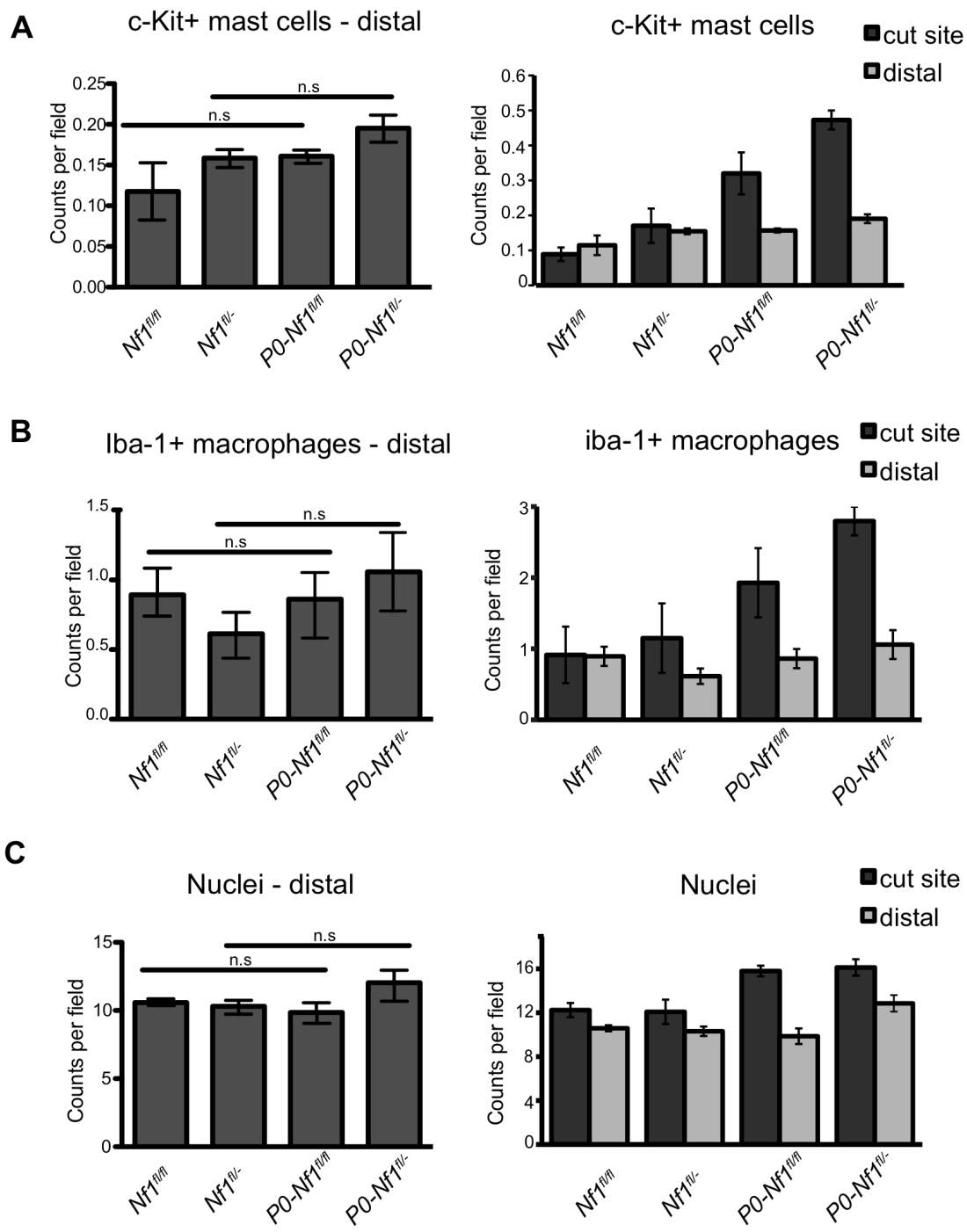

Figure 4-20: Analysis of the region distal to the injury site, 8 months following wounding. No significant differences were found in the numbers of (**A**) c-Kit+ mast cells, (**B**) Iba-1+ macrophages and (**C**) total nuclei in the distal regions of control and mutant animals. On the right, a comparison between distal stumps and cut sites is shown. The few mutant nerves in which the tumours spread to the distal stumps were not included in this analysis; the "cut site" in NF1 tumours refers to tumours only - macroscopically normal nerves were not analysed (n=3 animals for each group, 10 fields were counted per section, 3 sections were analysed for each animal, data are represented as mean values ±SEM).

A

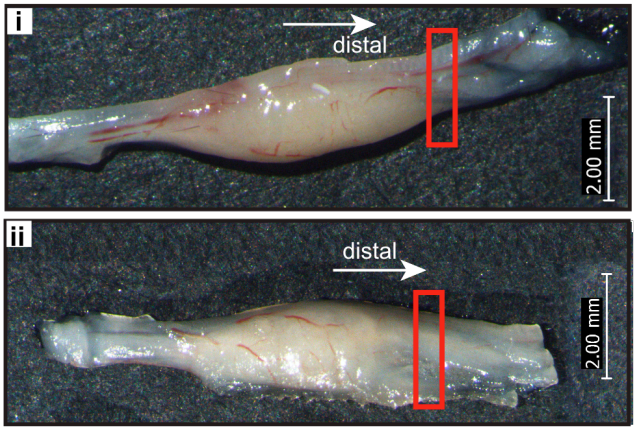

B

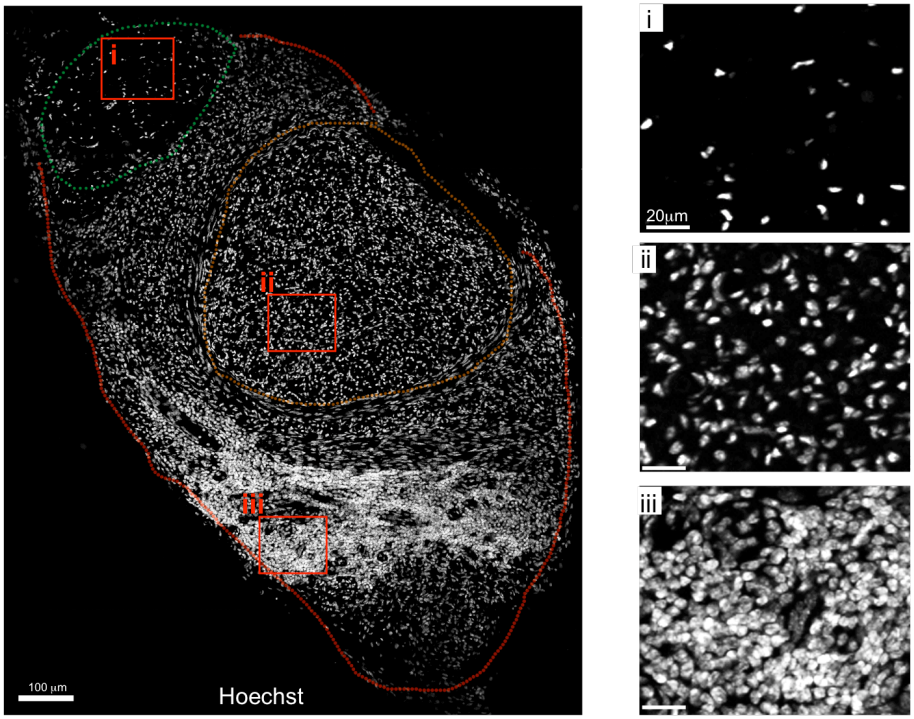

C

	total number of tumours	tumours spreading to the distal region
P0-Nf1$^{fl/fl}$	25	3
P0-Nf1$^{fl/-}$	18	1

Figure 4-21: A few tumours spread along the distal stump of the nerve. A) Macroscopic appearance of tumours that developed in (**i**) *P0-Nf1$^{fl/fl}$* (ii) and *P0-Nf1$^{fl/-}$* mice. Red boxes indicate the regions cross-sections were prepared from **B**) Hoechst staining of the distal region of the nerve shown in A-i. Dashed lines delineate uninjured (green line), regenerated (orange) and tumour (red) areas. Right panel shows zoomed areas. **C**) Table showing the number of tumours that spread along the distal stump.

neurofibromas in which tumours can be found growing along large nerve plexus (Hrehorovich et al., 2003).

4.10 Distal to the tumour, *Nf1*$^{-/-}$ Schwann cells redifferentiate and remyelinate axons

The absence of tumours in the distal stump of injured *Nf1*-deficient nerves could be explained by two distinct hypotheses: 1) at this region of the nerve *Nf1*$^{-/-}$ Schwann cells die following dedifferentiation; 2) *Nf1*$^{-/-}$ Schwann cells persist, but the presence of pro-differentiative signals (and/or the absence of pro-tumourigenic cues) induce them to redifferentiate.

To discriminate between these possibilities we took advantage of the YFP reporter described earlier and traced the fate of *Nf1*$^{-/-}$ Schwann cells. Six months following injury, we harvested *Nf1*-deficient mice and analysed the nerve region downstream of the tumours that had formed at the wound-site (see Figure 4-19A). Remarkably, *Nf1*$^{-/-}$ Schwann cells were found redifferentiated and remyelinating axons, as illustrated in Figure 4-22. In contrast to what we encounter at the tumour site, where most GFP positive cells are deprived of axonal contact and are S100 negative, at the distal stump we found that nearly all GFP positive cells were associated with axons and expressing S100 (Figure 4-22). The same was true in the equivalent region of regenerated control nerves (Figure 4-23). It is noteworthy that a few GFP+S100-negative cells were also identified, some of which were GFP+p75+. Based on this observation, we may hypothesize that once dedifferentiated, originally P0-expressing, myelinated Schwann cells can re-differentiate into non-myelinating Schwann cells. This needs further analysis to be confirmed but, if proven true, provides additional evidence of the remarkable plasticity of these cells.

This data demonstrates that the same genetic insult (*Nf1* loss) has opposing outcomes depending on the microenvironmental context; dedifferentiated Schwann cells at the distal site undergo redifferentiation, whereas at the wound site, unknown signals specific for this region induce dedifferentiated *Nf1*$^{-/-}$ Schwann cells to form neurofibromas.

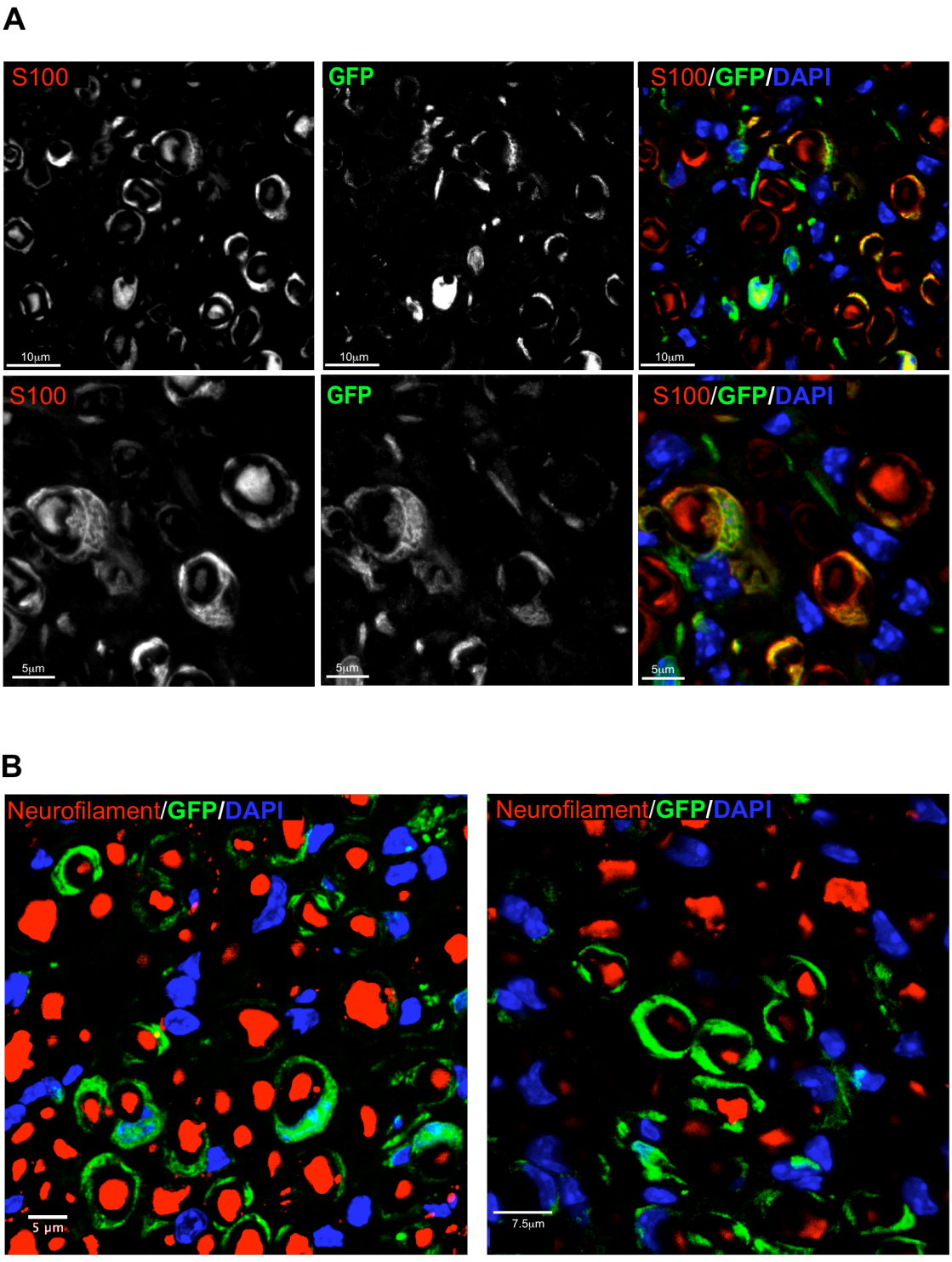

Figure 4-22: Distal to the tumour region, *Nf1*$^{-/-}$ Schwann cells are found redifferentiated and remyelinating. Sections were prepared from the nerve region distal to the neurofibroma formed in a *P0:YFP-Nf1*$^{fl/fl}$ mouse (see Figure 4-16) and immunolabelled for **A**) GFP (green) and the mature Schwann cell marker, S100 (red); **B**) GFP (green) and the axonal marker neurofilament (red). Nuclei were stained with DAPI. In contrast to what was observed in the tumour itself, at this region of the nerve, *Nf1*$^{-/-}$ Schwann cells redifferentiated and remyelinated normally after injury.

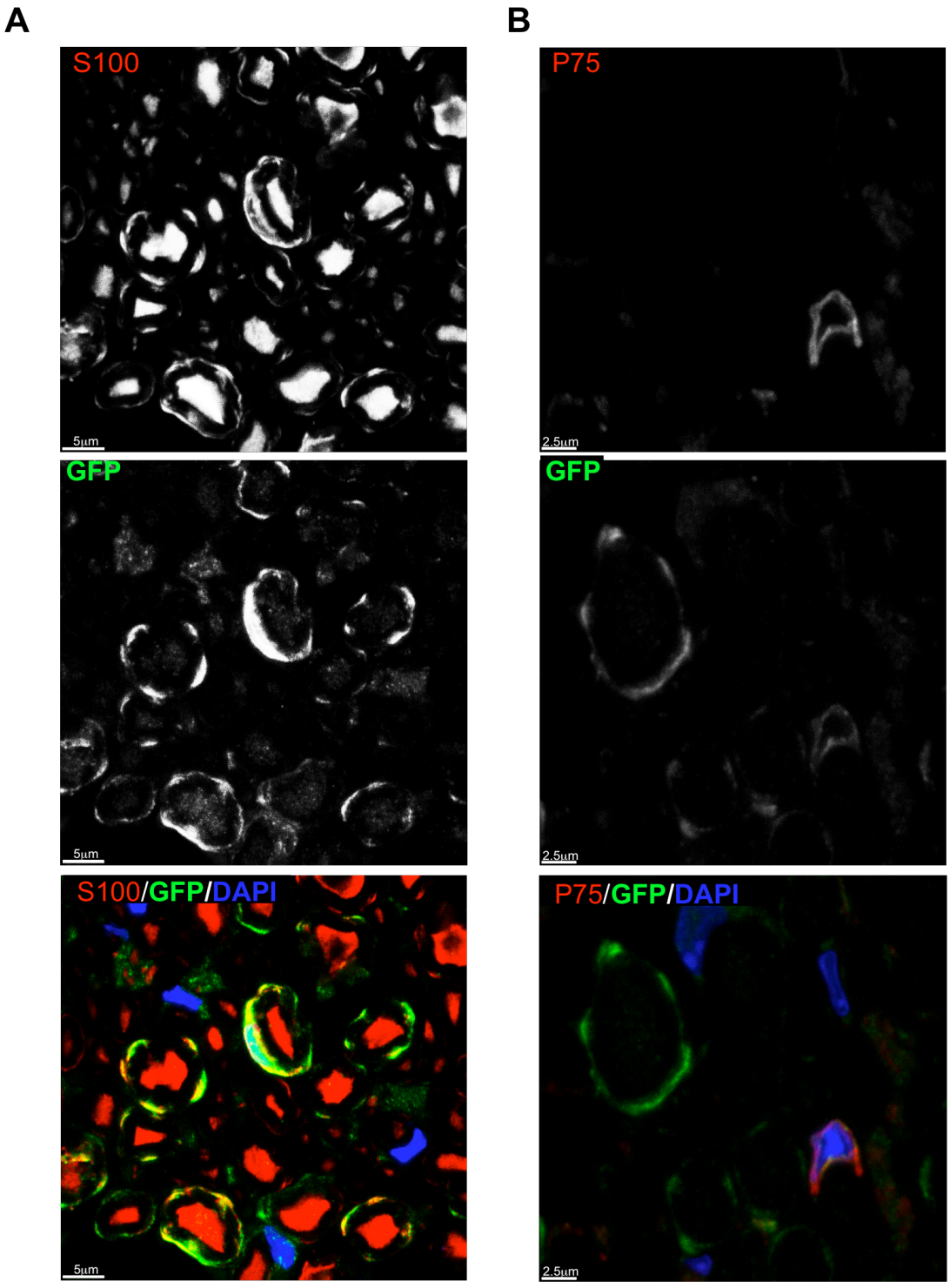

Figure 4-23: GFP-expressing cells persist in the regenerated control nerves, 6 months following injury. Distal nerves from *P0:YFP* controls were sectioned and stained for **A**) S100 (red), GFP (green) and DAPI (blue); **B**) p75 (red), GFP (green) and DAPI (blue). Six months after Tmx and nerve transection, most of the Cre expressing cells were found remyelinating and expressing the S100 marker. A few GFP+p75+ were found, suggesting that mSCs can redifferentiate into non-myelinating Schwann cells, after injury. Further confirmation is needed.

4.11 Chapter summary and conclusions

In the previous chapter we had shown that loss of the tumour suppressor neurofibromin was unable to perturb myelinating Schwann cell behaviour and induce tumour formation in adult mice. Here we tested whether nerve wounding would be able to alter the tumourigenic properties of *Nf1*$^{-/-}$ Schwann cells. To this end, we performed nerve transection in Tmx treated control and NF1 mutants and, 6-8 months later, analysed the nerves. We found that by this time-point, control nerves repaired normally and only a basal inflammatory response remained. In contrast, NF1 mutants developed nerve sheath tumours at the site of injury. Importantly, the frequency of tumour formation was independent of the genetic background, eliminating a decisive role for *Nf1* haploinsufficiency. We characterized the tumours by means of histological and ultrastructural analysis and classified them as neurofibromas. Strikingly, we traced *Nf1*$^{-/-}$ cells using *P0:YFP-Nf1*$^{fl/fl}$ animals and identified them as a major cellular component of the tumours. Not all the GFP+ cells were S100 positive, raising the exciting possibility that myelinating, P0-expressing Schwann cells may transdifferentiate into different cell types, upon injury. In particular, we noticed a remarkable similarity between GFP+/S100- cells and a frequent cellular constituent of neurofibromas, usually identified as "perineurial-like" cells. Hence it seems likely that these morphological distinct cells are, in fact, mSchwann cell derived. Further work will be done to better characterize these cells and to test if they also occur in injured control nerves or if this phenomenon is specific to an *Nf1*$^{-/-}$ context.

We described a strong inflammatory component associated with the neurofibromas that develop in *Nf1* mutants and confirmed the highly heterogeneous nature of the tumours.

The data described revealed that, unlike their differentiated counterpart, dedifferentiated progenitor-like Schwann cells can be rendered tumourigenic by *Nf1* loss. However, the switch in differentiation state is not, by itself, sufficient. Indeed, although Schwann cells dedifferentiate along the entire length of the nerve downstream of the injury, we found that tumours arose exclusively at the wound-site. Remarkably, when we analysed sciatic nerves distally to the wound site, we found that *Nf1*$^{-/-}$ Schwann cells had redifferentiated and remyelinated axons. Consistent with this, distal regions of both controls and mutants showed equivalent regeneration.

Taken together, this data shows that the tumourigenic potential of *Nf1*$^{-/-}$ mSchwann cells can be strongly modulated by microenvironmental cues. Otherwise refractory to tumourigenesis, dedifferentiated Schwann cells are susceptible to drive tumour

formation, but only when *Nf1* loss happens in concert with specific signals present exclusively at the site of injury. This new mouse model for neurofibroma formation offers excellent opportunities to further dissect microenvironmental components that are critical in determining the fate of genetically altered Schwann cells.

Chapter 5: Results III

5.1 Chapter introduction

In the previous chapter I have shown that wounding cooperates with *Nf1* loss to induce neurofibroma formation. Unexpectedly, all the tumours developed at the injury site, despite the Schwann cells dedifferentiating, with an associated inflammatory response, along the length of the nerve. This indicated that reverting to a dedifferentiated state is not sufficient to induce $Nf1^{-/-}$ SCs to form tumours. Instead, it shows that signals, or a threshold of signals, specific to the site of wounding are required to synergize with loss of *Nf1* in mSchwann cells to drive tumourigenesis. To start to dissect the microenvironmental cues that may be cooperating with the tumour suppressor loss we characterized NF1 mutants and control nerves shortly after injury, both at the injury site and distal to the wound.

5.2 The ERK pathway is deregulated in *Nf1*-deficient mice following injury

In chapter 3 of this thesis, I have shown that, despite its well-established role as a negative regulator of Ras signalling, neurofibromin loss in adult mSchwann cells does not cause a detectable effect on the relatively low basal levels of Ras/ERK signalling (Figure 3-10B). As mentioned, injury to the PNS induces Schwann cell dedifferentiation downstream of the site of injury through strong and rapid activation of the Ras/Raf/ERK pathway. We therefore wanted to investigate the ability of *Nf1*-deficient nerves to cope with the robust activation of this pathway, following nerve wounding. To do this, sciatic nerves of Tmx treated animals were dissected and processed for protein analysis, two, five and seven days following nerve transection. As expected, in the control mice we observed strong ERK activation, two days following injury. However, p-ERK levels markedly decreased by day 5 and 7 days following the surgeries were almost back to basal levels. In contrast, in NF1 mutant mice the levels of activated ERK were consistently found sustained at day 7. This was found in both $Nf1^{+/+}$ and $Nf1^{+/-}$ backgrounds, once again ruling out an effect of *Nf1* heterozygosity (Figure 5-1A). These results indicate that the ERK pathway is deregulated upon injury in mice with $Nf1^{-/-}$ mSCs.

Interestingly, when we immunostained sciatic nerve cross-sections prepared from the wound site and the distal area of the injured nerve, 7 days following surgery, we found a remarkable difference between the regions. Downstream of the injury site, activated

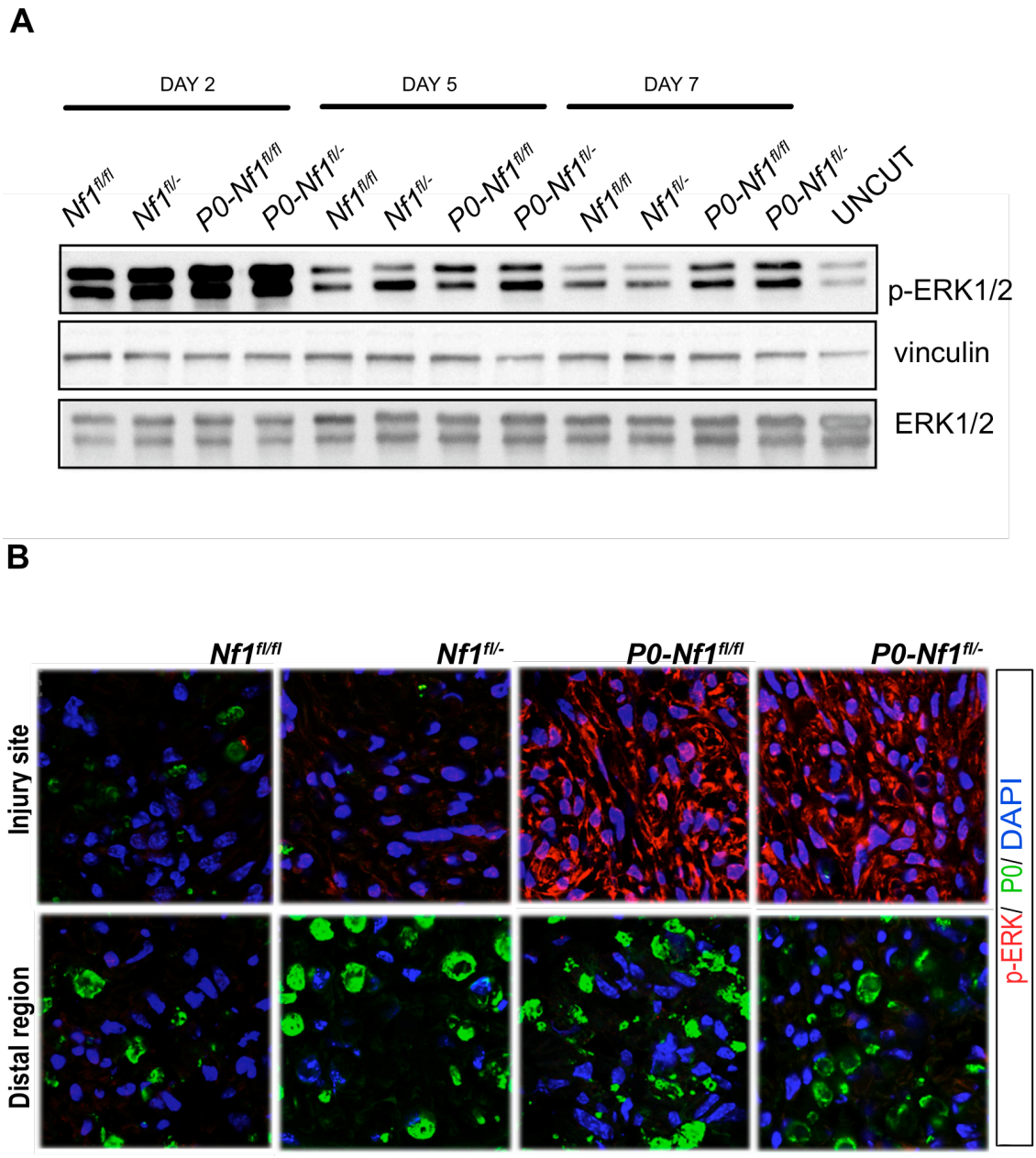

Figure 5-1: ERK signalling is deregulated in sciatic nerves of *Nf1*-deficient mice, following injury. **A**) Western blot analysis of nerves from control (*Nf1*$^{fl/fl}$ and *Nf1*$^{fl/-}$) and mutant (*P0-Nf1*$^{fl/fl}$ and *P0-Nf1*$^{fl/-}$) mice at indicated time-points after injury. Note the ERK signal is sustained at day 7 in mutant mice (blot representative of 4 different animals for each genotype) **B**) 7 days following injury, cryosections of sciatic nerves were immunolabelled for the mSC marker P0 (green) and p-ERK (red). Nuclei were counterstained with DAPI. Upper panel: site of injury; bottom panel: distal region. ERK pathway is sustained only at the site of injury, in NF1 mutants (representative images of 3 animals analysed for each group).

ERK could no longer be detected in both *Nf1*-deficient and control nerves. In sharp contrast, at the wound site, strong p-ERK staining was still observed, exclusively in NF1 mutant nerves (Figure 5-1B). This showed that, despite ERK activation occurring throughout the entire length of the distal stump, it is only at the injury site that the pathway is deregulated in the absence of NF1. We can envision two possible explanations for this: 1) the deregulation of ERK is dependent on a specific signal (or on a specific level of a signal) that is present exclusively at the wounding site; 2) at the distal region of the nerve, the microenvironment is more pro-differentiative, resulting in Ras/ERK suppression and consequently allowing normal redifferentiation of Schwann cells.

These observations are in agreement with our previous findings that downstream of the injury site, $Nf1^{-/-}$ Schwann cells were refractory to tumourigenesis and instead were found redifferentiated and remyelinating axons, 6-8 months following wounding. Furthermore, it strongly suggests a link between the presence of deregulated Ras/ERK signalling at the injury site and neurofibroma formation.

5.3 Increased proliferation in $Nf1^{-/-}$ Schwann cells

Upon injury, Schwann cells associated with degenerating axons dedifferentiate to a progenitor-like cell and re-enter the cell-cycle. The onset of mitogenesis is synchronous and has been described to peak 3-5 days following injury (Triolo et al., 2006). After this period, Schwann cells interact with the extracellular-matrix (ECM), reorganize their basement membrane and rearrange themselves into bands of Bungner. Importantly, Schwann cells mitotic activity is dependent on ERK signalling (Newbern et al., 2011; Napoli et al., 2012). We therefore tested if the deregulated levels of activated ERK detected in NF1 mutants would correlate with an effect on Schwann cell proliferation. Proliferation rates were assessed 7 days following injury (the time point at which we find that, contrary to controls, *Nf1*-deficient mice still exhibit elevated levels of p-ERK at the wound-site), in *P0:YFP-*$Nf1^{+/+}$ and *P0:YFP-*$Nf1^{+/-}$ controls and in *P0:YFP-*$Nf1^{fl/fl}$ and *P0:YFP-*$Nf1^{fl/-}$ mutants. Although not statistically significant we found that, at this stage, $Nf1^{-/-}$ Schwann cells appeared to proliferate more than *Nf1* positive or heterozygous cells (Figure 5-2A). Strikingly, this difference was only detected at the wound-site and not at the distal region, mirroring the differences in ERK activity and suggesting that by maintaining sustained activated levels of ERK, $Nf1^{-/-}$ Schwann cells are kept in a more proliferative-state (Figure 5-2B and C).

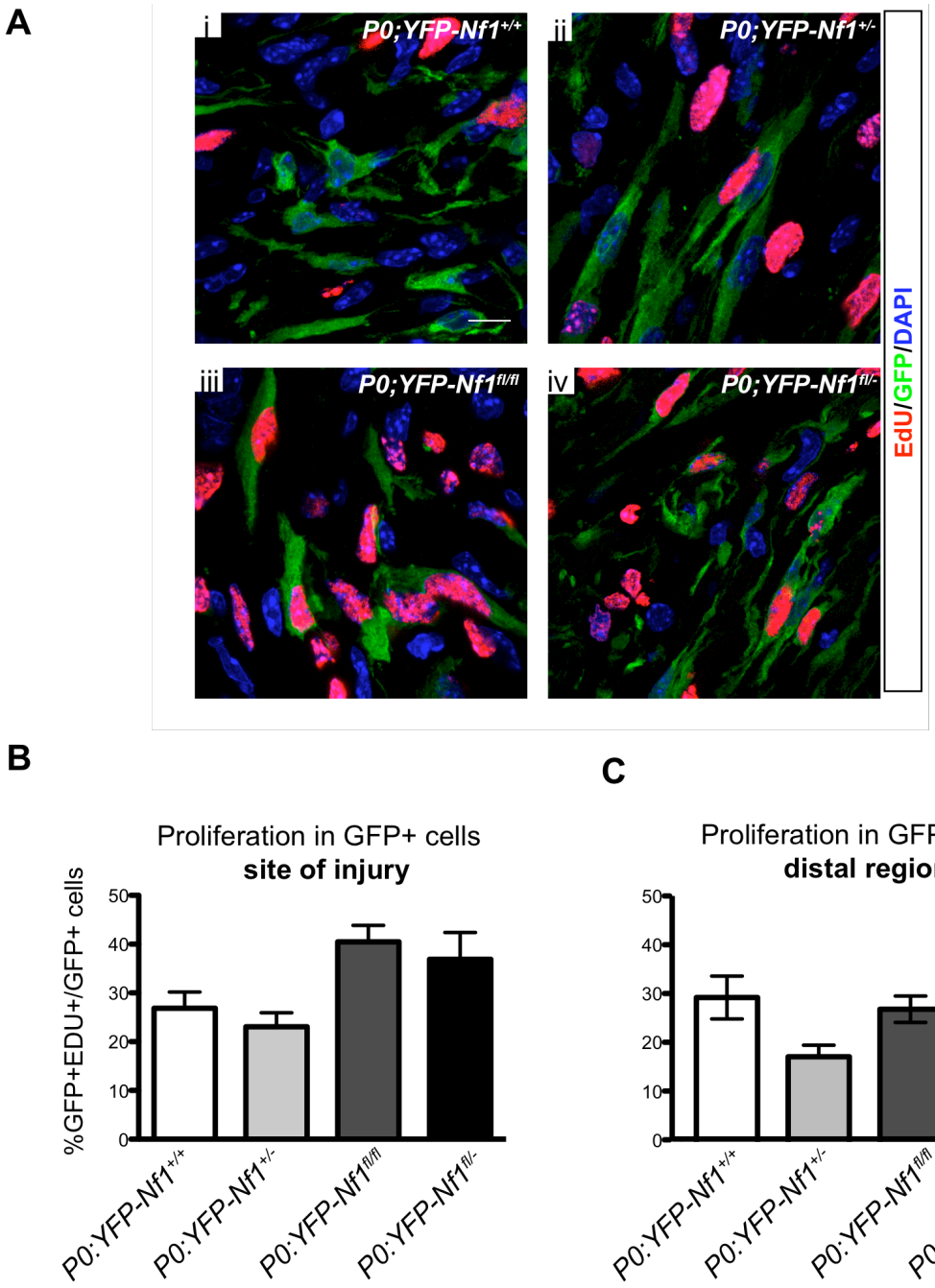

Figure 5-2: Increased proliferation in *Nf1*$^{-/-}$ Schwann cells 7 days following injury. EdU incorporation was assessed 7 days following injury in control (i and ii) and mutant mice (iii and iv). **A**) GFP labels Cre+ Schwann cells, EdU is stained in red. At the injury site of mutant mice, *Nf1*$^{-/-}$ Schwann cells (iii and v) showed increased proliferation when compared to GFP+ NF1+ cells in the same region of control mice (green in i and ii). **B**) Quantification of the % of GFP+EdU+ cells in control and mutant groups, at the site of injury. **C**) Similar quantification to B shows that at the distal region, similar rates of proliferation are observed in Schwann cells both in controls and mutant animals (n=3 of each animal group, 3 sections were analysed for each animal, 10 fields were counted per section, data represent means ±SEM).

5.4 Analysis of the extracellular matrix components

We next wanted to dissect putative signals differentially expressed at the injury site and the distal stump that could be affecting the behaviour of *Nf1*$^{-/-}$ Schwann cells specifically at the site of injury. First, we assessed the expression of ECM components. A variety of ECM proteins are upregulated following injury in the PNS and are thought to contribute to successful nerve repair by promoting axonal repair and SC remyelination (Akassoglou et al., 2002). During regeneration, ECM proteins (that can be organized in an interstitial matrix or at cell basement membranes) influence Schwann cell behaviour through sequestration and release of growth factors, and, through interaction with cell-adhesion receptors (Gardiner, 2011). Importantly, cell-matrix interactions are known to activate ERK signalling in several cell types (Sanders and Basson, 2000).

To investigate the distribution of ECM components following injury, we harvested mice 7 days following injury and compared the expression of the main ECM components – laminin 1, fibronectin, collagen I and collagen IV - at the injury site and distal stump, in control and *Nf1*-deficient nerves. As illustrated in Figures 5-3 to 5-6, laminin 1, collagen I and collagen IV localized specifically in the basal lamina of Schwann cells and epineurial cells (collagen IV was also found surrounding blood vessels), whereas fibronectin was abundantly expressed throughout the interstitial matrix (Figure 5-7). Overall, despite finding, as previously reported, increased expression of these proteins in injured nerves as compared to unwounded nerves, we failed to notice any striking difference in their expression levels between the injury site and the normal behaving distal region. Given this, we conclude that these components of the ECM are not the specific signal altering the behaviour of *Nf1*$^{-/-}$ Schwann cells.

A

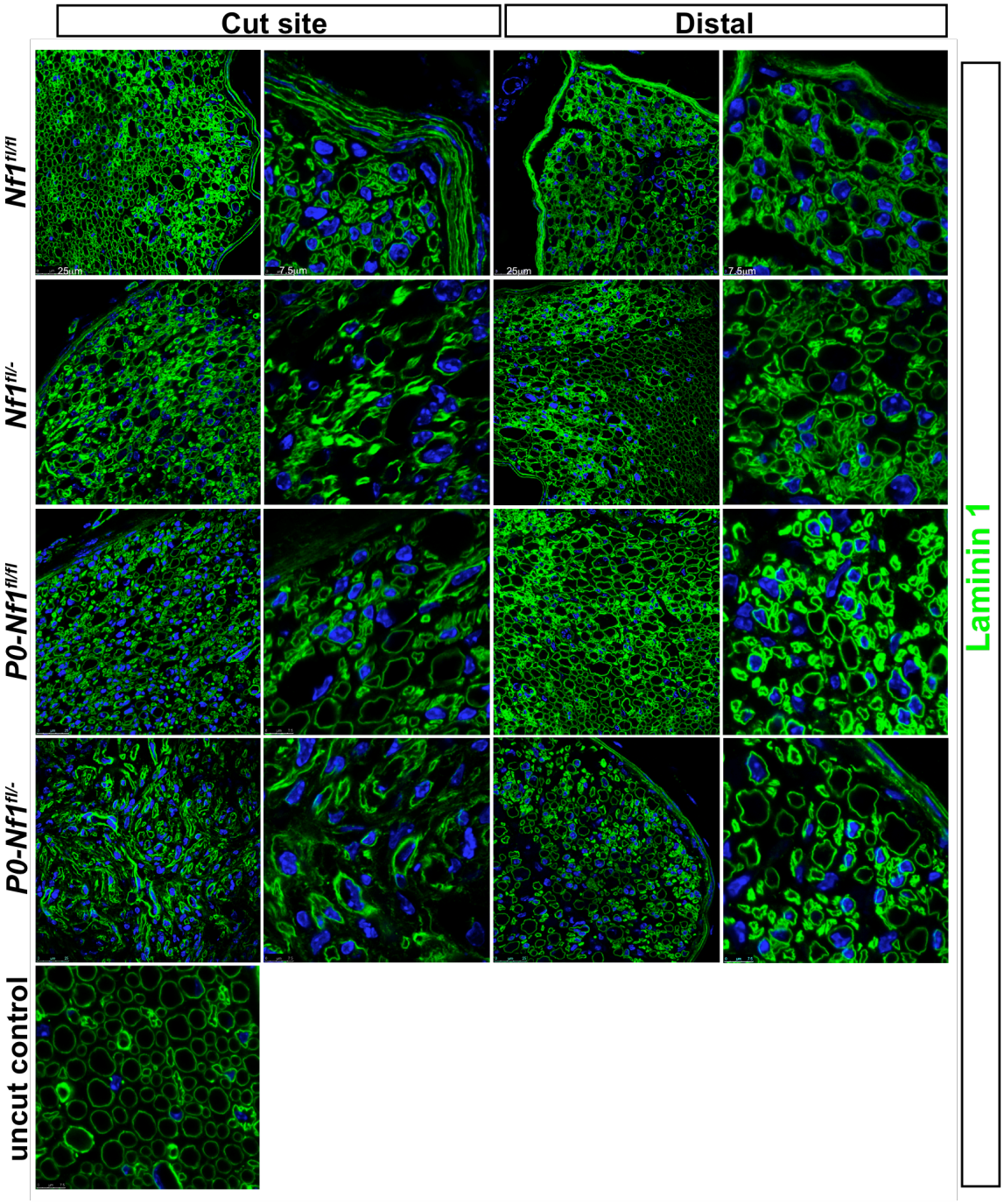

Figure 5-3: Analysis of the extracellular matrix components, 7 days following injury- laminin1. A) Sciatic nerves of Tmx-treated mice were partially transected and harvested for immunostaining, one week later. Immunolabelling for the ECM component laminin1 (green) shows no differences in the expression of this protein between controls and mutants and between the injury site and distal regions. **B**) (in the next page) The same as in A, but only the green channel is displayed, for better visualization. **C**) Amplification of A (n=3 for each genotype, shown are representative images).

B

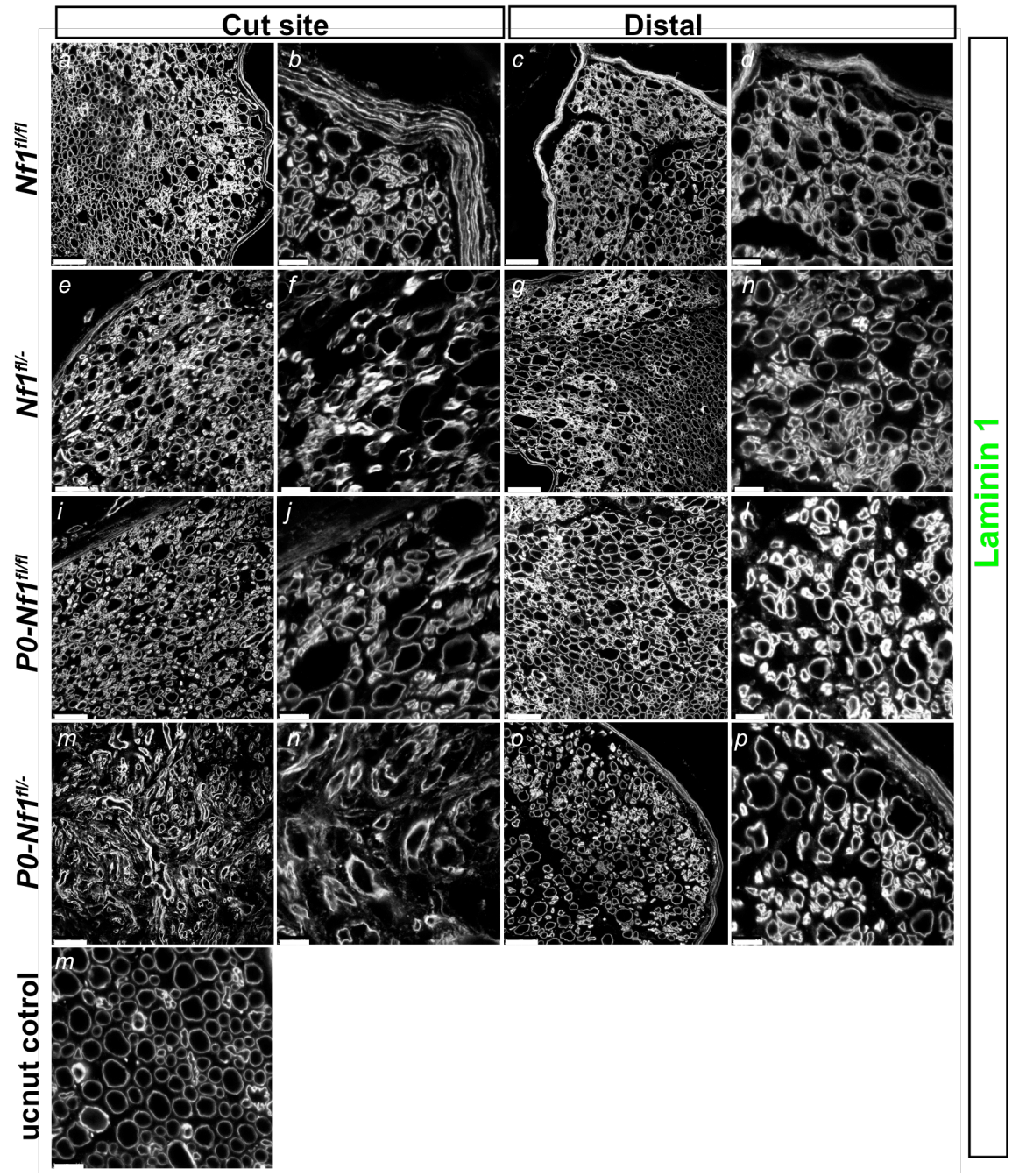

Figure 5-3: Analysis of the extracellular matrix, 7 days following injury- laminin1. B) The same as in A, but only the green channel is displayed, for better visualization. Shown are representative images (n=3 for each genotype).

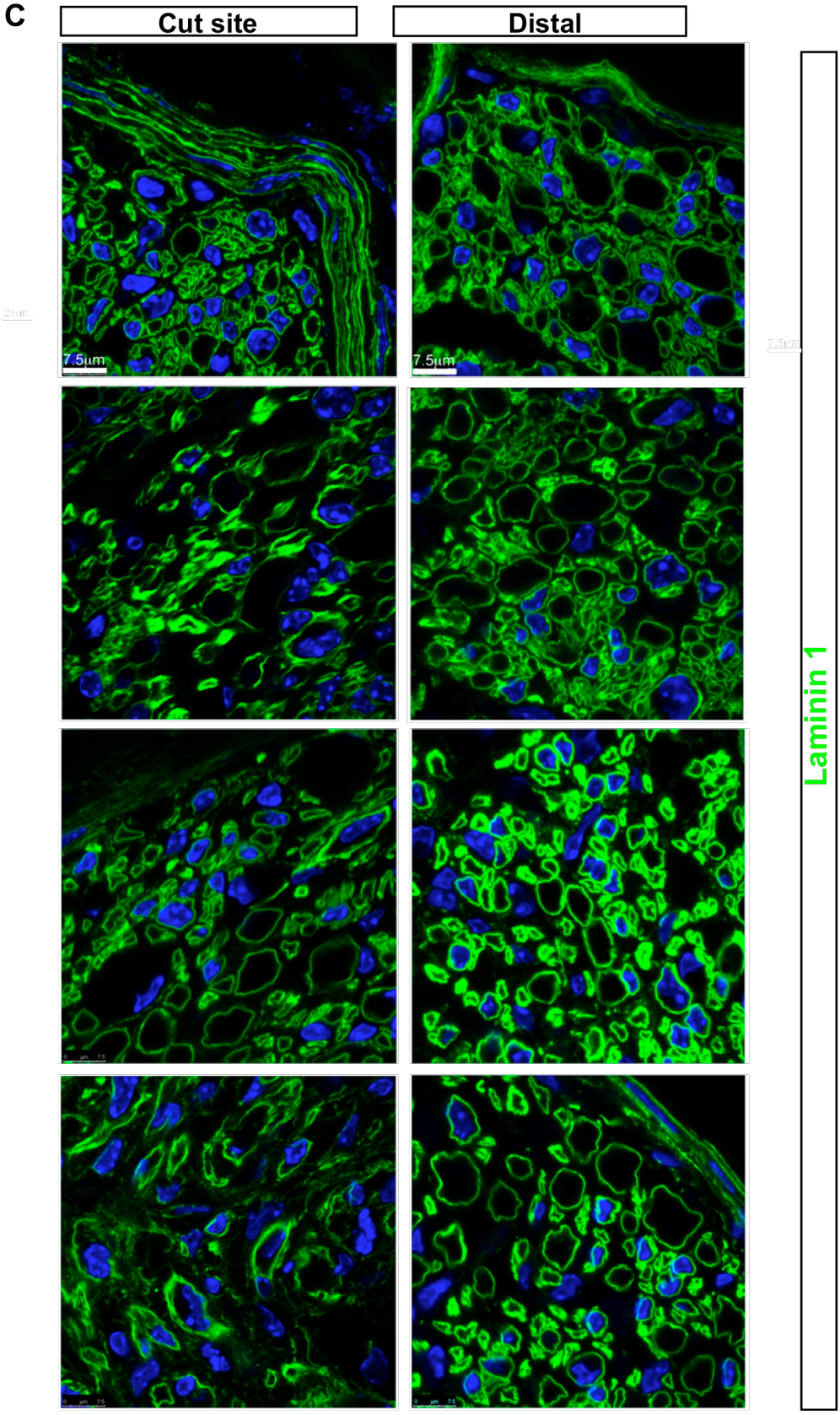

Figure 5-3: Analysis of the extracellular matrix, 7 days following injury- laminin1. C) Amplification of 5-3A. Note: In the images of the distal stump, axons have degenerated, but the structure is maintained, as clearly shown by the tubular organization of the ECM.

A

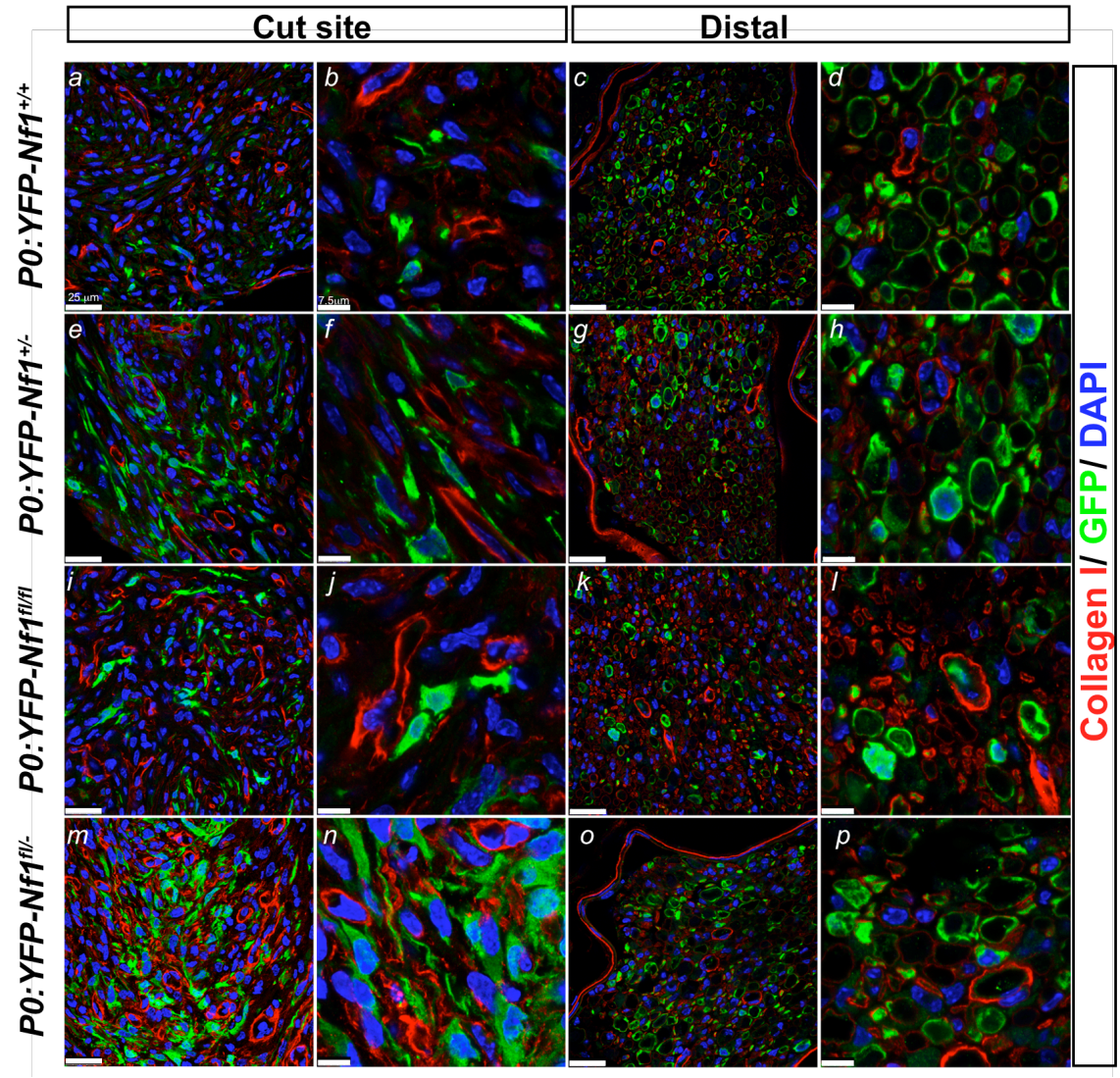

Figure 5-4: Analysis of the ECM, 7 days following injury- collagen I.

A) Cross-sections of sciatic nerves from controls *P0:YFP-Nf1*$^{+/+}$ and *P0:YFP-Nf1*$^{+/-}$ and mutants *P0:YFP-Nf1*$^{fl/fl}$ *and P0:YFP-Nf1*$^{fl/-}$ were stained for the ECM component collagen I (red) and GFP (green). No differences were observed between genotypes and between the two regions of the nerve analysed. **B**) The red channel alone is shown for easier visualization (next page); **C**) Amplification of A (n=3 for each genotype, shown are representative images).

B

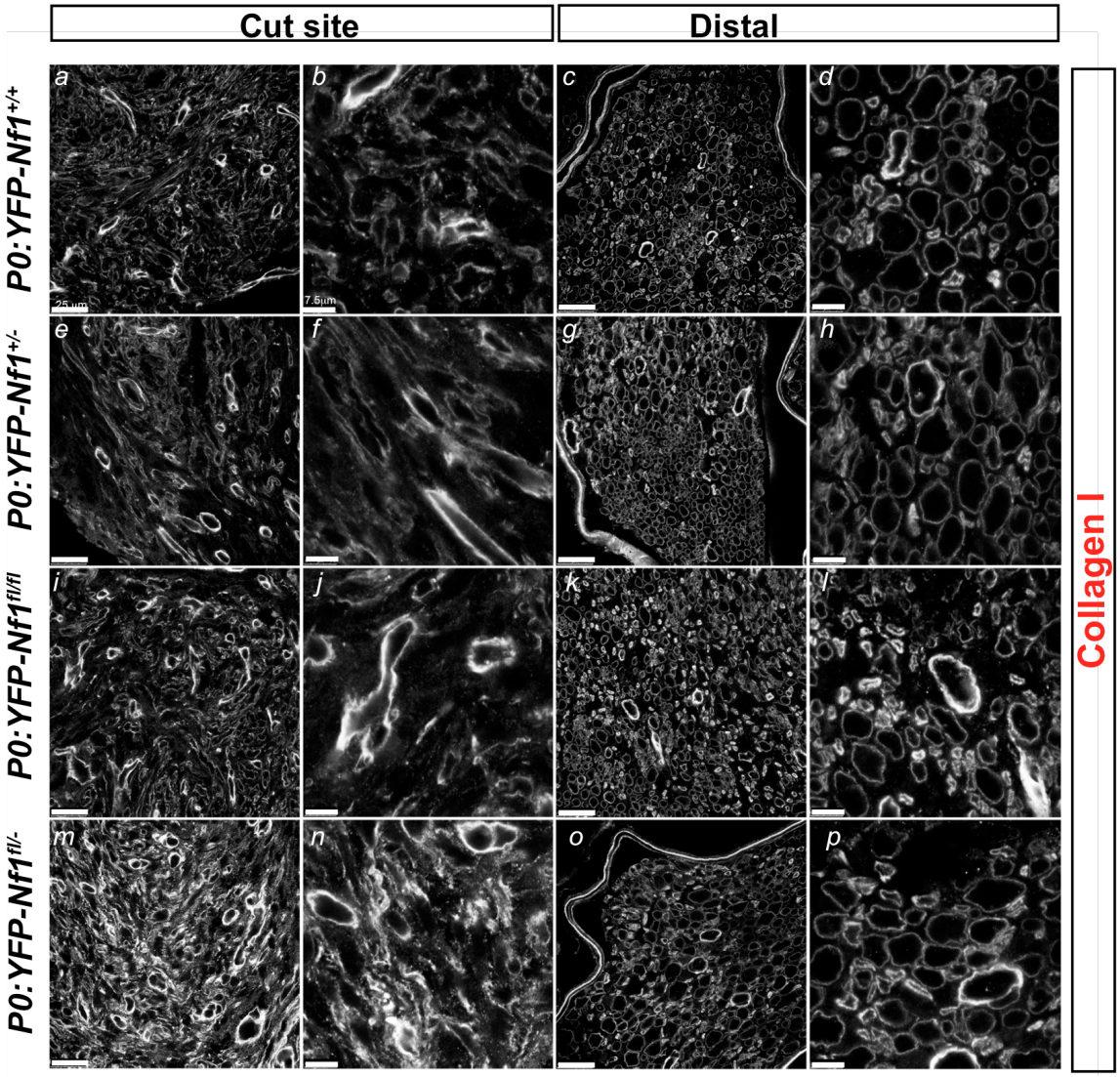

Figure 5-4: Analysis of the ECM, 7 days following injury- collagen I.

B) The red channel alone is shown for easier visualization (n=3 for each animal group, shown are representative images).

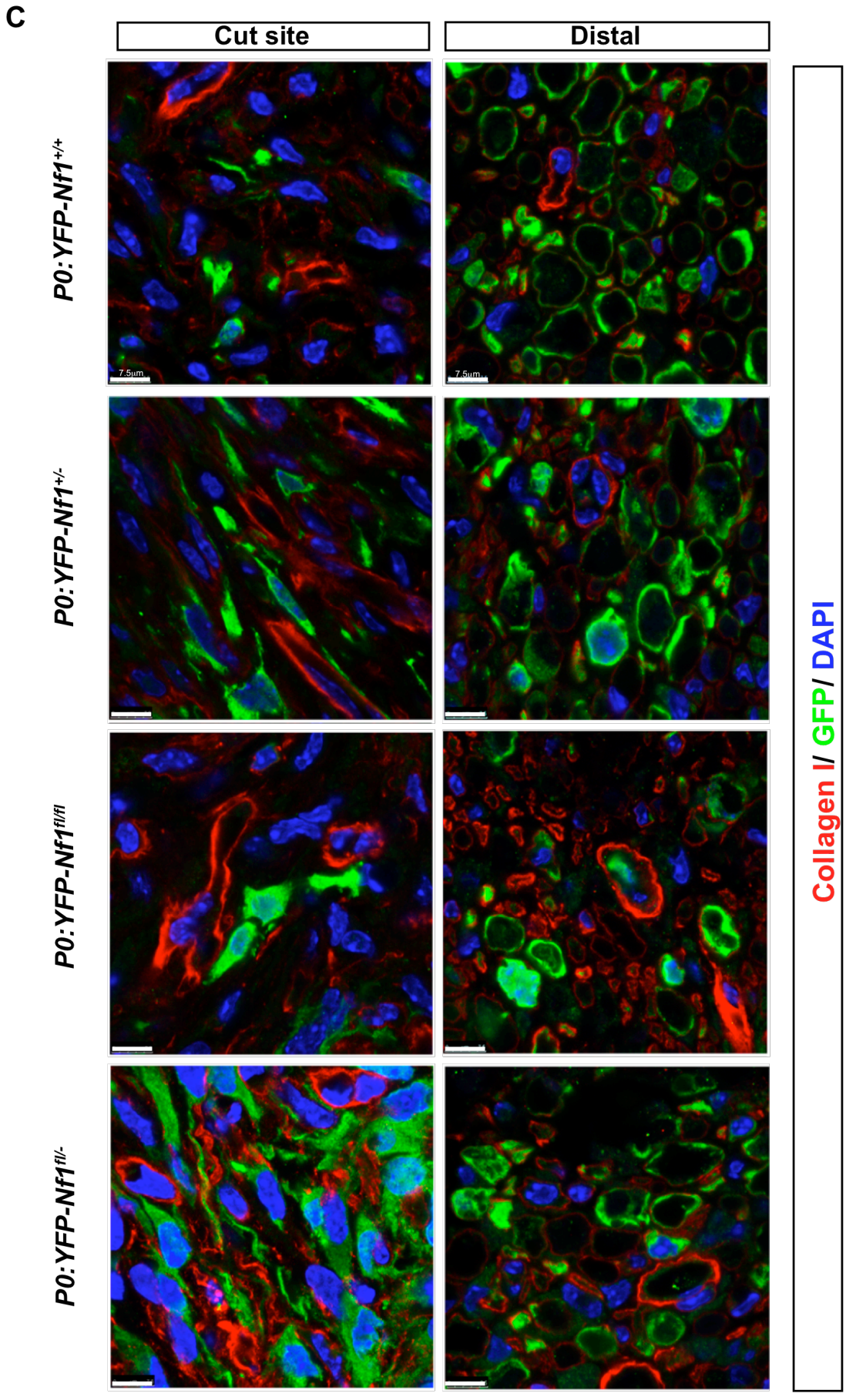

Figure 5-4C: Analysis of the ECM, 7 days following injury- collagen I

C) Amplification of 5-4A.

A

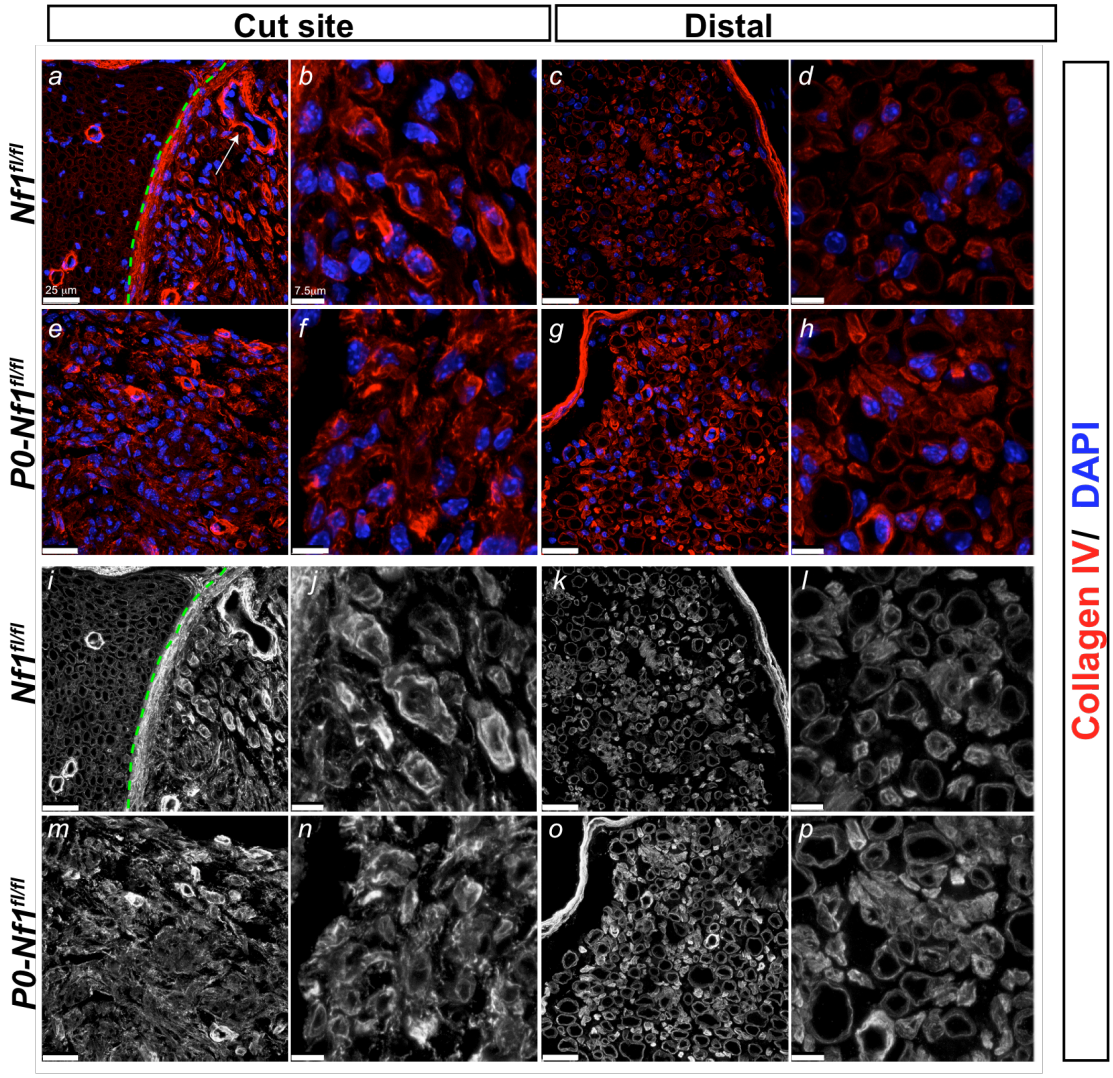

Figure 5-5: Analysis of the ECM, 7 days following injury – collagen IV.

A) Cross-sections of sciatic nerves from controls *Nf1*$^{fl/fl}$ and mutants *P0-Nf1*$^{fl/fl}$ were stained for the ECM component collagen 1V (red), one week following surgery. Collagen IV is strongly expressed at this time point, but in similar levels in all the genotypes and in both injury site and distal stump. Dashed line in **a** and **i** delineates injured area and unwounded nerve. Arrow in **A** points to a strongly positive blood vessel. The two lower panels show the red channel alone. **B**) Amplification of j, i, n and p (n=2 for each genotype, shown are representative images).

B

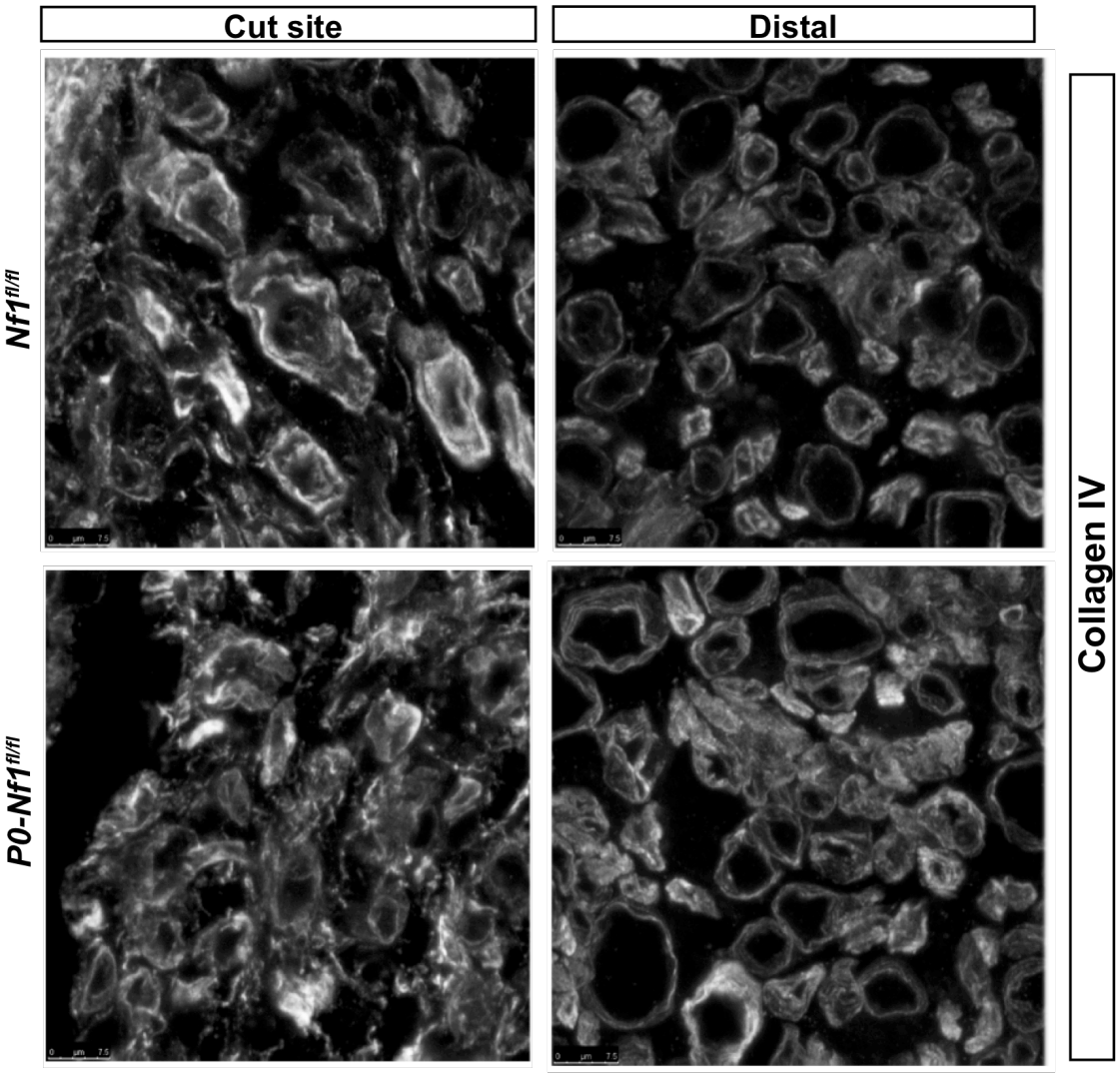

Figure 5-5: Analysis of the ECM, 7 days following injury- collagen IV.

B) Amplification of 5-5A. Note: Similarly to Figure 5-3, ECM staining in the distal stump shows tubular organization, reflecting a well-preserved structure despite of axonal degeneration.

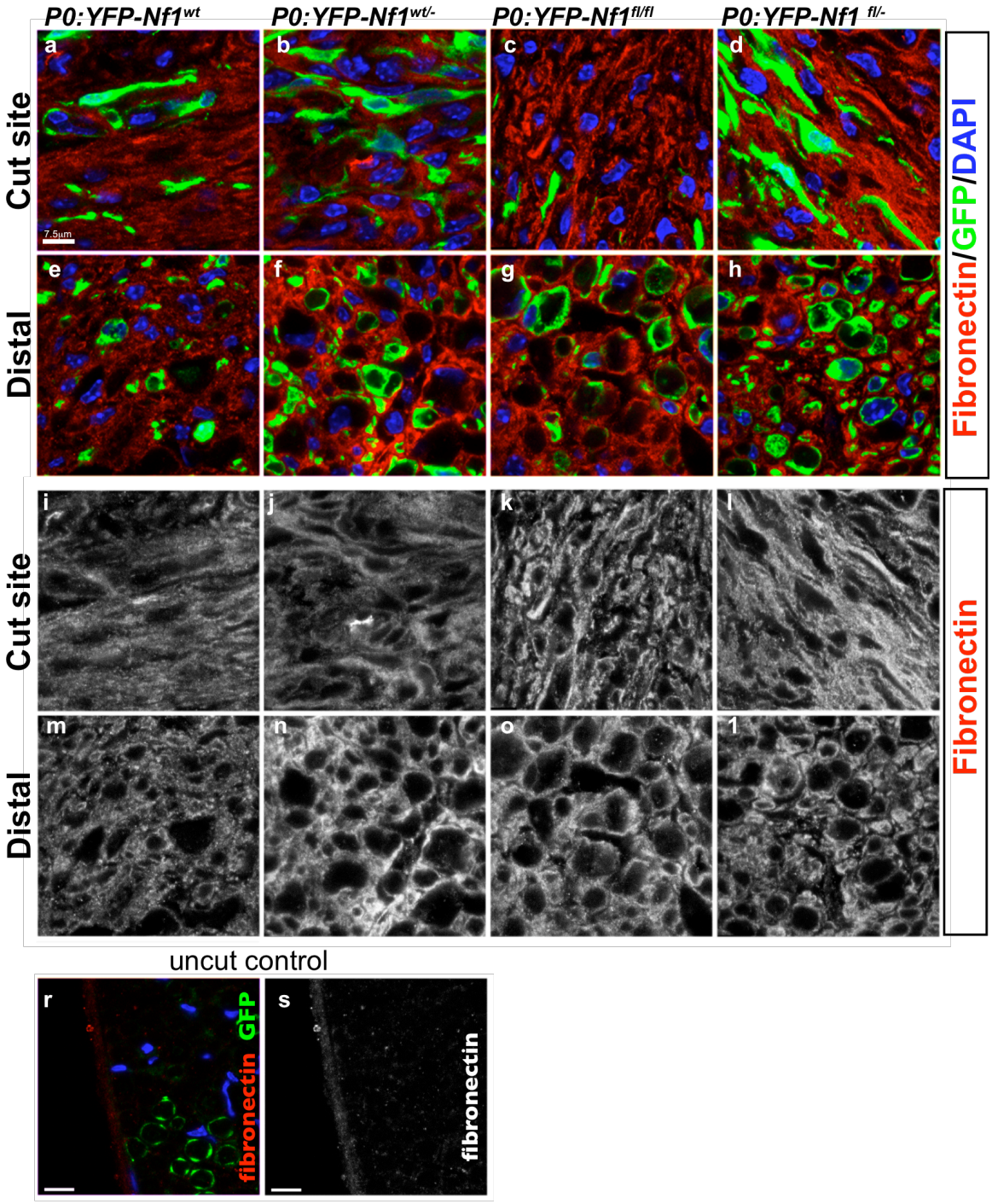

Figure 5-6: Analysis of the ECM, 7 days following injury - fibronectin.

A) YFP positive control and mutant mice were injected with Tamoxifen and their sciatic nerves were transected. One week after, nerves were immunostained for the ECM component fibronectin (red) and GFP (green). **r** and **s** show unwounded controls. Representative fluorescent images of cross-sections are shown. No observable differences were detected between genotypes and between the injury site and distal regions of the nerve (n=3 for each group).

5.5 Enrichment of macrophages at the wound-site

As mentioned before, injury induces a robust inflammatory response along the nerve. The presence of these immune cells at the wound site is known to be key for the successful repair of the damaged tissue; in the PNS specifically, they contribute to axonal and myelin debris clearance and remodelling of the nerve structure following damage. However, besides this well-established role in promoting healing, the presence of inflammatory cells has also been shown to play a primordial role in tumour-initiation. For example, an early study showed that the development of wound-induced tumour in chickens infected with Rous Sarcoma virus was shown to be dependent on the action of cytokines released by inflammatory cells at the site of wounding (Martins-Green et al., 1994). In order to identify any differential distribution of specific immune cells along the nerve, we performed immunostainings for inflammatory cells, 7 days following injury. No significant differences were observed in the recruitment of inflammatory cells between cells mutants and controls, suggesting that at this time point after injury, NF1 deficiency does not detectably affect the inflammatory response. Furthermore, analysis of the neutrophil marker NIMP and the T-cell marker CD3 revealed very few positive cells in all genotypes (less than 1 positive cell per section), both at the injury site and distal stump, suggesting that these cells do not play a relevant role in promoting tumourigenesis (not shown). However, we did observe that increased numbers of macrophages were present at the wound site in comparison with the region downstream of the damage (Figure 5-7C). Although consistent, this difference was not statistically significant with the number of animals I have analysed. In addition, the number of mast cells also tended to be slightly higher at the wound site, in both controls and mutant nerves (Figure 5-7B). Again, the same results were obtained with $Nf1^{+/+}$ and $Nf1^{+/-}$ backgrounds, eliminating a contribution of *Nf1* heterozygosity. It is thus possible that the presence of relatively higher levels of mediators secreted by these immune cells may affect the behaviour of $Nf1^{-/-}$ Schwann cells, perhaps by providing a continuous stimulus to the Ras/ERK pathway. Further work is required to dissect which specific signals are synergizing with *Nf1* loss to induce neurofibroma formation.

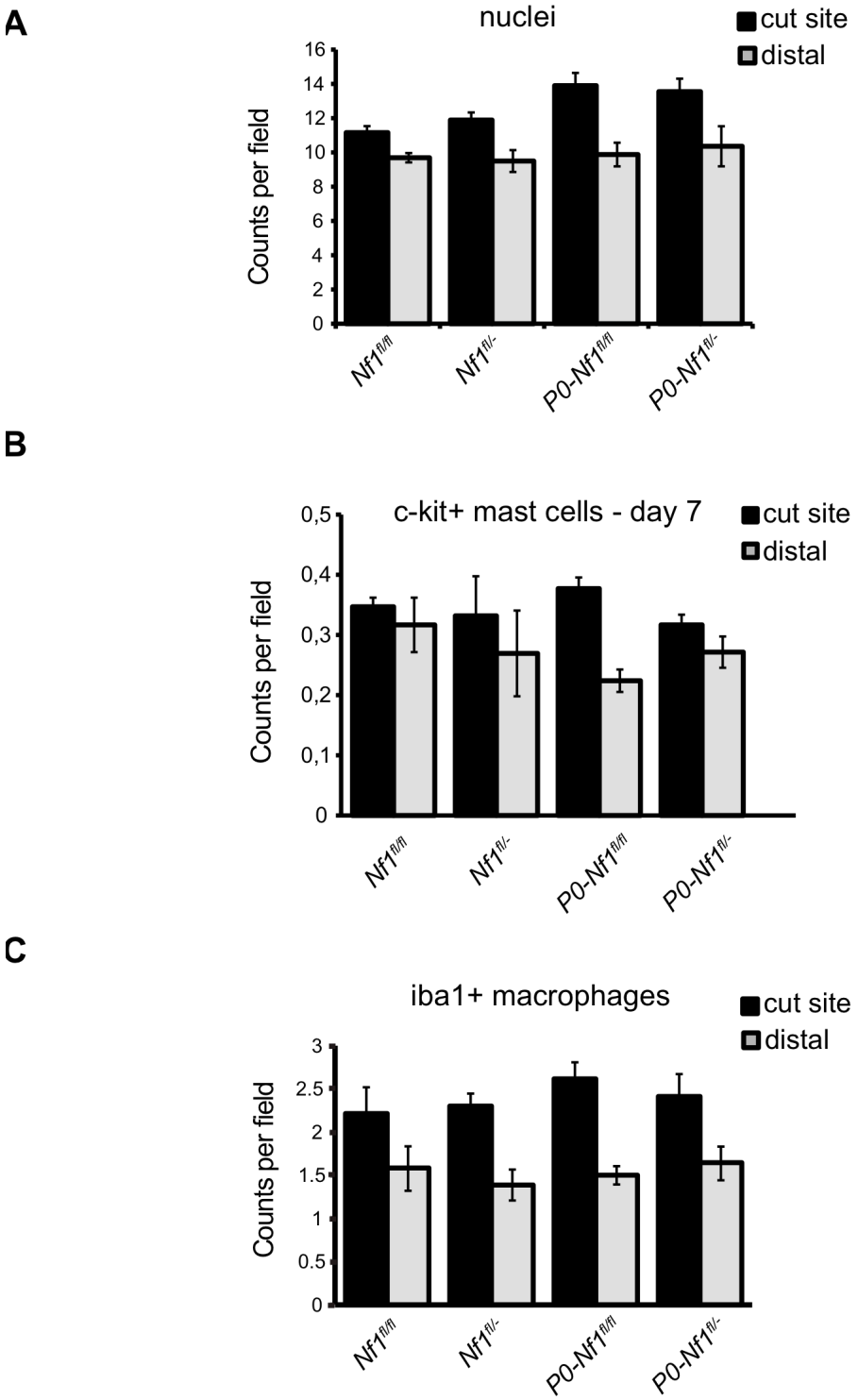

Figure 5-7: Enrichment of immune cells at the injury site, compared to the distal region of the nerve, 7 days following injury. A) Quantification of total nuclei at the site of injury (dark grey) and in the distal region (light grey) of sciatic nerves in controls (*Nf1*$^{fl/fl}$ and *Nf1*$^{fl/-}$) and mutant mice (*P0-Nf1*$^{fl/fl}$ and *P0-Nf1*$^{fl/-}$). **B**) Quantification of mast cells as determined by c-Kit staining. **C**) Quantification of Iba-1+ macrophages (for all experiments, data represent means of 3-4 animals; 8 fields were counted per section; 3 sections per animal, data represents mean values ±SEM).

5.6 Testing the therapeutic potential of MEK inhibitors

I have shown that shortly following injury, *Nf1*-deficient mice exhibit deregulated ERK signalling in the region that later gives rise to tumours. To investigate the requirement of ERK deregulation in neurofibroma formation we are currently testing the effect of the highly selective MEK1/2 inhibitor PD 03255901 (Solit et al., 2006) on tumour development. We have chosen to use the inhibitor at a relatively low dosage (8 mg/kg) to try to reduce but not completely block signalling through the Ras/Raf/ERK pathway, because ERK activation is required for Schwann cell dedifferentiation and recruitment of inflammatory response (Napoli et al, 2012). To do this, we have developed an experimental plan, which is depicted in Figure 5-8A. Briefly, NF1 mutant animals are Tmx treated and their right sciatic nerve injured, as detailed before. Two days following surgery, the animals are either placed into the control DMSO group or treated i.p. with the PD inhibitor. The treatment is administered daily for 14 days in order to cover the period of time that corresponds to the most drastic cellular events, including the peak of the inflammatory response (Zochodne, 2008). So far, we have tested the effect of PD treatment at day 7 of treatment and 1 month following the beginning of the protocol and verified that PD treatment is not impairing either SC dedifferentiation (Figure 5-8C) or axonal regrowth (Figure 5-8D). However, the levels of activated ERK are substantially reduced when compared to untreated or DMSO treated animals (Figure 5-8B). We will be examining the longer-term effects of MEK/ERK inhibition in 3-4 months; if a reduction in the frequency of tumour development is observed, this will unveil MEK inhibitors as useful therapeutics for the treatment of neurofibromas, in particular following injuries and surgeries.

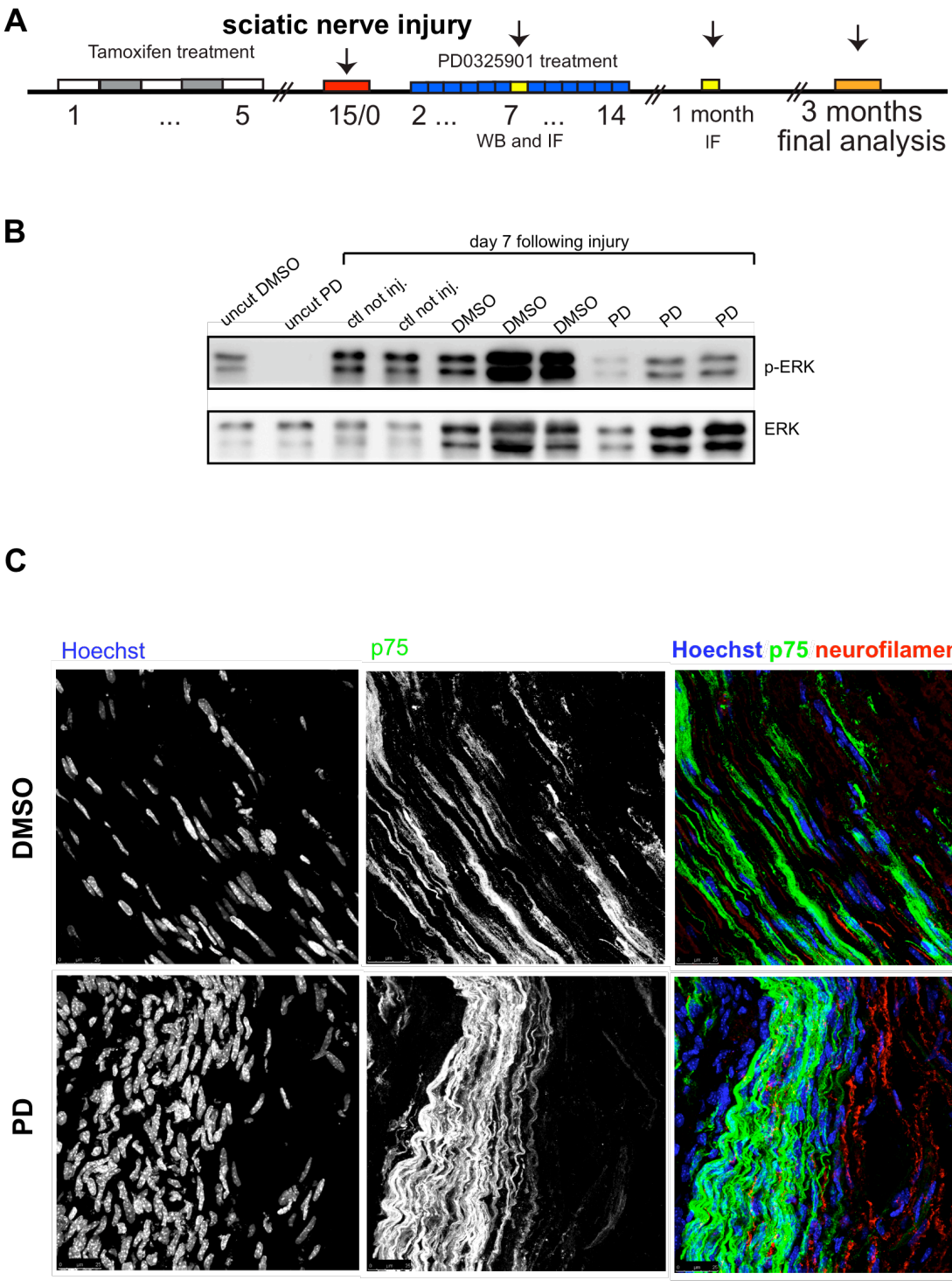

Figure 5-8: PD treatment efficiently reduces activation of the ERK pathway. **A**) Protocol of PD treatment; 8mg/kg of PD were injected i.p. daily, for 14 days starting on day 2 after injury. **B**) PD or vehicle (DMSO) treated animals were sacrificed 7 days following injury; sciatic nerves were harvested and analysed by Western blotting for p-ERK activity. **C** and **D**) Sciatic nerves from PD and vehicle treated animals were processed for p75 (green) and neurofilament (red) immunofluorescence; nuclei were stained with Hoechst (blue).

→

D

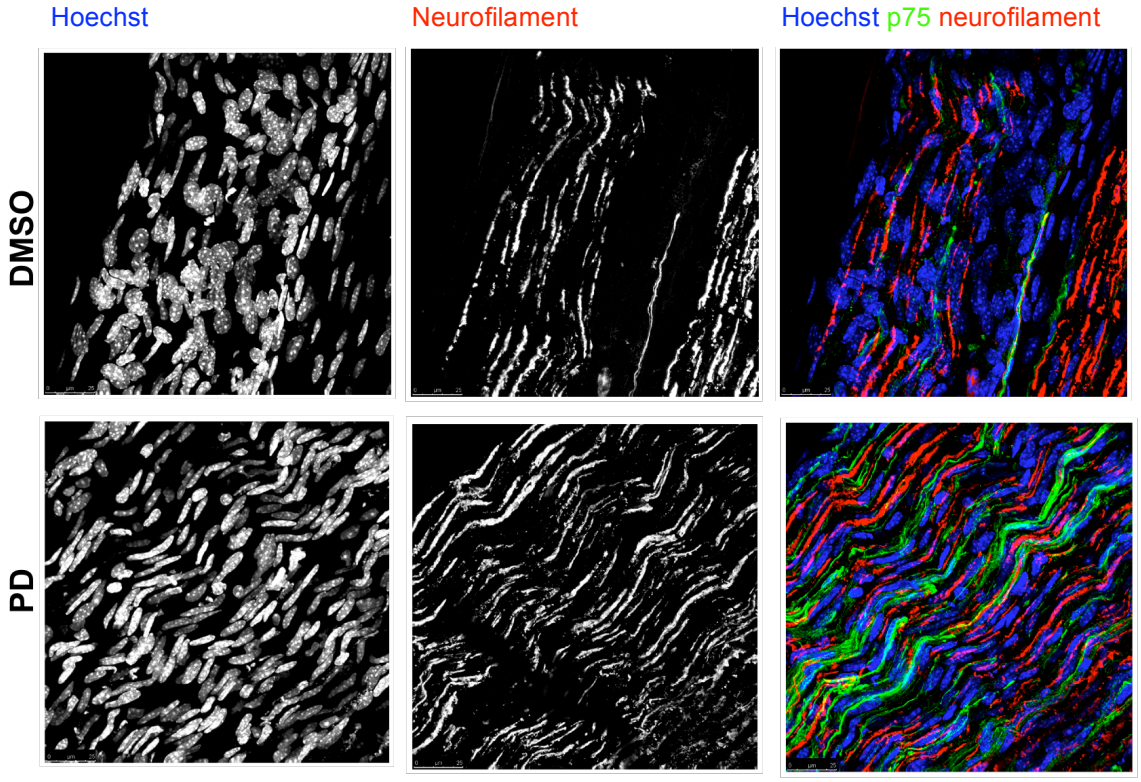

(continuation from previous page) **C** shows that 7 days after injury, Schwann cells dedifferentiate despite PD treatment (note the strong p75 staining); **D**) 1 month following injury, axons have regrown similarly in control and PD animals. Figures represent region of the nerve distal to the site of injury.

5.7 Chapter summary and conclusions

In this chapter I have shown that following injury, the ERK pathway is deregulated and sustained in *Nf1*-deficient nerves. Strikingly, this deregulation is only observed at the injury site, despite wounding inducing ERK activation throughout the entire distal stump of the damaged peripheral nerve. This correlates with the location of neurofibroma formation and suggests a link between deregulation of the Ras/ERK signalling and tumourigenesis. In addition, we found that $Nf1^{-/-}$ mSchwann cells exhibit slightly higher proliferations rates than control nerves, exclusively at the location of the injury. Thus, it appears that microenvironmental cues specific to the wound site are able to alter $Nf1^{-/-}$ mSchwann cells early following injury. In contrast, $Nf1^{-/-}$ Schwann cells downstream of the wound seem protected from these signals; the regulation of the ERK pathway does not seem impaired and $Nf1^{-/-}$ Schwann cell proliferate similarly to control nerves. This is in striking accordance with the longer-term studies that showed that at this region of the nerve, $Nf1^{-/-}$ Schwann cells behave normally and do not form tumours.

Next, we compared nerve sections prepared from both the site of injury and the distal stump. We started by analyzing the expression of the ECM components laminin 1, fibronectin, collagen I and collagen IV. However, despite finding that all components were highly expressed following injury, we failed to detect any differences between the injury site and the distal stump, eliminating a role for these ECM components in promoting $Nf1^{-/-}$ Schwann cell tumourigenesis. We have also analysed the distribution of the inflammatory response along the injured nerves. Although we have detected, as expected, recruitment of immune cells throughout the entire length of the nerve, we found that at the injury site there was a small, but consistent, enrichment of mast cells and, more pronouncedly, macrophages. This may suggest that at the site of injury, a threshold of specific signals released by these cells is present and is necessary for the transformation of $Nf1^{-/-}$ Schwann cells.

Finally, I have described current work that aims to test if ERK inhibition has therapeutic potential for the treatment of neurofibromas.

In conclusion, I have shown that neurofibroma formation correlates with an early deregulation of Ras/ERK pathway. The signal(s) behind this is still unknown, but it may be related to increased numbers of inflammatory cells, present at the injury site. Importantly, as a result of the data described in this thesis, we are currently testing the potential therapeutic impact of MEK inhibitors in wound-induced neurofibromas.

Chapter 6: Results IV

6.1 Chapter introduction

Ras/Raf/ERK signalling regulates major cellular processes as diverse as apoptosis, survival, proliferation and differentiation (Downward, 1998). This pivotal regulation is mainly achieved through modulation of signal amplitude and duration, which is afforded through manipulation of multiple regulatory controls; subcellular compartmentalization, crosstalk with other pathways and protein interactions between components of the pathway and scaffolds, phosphatases and adaptor proteins that enhance, inhibit or redirect the signal flux.

The plethora of biological effects controlled by this pathway is well illustrated in Schwann cells in which Ras/ERK signalling has been implicated in mutually exclusive biological functions such as proliferation (Echave et al., 2009), differentiation (Newbern et al., 2011) and dedifferentiation (Harrisingh et al., 2004; Napoli et al., 2012). Given this central role, it is not surprising that aberrant Ras signalling is found in a range of syndromes affecting the nervous system and, importantly, in Schwann cells isolated from neurofibromas. It is therefore clear that this pathway must be under tight regulatory mechanisms in the PNS. Consistent with this idea, I have shown in chapter 3 that *Nf1* loss in adult mice does not automatically alter ERK signalling, suggesting that other mechanisms of control must be in place. Similarly, studies in transgenic mice engineered to lose *Nf1* during development showed that Schwann cells differentiated normally, indicating that ERK is not deregulated and suggesting that also during development Ras/ERK is subjected to additional regulatory mechanisms besides NF1 (Joseph et al., 2008; Wu et al., 2008; Zheng et al., 2008). Nevertheless, these mice still developed tumours later in adulthood, perhaps suggesting that a trigger acts to perturb the flux of Ras/ERK and this may initiate tumourigenesis. In line with this, I have shown in the previous chapters that ERK deregulation precedes neurofibroma development, indicating that in this mouse model the Ras/ERK pathway might be involved in the early steps of tumour formation. In contrast, in the nerve regions where $Nf1^{-/-}$ Schwann cells exhibited normal ERK regulation, no tumours formed and Schwann cells redifferentitated normally. Collectively, these observations suggest that the flux of signalling through the ERK pathway is crucial in determining the fate of $Nf1^{-/-}$ SC. Understanding the normal mechanisms of ERK regulation in Schwann cells may provide insights into how ERK signalling contributes to tumourigenesis in the context of NF1 and identify potential therapeutic strategies.

Given this, we employed a simple *in vitro* system that would allow us to investigate mechanisms by which ERK is regulated during Schwann cell differentiation. We have used rat primary Schwann cells that can be dissociated from rat peripheral nerves and expanded indefinitely *in vitro* in their undifferentiated, more "progenitor-like" state (Mathon et al., 2001). Importantly, these cells can be induced to express myelination-associated markers by activation of cAMP signalling (Monuki et al., 1989; Shuman et al., 1988; Sobue and Pleasure, 1984; Zorick et al., 1996b), which is implicated in Schwann cell development *in vivo* (Monk et al., 2009; Monk et al., 2011). This system has been extensively used to study mechanisms involved in Schwann cell differentiation and is amenable to efficient silencing with siRNA and shRNA.

6.2 cAMP-differentiated Schwann cells show a dampened ERK signalling

One of the best-studied pathways that crosstalks with and regulates Ras/Raf/ERK to control proliferation and differentiation is cAMP (Stork and Schmitt, 2002). Depending on the cell type, cAMP can either activate or inhibit ERK signalling. For example, in adipocytes and hepatocytes cAMP inhibits proliferation through ERK inhibition (Sevetson et al., 1993; Thoresen et al., 1999). In primary Schwann cells, cAMP signalling has different outcomes depending on the cellular context; at low concentrations and in the presence of mitogens cAMP promotes proliferation, whilst at elevated concentrations and in the absence of mitogenic signalling, it induces differentiation (Arthur-Farraj et al., 2011). Given its role in promoting SC differentiation and its known ability to regulate ERK signalling in different systems, we asked if the cAMP pathway is involved in ERK regulation in Schwann cells. To test this, primary Schwann cells cultured in defined medium without serum were treated with the cell-permeable cAMP analogue dibutyryl-cAMP (db-cAMP) for 2 hours, followed by stimulation with the mitogen NRG1 (specifically, the EGF domain of human recombinant NRG1 - see Figure 1-3) to activate ERK signalling, 10 minutes before lysis. Activation of the Ras/ERK pathway was measured using an antibody against pERK. NRG1 elicited strong phosphorylation of ERK in both untreated and cAMP treated cells, indicating that in these experimental conditions, cAMP does not detectably affect ERK signalling (Figure 6-1A). This data suggests that cAMP does not have a direct effect on the Ras/ERK pathway in primary Schwann cells. Next, we tested if longer-exposure to cAMP (the upregulation of differentiation markers by cAMP is more evident at 24 to 48 hours of treatment), would unveil an indirect effect of cAMP on ERK regulation. To do this,

Schwann cells were kept in db-cAMP for 48 hours and then stimulated with NRG1. Remarkably, we found that the pronounced ERK activation evoked by NRG1 was severely blunted in db-cAMP treated cells (Figure 6-1B), indicating that the pro-differentiative effect of cAMP dampens the flux of signalling downstream of Ras/ERK.

6.3 Pro-differentiating conditions quench ERK activation in *Nf1*-deficient Schwann cells

As mentioned, studies in mouse models of NF1 have shown that *Nf1*$^{-/-}$ Schwann cells are able to differentiate normally and give rise to the right numbers of myelinating and non-myelinating Schwann cells. We hypothesized that this is made possible by the existence of additional regulatory mechanisms that maintain ERK signalling quenched during development. As we found that cAMP signalling regulates ERK, we tested its effects on *Nf1*$^{-/-}$ Schwann cells using siRNA knockdowns (kd).

To do this, we optimized the siRNA-mediated silencing protocol by using two transfections separated by 48 hours in order to maintain the suppression of NF1 levels for the duration of the experiment (Figure 6-2A-C). Using this system we tested the effects of *Nf1* loss on ERK signalling. NF1 kd cells were induced to differentiate for 48 hours in the presence of db-cAMP and then harvested 10 minutes after NRG1 stimulation. As shown in Figure 6-2D, in unstimulated conditions we failed to detect any differences in ERK expression between scrambled control and NF1 kd cells, likely due to the low basal levels of ERK. In contrast, 10 minutes following NRG1 stimulation, *Nf1* deficient cells displayed slightly increased levels of activated ERK, consistent with the role of NF1 as a negative regulator of the pathway. Importantly, we observed that in the presence of cAMP, *Nf1*-deficient cells, similarly to controls cells, showed a marked dampening of ERK indicating that even in the absence of *Nf1,* cAMP signalling results in a dampened flux through the ERK pathway. These data may help to elucidate how *Nf*1 loss during development does not impair Schwann cell differentiation.

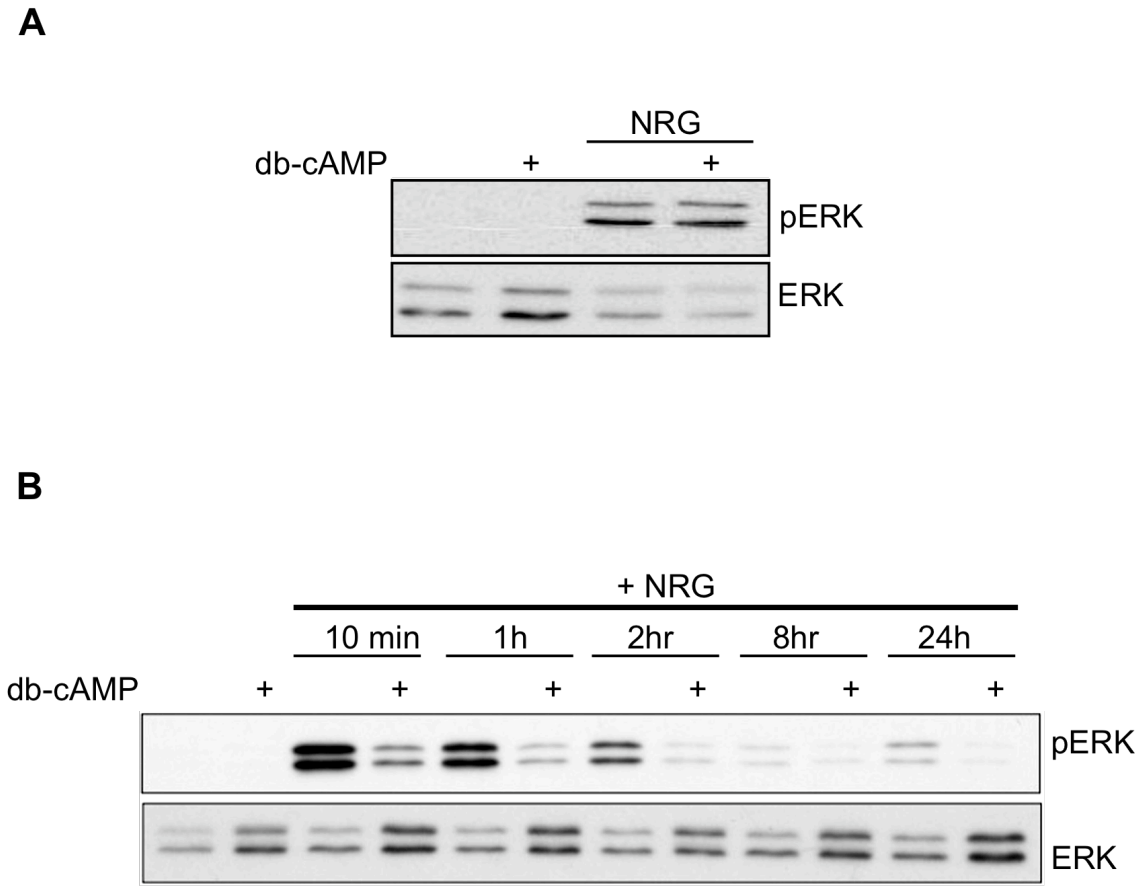

Figure 6-1: NRG1 stimulation elicits dampened ERK activation in Schwann cells induced to differentiate in the presence of db-cAMP.

A) Short exposure to cAMP does not affect ERK signalling. Primary cultures of Schwann cells were grown to confluence and then incubated with either defined medium (SATO) or defined medium plus 1mM of db-cAMP. 2 hours later, cells were stimulated with NRG1 for 10 minutes and processed for Western blot analysis of p-ERK. **B**) Schwann cells were induced to differentiate by treatment with db-cAMP for 48 hours, and then stimulated with NRG1 for the indicated time-points. Western blot for p-ERK show that differentiated Schwann cells display quenched ERK activation when compared to undifferentiated cells (blot is representative of 4 independent experiments).

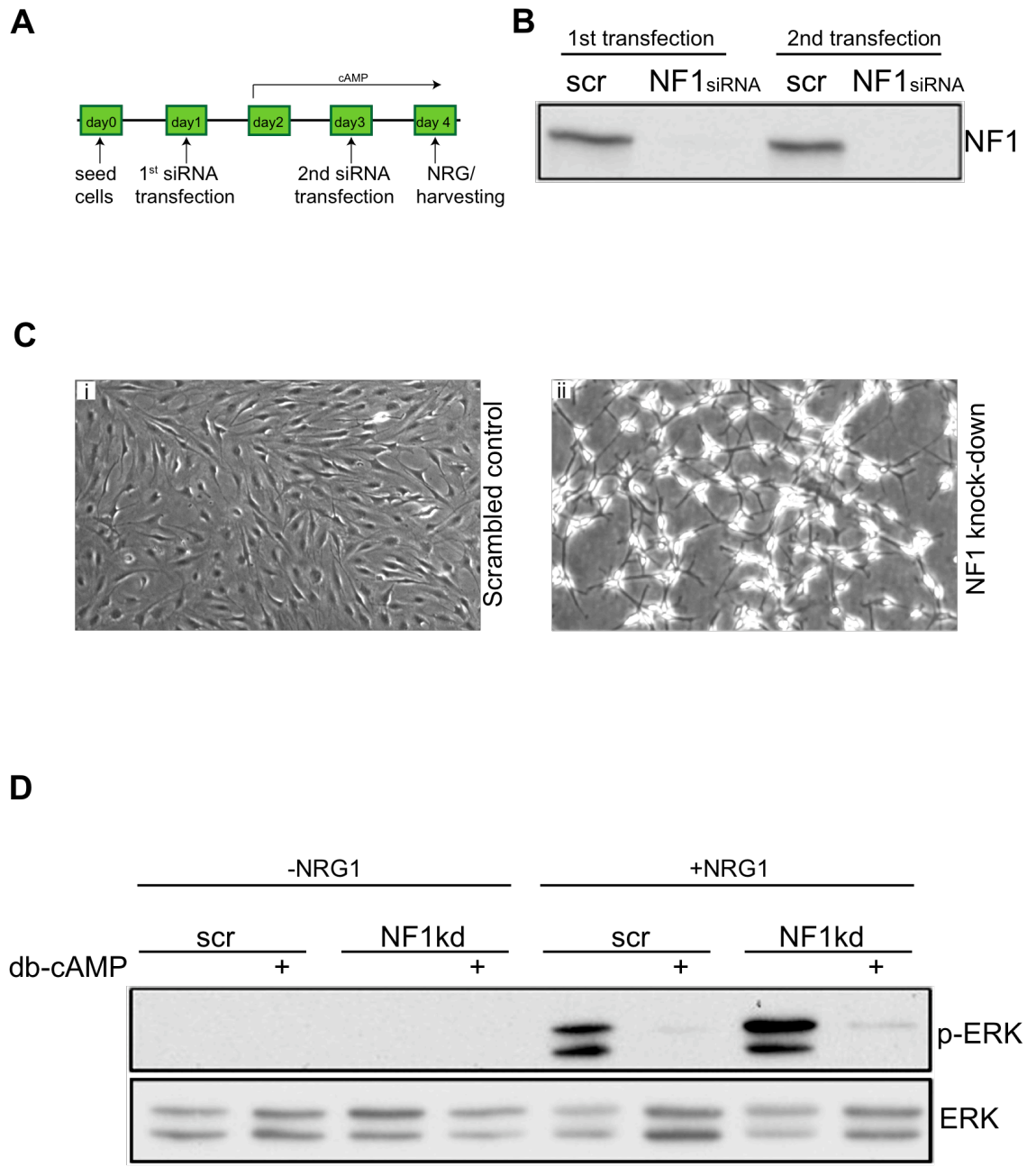

Figure 6-2: NF1 knockdown cells exhibit a marked quenching of ERK activation upon NRG1 stimulation. **A**) Protocol of siRNA transfection. **B**) Western blot analysis shows that NF1 is efficiently knocked-down using siRNA and that protein levels remain low up to 80 hours following the first transfection. **C**) Schwann cells transfected with scrambled control appeared more rounded and flattened, while the NF1 knocked-down cells showed the refractile morphology characteristic of Ras hyperactivation. **D**) Scrambled control and NF1 knocked-down cells were kept in db-cAMP for 2 days and stimulated with NRG1 for 10 minutes. Blot shows levels of p-ERK.

6.4 MKP3 is strongly induced by cAMP exposure

In many systems cAMP inhibits ERK activation by uncoupling Raf from Ras activation (Cook and McCormick, 1993; Wu, 1993). To test if a similar mechanism operated in our system, Schwann cells were allowed to differentiate in the presence of cAMP and stimulated with NRG1 shortly before processing for Western blot analysis. As illustrated in Figure 6-3, cAMP did not significantly affect the levels of the activated upstream kinases Raf and MEK (Figure 6-3iii and iv). In addition, we analysed the levels of AKT activation, another Ras effector downstream of ErbB2, and detected no significant changes (Figure 6-3i). Together, these results suggest that cAMP specifically quenches ERK signalling downstream of MEK.

The regulated dephosphorylation of the essential threonine and tyrosine residues in the ERK activation loop plays a key role in determining the magnitude and duration of the kinase activation and, hence, the physiological outcome of signalling (Owens and Keyse, 2007). The major players involved in this type of regulation belong to the family of dual specificity MAP kinase phosphatases (MKPs also known as DUSPs). Interestingly, it has been suggested that these phosphatases may be involved in regulating the extent of ERK activation to control the decision between differentiation and proliferation (Camps et al., 1998; Misra-Press et al., 1995). Moreover, cAMP signalling has been shown to transcriptionally activate MKPs (Burgun et al., 2000). To test whether these proteins play a role in the regulation of ERK signalling in Schwann cells, we cultured the cells for two days in db-cAMP and stimulated them with NRG1. Shortly before harvesting, cells were treated with a cocktail of phosphatase inhibitors (1mM NaF, 1mM NaO3 and phosphatase cocktail from Sigma). As shown in Figure 6-4A, in the presence of phosphatase inhibitors, the ERK pathway was similarly induced in both differentiated and undifferentiated cells. This suggested that phosphatases are indeed contributing to the regulation of ERK signalling under differentiating conditions.

A previous study reported that the ERK-specific phosphatase MKP3 is strongly upregulated at the mRNA level upon Schwann cell differentiation *in vitro*, in response to forskolin (an activator of adenylyl cyclase) (Bermingham et al., 2001). We therefore decided to determine the role of this phosphatase in ERK regulation in response to cAMP. To do this, Schwann cells were maintained in the presence of db-cAMP for different periods of time and then processed for Western blot analysis. As illustrated in Figure 6-4B, we detected a strong induction of MKP3 expression 24 hours after cAMP treatment, which was sustained for at least 48 hours. In contrast, we did not find any induction of the serine/threonine protein phosphatase 1 (PP1) (Figure 6-4C).

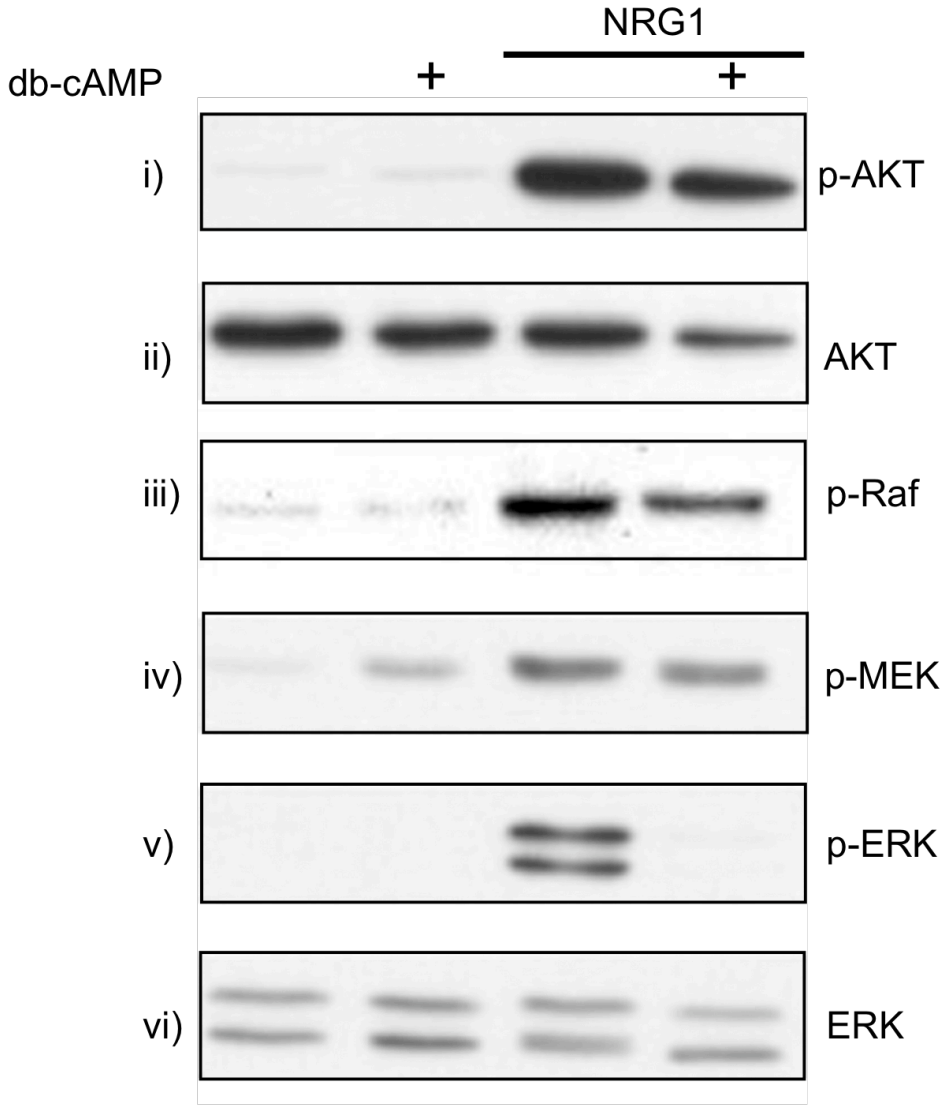

Figure 6-3: Dampening of ERK signalling occurs downstream of MEK.

Schwann cells were differentiated in db-cAMP for 2 days before NRG1 stimulation. Ten minutes after NRG treatment, cells were harvested and analysed by Western blotting with the specified antibodies. ERK is the only kinase quenched in the presence of db-cAMP (blots are representative of 2-4 experiments).

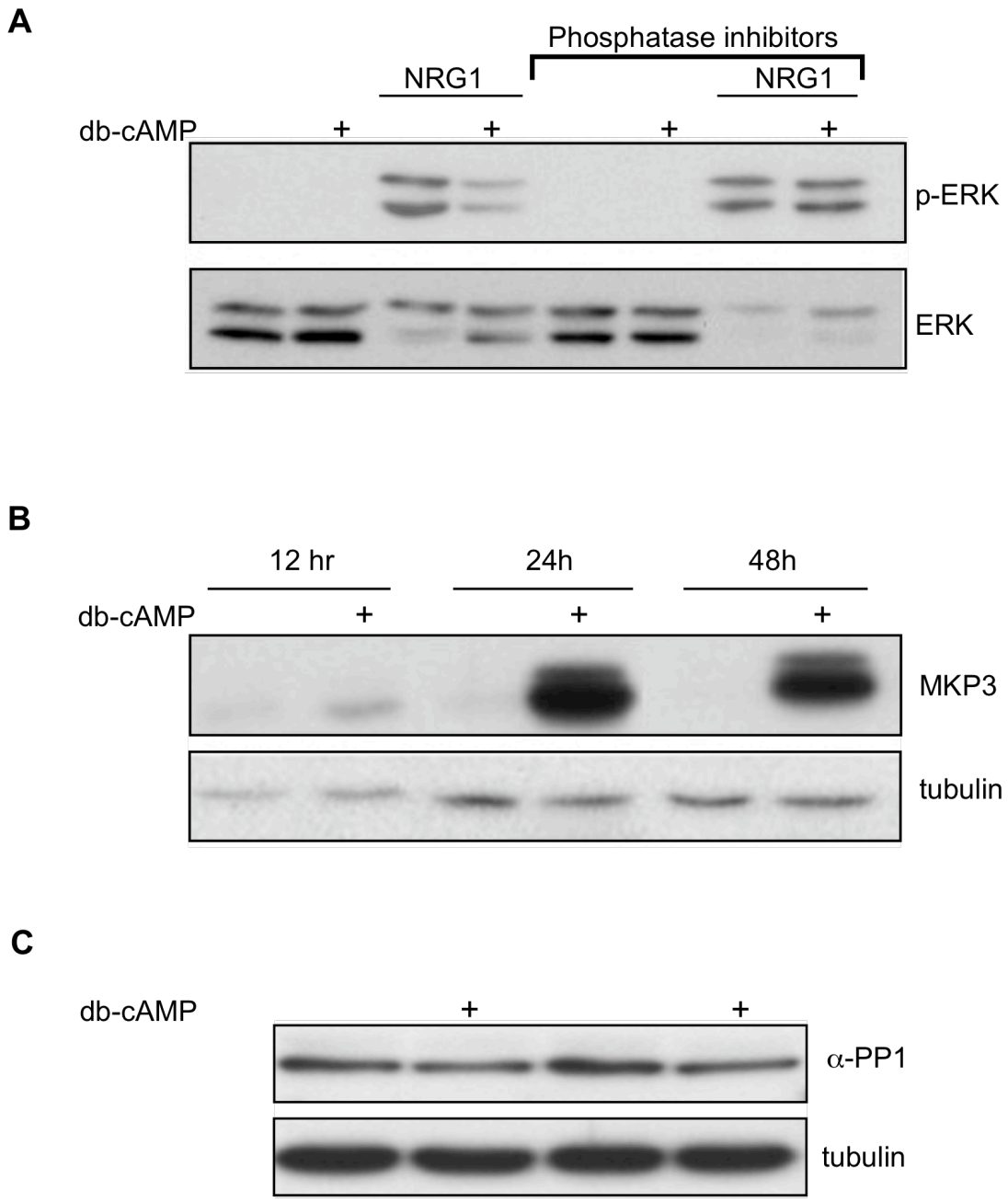

Figure 6-4: The ERK-specific phosphatase MKP3 is strongly induced by cAMP signalling. **A**) Cells were differentiated in the presence of cAMP and stimulated with NRG1 for 10 minutes. After stimulation, cells were treated with a cocktail of phosphatase inhibitors or left untreated. Cells were harvested and processed for p-ERK analysis. Blot shows that in the presence of the phoshatase inhibitors, the ERK pathway is activated similarly in differentiated and undifferentiated SCs (blot is representative of two independent experiments). **B**) Cells were exposed to db-cAMP and harvested at 12, 24 and 48 hours. Shown are levels of the phosphatase MKP3 (blot is representative of 3 independent experiments). **C**) Cells treated with db-cAMP for 48 hours were processed for phosphoprotein phosphatase 1 (PP1) analysis.

This data suggested that cAMP might exert its pro-differentiating effects, at least in part, by quenching ERK signalling through MKP3 induction. To test this more directly, we used the double transfection protocol described above to efficiently knockdown MKP3 (Figure 6-5A). MKP3 knockdown cells were either kept in defined medium or exposed to 1mM db-cAMP for two days and then stimulated with NRG1 and processed for Western blot analysis. Surprisingly, we found that in the absence of this phosphatase, db-cAMP still induced a strong dampening of ERK signalling, indicating that either MKP3 is not involved in ERK quenching or that MKP3 might act in conjunction with other phosphatases (Figure 6-5B). To discriminate between the two possibilities we compared the kinetics of ERK activation in response to NRG1 in control and MKP3 kd cells. As shown in Figure 6-5C, in the absence of MKP3, cAMP treated cells showed a stronger and more rapid activation of ERK following NRG1 stimulation, suggesting that indeed MKP3 plays a role in regulating signalling through the ERK pathway.

6.5 MKP3 loss impairs Schwann cell cAMP-induced differentiation *in vitro*, but not in SC-DRG co-cultures

We next tested if MKP3, through regulation of ERK signalling, had an effect on Schwann cell cAMP-induced differentiation. To assess this, we transiently knocked-down MKP3 in Schwann cells and then induced them to differentiate in the presence of high levels of cAMP. Forty-eight hours later, cells were harvested and RNA was extracted for analysis by quantitative RT-PCR. As shown in Figure 6-6, in the absence of the phosphatase, the mRNA expression of the myelin-protein P0 and the transcription factor Krox-20 (considered the master regulator of SC differentiation) were significantly impaired. This data suggests that MKP3 might regulate the outcome of cAMP signalling by setting the appropriate level of activated ERK. We then assessed the effect of MKP3 kd in a more physiological system. *In vivo*, Schwann cell differentiation is strictly dependent on axoglial signalling (Jessen and Mirsky, 2005). This can be mimicked *in vitro* by co-culturing Schwann cells with dorsal root ganglia (DRG) explants extracted from P0 (postanatal day 0) rats. In these cultures, Schwann cells are induced to differentiate and myelinate by axonal cues. In order to test the role of MKP3 in Schwann cell differentiation in these cultures we needed a more long-lasting knockdown (it takes 3-4 weeks to achieve significant myelination). To achieve this we

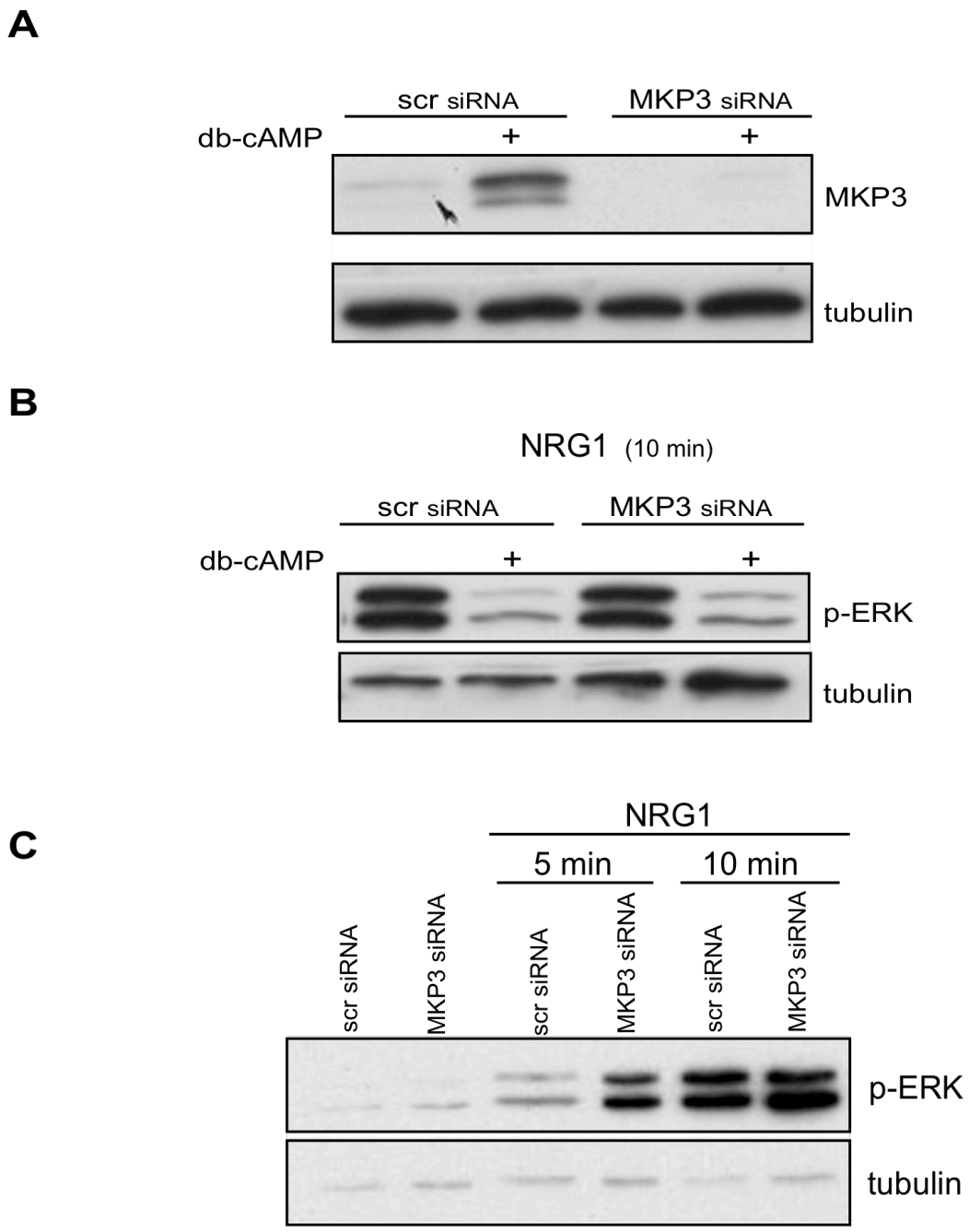

Figure 6-5: MKP3 knockdown does not prevent cAMP-mediated ERK dampening, but affects the kinetics of ERK activation following NRG stimulation. **A**) MKP3 is efficiently knocked-down using siRNA. **B**) MKP3 knockdown cells still show dampened ERK signalling in the presence of cAMP. Scrambled control and MKP3 kd cells were either left untreated or exposed to db-cAMP for two days. Cells were stimulated with NRG1 for 10 min before lysis. **C**) In MKP3 kd cells, ERK activation occurs faster than in control cells, implicating this phosphatase in ERK regulation in differentiating conditions. Cells were kept in db-cAMP, stimulated with NRG1 for 5 and 10 min and then processed for Western blot analysis of activated ERK (all the blots are representative of 2-3 independent experiments).

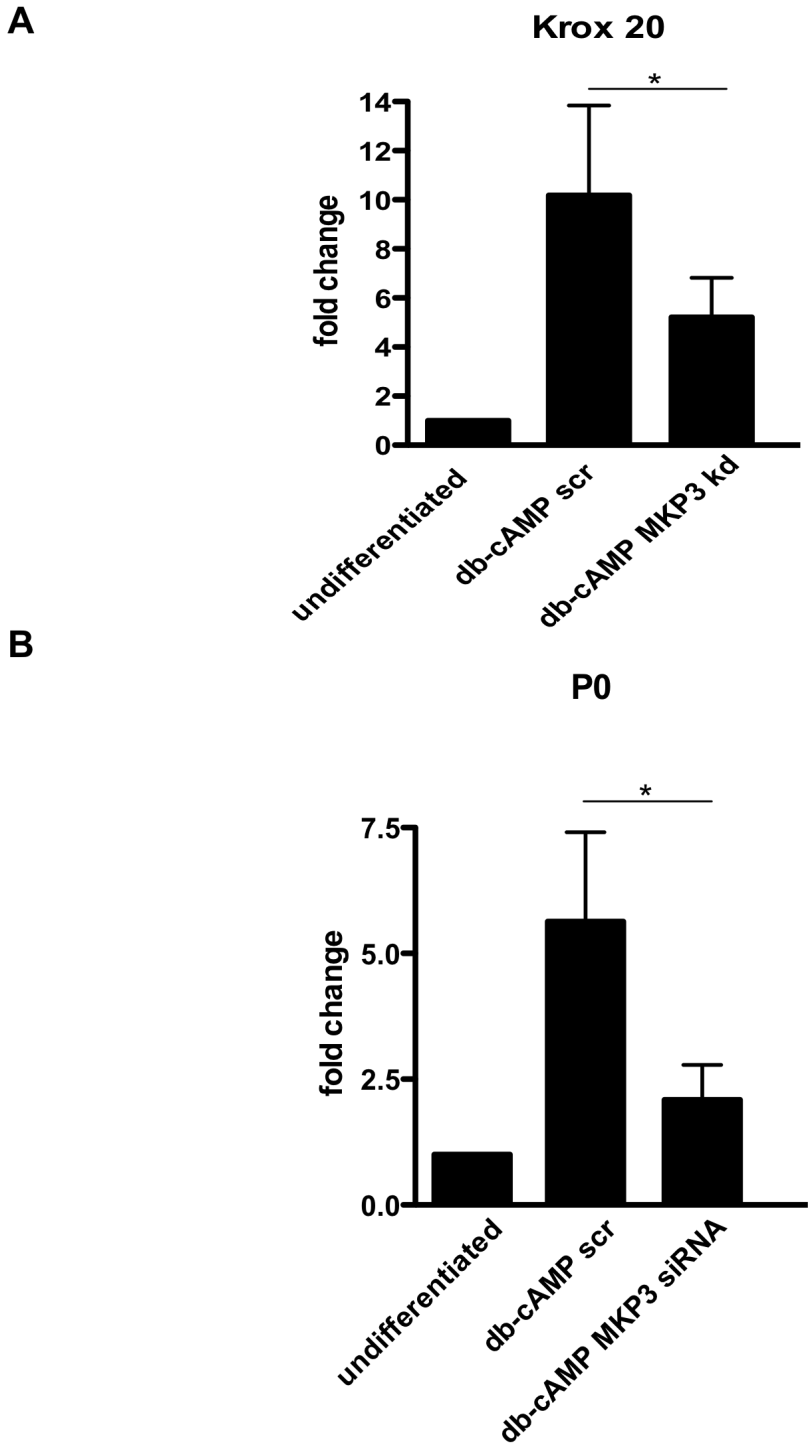

Figure 6-6: MKP3 knockdown impairs db-cAMP induced Schwann cell differentiation. Control and MKP3 knocked-down Schwann cells were cultured in defined medium alone (undifferentiated) or with db-cAMP for 48 hours. **A**) Krox-20 and **B**) P0 expression levels were then analysed using RT-PCR. *B2M* was used as loading control. The results are expressed as fold induction ±SEM of 3-5 independent experiments (*$p \leq 0.05$, significant difference, Repeated Measures ANOVA with post-hoc Newman-Keuls analyses).

cloned short hairpin RNA constructs (shRNAs) targeting the MKP3 sequence into the pSiren-RetroQ vector (see Chapter 2). This retroviral vector plasmid allows constitutive expression of the shRNA constructs and selection of the infected cells by puromycin treatment. We successfully obtained Schwann cells expressing 3 different shRNAs for MKP3, all of them leading to reduced levels of the phosphatase (Figure 6-7A). Nevertheless, it is worth noting that the depletion of MKP3 achieved by this method was not as dramatic as the one obtained using siRNA. MKP3-shRNA expressing Schwann cells were seeded onto the DRG cultures, as described in Materials and Methods, and myelination efficiency was assessed 3 weeks later by quantification of fibres positive for the myelin protein zero (P0). As depicted in Figure 6-7B and C, we did not find MKP3 knockdown caused any consistent effect on myelination efficiency. This may suggest that in SC-DRG co-cultures other mechanisms, including other phosphatases, might compensate for MKP3 reduction, or, that the remaining levels of the phosphatase, although low, are sufficient to regulate ERK therefore allowing efficient differentiation.

6.6 MKP3 is expressed *in vivo* at the onset of myelination and re-expressed following injury in the PNS

Finally, we analysed the expression of the protein *in vivo*. As shown in Figure 6-8A, MKP3 is expressed in rat at postnatal day zero (P0) and its expression gradually decreases after that, consistent with a role in controlling ERK signalling during Schwann cell myelination. Interestingly, we also observed that the phosphatase is re-expressed following injury, which may suggest that upon the ERK activation that rapidly follows injury, MKP3 again plays a role in setting the appropriate levels of ERK signalling. However, a more systematic analysis, including characterization of MKP3/pERK expression during embryogenesis, is still required.

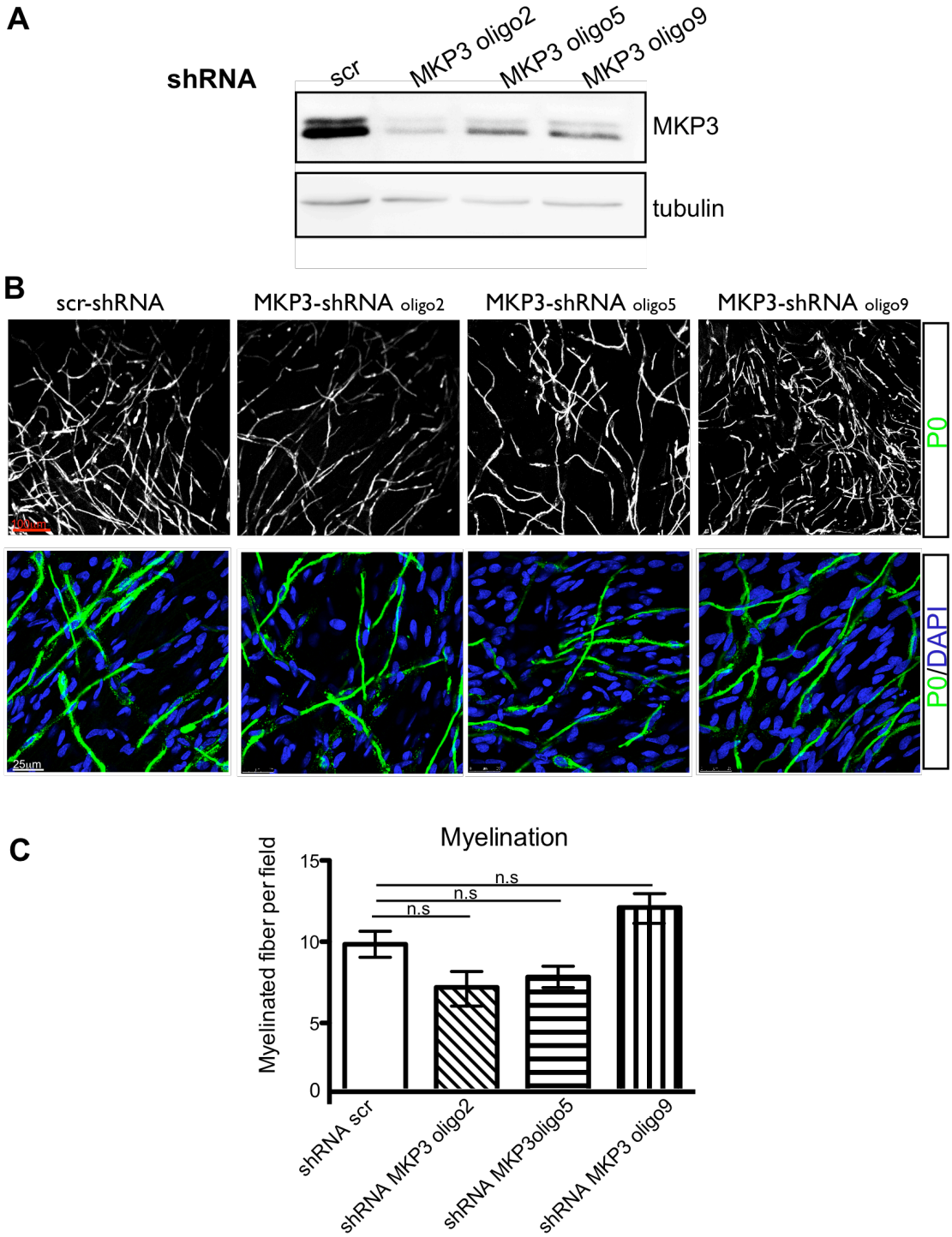

Figure 6-7: MKP3 knockdown does not impair Schwann cell differentiation in SC-DRG co-cultures. Schwann cells were infected with pRetroSiren vector expressing 3 different shRNAs against MKP3. **A**) Blot shows reduced levels of MKP3 in MKP3-shRNA cells compared to scr-shRNA control. **B**) MKP3-shRNA Schwann cells were co-cultured with DRG and induced to differentiate for 3 weeks, by the addition of ascorbic acid and matrigel. Shown are representative images of immunostainings for the myelin protein P0. **C**) Quantification of B. Graph represents mean results from 4-5 coverslips; 20 fields were counted in each coverslip. Error bars indicate ±SEM. n.s, not significantly different (one-way ANOVA, Bonferroni post-test).

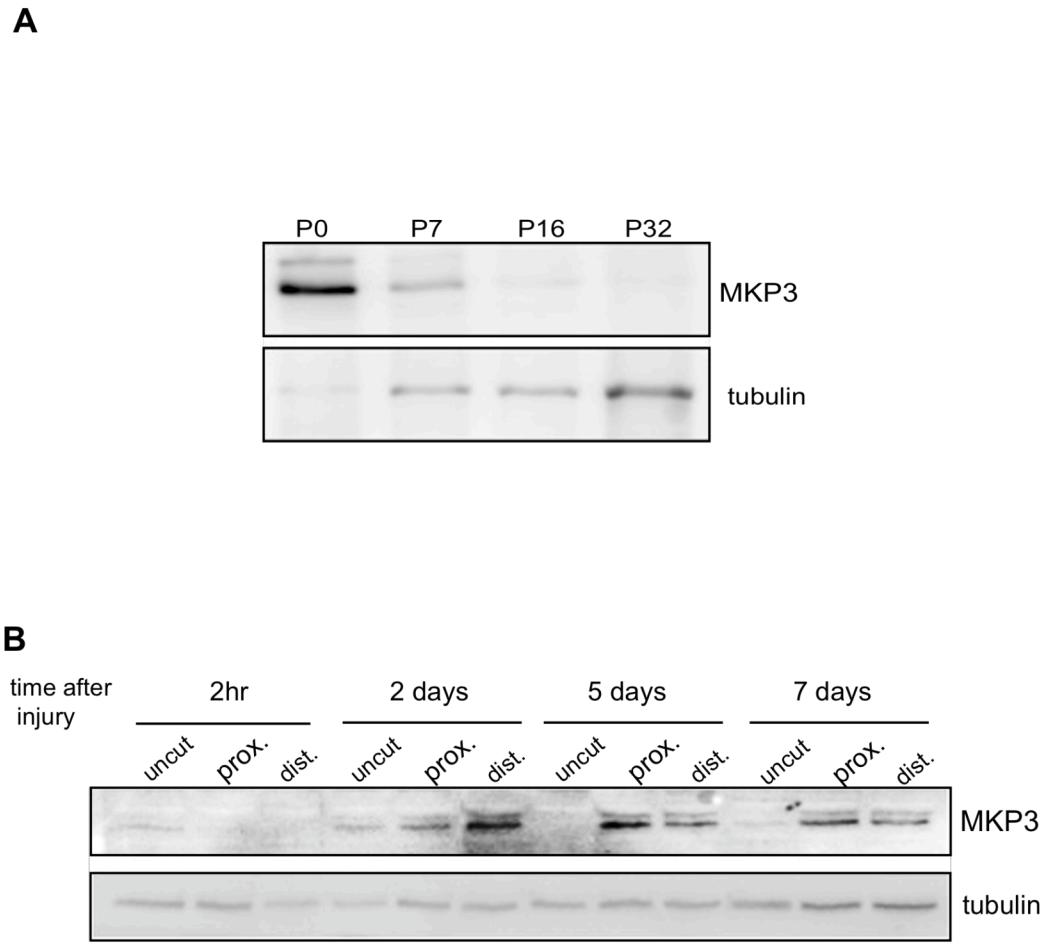

Figure 6-8: MKP3 is expressed at P0 and re-expressed following injury to the PNS, in rats. A) Sciatic nerves from P0, P7, P16 and P32 rats were harvested and processed for Western blot analysis of MKP3. **B**) 4 weeks-old rats were injured in the right sciatic nerve. Blot shows MKP3 levels at the indicated time points following injury, in the proximal and distal stumps and in the uncut contralateral nerve (n=3 for each time-point).

6.7 Chapter summary and conclusions

In this chapter we have used an *in vitro* system of primary Schwann cells to show that the flux of signalling through Ras/ERK in response to NRG1 is dampened in db-cAMP-differentiated Schwann cells, as compared to undifferentiated cells. Importantly, we observed that this effect was still in place in NF1 depleted Schwann cells, suggesting a possible mechanism by which *Nf1*$^{-/-}$ Schwann cells differentiate during development. Also, we have shown that cAMP signalling induces the strong expression of an ERK-specific phosphatase, MKP3, indicating a potential role for this mechanism in the regulatory control of the Ras/ERK pathway. However, we showed that MK3P depleted cells still exhibited ERK quenching, implicating other phosphatases/mechanisms in the regulation of this pathway. Nevertheless, the induction of the differentiation markers P0 and Krox-20 was impaired in MKP3 deficient cells, indicating that cAMP signalling likely exerts part of its pro-differentiating effects by setting ERK at appropriate levels, through induction of the phosphatase MKP3. The presence of other phosphatases or mechanisms was further suggested by the observation that SCs infected with shRNA for MKP3 myelinated to a similar extent as control cells. Alternatively, it is possible that the low levels of MKP3 that remained in shRNA-infected cells were enough to regulate ERK and allow differentiation to proceed.

Importantly, we have detected expression of MKP3 at the onset of myelination in P0 rats (earlier expression was not assessed yet) and later, in adult animals following nerve injury, suggesting that this protein plays a role in regulating ERK signalling *in vivo*. In the future it would be interesting to pursue further studies to investigate how this phosphatase (and others) may be involved in pathologies affecting the Ras/ERK pathway in the PNS, including neurofibroma formation.

Chapter 7: Discussion

Although NF1 is widely expressed, NF1 patients are predisposed to a unique and restricted set of tumours, suggesting that certain cell types are particularly sensitive to loss of this specific tumour suppressor. The most common tumourigenic manifestation in these patients is the development of neurofibromas, benign tumours of Schwann cell origin that arise in peripheral nerves. Schwann cells, or cells within the Schwann cell lineage are therefore, highly sensitive to loss of *Nf1*. Neurofibromin loss is thought to induce tumourigenesis by leading to Ras hyperactivation. However, the mechanisms by which Ras becomes activated in the peripheral nerves and through which precise downstream effectors it exerts its tumourigenic effects remain elusive.

Previous work in mouse models showed that disruption of the *Nf1* gene in early stages of SC development (NCSC-SCP) resulted in neurofibroma formation. Surprisingly, analysis of post-natal nerves demonstrated that embryonic loss of *Nf1* did not automatically impact SC differentiation in that $Nf1^{-/-}$ SCs appeared to have developed normally and were present in the right numbers in post-natal nerves. Instead, the embryonic loss of *Nf1* had "primed" the downstream/differentiated progeny with aberrant properties that ultimately led to tumour formation in adult life. The lack of a detectable effect of *Nf1* loss on SC differentiation was particularly intriguing in light of the findings in our laboratory that sustained activation of Ras/Raf/ERK signalling in Schwann cells induces dedifferentiation and proliferation. To explain these apparently contradictory observations, we hypothesized that during development, the normal nerve microenvironment (perhaps through axonal signals), acts to quench the Ras pathway thereby enabling normal differentiation. However, when later in life, as yet unknown signals activate Ras, Schwann cells that in the adult life rely on NF1 for the proper regulation of Ras signalling, fail to dampen the signal in the absence of neurofibromin and, probably in concert with additional microenvironmental/epigenetic factors, culminate in uncontrolled proliferation and tumour formation. In this thesis, I presented worked aimed at testing these hypotheses.

7.1 Adult, quiescent myelinating Schwann cells are not susceptible to *Nf1* loss

Contrary to other cell types that rely on a population of self-renewing stem cells to generate new cells, there does not seem to be a pool of stem cells capable of generating new Schwann cells in an adult individual. Instead, the demand for new cells

is met by the ability of fully differentiated SCs to dedifferentiate to a "progenitor-like" state with proliferative capabilities. This feature is particularly obvious and relevant following an injury to the peripheral nervous system, upon which SCs revert to a dedifferentiated state, proliferate and create a microenvironment conducive for nerve regeneration. Keeping in mind the remarkable plasticity that SCs retain throughout their life, I tested the susceptibility of adult myelinating Schwann cells to give rise to tumours upon loss of *Nf1*. However, I found that the specific disruption of the *Nf1* gene in adult, myelinating Schwann cells did not alter SC differentiation status and accordingly, did not result in neurofibroma formation. The resistance of adult mSCs to *Nf1*-induced neurofibromas is likely a consequence of the limited proliferation of adult myelinating Schwann cells. To test this possibility we have investigated the homeostatic dynamics of the SC population in the adult intact nerve. We have assessed SC proliferation in the adult sciatic nerve by continual administration of EdU over periods up to 70 days. Interestingly, we have found that whilst non-myelinating SCs do proliferate, albeit in a slow rate (approximately 4% per month), myelinating SCs appear to be remarkably quiescent in the adult peripheral nerve (we have failed to identify a single EdU positive nuclei in more than 14,000 cells counted) (Nihouarn et al., unpublished data). It is therefore likely that very low levels of Ras signalling are required to maintain SCs in this highly quiescent state. In this scenario, the Ras pathway in myelinating Schwann cells may not get sufficiently activated to require the activity of NF1. This is consistent with the very low levels of basal ERK detected in the adult peripheral nerve and with the lack of any detectable change in ERK activation, following *Nf1* loss. Furthermore, if myelinating SCs in an intact nerve do not normally proliferate (or at least exhibit an extraordinarily slow turnover rate), it would not be expected that in human patients, under these circumstances, the inactivation of the second *Nf1* allele is a frequent event.

During the course of this thesis, two independent studies from the Parada and Ratner laboratories have addressed if *Nf1* loss in late stages of SC development (immature stage) or in adult SCs had tumourigenic potential (Le et al., 2011; Mayes et al., 2011). For this purpose, they have used a Tamoxifen-inducible Cre recombinase under the control of two distinct *Plp* drivers. Importantly, the results in both studies argued against the idea that there is a limited window of opportunity for neurofibroma formation (discussed in chapter 1), because when Tmx was administered to pregnant/lactating females or adult mice, inducing *Nf1* loss at the immature stage and beyond, it resulted in the development of neurofibromas. Both studies found that loss

of *Nf1* at the SCP and immature stage resulted in tumourigenesis with high penetrance. However, the studies diverged when they considered loss of *Nf1* in mature SCs (2-4 months old mice). Whereas Mayes and colleagues reported that $Nf1^{-/-}$ adult SCs gave rise to neurofibromas with 100% penetrance, beginning 5 months post-injection, Le and colleagues found that adult loss of *Nf1* resulted in neurofibromas only in rare cases (2 out 19) and late in life, suggesting that only a very special set of circumstances can render an $Nf1^{-/-}$ mature SC capable of developing into a tumour. The reasons behind these discrepancies were not further investigated by the authors. Importantly, in the mouse model used by Mayes, PlpCre-mediated recombination was found in a broad range of cells: in addition to glial cells (satellite and SCs), spleen and thymus, recombination was also found in the heart, lung, thyroid, skin, fat and bone (mice developed hematopoietic-containing tumours in a variety of locations: liver, spleen, lung, kidney, lymph nodes). Given this ubiquitous expression, the study of the specific effect of *Nf1* loss in mature SCs is hard to interpret. On the other hand, in the mouse model used by Le and co-workers, *Nf1* recombination appeared to be more restricted and no other types of tumours developed, besides neurofibromas. Importantly, *Plp* is expressed in both myelinating and non-myelinating Schwann cells. In fact, Mayes performed an ultrastructural analysis of the nerve following *Nf1* loss and, similarly to what has been described for some of the previous NF1 mouse models (*P0aCre:*$Nf1^{fl/-}$ discussed in chapter 1), observed that myelinating SCs seemed unaffected by *Nf1* ablation whilst Remak bundles appeared disrupted. This is in accordance with our observations that *Nf1* loss in adult myelinating SCs does not seem to alter SC differentiation state. Furthermore, it is also in agreement with our findings, that unlike mSCs that appear completely quiescent, non-myelinating SCs proliferate in the adult nerve, even if at a slow rate, which may make them more susceptible to Ras deregulation in an $Nf1^{-/-}$ context. In conclusion, myelinating SCs appear to be a remarkable stable entity under normal homeostatic conditions and are not altered by *Nf1* loss. Non-myelinating SCs, on the other hand, do proliferate in the adult sciatic nerve (although slowly), and for this reason are likely more sensitive to deregulation through Ras signalling upon *Nf1* loss. Non-myelinating Schwann cells may therefore, be the cell of origin in the mouse models described by Mayes and Le.

7.2 Adult *Nf1*$^{-/-}$ myelinating SCs form tumours, following injury

Human tumours frequently develop at sites of chronic injury. This was recognized more than a century ago by Rudolf Virchow, who postulated that previous injuries and chronic inflammation are a precondition for tumourigenesis (Virchow, 1863). Indeed, the relationship between chronic inflammation and the development of cancer has been well established in cases such as the *Helicobacter pylori*-induced gastritis/gastric cancer and chronic viral hepatitis/hepatic cancer, among others (Schafer and Werner, 2008). Experimental studies in animal models have also supported this concept. In the pancreas for instance, expression of an endogenous K-Ras^{G12V} oncogene in adult acinar cells has no detectable consequences in the context of a healthy tissue. However, when these mice are challenged with chronic pancreatitis, they develop pancreatic tumours and cancer (Guerra et al., 2007). Therefore injury/inflammation can dramatically alter the potential of a genetically mutated cell to become a tumour-initiating cell. Injury or infection-associated inflammation may promote tumourigenesis in a variety of ways. First, inflammatory cells may produce cytokines that promote cell division. Secondly, inflammation is associated with increased formation of reactive species (ROS) and genomic stress that can directly promote oncogenic mutations (Lin and Karin, 2007). Furthermore, it is becoming increasingly acknowledged that wounding may also promote tumourigenesis through mechanisms that are independent of inflammation. An example of how this may happen came from a recent study on a model of basal cell carcinoma (BCC). The conditional expression of an oncogenic allele of Smo - a central mediator of the Hedgehog (*Hh*) pathway- in follicular stem cells of an adult mouse model does not automatically result in hyperactivation of the pathway and does not induce tumour formation. However, upon cutaneous injury, these oncogene-expressing cells gave rise to BCC-like tumours (Wong and Reiter, 2011). Following injury, both wild-type and oncogene-expressing follicular stem cells leave their original location - the follicular bulge - and migrate to the wound site where Smo-expressing cells (and not wild-type cells) exhibit strong activation of *Hh* signalling. This suggested that in the bulge, the presence of negative regulators of HH act to inhibit Smo-mediated oncogenesis. However, when cells leave the bulge to migrate to the wound site, stem cells escape from this growth-restrictive niche and the downstream HH signal transduction is derepressed, giving rise to BCC-like tumours. Hence, extrinsic factors that may be independent of inflammation, such as mobilization to distinct locations, may alter the tumourigenic potential of genetically altered cells.

In this thesis I presented experimental work establishing a relationship between wounding and neurofibroma development. I have found that whilst otherwise refractory to tumourigenesis, adult *Nf1*$^{-/-}$ myelinating SCs can form tumours in the context of a nerve injury. Importantly, besides creating the pro-tumourigenic microenvironment required by the *Nf1* deficient cells to induce tumourigenesis, injury may also play an additional and critical role. As stated before, NF1 patients are born heterozygous and the loss of the second *Nf1* allele is the bottleneck event for neurofibroma formation. This raises the question of under which circumstances inactivation of the second allele is made possible. Critically, unlike the highly quiescent intact nerve, following injury SCs exhibit elevated proliferation (Kim et al., 2000), which may create opportunities for somatic mutations to occur. Indeed, the observation that one of the *Nf1*$^{+/-}$ mice developed a tumour at a wound site may support this possibility. Identification of somatic mutations inactivating the second allele would nevertheless be required to confirm this.

We have tracked *Nf1*$^{-/-}$ SCs by crossing our *P0Cre-Nf1* models with a YFP reporter. We observed that *Nf1*$^{-/-}$ mSchwann cell-derived cells are a major component of the tumours that developed at the injury site. Surprisingly, we observed that contrary to the YFP-negative *Nf1* positive-Schwann cells that exhibit immunoreactivity for the marker S100, the majority of the YFP-positive *Nf1*$^{-/-}$ mSC-derived cells within the tumour region, were negative for this marker. A similar phenomenon has been described by Cichowski and colleagues in the neurofibromas that developed in the *Nf1*$^{+/-}$*;Nf1*$^{-/-}$ chimeric mouse model (Cichowski et al., 1999). In this mouse model, S100 staining was only observed at the areas of normal nerve, whereas at the neoplastic lesion itself, only minimal staining was present. Interestingly, experiments in our laboratory have shown that Ras-expressing SCs exhibit a marked reduction in S100 expression (Quereda, unpublished data). It is thus plausible that the lack of S100 expression in *Nf1*$^{-/-}$ SCs is related to the presence of higher levels of Ras signalling. However, direct evidence for this is still lacking. I will address this in the future by performing in vitro knockdown of *Nf1* and determining if and how the resulting elevated levels of Ras signalling may affect S100 expression. These findings are relevant, as they may have implications for the pathological classification of human neurofibromas. The presence of S100 positive cells is frequently used as a diagnostic criteria for neurofibromas. However, if S100 positive cells are specifically marking *Nf1*-positive Schwann cells and not the neoplastic *Nf1*$^{-/-}$ SCs, it would be appropriate to consider alternative SC markers when assessing for the presence of neurofibromas.

Interestingly, analysis of immunofluorescence images of $GFP^+/S100^-/p75^+$cells revealed that a great number of these cells, that are derived from mSCs and express the p75 marker, therefore were presumably dedifferentiated SCs, appeared morphologically distinct from SCs. Indeed, their characteristic morphology - exhibiting long cytoplasmic processes either displayed in parallel arrays or enwrapping other cells - more resembled the one of "perineurial-like" cells, a frequent cellular component of neurofibromas. Perineurial-like cells although ultrastructurally similar to the fibroblast-like cells that compose the perineurium, frequently lack markers expressed by perineurial cells such as the epithelial membrane antigen (EMA) (Perentes et al., 1987; Theaker and Fletcher, 1989; Theaker et al., 1988). It is therefore unclear if the "perineurial-like" cells present in neurofibromas derive from perineurial cells or other cellular components. Furthermore, as discussed in chapter 1, the origin of perineurial cells also remains unclear. Interestingly, it has been previously reported, that neurofibromas contain intermediate/transitional cells that share characteristics with both SCs and perineurial cells, which had led to the suggestion that SCs and "perineurial-like" cells are functional variants of the same cell type (Hirose et al., 1986). These cells were characterized by presence of pinocytic vesicles (characteristic of perineurial cells) and continuous basal lamina (characteristic of SCs) (Erlandson, 1991; Hirose et al., 1986). Based on our observations, it appears that in fact, "perineurial-like" cells, or at least some of them, derive from *Nf1*$^{-/-}$ myelinating Schwann cells. It is, nonetheless, important to mention that a definitive confirmation that "perineurial-like" cells derive from *Nf1*-deficient Schwann cells can only be achieved by performing gold-labelling staining for GFP in neurofibroma EM sections of *P0:YFP-Nf1*$^{fl/fl}$ mice. Curiously, it has been reported that *gpr126*-null mice, that lack differentiated SCs cells due to the absence of signalling through cAMP, exhibit an elevated number of fascicle-forming "perineurial-like" cells (Monk et al., 2011). It is therefore tempting to speculate that also in this case, "perineurial-like" cells derive from Schwann cell progenitors, that lacking signals required to differentiate into mature SCs, abnormally differentiate into "perineurial-like" cells.

In addition, we also identified a population of mSC-derived GFP positive cells that lacked the expression of the SC markers S100 and p75, raising the possibility that dedifferentiated SCs can also give rise to a distinct, as yet unidentified cellular component. An extensive molecular profiling of these cells is required to draw further conclusions. Importantly, a more exhaustive analysis of injured controls is still needed to test if this apparent potential of dedifferentiated SCs to give rise to different cells is

restricted to the *Nf1*$^{-/-}$ genotype or if it is a general characteristic of normal dedifferentiated SCs. The *P0:YFP* mice will be, in this sense, a valuable tool to further study the plastic behaviour of SCs following injury.

The initial extensive characterization of the P0-Cre-mediated recombination revealed that, at least in the sciatic nerve, Cre recombinase appears to be specifically expressed by myelinating Schwann cells, arguing against the possibility that an as yet unidentified population of progenitors may be the neurofibroma-initiating cell in adult peripheral nerves. Nevertheless, although unlikely, the existence of a P0-expressing progenitor cell, which may reside in a distinct location and migrate to the injury site upon wounding, cannot be excluded.

Our results indicate that mature myelinating Schwann cells can indeed be the cell of origin for neurofibromas, but only when they leave their quiescent state and are induced to dedifferentiate.

7.3 Following injury, tumours form independently of the *Nf1* background

Tumour cells do not grow in isolation. Indeed, the tumour microenvironment controls the behaviour of genetically altered cells, either suppressing their tumourigenic properties or supporting and promoting their survival, proliferation and transformation. Neurofibromas - highly heterogeneous tumours composed of a mixture of cells that besides the neoplastic SCs, includes and a variety of non-neoplastic elements including "perineurial-like" cells, fibroblasts, axons and mast cells - are a good example of the complexity of cellular interactions within tumours. In particular, in the *Krox-20Cre-Nf1*^{flox} mouse model, the ability of *Nf1*$^{-/-}$ SCs to drive tumours was shown to be dependent on the presence of an *Nf1* haploinsufficient stroma (Zhu et al., 2002). As discussed in chapter 1, later studies in *Krox-20Cre-Nf1*^{flox} animals have narrowed the requirement of *Nf1* heterozygosity to the presence of *Nf1*$^{+/-}$ mast cells. Accordingly, transplantation of *Nf1*$^{+/-}$ bone marrow into *Krox-20Cre-Nf1*^{flox} animals (that normally do not develop tumours) was sufficient to allow *Nf1*$^{-/-}$ Schwann cells to form neurofibromas in an *Nf1*$^{+/+}$ background. Importantly, this effect could be reverted by the inhibition of Kit signalling (required for mast cell migration and maturation), which pinpointed mast cells as the critical *Nf1*$^{+/-}$ player (Yang et al., 2008). However, these studies did not clarify exactly how mast cell *Nf1* heterozygosity promotes tumourigenesis. Importantly, *Nf1* haploinsufficient mast cells are hypersensitive to KitL, a migratory stimuli secreted in elevated levels by *Nf1*$^{-/-}$ Schwann

cells. Thus, it is possible that rather than conferring specific pro-tumourigenic effects at the site of the developing tumour (e.g secretion of growth factors that *Nf1*^{wt} cells do not), *Nf1* haploinsufficiency may act by attributing mast cells enhanced migration and recruitment to the mutant nerve.

Importantly, in our mouse model, *Nf1*$^{-/-}$ Schwann cells developed tumours following injury in both *Nf1*$^{+/+}$ and *Nf1*$^{+/-}$ backgrounds and at similar frequencies, indicating that *Nf1* heterozygosity is not required for neurofibroma development.

The requirement for *Nf1* haploinsufficiency had been previously been challenged by the work in the Ratner lab with the *Dhh;Nf1*$^{fl/fl}$ and *PlpCreER;Nf1*$^{fl/fl}$ mouse models which also developed neurofibromas in a wild-type background (Mayes et al., 2011; Wu et al., 2008). Nevertheless, it is important to take into consideration that both mouse models presented important differences in comparison with the model described in this thesis. Most critically, in both mouse models, Cre recombination was not targeted exclusively to Schwann cells, which brings additional hurdles in the interpretation of the results. In the *Dhh* model in particular, neurofibromas developed rapidly and extensively at the nerve roots, which was more consistent with a boundary cap rather than a SC origin (see chapter 1 for more details). Furthermore, *Dhh* is also expressed by additional embryonic cells such as SKPs. On the other hand, in the *PlpCreER* model Cre activity was also observed on a variety of cells in addition to Schwann cells. In contrast, in the *P0-Nf1*^{flox} model here described, P0Cre appears to target exclusively myelinating Schwann cells. Hence, our mouse model provides a "cleaner" system to show that given the right microenvironmental conditions, *Nf1*$^{-/-}$ Schwann cells may form tumours even in the context of an *Nf1*$^{+/+}$ background. However, this does not mean that the nerve microenvironment does not play a critical role in controlling the fate of *Nf1*$^{-/-}$ SCs. Indeed, in our mouse model, a variety of inflammatory cells including mast cells are recruited to the peripheral nerve in response to the injury in both *Nf1*$^{+/+}$ and *Nf1*$^{+/-}$ backgrounds. Hence, it is possible that once at the *Nf1*-deficient nerve, immune cells may critically alter the behaviour of *Nf1*$^{-/-}$ SCs. Mast cells in particular, may also in this mouse model, exert essential pro-tumourigenic effects. This would be consistent with the hypothesis that in the specific case of the Krox-20 model, haploinsufficiency is required to attribute an increased migration of mast cells to the nerve. If this is overcome (in our case, by eliciting an inflammatory response), *Nf1* heterozygosity is no longer compulsory. The requirement, in our mouse model, for the presence of mast cells at the sciatic nerve may be tested by treating the injured

animals with c-Kit inhibitors (e.g Imatibib mesylate), as c-Kit activity in mast cells is key in governing mast cell behaviour (Ingram et al., 2001; Yang et al., 2003).

7.4 The nerve is tumour-suppressive

We have shown that adult, mature mSC can induce tumour formation, but only after reverting to a dedifferentiated state in response to injury. Nevertheless, we observed that reverting to a "progenitor-like" state is not, *per se*, sufficient for tumourigenesis. Following injury, strong and sustained activation of Ras/Raf/ERK signalling induces SCs at the injury site and downstream of the lesion to dedifferentiate. The damage response is also associated with a robust inflammatory response, involving the influx of mast cells, macrophages, neutrophils, T-cells and fibroblasts throughout the entire length of the nerve, distal to the wound-site. However, despite this remarkable remodelling of the nerve downstream of the injury, we observed that dedifferentiated *Nf1*$^{-/-}$ cells formed tumours exclusively at the injury site. Strikingly, the nerve stump distal to the lesion site was indistinguishable between controls and NF1 mutants and remarkably, *Nf1*$^{-/-}$ Schwann cell at this region of the nerve, redifferentiated normally and remyelinated axons. Accordingly, the kinetics of Ras/ERK signalling did not seem to be altered in *Nf1*$^{-/-}$ SCs at the distal stump since, 7 days following injury, ERK was dampened in both wild-type and NF1 mutant nerves. These observations strongly suggest that the nerve microenvironment is highly tumour-suppressive, because even in the presence of strong activation of Ras signalling and in the presence of an inflammatory environment, is able to suppress Ras/ERK in the absence of NF1 thereby allowing normal redifferentiation. This is somehow reminiscent of what seems to happen during SC development in NF1 mutants. As mentioned before *Nf1*$^{-/-}$ Schwann cells differentiate normally, although Ras/Raf/ERK signalling is activated during the initial stages of differentiation (Newbern et al., 2011). Bringing together the observation that strong activation of Ras/ERK drives SCs dedifferentiation with the fact that in fully differentiated SCs the basal levels of activated ERK are very low, we may speculate that following the initial requirement for Ras/ERK during embryogenesis, ERK signalling has to be dampened to allow the completion of SC differentiation. This speculation is backed up by two main findings. First, ERK appears to be required for Krox-20 induction, which places its effects in early differentiation (Newbern et al., 2011; Rosenberg et al., in prep.). Second, experiments in our laboratory using SC-DRG co-cultures have shown that ERK is found strongly activated in SCs that are aligned with axons – and are therefore in preparation for myelination, whilst is no longer activated

when SCs are fully differentiated (Napoli et al., unpublished data). Collectively, these findings suggest that the nerve microenvironment (probably pro-differentiative axonal signals) is strongly suppressive for Ras/ERK signalling. Our work suggests that only when *Nf1*$^{-/-}$ SCs escape from this suppressive environment they have the capacity to form tumours.

7.5 The microenvironment at the injury site is tumour-promoting

We found that only at the location of the injury, *Nf1*$^{-/-}$ SCs find the conditions required to drive tumour formation. In accordance with the differential behaviour of SCs at the wound site and SCs at the distal stump, the ERK activation that seems normal in *Nf1*$^{-/-}$ SCs distal to the cut, appears sustained and deregulated in NF1 mutants at the injury site. The connection between deregulated Ras/ERK signalling and tumour development is currently being tested in experiments using the MEK inhibitor PD 0325901. Importantly, if an effect on preventing tumour development is observed, this may unveil a possible therapeutic strategy to treat NF1 patients.

How can we explain that genotypically identical cells behave so differently depending on the location in the injured nerve? The answer seems to involve cell-exogenous factors. As discussed in Chapter 1, upon nerve transection both stumps on each side of the injured nerve retract, leaving a gap between them. This gap - the nerve bridge - consists of a unique microenvironment that includes elevated amounts of ECM and a variety of cells such as immune cells and fibroblasts. We may therefore speculate that some specific component of the bridge microenvironment that we have not yet identified, is responsible for the different behaviour.

Another critical difference between the injury site and the distal stumps is the stability of the Schwann cell basal lamina. Importantly, whilst the basal lamina is physically disrupted at the lesion site, in the distal stump of the nerves SC basal lamina remains well-organized and fairly intact, despite Schwann cells dedifferentiating within the tubes. We may therefore speculate that the lack of a tightly associated and organized basal membrane in the SCs at the injury site, might make SCs at this location more freely accessible to various proteins, including growth factors and cytokines which may influence proliferation of *Nf1*$^{-/-}$ Schwann cells. In contrast, in the distal stump, SCs are kept more protected and their access to extracellular factors may be more restricted, hence reducing the upstream signals feeding Ras signalling. In other words, at the injury site, disruption of the basal lamina may leave Schwann cells more susceptible to the

pro-tumourigenic microenvironment of the wound. Importantly, this hypothesis may be tested by studying the effects of less severe injuries such as nerve crush. Importantly, crush does not disrupt the structure of the basal lamina. Thus, by comparing the consequences of nerve transection to the ones of nerve crush, one could address the importance of the preservation of the basal lamina.

The importance of the severity of the injury has been also implicated in a rather distinct mouse model. Specifically, in a transgenic mouse model expressing the *jun* oncogene it was shown that the development of tumours of the connective tissue, termed dermal fibrosarcomas, only arise upon complete transection of the skin. When a more superficial injury is performed tumours do not develop, suggesting that a more dramatic disruption of the tissue architecture is required for oncogene expressing cells to develop into tumours (Schuh et al., 1990).

7.6 Possible signals upstream of the Ras pathway

Neurofibromin is a Ras-GAP meaning that its effects on Ras signalling are dependent on external activation of the pathway. For example, *Nf1*$^{-/-}$ hematopoietic progenitors exhibit Ras hyperactivation and increased proliferation only in response to specific growth factors and/or cytokines such as GM-CSF (granulocyte-macrophage colony stimulating factor), SCF (stem cell factor) and IL-3 (Largaespada et al., 1996; Zhang et al., 1998).

Which pro-tumourigenic factors may one expect to find at the wound site? Early work on the tumourigenic effects of the Rous sarcoma virus showed that chickens infected with the virus only developed tumours at the site of wounding (Dolberg et al., 1985). Interestingly, the effect of wounding on the development of the tumours was later demonstrated to be mimicked by local application of pro-inflammatory growth factors, such as transforming growth factor-β (TGF-β) and acidic and basic fibroblast growth factor (aFGF and bFGF) (Martins-Green et al., 1994). This led to the conclusion that tumour development in this animal model was accomplished through the cytokines released by the inflammatory cells at the wound site.

Importantly, we found that following injury macrophages are enriched at the site of injury compared to the distal areas of the nerve (in both controls and NF1 mutants). Activated macrophages have been shown to produce and secrete both TGF-β (Assoian et al., 1987) and FGF (Baird et al., 1985; Schulze-Osthoff et al., 1990). Additional growth factors are also produced by macrophages including platelet-derived growth factor BB (Watabe et al., 1994), which is a known mitogenic signal to Schwann cells

(when in the presence of cAMP) (Kim et al., 2001). It is thus plausible that the wound microenvironment provides a variety of signals or specific thresholds of signals that may promote tumourigenesis by activating Ras and thus stimulating the proliferation, migration and/or survival of Schwann cells. Consistent with a role for growth factors in promoting deregulated signalling through Ras, PDGF and TGF-β are found at increased levels in neurofibromas *in vivo* (Carroll and Stonecypher, 2005; Kadono et al., 2000; Watanabe et al., 2001). The effect of specific growth factors or cytokines could also be tested in our mouse model, by locally administrating putative factors in the distal stump of injured NF1 mutant nerves.

7.7 Penetrance

In our model, neurofibroma development occurred in approximately 30% of the injured animals. We may only speculate on the reasons underlying this incomplete penetrance. One possible explanation is related to the remarkable variability in Cre-recombinase efficiency (that ranged between 15 and 50%). A more careful analysis, comparing Cre recombination and the presence/absence of tumours can now be done using *P0:YFP-Nf1*^{flox} mutants. Another possibility is that slight biological differences in the wounding process varying from animal to animal may dictate the behaviour of *Nf1*$^{-/-}$ SCs. We did not observe any differences between females and males, excluding a prominent role for hormonal components. Still, slight inter-individual differences in the inflammatory response may result in different thresholds of specific factors present at the wound site, which may be critical for the outcome of *Nf1* loss. Furthermore, differences in the regeneration process, such as the speed of repair, may also influence the likelihood of tumour formation. Lastly, it is also possible that additional genetic and/or epigenetic changes are required for *Nf1*$^{-/-}$ to exhibit abnormal proliferation and culminate in tumour development, and thus it may involve stochastic changes.

7.8 Ras/Raf/ERK regulation in differentiating Schwann cells

As discussed in section 7.4, both during developmental differentiation and re-differentiation (in the distal stump) following injury, the nerve microenvironment appears to be able to regulate and suppress Ras/ERK signalling even in the absence of neurofibromin. These observations imply that additional regulatory mechanisms are in place during SC differentiation and may override *Nf1* loss. In this regard, we have studied possible mechanisms of ERK regulation in differentiating SCs. Importantly, we

found that the ERK1/2 phosphatase MKP3 (Dusp6) is strongly induced in SCs by the pro-differentiative signal cAMP. Consistent with a role for MKP3 in regulating ERK levels during differentiation, MKP3 depleted cells exhibited an impaired differentiation in SC monocultures. In Drosophila, MKP3 null mutation results in embryonic lethality and severe defects in oogenesis (Maillet et al., 2008). In sharp contrast, MKP3 knockout mice are viable and exhibit no major developmental defects, except an increased basal ERK1/2 phosphorylation in the heart, which results in cardiac hypercellularity (Maillet et al., 2008). The most likely explanation for the lack of a more striking phenotype is that other phosphatases compensate for the embryonic loss of MKP3. Indeed, the closely related DUSP7 (MKP-X) and DUSP9 (MKP4) also dephosphorylate ERK1/2, suggesting that these phosphatases could play a compensatory effect in the absence of MKP3 (Dickinson and Keyse, 2006). To overcome this possible effect, one could test the effects of MKP3 loss in a situation of acute activation of ERK signalling, such as the one experienced by Schwann cells following an injury. Importantly we observed that MKP3 is re-expressed in peripheral nerves after wounding. If MKP3 is indeed important in the regulation of Ras/ERK levels during differentiation/re-differentiation one could expect that following injury, redifferentiation may be impaired in the MKP3 null mice. In any case, it seems clear that the right balance of Ras/ERK signalling is critical for SC development and behaviour in the adult life, in particular following injury. Importantly, deregulation of this pathway seems to play a critical role in neurofibroma formation.

7.9 Conclusions and therapeutic relevance

The peripheral nerve is a remarkably regenerative structure, owing much to the plasticity of Schwann cells. Following an injury, fully differentiated Schwann cells via a Ras/Raf/ERK-mediated mechanism dedifferentiate to a progenitor-like state, which proliferate and aid in the nerve repair process. Once axons have regrown, SCs re-associate with axons and redifferentiate. The molecular switch that allows SCs to change differentiation status has to be tightly regulated.

We have generated a new mouse model of neurofibroma formation. In this thesis, I have shown that adult, highly quiescent myelinating Schwann cells are not made tumourigenic by *Nf1* loss. However, upon injury, *Nf1*$^{-/-}$ Schwann cells residing at the wound site, probably in response to a variety of growth factors and cytokines produced by cells involved in the wounding process (and made accessible by the physical disruption of the basal lamina), exhibit deregulated Ras/ERK signalling.

Abnormal Ras/Raf/ERK signalling, probably in cooperation with other genetic/epigenetic changes, may ultimately lead to neurofibroma formation. A schematic representation of this model is shown in Figure 7-1.

During this thesis I have started to test the therapeutic effect of the treatment with MEK inhibitors in wound-induced neurofibromas. If this proves successful, it may have important implications in the treatment of human patients.

Crucially, there is anecdotal evidence linking mechanical trauma and the development of neurofibromas. Patients have reported that neurofibromas frequently arise in sites of trauma (e.g. after bites, scratches, cuts) (Riccardi, 1992). Importantly, it has been suggested that given the high quality of peripheral nerve repair, it is likely that many cases of nerve injury may go entirely unnoticed and subclinical injury may be more common than it is presently though to be (Nguyen et al., 2002). Therefore is even possible that neurofibromas may develop from unnoticed nerve injuries. Furthermore, it may be the case that Ras/ERK signalling deregulation may also be involved in neurofibroma formation in cases with no apparent connection with trauma, which may imply a wider impact for treatments with MEK inhibitors.

7.10 Further work

Future studies should aim at dissecting the signals involved in promoting the distinct behaviour of *Nf1*$^{-/-}$ Schwann cells at the injury site and distal stump of the peripheral nerve. As discussed before, several factors may be involved including TGF-β and PDGF, amongst others. Systematic approaches, such as microarray analysis comparing upregulation of genes at the cut versus distal sites in mutant mice, should be taken. A more simple *in vitro* system could also be used to test the susceptibility of *Nf1*$^{-/-}$ Schwann cells to engage in deregulated Ras signalling upon stimulation with a variety of factors, including the ones mentioned above and others, also associated with wounding such as ATP, H_2O_2 and VEGF. Furthermore, if the MEK inhibitor treatment does not yield promising results, others therapeutic approaches may be tested. In particular, given the role that inflammatory-derived factors may play in neurofibroma development, anti-inflammatory drugs may be an alternative strategy to consider.

We have generated a powerful system to study the early events of tumourigenesis. In particular, this novel mouse model has the great advantage of developing frequent tumours in specific locations. This, together with the ability to track genetically altered cells (YFP+), provides great opportunities to investigate the, as yet fairly obscure, very early steps of tumour development.

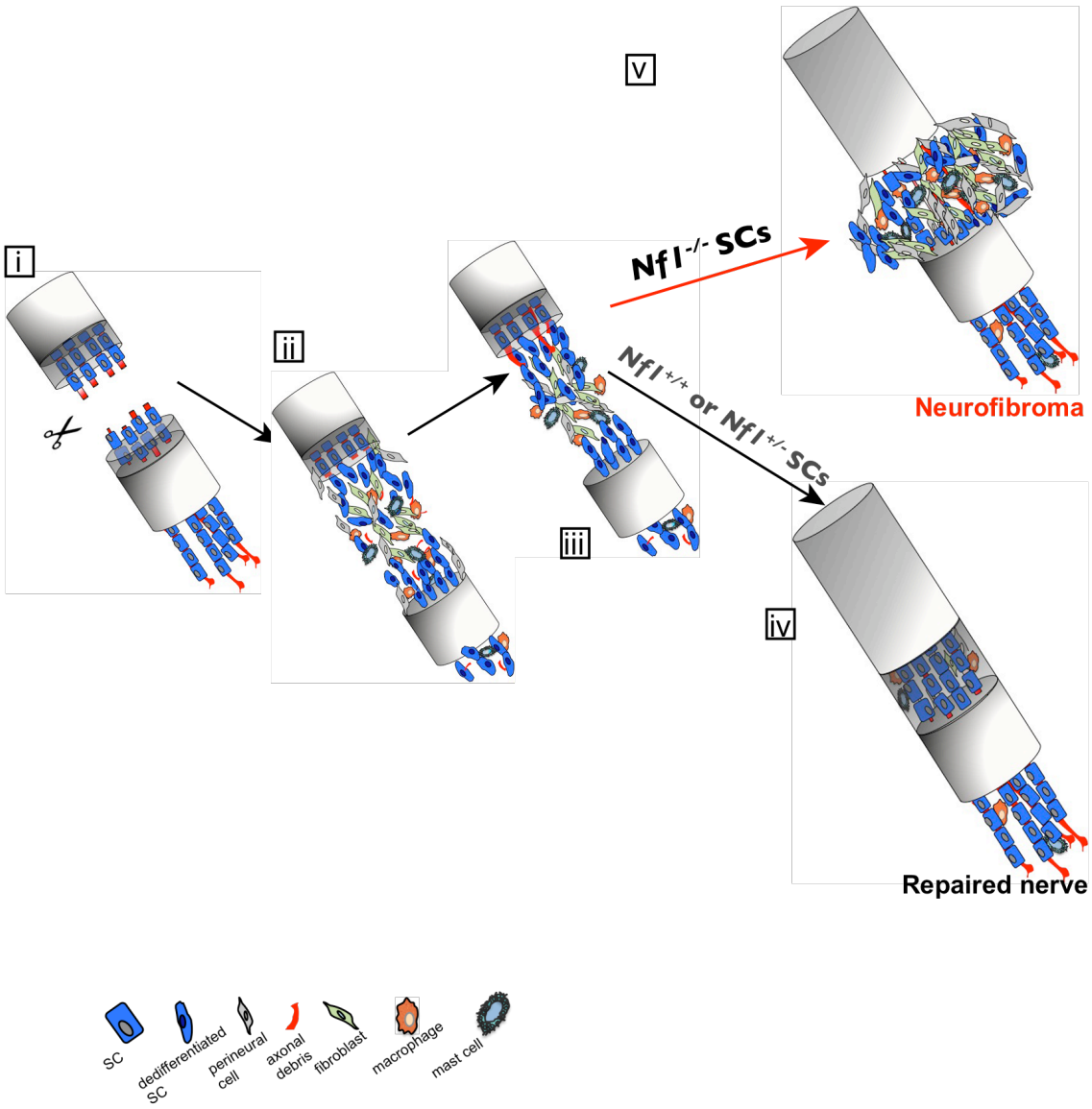

Figure 7-1: Model for neurofibroma formation. Following a nerve injury, at the wound site and distally to the injury site, axons (red) degenerate and Schwann cells (blue) dedifferentiate. A robust inflammatory response (orange and purple) and fibroblasts (green) are also recruited (**i** and **ii**). In wild-type animals, axons regrow, the inflammatory response is attenuated and Schwann cells redifferentiate (**iii** and **iv**). In this thesis, I have shown that if *Nf1* is deleted specifically in mSchwann cells in the adult mouse, neurofibroma-like tumours arise at the injury site (**v**). In contrast, in the distal stump of NF1 nerves, regeneration was indistinguishable from controls, suggesting that the nerve microenvironment is tumour suppressive.

References

Abe, I., Ochiai, N., Ichimura, H., Tsujino, A., Sun, J., and Hara, Y. (2004). Internodes can nearly double in length with gradual elongation of the adult rat sciatic nerve. J Orthop Res *22*, 571-577.

Adlkofer, K., and Lai, C. (2000). Role of neuregulins in glial cell development. Glia *29*, 104-111.

Adameyko, I., Lallemend, F., Aquino, J. B., Pereira, J. A., Topilko, P., Muller, T., Fritz, N., Beljajeva, A., Mochii, M., Liste, I., Usoskin, D., Suter, U., Birchmeier, C., Ernfors, P. (2009) Schwann Cell Precursors from Nerve Innervation Are a Cellular Origin of Melanocytes in Skin. Cell *139*, 366–379

Agius, E., and Cochard, P. (1998). Comparison of neurite outgrowth induced by intact and injured sciatic nerves: a confocal and functional analysis. J Neurosci *18*, 328-338.

Aguayo, A.J., Peyronnard, J.M., and Bray, G.M. (1973). A quantitative ultrastructural study of regeneration from isolated proximal stumps of transected unmyelinated nerves. J Neuropathol Exp Neurol *32*, 256-270.

Akassoglou, K., Kombrinck, K.W., Degen, J.L., and Strickland, S. (2000). Tissue plasminogen activator-mediated fibrinolysis protects against axonal degeneration and demyelination after sciatic nerve injury. J Cell Biol *149*, 1157-1166.

Akassoglou, K., Yu, W.M., Akpinar, P., and Strickland, S. (2002). Fibrin inhibits peripheral nerve remyelination by regulating Schwann cell differentiation. Neuron *33*, 861-875.

Akert, K., Sandri, C., Weibel, E.R., Peper, K., and Moor, H. (1976). The fine structure of the perineural endothelium. Cell Tissue Res *165*, 281-295.

Alcantara Llaguno, S., Chen, J., Kwon, C.H., Jackson, E.L., Li, Y., Burns, D.K., Alvarez-Buylla, A., and Parada, L.F. (2009). Malignant astrocytomas originate from neural stem/progenitor cells in a somatic tumor suppressor mouse model. Cancer Cell *15*, 45-56.

Aravind, L., Neuwald, A.F., and Ponting, C.P. (1999). Sec14p-like domains in NF1 and Dbl-like proteins indicate lipid regulation of Ras and Rho signaling. Curr Biol *9*, R195-197.

Arroyo, E.J., Bermingham, J.R., Jr., Rosenfeld, M.G., and Scherer, S.S. (1998). Promyelinating Schwann cells express Tst-1/SCIP/Oct-6. J Neurosci *18*, 7891-7902.

Arthur-Farraj, P., Wanek, K., Hantke, J., Davis, C.M., Jayakar, A., Parkinson, D.B., Mirsky, R., and Jessen, K.R. (2011). Mouse schwann cells need both NRG1 and cyclic AMP to myelinate. Glia *59*, 720-733.

Assoian, R.K., Fleurdelys, B.E., Stevenson, H.C., Miller, P.J., Madtes, D.K., Raines, E.W., Ross, R., and Sporn, M.B. (1987). Expression and secretion of type beta transforming growth factor by activated human macrophages. Proc Natl Acad Sci U S A *84*, 6020-6024.

Atanasoski, S., Scherer, S.S., Sirkowski, E., Leone, D., Garratt, A.N., Birchmeier, C., and Suter, U. (2006). ErbB2 signaling in Schwann cells is mostly dispensable for maintenance of myelinated peripheral nerves and proliferation of adult Schwann cells after injury. J Neurosci *26*, 2124-2131.

Atit, R.P., Crowe, M.J., Greenhalgh, D.G., Wenstrup, R.J., and Ratner, N. (1999). The Nf1 tumor suppressor regulates mouse skin wound healing, fibroblast proliferation, and collagen deposited by fibroblasts. J Invest Dermatol *112*, 835-842.

Bader, A.G., Kang, S., Zhao, L., and Vogt, P.K. (2005). Oncogenic PI3K deregulates transcription and translation. Nat Rev Cancer *5*, 921-929.

Bader, J.L. (1986). Neurofibromatosis and cancer. Ann N Y Acad Sci *486*, 57-65.

Baird, A., Mormede, P., and Bohlen, P. (1985). Immunoreactive fibroblast growth factor in cells of peritoneal exudate suggests its identity with macrophage-derived growth factor. Biochem Biophys Res Commun *126*, 358-364.

Balkwill, F., and Mantovani, A. (2001). Inflammation and cancer: back to Virchow? Lancet *357*, 539-545.

Ballester, R., Marchuk, D., Boguski, M., Saulino, A., Letcher, R., Wigler, M., and Collins, F. (1990). The NF1 locus encodes a protein functionally related to mammalian GAP and yeast IRA proteins. Cell *63*, 851-859.

Barker, D., Wright, E., Nguyen, K., Cannon, L., Fain, P., Goldgar, D., Bishop, D.T., Carey, J., Baty, B., Kivlin, J., *et al.* (1987). Gene for von Recklinghausen neurofibromatosis is in the pericentromeric region of chromosome 17. Science *236*, 1100-1102.

Baron, P., Shy, M., Honda, H., Sessa, M., Kamholz, J., and Pleasure, D. (1994). Developmental expression of P0 mRNA and P0 protein in the sciatic nerve and the spinal nerve roots of the rat. J Neurocytol *23*, 249-257.

Basu, T.N., Gutmann, D.H., Fletcher, J.A., Glover, T.W., Collins, F.S., and Downward, J. (1992). Aberrant regulation of ras proteins in malignant tumour cells from type 1 neurofibromatosis patients. Nature *356*, 713-715.

Be'eri, H., Reichert, F., Saada, A., and Rotshenker, S. (1998). The cytokine network of wallerian degeneration: IL-10 and GM-CSF. Eur J Neurosci *10*, 2707-2713.

Benninger, Y., Thurnherr, T., Pereira, J.A., Krause, S., Wu, X., Chrostek-Grashoff, A., Herzog, D., Nave, K.A., Franklin, R.J., Meijer, D., *et al.* (2007). Essential and distinct roles for cdc42 and rac1 in the regulation of Schwann cell biology during peripheral nervous system development. J Cell Biol *177*, 1051-1061.

Bermingham, J.R., Jr., Scherer, S.S., O'Connell, S., Arroyo, E., Kalla, K.A., Powell, F.L., and Rosenfeld, M.G. (1996). Tst-1/Oct-6/SCIP regulates a unique step in peripheral myelination and is required for normal respiration. Genes Dev *10*, 1751-1762.

Bermingham, J.R., Jr., Shumas, S., Whisenhunt, T., Rosenfeld, M.G., and Scherer, S.S. (2001). Modification of representational difference analysis applied to the isolation of forskolin-regulated genes from Schwann cells. J Neurosci Res *63*, 516-524.

Bernards, A., Snijders, A.J., Hannigan, G.E., Murthy, A.E., and Gusella, J.F. (1993). Mouse neurofibromatosis type 1 cDNA sequence reveals high degree of conservation of both coding and non-coding mRNA segments. Hum Mol Genet *2*, 645-650.

Birindelli, S., Perrone, F., Oggionni, M., Lavarino, C., Pasini, B., Vergani, B., Ranzani, G.N., Pierotti, M.A., and Pilotti, S. (2001). Rb and TP53 pathway alterations in sporadic and NF1-related malignant peripheral nerve sheath tumors. Lab Invest *81*, 833-844.

Bixby, J.L., Lilien, J., and Reichardt, L.F. (1988). Identification of the major proteins that promote neuronal process outgrowth on Schwann cells in vitro. J Cell Biol *107*, 353-361.

Bixby, J.L., and Zhang, R. (1990). Purified N-cadherin is a potent substrate for the rapid induction of neurite outgrowth. J Cell Biol *110*, 1253-1260.

Blanchard, A.D., Sinanan, A., Parmantier, E., Zwart, R., Broos, L., Meijer, D., Meier, C., Jessen, K.R., and Mirsky, R. (1996). Oct-6 (SCIP/Tst-1) is expressed in Schwann cell precursors, embryonic Schwann cells, and postnatal myelinating Schwann cells: comparison with Oct-1, Krox-20, and Pax-3. J Neurosci Res *46*, 630-640.

Bollag, G., McCormick, F., and Clark, R. (1993). Characterization of full-length neurofibromin: tubulin inhibits Ras GAP activity. EMBO J *12*, 1923-1927.

Bosio, A., Binczek, E., Haupt, W.F., and Stoffel, W. (1998). Composition and biophysical properties of myelin lipid define the neurological defects in galactocerebroside- and sulfatide-deficient mice. J Neurochem *70*, 308-315.

Brannan, C.I., Perkins, A.S., Vogel, K.S., Ratner, N., Nordlund, M.L., Reid, S.W., Buchberg, A.M., Jenkins, N.A., Parada, L.F., and Copeland, N.G. (1994). Targeted disruption of the neurofibromatosis type-1 gene leads to developmental abnormalities in heart and various neural crest-derived tissues. Genes Dev *8*, 1019-1029.

Bremer, M., Frob, F., Kichko, T., Reeh, P., Tamm, E.R., Suter, U., and Wegner, M. (2011). Sox10 is required for Schwann-cell homeostasis and myelin maintenance in the adult peripheral nerve. Glia *59*, 1022-1032.

Brill, M.S., Lichtman, J.W., Thompson, W., Zuo, Y., and Misgeld, T. (2011). Spatial constraints dictate glial territories at murine neuromuscular junctions. J Cell Biol *195*, 293-305.

Brinkmann, B.G., Agarwal, A., Sereda, M.W., Garratt, A.N., Muller, T., Wende, H., Stassart, R.M., Nawaz, S., Humml, C., Velanac, V.*, et al.* (2008). Neuregulin-1/ErbB signaling serves distinct functions in myelination of the peripheral and central nervous system. Neuron *59*, 581-595.

Britsch, S., Goerich, D.E., Riethmacher, D., Peirano, R.I., Rossner, M., Nave, K.A., Birchmeier, C., and Wegner, M. (2001). The transcription factor Sox10 is a key regulator of peripheral glial development. Genes Dev *15*, 66-78.

Britsch, S., Li, L., Kirchhoff, S., Theuring, F., Brinkmann, V., Birchmeier, C., and Riethmacher, D. (1998). The ErbB2 and ErbB3 receptors and their ligand, neuregulin-1, are essential for development of the sympathetic nervous system. Genes Dev *12*, 1825-1836.

Brossier, N.M., and Carroll, S.L. (2011). Genetically engineered mouse models shed new light on the pathogenesis of neurofibromatosis type I-related neoplasms of the peripheral nervous system. Brain Res Bull.

Brown, M.C., Perry, V.H., Hunt, S.P., and Lapper, S.R. (1994). Further studies on motor and sensory nerve regeneration in mice with delayed Wallerian degeneration. Eur J Neurosci *6*, 420-428.

Bruck, W. (1997). The role of macrophages in Wallerian degeneration. Brain Pathol *7*, 741-752.

Bruck, W., and Friede, R.L. (1990). Anti-macrophage CR3 antibody blocks myelin phagocytosis by macrophages in vitro. Acta Neuropathol *80*, 415-418.

Bruck, W., and Friede, R.L. (1991). The role of complement in myelin phagocytosis during PNS wallerian degeneration. J Neurol Sci *103*, 182-187.

Buchberg, A.M., Cleveland, L.S., Jenkins, N.A., and Copeland, N.G. (1990). Sequence homology shared by neurofibromatosis type-1 gene and IRA-1 and IRA-2 negative regulators of the RAS cyclic AMP pathway. Nature *347*, 291-294.

Bunge, M.B., Wood, P.M., Tynan, L.B., Bates, M.L., and Sanes, J.R. (1989). Perineurium originates from fibroblasts: demonstration in vitro with a retroviral marker. Science *243*, 229-231.

Bunge, R.P. (1993). Expanding roles for the Schwann cell: ensheathment, myelination, trophism and regeneration. Curr Opin Neurobiol *3*, 805-809.

Burgun, C., Esteve, L., Humblot, N., Aunis, D., and Zwiller, J. (2000). Cyclic AMP-elevating agents induce the expression of MAP kinase phosphatase-1 in PC12 cells. FEBS Lett *484*, 189-193.

Camps, M., Chabert, C., Muda, M., Boschert, U., Gillieron, C., and Arkinstall, S. (1998). Induction of the mitogen-activated protein kinase phosphatase MKP3 by nerve growth factor in differentiating PC12. FEBS Lett *425*, 271-276.

Carroll, S.L. (2011). Molecular mechanisms promoting the pathogenesis of Schwann cell neoplasms. Acta Neuropathol.

Carroll, S.L., Miller, M.L., Frohnert, P.W., Kim, S.S., and Corbett, J.A. (1997). Expression of neuregulins and their putative receptors, ErbB2 and ErbB3, is induced during Wallerian degeneration. J Neurosci *17*, 1642-1659.

Carroll, S.L., and Ratner, N. (2008). How does the Schwann cell lineage form tumors in NF1? Glia *56*, 1590-1605.

Carroll, S.L., and Stonecypher, M.S. (2005). Tumor suppressor mutations and growth factor signaling in the pathogenesis of NF1-associated peripheral nerve sheath tumors: II. The role of dysregulated growth factor signaling. J Neuropathol Exp Neurol *64*, 1-9.

Causey, G., and Barton, A.A. (1959). The cellular content of the endoneurium of peripheral nerve. Brain *82*, 594-598.

Cawthon, R.M., Andersen, L.B., Buchberg, A.M., Xu, G.F., O'Connell, P., Viskochil, D., Weiss, R.B., Wallace, M.R., Marchuk, D.A., Culver, M., *et al.* (1991). cDNA sequence and genomic structure of EV12B, a gene lying within an intron of the neurofibromatosis type 1 gene. Genomics *9*, 446-460.

Cawthon, R.M., O'Connell, P., Buchberg, A.M., Viskochil, D., Weiss, R.B., Culver, M., Stevens, J., Jenkins, N.A., Copeland, N.G., and White, R. (1990a). Identification and characterization of transcripts from the neurofibromatosis 1 region: the sequence and genomic structure of EVI2 and mapping of other transcripts. Genomics *7*, 555-565.

Cawthon, R.M., Weiss, R., Xu, G.F., Viskochil, D., Culver, M., Stevens, J., Robertson, M., Dunn, D., Gesteland, R., O'Connell, P., *et al.* (1990b). A major segment of the neurofibromatosis type 1 gene: cDNA sequence, genomic structure, and point mutations. Cell *62*, 193-201.

Chan, J.R., Cosgaya, J.M., Wu, Y.J., and Shooter, E.M. (2001). Neurotrophins are key mediators of the myelination program in the peripheral nervous system. Proc Natl Acad Sci U S A *98*, 14661-14668.

Chan, J.R., Jolicoeur, C., Yamauchi, J., Elliott, J., Fawcett, J.P., Ng, B.K., and Cayouette, M. (2006). The polarity protein Par-3 directly interacts with p75NTR to regulate myelination. Science *314*, 832-836.

Charles, P., Tait, S., Faivre-Sarrailh, C., Barbin, G., Gunn-Moore, F., Denisenko-Nehrbass, N., Guennoc, A.M., Girault, J.A., Brophy, P.J., and Lubetzki, C. (2002). Neurofascin is a glial receptor for the paranodin/Caspr-contactin axonal complex at the axoglial junction. Curr Biol *12*, 217-220.

Chavrier, P., Vesque, C., Galliot, B., Vigneron, M., Dolle, P., Duboule, D., and Charnay, P. (1990). The segment-specific gene Krox-20 encodes a transcription factor with binding sites in the promoter region of the Hox-1.4 gene. EMBO J *9*, 1209-1218.

Chen, S., Burgin, S., McDaniel, A., Li, X., Yuan, J., Chen, M., Khalaf, W., Clapp, D.W., and Yang, F.C. (2010). Nf1-/- Schwann cell-conditioned medium modulates mast cell degranulation by c-Kit-mediated hyperactivation of phosphatidylinositol 3-kinase. Am J Pathol *177*, 3125-3132.

Chen, S., Rio, C., Ji, R.R., Dikkes, P., Coggeshall, R.E., Woolf, C.J., and Corfas, G. (2003). Disruption of ErbB receptor signaling in adult non-myelinating Schwann cells causes progressive sensory loss. Nat Neurosci *6*, 1186-1193.

Chen, Y., Wang, H., Yoon, S.O., Xu, X., Hottiger, M.O., Svaren, J., Nave, K.A., Kim, H.A., Olson, E.N., and Lu, Q.R. (2011). HDAC-mediated deacetylation of NF-kappaB is critical for Schwann cell myelination. Nat Neurosci *14*, 437-441.

Chen, Y.Y., McDonald, D., Cheng, C., Magnowski, B., Durand, J., and Zochodne, D.W. (2005). Axon and Schwann cell partnership during nerve regrowth. J Neuropathol Exp Neurol *64*, 613-622.

Chen, Z.L., and Strickland, S. (2003). Laminin gamma1 is critical for Schwann cell differentiation, axon myelination, and regeneration in the peripheral nerve. J Cell Biol *163*, 889-899.

Chen, Z.L., Yu, W.M., and Strickland, S. (2007). Peripheral regeneration. Annu Rev Neurosci *30*, 209-233.

Cheng, L., Khan, M., and Mudge, A.W. (1995). Calcitonin gene-related peptide promotes Schwann cell proliferation. J Cell Biol *129*, 789-796.

Chernousov, M.A., and Carey, D.J. (2000). Schwann cell extracellular matrix molecules and their receptors. Histol Histopathol *15*, 593-601.

Cichowski, K., and Jacks, T. (2001). NF1 tumor suppressor gene function: narrowing the GAP. Cell *104*, 593-604.

Cichowski, K., Santiago, S., Jardim, M., Johnson, B.W., and Jacks, T. (2003). Dynamic regulation of the Ras pathway via proteolysis of the NF1 tumor suppressor. Genes Dev *17*, 449-454.

Cichowski, K., Shih, T.S., Schmitt, E., Santiago, S., Reilly, K., McLaughlin, M.E., Bronson, R.T., and Jacks, T. (1999). Mouse models of tumor development in neurofibromatosis type 1. Science *286*, 2172-2176.

Conforti, L., Wilbrey, A., Morreale, G., Janeckova, L., Beirowski, B., Adalbert, R., Mazzola, F., Di Stefano, M., Hartley, R., Babetto, E., *et al.* (2009). Wld S protein requires Nmnat activity and a short N-terminal sequence to protect axons in mice. J Cell Biol *184*, 491-500.

Corfas, G., Velardez, M.O., Ko, C.P., Ratner, N., and Peles, E. (2004). Mechanisms and roles of axon-Schwann cell interactions. J Neurosci *24*, 9250-9260.

Cosgaya, J.M., Chan, J.R., and Shooter, E.M. (2002). The neurotrophin receptor p75NTR as a positive modulator of myelination. Science *298*, 1245-1248.

Costa, R.M., Federov, N.B., Kogan, J.H., Murphy, G.G., Stern, J., Ohno, M., Kucherlapati, R., Jacks, T., and Silva, A.J. (2002). Mechanism for the learning deficits in a mouse model of neurofibromatosis type 1. Nature *415*, 526-530.

Court, F.A., Wrabetz, L., and Feltri, M.L. (2006). Basal lamina: Schwann cells wrap to the rhythm of space-time. Curr Opin Neurobiol *16*, 501-507.

Courtois-Cox, S., Genther Williams, S.M., Reczek, E.E., Johnson, B.W., McGillicuddy, L.T., Johannessen, C.M., Hollstein, P.E., MacCollin, M., and Cichowski, K. (2006). A negative feedback signaling network underlies oncogene-induced senescence. Cancer Cell *10*, 459-472.

Cui, Y., Costa, R.M., Murphy, G.G., Elgersma, Y., Zhu, Y., Gutmann, D.H., Parada, L.F., Mody, I., and Silva, A.J. (2008). Neurofibromin regulation of ERK signaling modulates GABA release and learning. Cell *135*, 549-560.

Curtis, R., Stewart, H.J., Hall, S.M., Wilkin, G.P., Mirsky, R., and Jessen, K.R. (1992). GAP-43 is expressed by nonmyelin-forming Schwann cells of the peripheral nervous system. J Cell Biol *116*, 1455-1464.

D'Angelo, I., Welti, S., Bonneau, F., and Scheffzek, K. (2006). A novel bipartite phospholipid-binding module in the neurofibromatosis type 1 protein. EMBO Rep *7*, 174-179.

Dang, I., and DeVries, G.H. (2005). Schwann cell lines derived from malignant peripheral nerve sheath tumors respond abnormally to platelet-derived growth factor-BB. J Neurosci Res *79*, 318-328.

Dasgupta, B., Dugan, L.L., and Gutmann, D.H. (2003). The neurofibromatosis 1 gene product neurofibromin regulates pituitary adenylate cyclase-activating polypeptide-mediated signaling in astrocytes. J Neurosci *23*, 8949-8954.

Daston, M.M., Scrable, H., Nordlund, M., Sturbaum, A.K., Nissen, L.M., and Ratner, N. (1992). The protein product of the neurofibromatosis type 1 gene is expressed at highest abundance in neurons, Schwann cells, and oligodendrocytes. Neuron *8*, 415-428.

Decker, L., Desmarquet-Trin-Dinh, C., Taillebourg, E., Ghislain, J., Vallat, J.M., and Charnay, P. (2006). Peripheral myelin maintenance is a dynamic process requiring constant Krox20 expression. J Neurosci *26*, 9771-9779.

DeClue, J.E., Cohen, B.D., and Lowy, D.R. (1991). Identification and characterization of the neurofibromatosis type 1 protein product. Proc Natl Acad Sci U S A *88*, 9914-9918.

DeClue, J.E., Papageorge, A.G., Fletcher, J.A., Diehl, S.R., Ratner, N., Vass, W.C., and Lowy, D.R. (1992). Abnormal regulation of mammalian p21ras contributes to malignant tumor growth in von Recklinghausen (type 1) neurofibromatosis. Cell *69*, 265-273.

Dickersin, G.R. (1987). The electron microscopic spectrum of nerve sheath tumors. Ultrastruct Pathol *11*, 103-146.

Dickinson, R.J., and Keyse, S.M. (2006). Diverse physiological functions for dual-specificity MAP kinase phosphatases. J Cell Sci *119*, 4607-4615.

Dirks, P.B. (2008). Cancer's source in the peripheral nervous system. Nat Med *14*, 373-375.

Doetsch, F. (2003). The glial identity of neural stem cells. Nat Neurosci *6*, 1127-1134.

Dolberg, D.S., Hollingsworth, R., Hertle, M., and Bissell, M.J. (1985). Wounding and its role in RSV-mediated tumor formation. Science *230*, 676-678.

Dong, Z., Brennan, A., Liu, N., Yarden, Y., Lefkowitz, G., Mirsky, R., and Jessen, K.R. (1995). Neu differentiation factor is a neuron-glia signal and regulates survival, proliferation, and maturation of rat Schwann cell precursors. Neuron *15*, 585-596.

Dong, Z., Sinanan, A., Parkinson, D., Parmantier, E., Mirsky, R., and Jessen, K.R. (1999). Schwann cell development in embryonic mouse nerves. J Neurosci Res *56*, 334-348.

Downward, J. (1998). Ras signalling and apoptosis. Curr Opin Genet Dev *8*, 49-54.

Du Plessis, D.G., Mouton, Y.M., Muller, C.J., and Geiger, D.H. (1996). An ultrastructural study of the development of the chicken perineurial sheath. J Anat *189 (Pt 3)*, 631-641.

Dupin, E., Real, C., Glavieux-Pardanaud, C., Vaigot, P., and Le Douarin, N.M. (2003). Reversal of developmental restrictions in neural crest lineages: transition from

Schwann cells to glial-melanocytic precursors in vitro. Proc Natl Acad Sci U S A *100*, 5229-5233.

Dupree, J.L., Coetzee, T., Suzuki, K., and Popko, B. (1998). Myelin abnormalities in mice deficient in galactocerebroside and sulfatide. J Neurocytol *27*, 649-659.

Dvorak H-F (1986) Tumors: Wounds that do not heal. Similarities between tumor stroma generation and wound healing. N Engl J Med 315:1650–165930.

Echave, P., Machado-da-Silva, G., Arkell, R.S., Duchen, M.R., Jacobson, J., Mitter, R., and Lloyd, A.C. (2009). Extracellular growth factors and mitogens cooperate to drive mitochondrial biogenesis. J Cell Sci *122*, 4516-4525.

Ehlers, M. D. (2004). Deconstructing the axon: Wallerian degeneration and the ubiquitin-proteasome system. Trends Neurosci *27*, 3-6

Erickson, S.L., O'Shea, K.S., Ghaboosi, N., Loverro, L., Frantz, G., Bauer, M., Lu, L.H., and Moore, M.W. (1997). ErbB3 is required for normal cerebellar and cardiac development: a comparison with ErbB2-and heregulin-deficient mice. Development *124*, 4999-5011.

Erlandson, R.A. (1991). The enigmatic perineurial cell and its participation in tumors and in tumorlike entities. Ultrastruct Pathol *15*, 335-351.

Eshed, Y., Feinberg, K., Poliak, S., Sabanay, H., Sarig-Nadir, O., Spiegel, I., Bermingham, J.R., Jr., and Peles, E. (2005). Gliomedin mediates Schwann cell-axon interaction and the molecular assembly of the nodes of Ranvier. Neuron *47*, 215-229.

Evans, D.G., Baser, M.E., McGaughran, J., Sharif, S., Howard, E., and Moran, A. (2002). Malignant peripheral nerve sheath tumours in neurofibromatosis 1. J Med Genet *39*, 311-314.

Fawcett, J. W., and Keynes, R. J. (1990) Peripheral nerve regeneration. Annu Rev Neurosci *13*, 43-60

Feltri, M.L., Graus Porta, D., Previtali, S.C., Nodari, A., Migliavacca, B., Cassetti, A., Littlewood-Evans, A., Reichardt, L.F., Messing, A., Quattrini, A., *et al.* (2002). Conditional disruption of beta 1 integrin in Schwann cells impedes interactions with axons. J Cell Biol *156*, 199-209.

Feng, Z., and Ko, C.P. (2008). The role of glial cells in the formation and maintenance of the neuromuscular junction. Ann N Y Acad Sci *1132*, 19-28.

Fernandes, K.J., McKenzie, I.A., Mill, P., Smith, K.M., Akhavan, M., Barnabe-Heider, F., Biernaskie, J., Junek, A., Kobayashi, N.R., Toma, J.G., *et al.* (2004). A dermal niche for multipotent adult skin-derived precursor cells. Nat Cell Biol *6*, 1082-1093.

Fernandes, K.J., Toma, J.G., and Miller, F.D. (2008). Multipotent skin-derived precursors: adult neural crest-related precursors with therapeutic potential. Philos Trans R Soc Lond B Biol Sci *363*, 185-198.

Fernandez-Valle, C., Bunge, R.P., and Bunge, M.B. (1995). Schwann cells degrade myelin and proliferate in the absence of macrophages: evidence from in vitro studies of Wallerian degeneration. J Neurocytol *24*, 667-679.

Fernandez-Valle, C., Wood, P.M., and Bunge, M.B. (1998). Localization of focal adhesion kinase in differentiating Schwann cell/neuron cultures. Microsc Res Tech *41*, 416-430.

Filbin, M.T., Walsh, F.S., Trapp, B.D., Pizzey, J.A., and Tennekoon, G.I. (1990). Role of myelin P0 protein as a homophilic adhesion molecule. Nature *344*, 871-872.

Finzsch, M., Schreiner, S., Kichko, T., Reeh, P., Tamm, E.R., Bosl, M.R., Meijer, D., and Wegner, M. (2010). Sox10 is required for Schwann cell identity and progression beyond the immature Schwann cell stage. J Cell Biol *189*, 701-712.

Fischer, S., Weishaupt, A., Troppmair, J., and Martini, R.(2008). Increase of MCP-1 (CCL2) in myelin mutant Schwann cells is mediated by MEK-ERK signaling pathway. Glia *56*, 836-43

Fricker, F.R., Lago, N., Balarajah, S., Tsantoulas, C., Tanna, S., Zhu, N., Fageiry, S.K., Jenkins, M., Garratt, A.N., Birchmeier, C.*, et al.* (2011). Axonally derived neuregulin-1 is required for remyelination and regeneration after nerve injury in adulthood. J Neurosci *31*, 3225-3233.

Fricker, F.R., Zhu, N., Tsantoulas, C., Abrahamsen, B., Nassar, M.A., Thakur, M., Garratt, A.N., Birchmeier, C., McMahon, S.B., Wood, J.N.*, et al.* (2009). Sensory axon-derived neuregulin-1 is required for axoglial signaling and normal sensory function but not for long-term axon maintenance. J Neurosci *29*, 7667-7678.

Funakoshi, H., Frisen, J., Barbany, G., Timmusk, T., Zachrisson, O., Verge, V.M., and Persson, H. (1993). Differential expression of mRNAs for neurotrophins and their receptors after axotomy of the sciatic nerve. J Cell Biol *123*, 455-465.

Gardiner, N.J. (2011). Integrins and the extracellular matrix: key mediators of development and regeneration of the sensory nervous system. Dev Neurobiol *71*, 1054-1072.

Garratt, A.N., Britsch, S., and Birchmeier, C. (2000a). Neuregulin, a factor with many functions in the life of a schwann cell. Bioessays *22*, 987-996.

Garratt, A.N., Voiculescu, O., Topilko, P., Charnay, P., and Birchmeier, C. (2000b). A dual role of erbB2 in myelination and in expansion of the schwann cell precursor pool. J Cell Biol *148*, 1035-1046.

Gaul, U., Mardon, G., and Rubin, G.M. (1992). A putative Ras GTPase activating protein acts as a negative regulator of signaling by the Sevenless receptor tyrosine kinase. Cell *68*, 1007-1019.

Gerdts, J., Sasaki, Y., Vohra, B., Marasa, J. and Milbrandt, J. (2011). Image-based screening identifies novel roles for IkappaB kinase and glycogen synthase kinase 3 in axonal degeneration. J Biol Chem *286*, 28011-8

Geuna, S., Raimondo, S., Ronchi, G., Di Scipio, F., Tos, P., Czaja, K., and Fornaro, M. (2009). Chapter 3: Histology of the peripheral nerve and changes occurring during nerve regeneration. Int Rev Neurobiol *87*, 27-46.

Ghislain, J., and Charnay, P. (2006). Control of myelination in Schwann cells: a Krox20 cis-regulatory element integrates Oct6, Brn2 and Sox10 activities. EMBO Rep *7*, 52-58.

Ghislain, J., Desmarquet-Trin-Dinh, C., Jaegle, M., Meijer, D., Charnay, P., and Frain, M. (2002). Characterisation of cis-acting sequences reveals a biphasic, axon-dependent regulation of Krox20 during Schwann cell development. Development *129*, 155-166.

Giese, K.P., Martini, R., Lemke, G., Soriano, P., and Schachner, M. (1992). Mouse P0 gene disruption leads to hypomyelination, abnormal expression of recognition molecules, and degeneration of myelin and axons. Cell *71*, 565-576.

Gilley, J., and Coleman, M.P. (2010). Endogenous Nmnat2 is an essential survival factor for maintenance of healthy axons. PLoS Biol *8*, e1000300.

Gitler, A.D., Zhu, Y., Ismat, F.A., Lu, M.M., Yamauchi, Y., Parada, L.F., and Epstein, J.A. (2003). Nf1 has an essential role in endothelial cells. Nat Genet *33*, 75-79.

Glass, J.D., Culver, D.G., Levey, A.I., and Nash, N.R. (2002). Very early activation of m-calpain in peripheral nerve during Wallerian degeneration. J Neurol Sci *196*, 9-20.

Golding, J.P., and Cohen, J. (1997). Border controls at the mammalian spinal cord: late-surviving neural crest boundary cap cells at dorsal root entry sites may regulate sensory afferent ingrowth and entry zone morphogenesis. Mol Cell Neurosci *9*, 381-396.

Gouzi, J.Y., Moressis, A., Walker, J.A., Apostolopoulou, A.A., Palmer, R.H., Bernards, A., and Skoulakis, E.M. (2011). The receptor tyrosine kinase Alk controls neurofibromin functions in Drosophila growth and learning. PLoS Genet *7*, e1002281.

Gregory, P.E., Gutmann, D.H., Mitchell, A., Park, S., Boguski, M., Jacks, T., Wood, D.L., Jove, R., and Collins, F.S. (1993). Neurofibromatosis type 1 gene product (neurofibromin) associates with microtubules. Somat Cell Mol Genet *19*, 265-274.

Grivennikov, S.I., Greten, F.R., and Karin, M. (2010). Immunity, inflammation, and cancer. Cell *140*, 883-899.

Grossmann, K.S., Wende, H., Paul, F.E., Cheret, C., Garratt, A.N., Zurborg, S., Feinberg, K., Besser, D., Schulz, H., Peles, E., *et al.* (2009). The tyrosine phosphatase Shp2 (PTPN11) directs Neuregulin-1/ErbB signaling throughout Schwann cell development. Proc Natl Acad Sci U S A *106*, 16704-16709.

Grove, M., Komiyama, N.H., Nave, K.A., Grant, S.G., Sherman, D.L., and Brophy, P.J. (2007). FAK is required for axonal sorting by Schwann cells. J Cell Biol *176*, 277-282.

Guerra, C., Schuhmacher, A.J., Canamero, M., Grippo, P.J., Verdaguer, L., Perez-Gallego, L., Dubus, P., Sandgren, E.P., and Barbacid, M. (2007). Chronic pancreatitis is essential for induction of pancreatic ductal adenocarcinoma by K-Ras oncogenes in adult mice. Cancer Cell *11*, 291-302.

Guertin, A.D., Zhang, D.P., Mak, K.S., Alberta, J.A., and Kim, H.A. (2005). Microanatomy of axon/glial signaling during Wallerian degeneration. J Neurosci *25*, 3478-3487.

Guo, H.F., The, I., Hannan, F., Bernards, A., and Zhong, Y. (1997). Requirement of Drosophila NF1 for activation of adenylyl cyclase by PACAP38-like neuropeptides. Science *276*, 795-798.

Guo, H.F., Tong, J., Hannan, F., Luo, L., and Zhong, Y. (2000). A neurofibromatosis-1-regulated pathway is required for learning in Drosophila. Nature *403*, 895-898.

Gutmann, D.H., Wood, D.L., and Collins, F.S. (1991). Identification of the neurofibromatosis type 1 gene product. Proc Natl Acad Sci U S A *88*, 9658-9662.

Hagedorn, L., Suter, U., and Sommer, L. (1999). P0 and PMP22 mark a multipotent neural crest-derived cell type that displays community effects in response to TGF-beta family factors. Development *126*, 3781-3794.

Hajra, A., Martin-Gallardo, A., Tarle, S.A., Freedman, M., Wilson-Gunn, S., Bernards, A., and Collins, F.S. (1994). DNA sequences in the promoter region of the NF1 gene are highly conserved between human and mouse. Genomics *21*, 649-652.

Hall, S. (2005). The response to injury in the peripheral nervous system. J Bone Joint Surg Br *87*, 1309-1319.

Hall, S.M., Li, H., and Kent, A.P. (1997). Schwann cells responding to primary demyelination in vivo express p75NTR and c-erbB receptors: a light and electron immunohistochemical study. J Neurocytol *26*, 679-690.

Hanemann, C.O., and Muller, H.W. (1998). Pathogenesis of Charcot-Marie-Tooth 1A (CMT1A) neuropathy. Trends Neurosci *21*, 282-286.

Harrisingh, M.C., Perez-Nadales, E., Parkinson, D.B., Malcolm, D.S., Mudge, A.W., and Lloyd, A.C. (2004). The Ras/Raf/ERK signalling pathway drives Schwann cell dedifferentiation. EMBO J *23*, 3061-3071.

Hayasaka, K., Himoro, M., Sato, W., Takada, G., Uyemura, K., Shimizu, N., Bird, T.D., Conneally, P.M., and Chance, P.F. (1993a). Charcot-Marie-Tooth neuropathy type 1B is associated with mutations of the myelin P0 gene. Nat Genet *5*, 31-34.

Hayasaka, K., Himoro, M., Sawaishi, Y., Nanao, K., Takahashi, T., Takada, G., Nicholson, G.A., Ouvrier, R.A., and Tachi, N. (1993b). De novo mutation of the myelin P0 gene in Dejerine-Sottas disease (hereditary motor and sensory neuropathy type III). Nat Genet *5*, 266-268.

Heumann, R., Korsching, S., Bandtlow, C., and Thoenen, H. (1987). Changes of nerve growth factor synthesis in nonneuronal cells in response to sciatic nerve transection. J Cell Biol *104*, 1623-1631.

Hikawa, N., and Takenaka, T. (1996). Myelin-stimulated macrophages release neurotrophic factors for adult dorsal root ganglion neurons in culture. Cell Mol Neurobiol *16*, 517-528.

Hirata, K., Mitoma, H., Ueno, N., He, J. W., and Kawabuchi, M. (1999) Differential response of macrophage subpopulations to myelin degradation in the injured rat sciatic nerve. J Neurocytol *28*, 685-95.

Hirose, T., Sano, T., and Hizawa, K. (1986). Ultrastructural localization of S-100 protein in neurofibroma. Acta Neuropathol *69*, 103-110.

Ho, W.H., Armanini, M.P., Nuijens, A., Phillips, H.S., and Osheroff, P.L. (1995). Sensory and motor neuron-derived factor. A novel heregulin variant highly expressed in sensory and motor neurons. J Biol Chem *270*, 26722.

Hoopfer, E. D., McLaughlin, T., Watts, R. J., Schuldiner, O., O'Leary, D. D., and Luo, L. (2006). Wlds protection distinguishes axon degeneration following injury from naturally occurring developmental pruning. Neuron 50, 883-95

Howe, D.G., and McCarthy, K.D. (2000). Retroviral inhibition of cAMP-dependent protein kinase inhibits myelination but not Schwann cell mitosis stimulated by interaction with neurons. J Neurosci *20*, 3513-3521.

Hrehorovich, P.A., Franke, H.R., Maximin, S., and Caracta, P. (2003). Malignant peripheral nerve sheath tumor. Radiographics *23*, 790-794.

Hu, X., He, W., Diaconu, C., Tang, X., Kidd, G.J., Macklin, W.B., Trapp, B.D., and Yan, R. (2008). Genetic deletion of BACE1 in mice affects remyelination of sciatic nerves. FASEB J *22*, 2970-2980.

Hu, X., Hicks, C.W., He, W., Wong, P., Macklin, W.B., Trapp, B.D., and Yan, R. (2006). Bace1 modulates myelination in the central and peripheral nervous system. Nat Neurosci *9*, 1520-1525.

Huijbregts, R.P., Roth, K.A., Schmidt, R.E., and Carroll, S.L. (2003). Hypertrophic neuropathies and malignant peripheral nerve sheath tumors in transgenic mice overexpressing glial growth factor beta3 in myelinating Schwann cells. J Neurosci *23*, 7269-7280.

Ingram, D.A., Hiatt, K., King, A.J., Fisher, L., Shivakumar, R., Derstine, C., Wenning, M.J., Diaz, B., Travers, J.B., Hood, A.*, et al.* (2001). Hyperactivation of p21(ras) and the hematopoietic-specific Rho GTPase, Rac2, cooperate to alter the proliferation of neurofibromin-deficient mast cells in vivo and in vitro. J Exp Med *194*, 57-69.

Ingram, D.A., Yang, F.C., Travers, J.B., Wenning, M.J., Hiatt, K., New, S., Hood, A., Shannon, K., Williams, D.A., and Clapp, D.W. (2000). Genetic and biochemical evidence that haploinsufficiency of the Nf1 tumor suppressor gene modulates melanocyte and mast cell fates in vivo. J Exp Med *191*, 181-188.

Izawa, I., Tamaki, N., and Saya, H. (1996). Phosphorylation of neurofibromatosis type 1 gene product (neurofibromin) by cAMP-dependent protein kinase. FEBS Lett *382*, 53-59.

Jacks, T., Shih, T.S., Schmitt, E.M., Bronson, R.T., Bernards, A., and Weinberg, R.A. (1994). Tumour predisposition in mice heterozygous for a targeted mutation in Nf1. Nat Genet *7*, 353-361.

Jacob, C., Christen, C.N., Pereira, J.A., Somandin, C., Baggiolini, A., Lotscher, P., Ozcelik, M., Tricaud, N., Meijer, D., Yamaguchi, T.*, et al.* (2011). HDAC1 and HDAC2 control the transcriptional program of myelination and the survival of Schwann cells. Nat Neurosci *14*, 429-436.

Jaegle, M., Ghazvini, M., Mandemakers, W., Piirsoo, M., Driegen, S., Levavasseur, F., Raghoenath, S., Grosveld, F., and Meijer, D. (2003). The POU proteins Brn-2 and Oct-6 share important functions in Schwann cell development. Genes Dev *17*, 1380-1391.

Jessen, K.R. (2004). Glial cells. Int J Biochem Cell Biol *36*, 1861-1867.

Jessen, K.R., Brennan, A., Morgan, L., Mirsky, R., Kent, A., Hashimoto, Y., and Gavrilovic, J. (1994). The Schwann cell precursor and its fate: a study of cell death and differentiation during gliogenesis in rat embryonic nerves. Neuron *12*, 509-527.

Jessen, K.R., and Mirsky, R. (1999). Developmental regulation in the Schwann cell lineage. Adv Exp Med Biol *468*, 3-12.

Jessen, K.R., and Mirsky, R. (2002). Signals that determine Schwann cell identity. J Anat *200*, 367-376.

Jessen, K.R., and Mirsky, R. (2005). The origin and development of glial cells in peripheral nerves. Nat Rev Neurosci *6*, 671-682.

Jessen, K.R., and Mirsky, R. (2008). Negative regulation of myelination: relevance for development, injury, and demyelinating disease. Glia *56*, 1552-1565.

Jessen, K.R., Morgan, L., Brammer, M., and Mirsky, R. (1985). Galactocerebroside is expressed by non-myelin-forming Schwann cells in situ. J Cell Biol *101*, 1135-1143.

Jia, H., Yan, T., Feng, Y., Zeng, C., Shi, X., and Zhai, Q. (2007). Identification of a critical site in Wld(s): essential for Nmnat enzyme activity and axon-protective function. Neurosci Lett *413*, 46-51.

Johannessen, C.M., Johnson, B.W., Williams, S.M., Chan, A.W., Reczek, E.E., Lynch, R.C., Rioth, M.J., McClatchey, A., Ryeom, S., and Cichowski, K. (2008). TORC1 is essential for NF1-associated malignancies. Curr Biol *18*, 56-62.

Johannessen, C.M., Reczek, E.E., James, M.F., Brems, H., Legius, E., and Cichowski, K. (2005). The NF1 tumor suppressor critically regulates TSC2 and mTOR. Proc Natl Acad Sci U S A *102*, 8573-8578.

Jones, E.A., Jang, S.W., Mager, G.M., Chang, L.W., Srinivasan, R., Gokey, N.G., Ward, R.M., Nagarajan, R., and Svaren, J. (2007). Interactions of Sox10 and Egr2 in myelin gene regulation. Neuron Glia Biol *3*, 377-387.

Joseph, N.M., Mosher, J.T., Buchstaller, J., Snider, P., McKeever, P.E., Lim, M., Conway, S.J., Parada, L.F., Zhu, Y., and Morrison, S.J. (2008). The loss of Nf1 transiently promotes self-renewal but not tumorigenesis by neural crest stem cells. Cancer Cell *13*, 129-140.

Kadono, T., Kikuchi, K., Nakagawa, H., and Tamaki, K. (2000). Expressions of various growth factors and their receptors in tissues from neurofibroma. Dermatology *201*, 10-14.

Kalluri, R., and Zeisberg, M. (2006). Fibroblasts in cancer. Nat Rev Cancer *6*, 392-401.

Kao, S.C., Wu, H., Xie, J., Chang, C.P., Ranish, J.A., Graef, I.A., and Crabtree, G.R. (2009). Calcineurin/NFAT signaling is required for neuregulin-regulated Schwann cell differentiation. Science *323*, 651-654.

Key, A. and Retzius, G. (1876). Studien in der Anatomie des Nervensystems und des Bindgewebes, Part 2. Stockholm: Samson and Wallis.

Kennedy, A.D., and DeLeo, F.R. (2009). Neutrophil apoptosis and the resolution of infection. Immunol Res *43*, 25-61.

Kim, H.A., Ling, B., and Ratner, N. (1997). Nf1-deficient mouse Schwann cells are angiogenic and invasive and can be induced to hyperproliferate: reversion of some phenotypes by an inhibitor of farnesyl protein transferase. Mol Cell Biol *17*, 862-872.

Kim, H.A., Pomeroy, S.L., Whoriskey, W., Pawlitzky, I., Benowitz, L.I., Sicinski, P., Stiles, C.D., and Roberts, T.M. (2000). A developmentally regulated switch directs regenerative growth of Schwann cells through cyclin D1. Neuron *26*, 405-416.

Kim, H.A., Ratner, N., Roberts, T.M., and Stiles, C.D. (2001). Schwann cell proliferative responses to cAMP and Nf1 are mediated by cyclin D1. J Neurosci *21*, 1110-1116.

Kim, H.A., Rosenbaum, T., Marchionni, M.A., Ratner, N., and DeClue, J.E. (1995). Schwann cells from neurofibromin deficient mice exhibit activation of p21ras, inhibition of cell proliferation and morphological changes. Oncogene *11*, 325-335.

King, D., Yang, G., Thompson, M.A., and Hiebert, S.W. (2002). Loss of neurofibromatosis-1 and p19(ARF) cooperate to induce a multiple tumor phenotype. Oncogene *21*, 4978-4982.

Kirschner, D.A., and Ganser, A.L. (1980). Compact myelin exists in the absence of basic protein in the shiverer mutant mouse. Nature *283*, 207-210.

Kourea, H.P., Orlow, I., Scheithauer, B.W., Cordon-Cardo, C., and Woodruff, J.M. (1999). Deletions of the INK4A gene occur in malignant peripheral nerve sheath tumors but not in neurofibromas. Am J Pathol *155*, 1855-1860.

Kristensson, K., and Olsson, Y. (1971). The perineurium as a diffusion barrier to protein tracers. Differences between mature and immature animals. Acta Neuropathol *17*, 127-138.

Kruger, G.M., Mosher, J.T., Bixby, S., Joseph, N., Iwashita, T., and Morrison, S.J. (2002). Neural crest stem cells persist in the adult gut but undergo changes in self-renewal, neuronal subtype potential, and factor responsiveness. Neuron *35*, 657-669.

Kucenas, S., Takada, N., Park, H.C., Woodruff, E., Broadie, K., and Appel, B. (2008). CNS-derived glia ensheath peripheral nerves and mediate motor root development. Nat Neurosci *11*, 143-151.

Kuhlmann, T., Bitsch, A., Stadelmann, C., Siebert, H., and Bruck, W. (2001). Macrophages are eliminated from the injured peripheral nerve via local apoptosis and circulation to regional lymph nodes and the spleen. J Neurosci *21*, 3401-3408.

Kweh, F., Zheng, M., Kurenova, E., Wallace, M., Golubovskaya, V., and Cance, W.G. (2009). Neurofibromin physically interacts with the N-terminal domain of focal adhesion kinase. Mol Carcinog *48*, 1005-1017.

La Fleur, M., Underwood, J.L., Rappolee, D.A., and Werb, Z. (1996). Basement membrane and repair of injury to peripheral nerve: defining a potential role for

macrophages, matrix metalloproteinases, and tissue inhibitor of metalloproteinases-1. J Exp Med *184*, 2311-2326.

La Marca, R., Cerri, F., Horiuchi, K., Bachi, A., Feltri, M.L., Wrabetz, L., Blobel, C.P., Quattrini, A., Salzer, J.L., and Taveggia, C. (2011). TACE (ADAM17) inhibits Schwann cell myelination. Nat Neurosci *14*, 857-865.

Largaespada, D.A., Brannan, C.I., Jenkins, N.A., and Copeland, N.G. (1996). Nf1 deficiency causes Ras-mediated granulocyte/macrophage colony stimulating factor hypersensitivity and chronic myeloid leukaemia. Nat Genet *12*, 137-143.

Le, L.Q., Liu, C., Shipman, T., Chen, Z., Suter, U., and Parada, L.F. (2011). Susceptible stages in Schwann cells for NF1-associated plexiform neurofibroma development. Cancer Res *71*, 4686-4695.

Le, L.Q., Shipman, T., Burns, D.K., and Parada, L.F. (2009). Cell of origin and microenvironment contribution for NF1-associated dermal neurofibromas. Cell Stem Cell *4*, 453-463.

Le, N., Nagarajan, R., Wang, J.Y., Araki, T., Schmidt, R.E., and Milbrandt, J. (2005). Analysis of congenital hypomyelinating Egr2Lo/Lo nerves identifies Sox2 as an inhibitor of Schwann cell differentiation and myelination. Proc Natl Acad Sci U S A *102*, 2596-2601.

Lee, K.F., Simon, H., Chen, H., Bates, B., Hung, M.C., and Hauser, C. (1995). Requirement for neuregulin receptor erbB2 in neural and cardiac development. Nature *378*, 394-398.

Lee, M., Brennan, A., Blanchard, A., Zoidl, G., Dong, Z., Tabernero, A., Zoidl, C., Dent, M.A., Jessen, K.R., and Mirsky, R. (1997). P0 is constitutively expressed in the rat neural crest and embryonic nerves and is negatively and positively regulated by axons to generate non-myelin-forming and myelin-forming Schwann cells, respectively. Mol Cell Neurosci *8*, 336-350.

Lefcort, F., Venstrom, K., McDonald, J.A., and Reichardt, L.F. (1992). Regulation of expression of fibronectin and its receptor, alpha 5 beta 1, during development and regeneration of peripheral nerve. Development *116*, 767-782.

Lemke, G., Kuhn, R., Monuki, E.S., and Weinmaster, G. (1991). Expression and activity of the transcription factor SCIP during glial differentiation and myelination. Ann N Y Acad Sci *633*, 189-195.

Lemke, G., Lamar, E., and Patterson, J. (1988). Isolation and analysis of the gene encoding peripheral myelin protein zero. Neuron *1*, 73-83.

Leone, D.P., Genoud, S., Atanasoski, S., Grausenburger, R., Berger, P., Metzger, D., Macklin, W.B., Chambon, P., and Suter, U. (2003). Tamoxifen-inducible glia-specific Cre mice for somatic mutagenesis in oligodendrocytes and Schwann cells. Mol Cell Neurosci *22*, 430-440.

Levy, P., Vidaud, D., Leroy, K., Laurendeau, I., Wechsler, J., Bolasco, G., Parfait, B., Wolkenstein, P., Vidaud, M., and Bieche, I. (2004). Molecular profiling of malignant peripheral nerve sheath tumors associated with neurofibromatosis type 1, based on large-scale real-time RT-PCR. Mol Cancer *3*, 20.

Lewallen, K.A., Shen, Y.A., De la Torre, A.R., Ng, B.K., Meijer, D., and Chan, J.R. (2011). Assessing the role of the cadherin/catenin complex at the Schwann cell-axon interface and in the initiation of myelination. J Neurosci *31*, 3032-3043.

Limpert, A.S., and Carter, B.D. (2010). Axonal neuregulin 1 type III activates NF-kappaB in Schwann cells during myelin formation. J Biol Chem *285*, 16614-16622.

Lin, W.W., and Karin, M. (2007). A cytokine-mediated link between innate immunity, inflammation, and cancer. J Clin Invest *117*, 1175-1183.

Liu, H.M., Yang, L.H., and Yang, Y.J. (1995). Schwann cell properties: 3. C-fos expression, bFGF production, phagocytosis and proliferation during Wallerian degeneration. J Neuropathol Exp Neurol *54*, 487-496.

Lloyd, A.C., Obermuller, F., Staddon, S., Barth, C.F., McMahon, M., and Land, H. (1997). Cooperating oncogenes converge to regulate cyclin/cdk complexes. Genes Dev *11*, 663-677.

Lobsiger, C.S., Schweitzer, B., Taylor, V., and Suter, U. (2000). Platelet-derived growth factor-BB supports the survival of cultured rat Schwann cell precursors in synergy with neurotrophin-3. Glia *30*, 290-300.

Lunn, E.R., Perry, V.H., Brown, M.C., Rosen, H., and Gordon, S. (1989). Absence of Wallerian Degeneration does not Hinder Regeneration in Peripheral Nerve. Eur J Neurosci *1*, 27-33.

Lyons, D.A., Pogoda, H.M., Voas, M.G., Woods, I.G., Diamond, B., Nix, R., Arana, N., Jacobs, J., and Talbot, W.S. (2005). erbb3 and erbb2 are essential for schwann cell migration and myelination in zebrafish. Curr Biol *15*, 513-524.

Ma, L., Chen, Z., Erdjument-Bromage, H., Tempst, P., and Pandolfi, P.P. (2005). Phosphorylation and functional inactivation of TSC2 by Erk implications for tuberous sclerosis and cancer pathogenesis. Cell *121*, 179-193.

MacInnis, B. L., Campenot, R. B. (2005). Regulation of Wallerian degeneration and nerve growth factor withdrawal-induced pruning of axons of sympathetic neurons by the proteasome and the MEK/Erk pathway. Mol Cell Neurosci *28*, 430-9

Mack, T.G., Reiner, M., Beirowski, B., Mi, W., Emanuelli, M., Wagner, D., Thomson, D., Gillingwater, T., Court, F., Conforti, L., *et al.* (2001). Wallerian degeneration of injured axons and synapses is delayed by a Ube4b/Nmnat chimeric gene. Nat Neurosci *4*, 1199-1206.

Maillet, M., Purcell, N.H., Sargent, M.A., York, A.J., Bueno, O.F., and Molkentin, J.D. (2008). DUSP6 (MKP3) null mice show enhanced ERK1/2 phosphorylation at baseline and increased myocyte proliferation in the heart affecting disease susceptibility. J Biol Chem *283*, 31246-31255.

Mangoura, D., Sun, Y., Li, C., Singh, D., Gutmann, D.H., Flores, A., Ahmed, M., and Vallianatos, G. (2006). Phosphorylation of neurofibromin by PKC is a possible molecular switch in EGF receptor signaling in neural cells. Oncogene *25*, 735-745.

Marchuk, D.A., Saulino, A.M., Tavakkol, R., Swaroop, M., Wallace, M.R., Andersen, L.B., Mitchell, A.L., Gutmann, D.H., Boguski, M., and Collins, F.S. (1991). cDNA cloning of

the type 1 neurofibromatosis gene: complete sequence of the NF1 gene product. Genomics *11*, 931-940.

Maro, G.S., Vermeren, M., Voiculescu, O., Melton, L., Cohen, J., Charnay, P., and Topilko, P. (2004). Neural crest boundary cap cells constitute a source of neuronal and glial cells of the PNS. Nat Neurosci *7*, 930-938.

Marshall, C.J. (1995). Specificity of receptor tyrosine kinase signaling: transient versus sustained extracellular signal-regulated kinase activation. Cell *80*, 179-185.

Martini, R., Mohajeri, M.H., Kasper, S., Giese, K.P., and Schachner, M. (1995). Mice doubly deficient in the genes for P0 and myelin basic protein show that both proteins contribute to the formation of the major dense line in peripheral nerve myelin. J Neurosci *15*, 4488-4495.

Martini, R., and Schachner, M. (1988). Immunoelectron microscopic localization of neural cell adhesion molecules (L1, N-CAM, and myelin-associated glycoprotein) in regenerating adult mouse sciatic nerve. J Cell Biol *106*, 1735-1746.

Martins-Green, M., Boudreau, N., and Bissell, M.J. (1994). Inflammation is responsible for the development of wound-induced tumors in chickens infected with Rous sarcoma virus. Cancer Res *54*, 4334-4341.

Mathon, N.F., Malcolm, D.S., Harrisingh, M.C., Cheng, L., and Lloyd, A.C. (2001). Lack of replicative senescence in normal rodent glia. Science *291*, 872-875.

Maurel, P., Einheber, S., Galinska, J., Thaker, P., Lam, I., Rubin, M.B., Scherer, S.S., Murakami, Y., Gutmann, D.H., and Salzer, J.L. (2007). Nectin-like proteins mediate axon Schwann cell interactions along the internode and are essential for myelination. J Cell Biol *178*, 861-874.

Maurel, P., and Salzer, J.L. (2000). Axonal regulation of Schwann cell proliferation and survival and the initial events of myelination requires PI 3-kinase activity. J Neurosci *20*, 4635-4645.

Mayes, D.A., Rizvi, T.A., Cancelas, J.A., Kolasinski, N.T., Ciraolo, G.M., Stemmer-Rachamimov, A.O., and Ratner, N. (2011). Perinatal or adult Nf1 inactivation using tamoxifen-inducible PlpCre each cause neurofibroma formation. Cancer Res *71*, 4675-4685.

McDonald, D., Cheng, C., Chen, Y., and Zochodne, D. (2006). Early events of peripheral nerve regeneration. Neuron Glia Biol *2*, 139-147.

McKerracher, L., David, S., Jackson, D.L., Kottis, V., Dunn, R.J., and Braun, P.E. (1994). Identification of myelin-associated glycoprotein as a major myelin-derived inhibitor of neurite growth. Neuron *13*, 805-811.

Mei, L., and Xiong, W.C. (2008). Neuregulin 1 in neural development, synaptic plasticity and schizophrenia. Nat Rev Neurosci *9*, 437-452.

Meier, C., Parmantier, E., Brennan, A., Mirsky, R., and Jessen, K.R. (1999). Developing Schwann cells acquire the ability to survive without axons by establishing an autocrine circuit involving insulin-like growth factor, neurotrophin-3, and platelet-derived growth factor-BB. J Neurosci *19*, 3847-3859.

Menon, A.G., Anderson, K.M., Riccardi, V.M., Chung, R.Y., Whaley, J.M., Yandell, D.W., Farmer, G.E., Freiman, R.N., Lee, J.K., Li, F.P., *et al.* (1990). Chromosome 17p deletions and p53 gene mutations associated with the formation of malignant neurofibrosarcomas in von Recklinghausen neurofibromatosis. Proc Natl Acad Sci U S A *87*, 5435-5439.

Messiaen, L.M., Callens, T., Mortier, G., Beysen, D., Vandenbroucke, I., Van Roy, N., Speleman, F., and Paepe, A.D. (2000). Exhaustive mutation analysis of the NF1 gene allows identification of 95% of mutations and reveals a high frequency of unusual splicing defects. Hum Mutat *15*, 541-555.

Messing, A., Behringer, R.R., Hammang, J.P., Palmiter, R.D., Brinster, R.L., and Lemke, G. (1992). P0 promoter directs expression of reporter and toxin genes to Schwann cells of transgenic mice. Neuron *8*, 507-520.

Messing, A., Behringer, R.R., Wrabetz, L., Hammang, J.P., Lemke, G., Palmiter, R.D., and Brinster, R.L. (1994). Hypomyelinating peripheral neuropathies and schwannomas in transgenic mice expressing SV40 T-antigen. J Neurosci *14*, 3533-3539.

Meyer, D., Yamaai, T., Garratt, A., Riethmacher-Sonnenberg, E., Kane, D., Theill, L.E., and Birchmeier, C. (1997). Isoform-specific expression and function of neuregulin. Development *124*, 3575-3586.

Michailov, G.V., Sereda, M.W., Brinkmann, B.G., Fischer, T.M., Haug, B., Birchmeier, C., Role, L., Lai, C., Schwab, M.H., and Nave, K.A. (2004). Axonal neuregulin-1 regulates myelin sheath thickness. Science *304*, 700-703.

Miller, S.J., Jessen, W.J., Mehta, T., Hardiman, A., Sites, E., Kaiser, S., Jegga, A.G., Li, H., Upadhyaya, M., Giovannini, M., *et al.* (2009). Integrative genomic analyses of neurofibromatosis tumours identify SOX9 as a biomarker and survival gene. EMBO Mol Med *1*, 236-248.

Miller, S.J., Rangwala, F., Williams, J., Ackerman, P., Kong, S., Jegga, A.G., Kaiser, S., Aronow, B.J., Frahm, S., Kluwe, L., *et al.* (2006). Large-scale molecular comparison of human schwann cells to malignant peripheral nerve sheath tumor cell lines and tissues. Cancer Res *66*, 2584-2591.

Misra-Press, A., Rim, C.S., Yao, H., Roberson, M.S., and Stork, P.J. (1995). A novel mitogen-activated protein kinase phosphatase. Structure, expression, and regulation. J Biol Chem *270*, 14587-14596.

Moalem, G., Xu, K., and Yu, L. (2004). T lymphocytes play a role in neuropathic pain following peripheral nerve injury in rats. Neuroscience *129*, 767-777.

Monk, K.R., Naylor, S.G., Glenn, T.D., Mercurio, S., Perlin, J.R., Dominguez, C., Moens, C.B., and Talbot, W.S. (2009). A G protein-coupled receptor is essential for Schwann cells to initiate myelination. Science *325*, 1402-1405.

Monk, K.R., Oshima, K., Jors, S., Heller, S., and Talbot, W.S. (2011). Gpr126 is essential for peripheral nerve development and myelination in mammals. Development *138*, 2673-2680.

Monuki, E.S., Kuhn, R., and Lemke, G. (1993). Repression of the myelin P0 gene by the POU transcription factor SCIP. Mech Dev *42*, 15-32.

Monuki, E.S., Kuhn, R., Weinmaster, G., Trapp, B.D., and Lemke, G. (1990). Expression and activity of the POU transcription factor SCIP. Science *249*, 1300-1303.

Monuki, E.S., Weinmaster, G., Kuhn, R., and Lemke, G. (1989). SCIP: a glial POU domain gene regulated by cyclic AMP. Neuron *3*, 783-793.

Morris, J.H., Hudson, A.R., and Weddell, G. (1972a). A study of degeneration and regeneration in the divided rat sciatic nerve based on electron microscopy. II. The development of the "regenerating unit". Z Zellforsch Mikrosk Anat *124*, 103-130.

Morris, J.H., Hudson, A.R., and Weddell, G. (1972b). A study of degeneration and regeneration in the divided rat sciatic nerve based on electron microscopy. IV. Changes in fascicular microtopography, perineurium and endoneurial fibroblasts. Z Zellforsch Mikrosk Anat *124*, 165-203.

Morrison, S.J., White, P.M., Zock, C., and Anderson, D.J. (1999). Prospective identification, isolation by flow cytometry, and in vivo self-renewal of multipotent mammalian neural crest stem cells. Cell *96*, 737-749.

Mueller, M., Leonhard, C., Wacker, K., Ringelstein, E.B., Okabe, M., Hickey, W.F., and Kiefer, R. (2003). Macrophage response to peripheral nerve injury: the quantitative contribution of resident and hematogenous macrophages. Lab Invest *83*, 175-185.

Muir, D. (1995). Differences in proliferation and invasion by normal, transformed and NF1 Schwann cell cultures are influenced by matrix metalloproteinase expression. Clin Exp Metastasis *13*, 303-314.

Mukhopadhyay, G., Doherty, P., Walsh, F.S., Crocker, P.R., and Filbin, M.T. (1994). A novel role for myelin-associated glycoprotein as an inhibitor of axonal regeneration. Neuron *13*, 757-767.

Murphy, P., Topilko, P., Schneider-Maunoury, S., Seitanidou, T., Baron-Van Evercooren, A., and Charnay, P. (1996). The regulation of Krox-20 expression reveals important steps in the control of peripheral glial cell development. Development *122*, 2847-2857.

Nadra, K., de Preux Charles, A.S., Médard, J.J., Hendricks, W.T., Han, G.S., Grès, S., Carman, G.M., Saulnier-Blache, J.S., Verheijen, M.H., and Chrast, R. (2008) Phosphatidic acid mediates demyelination in Lpin1 mutant mice. Genes Dev. *22*, 1647-1661

Nagarajan, R., Svaren, J., Le, N., Araki, T., Watson, M., and Milbrandt, J. (2001). EGR2 mutations in inherited neuropathies dominant-negatively inhibit myelin gene expression. Neuron *30*, 355-368.

Nagy, A. (2000). Cre recombinase: the universal reagent for genome tailoring. Genesis *26*, 99-109.

Napoli, I., Noon, L.A., Ribeiro, S., Kerai, A.P., Parrinello, S., Rosenberg, L.H., Collins, M.J., Harrisingh, M.C., White, I.J., Woodhoo, A., and Lloyd, A.C. A central role for the ERK-signalling pathway in controlling Schwann cell plasticity and peripheral nerve regeneration in vivo, Neuron (2012), doi:10.1016/j.neuron.2011011.031

Nathan, C. (2006). Neutrophils and immunity: challenges and opportunities. Nat Rev Immunol *6*, 173-182.

Nave, K.A. (2010). Myelination and the trophic support of long axons. Nat Rev Neurosci *11*, 275-283.

Nave, K.A., and Salzer, J.L. (2006). Axonal regulation of myelination by neuregulin 1. Curr Opin Neurobiol *16*, 492-500.

Newbern, J., and Birchmeier, C. (2010). Nrg1/ErbB signaling networks in Schwann cell development and myelination. Semin Cell Dev Biol *21*, 922-928.

Newbern, J.M., Li, X., Shoemaker, S.E., Zhou, J., Zhong, J., Wu, Y., Bonder, D., Hollenback, S., Coppola, G., Geschwind, D.H., *et al.* (2011). Specific functions for ERK/MAPK signaling during PNS development. Neuron *69*, 91-105.

Nguyen, Q.T., Sanes, J.R., and Lichtman, J.W. (2002). Pre-existing pathways promote precise projection patterns. Nat Neurosci *5*, 861-867.

Nickols, J.C., Valentine, W., Kanwal, S., and Carter, B.D. (2003). Activation of the transcription factor NF-kappaB in Schwann cells is required for peripheral myelin formation. Nat Neurosci *6*, 161-167.

Niederlander, C., and Lumsden, A. (1996). Late emigrating neural crest cells migrate specifically to the exit points of cranial branchiomotor nerves. Development *122*, 2367-2374.

Nielsen, G.P., Stemmer-Rachamimov, A.O., Ino, Y., Moller, M.B., Rosenberg, A.E., and Louis, D.N. (1999). Malignant transformation of neurofibromas in neurofibromatosis 1 is associated with CDKN2A/p16 inactivation. Am J Pathol *155*, 1879-1884.

Nodari, A., Zambroni, D., Quattrini, A., Court, F.A., D'Urso, A., Recchia, A., Tybulewicz, V.L., Wrabetz, L., and Feltri, M.L. (2007). Beta1 integrin activates Rac1 in Schwann cells to generate radial lamellae during axonal sorting and myelination. J Cell Biol *177*, 1063-1075.

Ogata, T., Iijima, S., Hoshikawa, S., Miura, T., Yamamoto, S., Oda, H., Nakamura, K., and Tanaka, S. (2004). Opposing extracellular signal-regulated kinase and Akt pathways control Schwann cell myelination. J Neurosci *24*, 6724-6732.

Olsson, Y. (1990). Microenvironment of the peripheral nervous system under normal and pathological conditions. Crit Rev Neurobiol *5*, 265-311.

Ousman, S.S., and David, S. (2001). MIP-1alpha, MCP-1, GM-CSF, and TNF-alpha control the immune cell response that mediates rapid phagocytosis of myelin from the adult mouse spinal cord. J Neurosci *21*, 4649-4656.

Owens, D.M., and Keyse, S.M. (2007). Differential regulation of MAP kinase signalling by dual-specificity protein phosphatases. Oncogene *26*, 3203-3213.

Parmantier, E., Lynn, B., Lawson, D., Turmaine, M., Namini, S.S., Chakrabarti, L., McMahon, A.P., Jessen, K.R., and Mirsky, R. (1999). Schwann cell-derived Desert hedgehog controls the development of peripheral nerve sheaths. Neuron *23*, 713-724.

Parrinello, S., and Lloyd, A.C. (2009). Neurofibroma development in NF1--insights into tumour initiation. Trends Cell Biol *19*, 395-403.

Parrinello, S., Napoli, I., Ribeiro, S., Digby, P.W., Fedorova, M., Parkinson, D.B., Doddrell, R.D., Nakayama, M., Adams, R.H., and Lloyd, A.C. (2010). EphB signaling directs peripheral nerve regeneration through Sox2-dependent Schwann cell sorting. Cell *143*, 145-155.

Parrinello, S., Noon, L.A., Harrisingh, M.C., Digby, P.W., Rosenberg, L.H., Cremona, C.A., Echave, P., Flanagan, A.M., Parada, L.F., and Lloyd, A.C. (2008). NF1 loss disrupts Schwann cell-axonal interactions: a novel role for semaphorin 4F. Genes Dev *22*, 3335-3348.

Pellegrino, R.G., and Spencer, P.S. (1985). Schwann cell mitosis in response to regenerating peripheral axons in vivo. Brain Res *341*, 16-25.

Pereira, J.A., Baumann, R., Norrmen, C., Somandin, C., Miehe, M., Jacob, C., Luhmann, T., Hall-Bozic, H., Mantei, N., Meijer, D., *et al.* (2010). Dicer in Schwann cells is required for myelination and axonal integrity. J Neurosci *30*, 6763-6775.

Perentes, E., Nakagawa, Y., Ross, G.W., Stanton, C., and Rubinstein, L.J. (1987). Expression of epithelial membrane antigen in perineurial cells and their derivatives. An immunohistochemical study with multiple markers. Acta Neuropathol *75*, 160-165.

Perkins, N.M., and Tracey, D.J. (2000). Hyperalgesia due to nerve injury: role of neutrophils. Neuroscience *101*, 745-757.

Perlin, J.R., Lush, M.E., Stephens, W.Z., Piotrowski, T., and Talbot, W.S. (2011). Neuronal Neuregulin 1 type III directs Schwann cell migration. Development *138*, 4639-4648.

Perry, V.H., Brown, M.C., and Gordon, S. (1987). The macrophage response to central and peripheral nerve injury. A possible role for macrophages in regeneration. J Exp Med *165*, 1218-1223.

Poliak, S., and Peles, E. (2003). The local differentiation of myelinated axons at nodes of Ranvier. Nat Rev Neurosci *4*, 968-980.

Previtali, S.C., Dina, G., Nodari, A., Fasolini, M., Wrabetz, L., Mayer, U., Feltri, M.L., and Quattrini, A. (2003a). Schwann cells synthesize alpha7beta1 integrin which is dispensable for peripheral nerve development and myelination. Mol Cell Neurosci *23*, 210-218.

Previtali, S.C., Nodari, A., Taveggia, C., Pardini, C., Dina, G., Villa, A., Wrabetz, L., Quattrini, A., and Feltri, M.L. (2003b). Expression of laminin receptors in schwann cell differentiation: evidence for distinct roles. J Neurosci *23*, 5520-5530.

Raphael, A.R., Lyons, D.A., and Talbot, W.S. (2011). ErbB signaling has a role in radial sorting independent of Schwann cell number. Glia *59*, 1047-1055.

Reichert, F., Saada, A., and Rotshenker, S. (1994). Peripheral nerve injury induces Schwann cells to express two macrophage phenotypes: phagocytosis and the galactose-specific lectin MAC-2. J Neurosci *14*, 3231-3245.

Repasky, G.A., Chenette, E.J., and Der, C.J. (2004). Renewing the conspiracy theory debate: does Raf function alone to mediate Ras oncogenesis? Trends Cell Biol *14*, 639-647.

Riccardi, V.M. (1981). Von Recklinghausen neurofibromatosis. N Engl J Med *305*, 1617-1627.

Riccardi, V.M. (1992) Neurofibromatosis: Phenotype, Natural History and Pathogenesis. The John Hopkins University Press, (Baltimore and London)

Richardson, W.D., Young, K.M., Tripathi, R.B., and McKenzie, I. (2011). NG2-glia as multipotent neural stem cells: fact or fantasy? Neuron *70*, 661-673.

Ridley, A.J., Paterson, H.F., Noble, M., and Land, H. (1988). Ras-mediated cell cycle arrest is altered by nuclear oncogenes to induce Schwann cell transformation. EMBO J *7*, 1635-1645.

Riethmacher, D., Sonnenberg-Riethmacher, E., Brinkmann, V., Yamaai, T., Lewin, G.R., and Birchmeier, C. (1997). Severe neuropathies in mice with targeted mutations in the ErbB3 receptor. Nature *389*, 725-730.

Rios, J.C., Melendez-Vasquez, C.V., Einheber, S., Lustig, M., Grumet, M., Hemperly, J., Peles, E., and Salzer, J.L. (2000). Contactin-associated protein (Caspr) and contactin form a complex that is targeted to the paranodal junctions during myelination. J Neurosci *20*, 8354-8364.

Rios, J.C., Rubin, M., St Martin, M., Downey, R.T., Einheber, S., Rosenbluth, J., Levinson, S.R., Bhat, M., and Salzer, J.L. (2003). Paranodal interactions regulate expression of sodium channel subtypes and provide a diffusion barrier for the node of Ranvier. J Neurosci *23*, 7001-7011.

Rubin, J.B., and Gutmann, D.H. (2005). Neurofibromatosis type 1 - a model for nervous system tumour formation? Nat Rev Cancer *5*, 557-564.

Ryu, E.J., Wang, J.Y., Le, N., Baloh, R.H., Gustin, J.A., Schmidt, R.E., and Milbrandt, J. (2007). Misexpression of Pou3f1 results in peripheral nerve hypomyelination and axonal loss. J Neurosci *27*, 11552-11559.

Salzer, J.L. (2003). Polarized domains of myelinated axons. Neuron *40*, 297-318.

Salzer, J.L., Brophy, P.J., and Peles, E. (2008). Molecular domains of myelinated axons in the peripheral nervous system. Glia *56*, 1532-1540.

Sanders, F.K., and Young, J.Z. (1946). The influence of peripheral connexion on the diameter of regenerating nerve fibres. J Exp Biol *22*, 203-212.

Sanders, M.A., and Basson, M.D. (2000). Collagen IV-dependent ERK activation in human Caco-2 intestinal epithelial cells requires focal adhesion kinase. J Biol Chem *275*, 38040-38047.

Schafer, M., Fruttiger, M., Montag, D., Schachner, M., and Martini, R. (1996). Disruption of the gene for the myelin-associated glycoprotein improves axonal regrowth along myelin in C57BL/Wlds mice. Neuron *16*, 1107-1113.

Schafer, M., and Werner, S. (2008). Cancer as an overhealing wound: an old hypothesis revisited. Nat Rev Mol Cell Biol *9*, 628-638.

Scherer, S.S. (1999). Nodes, paranodes, and incisures: from form to function. Ann N Y Acad Sci *883*, 131-142.

Scherer, S.S., Wang, D.Y., Kuhn, R., Lemke, G., Wrabetz, L., and Kamholz, J. (1994). Axons regulate Schwann cell expression of the POU transcription factor SCIP. J Neurosci *14*, 1930-1942.

Scherer, S.S., and Wrabetz, L. (2008). Molecular mechanisms of inherited demyelinating neuropathies. Glia *56*, 1578-1589.

Schneider-Maunoury, S., Topilko, P., Seitandou, T., Levi, G., Cohen-Tannoudji, M., Pournin, S., Babinet, C., and Charnay, P. (1993). Disruption of Krox-20 results in alteration of rhombomeres 3 and 5 in the developing hindbrain. Cell *75*, 1199-1214.

Schreiner, S., Cossais, F., Fischer, K., Scholz, S., Bosl, M.R., Holtmann, B., Sendtner, M., and Wegner, M. (2007). Hypomorphic Sox10 alleles reveal novel protein functions and unravel developmental differences in glial lineages. Development *134*, 3271-3281.

Scherer, S.S., and Salzer, J.L. (2001). Axon-Schwann Cell Interactions during Peripheral Nerve Degeneration and Regeneration (Oxford: Oxford University Press).

Schubbert, S., Shannon, K., and Bollag, G. (2007). Hyperactive Ras in developmental disorders and cancer. Nat Rev Cancer *7*, 295-308.

Schuh, A.C., Keating, S.J., Monteclaro, F.S., Vogt, P.K., and Breitman, M.L. (1990). Obligatory wounding requirement for tumorigenesis in v-jun transgenic mice. Nature *346*, 756-760.

Schulze-Osthoff, K., Risau, W., Vollmer, E., and Sorg, C. (1990). In situ detection of basic fibroblast growth factor by highly specific antibodies. Am J Pathol *137*, 85-92.

Sela-Donenfeld, D., and Kalcheim, C. (1999). Regulation of the onset of neural crest migration by coordinated activity of BMP4 and Noggin in the dorsal neural tube. Development *126*, 4749-4762.

Serra, E., Rosenbaum, T., Winner, U., Aledo, R., Ars, E., Estivill, X., Lenard, H.G., and Lazaro, C. (2000). Schwann cells harbor the somatic NF1 mutation in neurofibromas: evidence of two different Schwann cell subpopulations. Hum Mol Genet *9*, 3055-3064.

Serrano, M., Lin, A.W., McCurrach, M.E., Beach, D., and Lowe, S.W. (1997). Oncogenic ras provokes premature cell senescence associated with accumulation of p53 and p16INK4a. Cell *88*, 593-602.

Sevetson, B.R., Kong, X., and Lawrence, J.C., Jr. (1993). Increasing cAMP attenuates activation of mitogen-activated protein kinase. Proc Natl Acad Sci U S A *90*, 10305-10309.

Shah, N.M., Marchionni, M.A., Isaacs, I., Stroobant, P., and Anderson, D.J. (1994). Glial growth factor restricts mammalian neural crest stem cells to a glial fate. Cell *77*, 349-360.

Shamash, S., Reichert, F., and Rotshenker, S. (2002). The cytokine network of Wallerian degeneration: tumor necrosis factor-alpha, interleukin-1alpha, and interleukin-1beta. J Neurosci *22*, 3052-3060.

Shapiro, L., Doyle, J.P., Hensley, P., Colman, D.R., and Hendrickson, W.A. (1996). Crystal structure of the extracellular domain from P0, the major structural protein of peripheral nerve myelin. Neuron *17*, 435-449.

Sheela, S., Riccardi, V.M., and Ratner, N. (1990). Angiogenic and invasive properties of neurofibroma Schwann cells. J Cell Biol *111*, 645-653.

Sherman, L.S., Atit, R., Rosenbaum, T., Cox, A.D., and Ratner, N. (2000). Single cell Ras-GTP analysis reveals altered Ras activity in a subpopulation of neurofibroma Schwann cells but not fibroblasts. J Biol Chem *275*, 30740-30745.

Sheu, J.Y., Kulhanek, D.J., and Eckenstein, F.P. (2000). Differential patterns of ERK and STAT3 phosphorylation after sciatic nerve transection in the rat. Exp Neurol *166*, 392-402.

Shuman, S., Hardy, M., Sobue, G., and Pleasure, D. (1988). A cyclic AMP analogue induces synthesis of a myelin-specific glycoprotein by cultured Schwann cells. J Neurochem *50*, 190-194.

Shy, M.E., Arroyo, E., Sladky, J., Menichella, D., Jiang, H., Xu, W., Kamholz, J., and Scherer, S.S. (1997). Heterozygous P0 knockout mice develop a peripheral neuropathy that resembles chronic inflammatory demyelinating polyneuropathy (CIDP). J Neuropathol Exp Neurol *56*, 811-821.

Silva, A.J., Frankland, P.W., Marowitz, Z., Friedman, E., Laszlo, G.S., Cioffi, D., Jacks, T., and Bourtchuladze, R. (1997). A mouse model for the learning and memory deficits associated with neurofibromatosis type I. Nat Genet *15*, 281-284.

Snipes, G.J., and Suter, U. (1995). Molecular anatomy and genetics of myelin proteins in the peripheral nervous system. J Anat *186 (Pt 3)*, 483-494.

Sobue, G., and Pleasure, D. (1984). Schwann cell galactocerebroside induced by derivatives of adenosine 3',5'-monophosphate. Science *224*, 72-74.

Solit, D.B., Garraway, L.A., Pratilas, C.A., Sawai, A., Getz, G., Basso, A., Ye, Q., Lobo, J.M., She, Y., Osman, I., *et al.* (2006). BRAF mutation predicts sensitivity to MEK inhibition. Nature *439*, 358-362.

Song, X.Y., Zhou, F.H., Zhong, J.H., Wu, L.L., and Zhou, X.F. (2006). Knockout of p75(NTR) impairs re-myelination of injured sciatic nerve in mice. J Neurochem *96*, 833-842.

Soriano, P. (1999). Generalized lacZ expression with the ROSA26 Cre reporter strain. Nat Genet *21*, 70-71.

Spiegel, I., Adamsky, K., Eshed, Y., Milo, R., Sabanay, H., Sarig-Nadir, O., Horresh, I., Scherer, S.S., Rasband, M.N., and Peles, E. (2007). A central role for Necl4 (SynCAM4) in Schwann cell-axon interaction and myelination. Nat Neurosci *10*, 861-869.

Srinivas, S., Watanabe, T., Lin, C.S., William, C.M., Tanabe, Y., Jessell, T.M., and Costantini, F. (2001). Cre reporter strains produced by targeted insertion of EYFP and ECFP into the ROSA26 locus. BMC Dev Biol *1*, 4.

Stemmer-Rachamimov, A.O., Louis, D.N., Nielsen, G.P., Antonescu, C.R., Borowsky, A.D., Bronson, R.T., Burns, D.K., Cervera, P., McLaughlin, M.E., Reifenberger, G.*, et al.* (2004). Comparative pathology of nerve sheath tumors in mouse models and humans. Cancer Res *64*, 3718-3724.

Stemple, D.L., and Anderson, D.J. (1992). Isolation of a stem cell for neurons and glia from the mammalian neural crest. Cell *71*, 973-985.

Stevens, B., and Fields, R.D. (2000). Response of Schwann cells to action potentials in development. Science *287*, 2267-2271.

Stevens, B., Ishibashi, T., Chen, J.F., and Fields, R.D. (2004). Adenosine: an activity-dependent axonal signal regulating MAP kinase and proliferation in developing Schwann cells. Neuron Glia Biol *1*, 23-34.

Stewart, H.J., Turner, D., Jessen, K.R., and Mirsky, R. (1997). Expression and regulation of alpha1beta1 integrin in Schwann cells. J Neurobiol *33*, 914-928.

Stoll, G., Griffin, J.W., Li, C.Y., and Trapp, B.D. (1989). Wallerian degeneration in the peripheral nervous system: participation of both Schwann cells and macrophages in myelin degradation. J Neurocytol *18*, 671-683.

Stoll, G., Jander, S., and Myers, R.R. (2002). Degeneration and regeneration of the peripheral nervous system: from Augustus Waller's observations to neuroinflammation. J Peripher Nerv Syst *7*, 13-27.

Stoll, G., and Muller, H.W. (1999). Nerve injury, axonal degeneration and neural regeneration: basic insights. Brain Pathol *9*, 313-325.

Stork, P.J., and Schmitt, J.M. (2002). Crosstalk between cAMP and MAP kinase signaling in the regulation of cell proliferation. Trends Cell Biol *12*, 258-266.

Sunderland, S. (1990). The anatomy and physiology of nerve injury. Muscle Nerve *13*, 771-784.

Sunderland, S., and Bradley, K.C. (1949). The cross-sectional area of peripheral nerve trunks devoted to nerve fibers. Brain *72*, 428-449.

Svaren, J., and Meijer, D. (2008). The molecular machinery of myelin gene transcription in Schwann cells. Glia *56*, 1541-1551.

Syed, N., Reddy, K., Yang, D.P., Taveggia, C., Salzer, J.L., Maurel, P., and Kim, H.A. (2010). Soluble neuregulin-1 has bifunctional, concentration-dependent effects on Schwann cell myelination. J Neurosci *30*, 6122-6131.

Tacke, R., and Martini, R. (1990). Changes in expression of mRNA specific for cell adhesion molecules (L1 and NCAM) in the transected peripheral nerve of the adult rat. Neurosci Lett *120*, 227-230.

Tapinos, N., Ohnishi, M., and Rambukkana, A.(2006). ErbB2 receptor tyrosine kinase

signaling mediates early demyelination induced by leprosy bacilli. Nat Med *12*, 961-6

Tanaka, K., Nakafuku, M., Satoh, T., Marshall, M.S., Gibbs, J.B., Matsumoto, K., Kaziro, Y., and Toh-e, A. (1990). S. cerevisiae genes IRA1 and IRA2 encode proteins that may be functionally equivalent to mammalian ras GTPase activating protein. Cell *60*, 803-807.

Taniuchi, M., Clark, H.B., and Johnson, E.M., Jr. (1986). Induction of nerve growth factor receptor in Schwann cells after axotomy. Proc Natl Acad Sci U S A *83*, 4094-4098.

Tao, Y., Dai, P., Liu, Y., Marchetto, S., Xiong, W.C., Borg, J.P., and Mei, L. (2009). Erbin regulates NRG1 signaling and myelination. Proc Natl Acad Sci U S A *106*, 9477-9482.

Taveggia, C., Feltri, M.L., and Wrabetz, L. (2010). Signals to promote myelin formation and repair. Nat Rev Neurol *6*, 276-287.

Taveggia, C., Zanazzi, G., Petrylak, A., Yano, H., Rosenbluth, J., Einheber, S., Xu, X., Esper, R.M., Loeb, J.A., Shrager, P.*, et al.* (2005). Neuregulin-1 type III determines the ensheathment fate of axons. Neuron *47*, 681-694.

The, I., Hannigan, G.E., Cowley, G.S., Reginald, S., Zhong, Y., Gusella, J.F., Hariharan, I.K., and Bernards, A. (1997). Rescue of a Drosophila NF1 mutant phenotype by protein kinase A. Science *276*, 791-794.

Theaker, J.M., and Fletcher, C.D. (1989). Epithelial membrane antigen expression by the perineurial cell: further studies of peripheral nerve lesions. Histopathology *14*, 581-592.

Theaker, J.M., Gatter, K.C., and Puddle, J. (1988). Epithelial membrane antigen expression by the perineurium of peripheral nerve and in peripheral nerve tumours. Histopathology *13*, 171-179.

Thomas, P.K. & Jones, D.G. (1967). The cellular response to nerve injury. 2. Regeneration of the perineurium after nerve section. Journal of Anatomy 101, 45-55.

Thomas, L., Kluwe, L., Chuzhanova, N., Mautner, V., and Upadhyaya, M. (2010). Analysis of NF1 somatic mutations in cutaneous neurofibromas from patients with high tumor burden. Neurogenetics *11*, 391-400.

Thomas, L., Spurlock, G., Eudall, C., Thomas, N.S., Mort, M., Hamby, S.E., Chuzhanova, N., Brems, H., Legius, E., Cooper, D.N.*, et al.* (2011). Exploring the somatic NF1 mutational spectrum associated with NF1 cutaneous neurofibromas. Eur J Hum Genet.

Thoresen, G.H., Johasen, E.J., and Christoffersen, T. (1999). Effects of cAMP on ERK mitogen-activated protein kinase activity in hepatocytes do not parallel the bidirectional regulation of DNA synthesis. Cell Biol Int *23*, 13-20.

Thornton, M.R., Mantovani, C., Birchall, M.A., and Terenghi, G. (2005). Quantification of N-CAM and N-cadherin expression in axotomized and crushed rat sciatic nerve. J Anat *206*, 69-78.

Tischler, A.S., Shih, T.S., Williams, B.O., and Jacks, T. (1995). Characterization of Pheochromocytomas in a Mouse Strain with a Targeted Disruptive Mutation of the Neurofibromatosis Gene Nf1. Endocr Pathol *6*, 323-335.

Toews, A.D., Barrett, C., and Morell, P. (1998). Monocyte chemoattractant protein 1 is responsible for macrophage recruitment following injury to sciatic nerve. J Neurosci Res *53*, 260-267.

Topilko, P., Schneider-Maunoury, S., Levi, G., Baron-Van Evercooren, A., Chennoufi, A.B., Seitanidou, T., Babinet, C., and Charnay, P. (1994). Krox-20 controls myelination in the peripheral nervous system. Nature *371*, 796-799.

Toyota, B., Carbonetto, S., and David, S. (1990). A dual laminin/collagen receptor acts in peripheral nerve regeneration. Proc Natl Acad Sci U S A *87*, 1319-1322.

Trapp, B.D., Hauer, P., and Lemke, G. (1988). Axonal regulation of myelin protein mRNA levels in actively myelinating Schwann cells. J Neurosci *8*, 3515-3521.

Triolo, D., Dina, G., Lorenzetti, I., Malaguti, M., Morana, P., Del Carro, U., Comi, G., Messing, A., Quattrini, A., and Previtali, S.C. (2006). Loss of glial fibrillary acidic protein (GFAP) impairs Schwann cell proliferation and delays nerve regeneration after damage. J Cell Sci *119*, 3981-3993.

Tsao, J.W., Brown, M.C., Carden, M.J., McLean, W.G., and Perry, V.H. (1994). Loss of the compound action potential: an electrophysiological, biochemical and morphological study of early events in axonal degeneration in the C57BL/Ola mouse. Eur J Neurosci *6*, 516-524.

Upadhyaya, M., Shaw, D.J., and Harper, P.S. (1994). Molecular basis of neurofibromatosis type 1 (NF1): mutation analysis and polymorphisms in the NF1 gene. Hum Mutat *4*, 83-101.

Vallat, J.M., Sindou, P., Preux, P.M., Tabaraud, F., Milor, A.M., Couratier, P., LeGuern, E., and Brice, A. (1996). Ultrastructural PMP22 expression in inherited demyelinating neuropathies. Ann Neurol *39*, 813-817.

Vandenbroucke, I., Van Oostveldt, P., Coene, E., De Paepe, A., and Messiaen, L. (2004). Neurofibromin is actively transported to the nucleus. FEBS Lett *560*, 98-102.

Vartanian, T., Goodearl, A., Lefebvre, S., Park, S.K., and Fischbach, G. (2000). Neuregulin induces the rapid association of focal adhesion kinase with the erbB2-erbB3 receptor complex in schwann cells. Biochem Biophys Res Commun *271*, 414-417.

Virchow R (1863) Aetiologie der neoplastischen Geschwulste/ Pathogenie der neoplastischen Geschwulste (Verlag von August Hirschwald, Berlin, Germany).

Viskochil, D., Buchberg, A.M., Xu, G., Cawthon, R.M., Stevens, J., Wolff, R.K., Culver, M., Carey, J.C., Copeland, N.G., Jenkins, N.A., *et al.* (1990). Deletions and a translocation interrupt a cloned gene at the neurofibromatosis type 1 locus. Cell *62*, 187-192.

Visvader, J.E. (2011). Cells of origin in cancer. Nature *469*, 314-322.

Vivanco, I., and Sawyers, C.L. (2002). The phosphatidylinositol 3-Kinase AKT pathway in human cancer. Nat Rev Cancer *2*, 489-501.

Vogel, K.S., Klesse, L.J., Velasco-Miguel, S., Meyers, K., Rushing, E.J., and Parada, L.F. (1999). Mouse tumor model for neurofibromatosis type 1. Science *286*, 2176-2179.

Vogelezang, M.G., Liu, Z., Relvas, J.B., Raivich, G., Scherer, S.S., and ffrench-Constant, C. (2001). Alpha4 integrin is expressed during peripheral nerve regeneration and enhances neurite outgrowth. J Neurosci *21*, 6732-6744.

Walikonis, R.S., and Poduslo, J.F. (1998). Activity of cyclic AMP phosphodiesterases and adenylyl cyclase in peripheral nerve after crush and permanent transection injuries. J Biol Chem *273*, 9070-9077.

Walker, J.A., Tchoudakova, A.V., McKenney, P.T., Brill, S., Wu, D., Cowley, G.S., Hariharan, I.K., and Bernards, A. (2006). Reduced growth of Drosophila neurofibromatosis 1 mutants reflects a non-cell-autonomous requirement for GTPase-Activating Protein activity in larval neurons. Genes Dev *20*, 3311-3323.

Wallace, M.R., Marchuk, D.A., Andersen, L.B., Letcher, R., Odeh, H.M., Saulino, A.M., Fountain, J.W., Brereton, A., Nicholson, J., Mitchell, A.L.*, et al.* (1990). Type 1 neurofibromatosis gene: identification of a large transcript disrupted in three NF1 patients. Science *249*, 181-186.

Wang, J.T., Medress, Z.A., and Barres, B.A. (2012). Axon degeneration: Molecular mechanisms of a self-destruction pathway. J Cell Biol *196*, 7-18.

Wanner, I.B., and Wood, P.M. (2002). N-cadherin mediates axon-aligned process growth and cell-cell interaction in rat Schwann cells. J Neurosci *22*, 4066-4079.

Warner, L.E., Hilz, M.J., Appel, S.H., Killian, J.M., Kolodry, E.H., Karpati, G., Carpenter, S., Watters, G.V., Wheeler, C., Witt, D.*, et al.* (1996). Clinical phenotypes of different MPZ (P0) mutations may include Charcot-Marie-Tooth type 1B, Dejerine-Sottas, and congenital hypomyelination. Neuron *17*, 451-460.

Wasylyk, B., Hagman, J., and Gutierrez-Hartmann, A. (1998). Ets transcription factors: nuclear effectors of the Ras-MAP-kinase signaling pathway. Trends Biochem Sci *23*, 213-216.

Watabe, K., Fukuda, T., Tanaka, J., Toyohara, K., and Sakai, O. (1994). Mitogenic effects of platelet-derived growth factor, fibroblast growth factor, transforming growth factor-beta, and heparin-binding serum factor for adult mouse Schwann cells. J Neurosci Res *39*, 525-534.

Watanabe, T., Oda, Y., Tamiya, S., Masuda, K., and Tsuneyoshi, M. (2001). Malignant peripheral nerve sheath tumour arising within neurofibroma. An immunohistochemical analysis in the comparison between benign and malignant components. J Clin Pathol *54*, 631-636.

Webster, H.D., Martin, R., and O'Connell, M.F. (1973). The relationships between interphase Schwann cells and axons before myelination: a quantitative electron microscopic study. Dev Biol *32*, 401-416.

Weiss, B., Bollag, G., and Shannon, K. (1999). Hyperactive Ras as a therapeutic target in neurofibromatosis type 1. Am J Med Genet *89*, 14-22.

Wilkinson, D.G., Bhatt, S., Chavrier, P., Bravo, R., and Charnay, P. (1989). Segment-specific expression of a zinc-finger gene in the developing nervous system of the mouse. Nature *337*, 461-464.

Willem, M., Garratt, A.N., Novak, B., Citron, M., Kaufmann, S., Rittger, A., DeStrooper, B., Saftig, P., Birchmeier, C., and Haass, C. (2006). Control of peripheral nerve myelination by the beta-secretase BACE1. Science *314*, 664-666.

Williams, P.L. (1999). "Gray's Anatomy." Churchill livingstone, London.

Williams, V.C., Lucas, J., Babcock, M.A., Gutmann, D.H., Korf, B., and Maria, B.L. (2009). Neurofibromatosis type 1 revisited. Pediatrics *123*, 124-133.

Wimmer, K., Roca, X., Beiglbock, H., Callens, T., Etzler, J., Rao, A.R., Krainer, A.R., Fonatsch, C., and Messiaen, L. (2007). Extensive in silico analysis of NF1 splicing defects uncovers determinants for splicing outcome upon 5' splice-site disruption. Hum Mutat *28*, 599-612.

Wimmer, K., Yao, S., Claes, K., Kehrer-Sawatzki, H., Tinschert, S., De Raedt, T., Legius, E., Callens, T., Beiglbock, H., Maertens, O., *et al.* (2006). Spectrum of single- and multiexon NF1 copy number changes in a cohort of 1,100 unselected NF1 patients. Genes Chromosomes Cancer *45*, 265-276.

Wolpowitz, D., Mason, T.B., Dietrich, P., Mendelsohn, M., Talmage, D.A., and Role, L.W. (2000). Cysteine-rich domain isoforms of the neuregulin-1 gene are required for maintenance of peripheral synapses. Neuron *25*, 79-91.

Wong, C.E., Paratore, C., Dours-Zimmermann, M.T., Rochat, A., Pietri, T., Suter, U., Zimmermann, D.R., Dufour, S., Thiery, J.P., Meijer, D., *et al.* (2006). Neural crest-derived cells with stem cell features can be traced back to multiple lineages in the adult skin. J Cell Biol *175*, 1005-1015.

Wong, S.Y., and Reiter, J.F. (2011). Wounding mobilizes hair follicle stem cells to form tumors. Proc Natl Acad Sci U S A *108*, 4093-4098.

Woodhoo, A., Alonso, M.B., Droggiti, A., Turmaine, M., D'Antonio, M., Parkinson, D.B., Wilton, D.K., Al-Shawi, R., Simons, P., Shen, J., *et al.* (2009). Notch controls embryonic Schwann cell differentiation, postnatal myelination and adult plasticity. Nat Neurosci *12*, 839-847.

Wu, J., Williams, J.P., Rizvi, T.A., Kordich, J.J., Witte, D., Meijer, D., Stemmer-Rachamimov, A.O., Cancelas, J.A., and Ratner, N. (2008). Plexiform and dermal neurofibromas and pigmentation are caused by Nf1 loss in desert hedgehog-expressing cells. Cancer Cell *13*, 105-116.

Xu, G.F., O'Connell, P., Viskochil, D., Cawthon, R., Robertson, M., Culver, M., Dunn, D., Stevens, J., Gesteland, R., White, R., *et al.* (1990). The neurofibromatosis type 1 gene encodes a protein related to GAP. Cell *62*, 599-608.

Yamazaki, S., Ema, H., Karlsson, G., Yamaguchi, T., Miyoshi, H., Shioda, S., Taketo, M.M., Karlsson, S., Iwama, A., and Nakauchi, H. (2011). Nonmyelinating schwann cells

maintain hematopoietic stem cell hibernation in the bone marrow niche. Cell *147*, 1146-1158.

Yang, D.P., Zhang, D.P., Mak, K.S., Bonder, D.E., Pomeroy, S.L. and Kim, H.A. (2008). Schwann cell proliferation during Wallerian degeneration is not necessary for regeneration and remyelination of the peripheral nerves: axon-dependent removal of newly generated Schwann cells by apoptosis. Mol Cell Neurosci *38*, 80-8

Yan, T., Feng, Y., Zheng, J., Ge, X., Zhang, Y., Wu, D., Zhao, J., and Zhai, Q. (2010). Nmnat2 delays axon degeneration in superior cervical ganglia dependent on its NAD synthesis activity. Neurochem Int *56*, 101-106.

Yang, F.C., Chen, S., Clegg, T., Li, X., Morgan, T., Estwick, S.A., Yuan, J., Khalaf, W., Burgin, S., Travers, J., *et al.* (2006). Nf1+/- mast cells induce neurofibroma like phenotypes through secreted TGF-beta signaling. Hum Mol Genet *15*, 2421-2437.

Yang, F.C., Ingram, D.A., Chen, S., Hingtgen, C.M., Ratner, N., Monk, K.R., Clegg, T., White, H., Mead, L., Wenning, M.J., *et al.* (2003). Neurofibromin-deficient Schwann cells secrete a potent migratory stimulus for Nf1+/- mast cells. J Clin Invest *112*, 1851-1861.

Yang, F.C., Ingram, D.A., Chen, S., Zhu, Y., Yuan, J., Li, X., Yang, X., Knowles, S., Horn, W., Li, Y., *et al.* (2008). Nf1-dependent tumors require a microenvironment containing Nf1+/- and c-kit-dependent bone marrow. Cell *135*, 437-448.

Yoon, C., Korade, Z., and Carter, B.D. (2008). Protein kinase A-induced phosphorylation of the p65 subunit of nuclear factor-kappaB promotes Schwann cell differentiation into a myelinating phenotype. J Neurosci *28*, 3738-3746.

Yu, W.M., Yu, H., and Chen, Z.L. (2007). Laminins in peripheral nerve development and muscular dystrophy. Mol Neurobiol *35*, 288-297.

Yu, W.M., Yu, H., Chen, Z.L., and Strickland, S. (2009). Disruption of laminin in the peripheral nervous system impedes nonmyelinating Schwann cell development and impairs nociceptive sensory function. Glia *57*, 850-859.

Zanazzi, G., Einheber, S., Westreich, R., Hannocks, M.J., Bedell-Hogan, D., Marchionni, M.A., and Salzer, J.L. (2001). Glial growth factor/neuregulin inhibits Schwann cell myelination and induces demyelination. J Cell Biol *152*, 1289-1299.

Zang, G.Q., Zhou, X.Q., Yu, H., Xie, Q., Zhao, G.M., Wang, B., Guo, Q., Xiang, Y.Q., and Liao, D. (2000). Effect of hepatocyte apoptosis induced by TNF-alpha on acute severe hepatitis in mouse models. World J Gastroenterol *6*, 688-692.

Zhai, Q., Wang, J., Kim, A., Liu, Q., Watts, R., Hoopfer, E., Mitchison, T., Luo, L., and He, Z. (2003) Involvement of the ubiquitin-proteasome system in the early stages of wallerian degeneration. Neuron *39*, 217-25

Zhang, J.Y., Luo, X.G., Xian, C.J., Liu, Z.H., and Zhou, X.F. (2000). Endogenous BDNF is required for myelination and regeneration of injured sciatic nerve in rodents. Eur J Neurosci *12*, 4171-4180.

Zhang, Y., Campbell, G., Anderson, P.N., Martini, R., Schachner, M., and Lieberman, A.R. (1995). Molecular basis of interactions between regenerating adult rat thalamic

axons and Schwann cells in peripheral nerve grafts. II. Tenascin-C. J Comp Neurol *361*, 210-224.

Zhang, Y.Y., Vik, T.A., Ryder, J.W., Srour, E.F., Jacks, T., Shannon, K., and Clapp, D.W. (1998). Nf1 regulates hematopoietic progenitor cell growth and ras signaling in response to multiple cytokines. J Exp Med *187*, 1893-1902.

Zheng, H., Chang, L., Patel, N., Yang, J., Lowe, L., Burns, D.K., and Zhu, Y. (2008). Induction of abnormal proliferation by nonmyelinating schwann cells triggers neurofibroma formation. Cancer Cell *13*, 117-128.

Zhu, Y., Ghosh, P., Charnay, P., Burns, D.K., and Parada, L.F. (2002). Neurofibromas in NF1: Schwann cell origin and role of tumor environment. Science *296*, 920-922.

Zhu, Y., Romero, M.I., Ghosh, P., Ye, Z., Charnay, P., Rushing, E.J., Marth, J.D., and Parada, L.F. (2001). Ablation of NF1 function in neurons induces abnormal development of cerebral cortex and reactive gliosis in the brain. Genes Dev *15*, 859-876.

Zielasek, J., Martini, R., and Toyka, K.V. (1996). Functional abnormalities in P0-deficient mice resemble human hereditary neuropathies linked to P0 gene mutations. Muscle Nerve *19*, 946-952.

Zochodne, D.W. (2008). Neurobiology of Peripheral Nerve Regeneration, First Edition (New York: Cambridge University Press).

Zorick, T.S., Syroid, D.E., Arroyo, E., Scherer, S.S., and Lemke, G. (1996a). The Transcription Factors SCIP and Krox-20 Mark Distinct Stages and Cell Fates in Schwann Cell Differentiation. Mol Cell Neurosci *8*, 129-145.

Zorick, T.S., Syroid, D.E., Arroyo, E., Scherer, S.S., and Lemke, G. (1996b). The transcription factors SCIP and Krox-20 mark distinct stages and cell fates in Schwann cell differentiation. Mol Cell Neurosci *8*, 129-145.